SEDIMENTATION AND CHEMICAL PROCESSES ON THE LOWER MKUZE FLOODPLAIN: IMPLICATIONS FOR WETLAND STRUCTURE AND FUNCTION

Submitted in fulfilment of the requirements for the degree of Doctor of Philosophy in the School of Chemistry, University of KwaZulu-Natal.

Marc Humphries

December 2008

ABSTRACT

The Mkuze Wetland System, situated in northern KwaZulu-Natal, is South Africa's largest freshwater wetland area. The system plays a vital role in the functioning of the local landscape and has been identified as an important site for the retention of a number of solutes. The mechanisms through which this retention occurs were investigated through analysis of sediment, groundwater and porewater samples collected from the lower floodplain. Sample analysis was achieved through the use of several techniques, including Inductively Coupled Plasma-Optical Emission Spectroscopy (ICP-OES), X-ray Diffraction (XRD), X-ray Fluorescence (XRF), electron microscopy and sequential extraction.

Data collected indicate that evapotranspiration is the primary mechanism controlling the retention of chemicals. Groundwater, introduced by flow from the Mkuze River, becomes increasingly concentrated under the effects of evapotranspiration, resulting in the precipitation of calcium carbonate, followed by silica compounds (amorphous/opaline silica, Mg-silicates). Evapotranspiration also indirectly influences the sediment redox status, which exerts control on the formation of Fe/Mn oxyhydroxides and sulphides. Clay mineralogy is dominated by Fe-rich smectite, which is inferred to be dominantly neogenetic in origin. Seasonal drying and flooding of floodplain sediments, as well as the build up of silicon in solution under evapotranspiration, results in the *in situ* formation of smectite. Under the influence of evapotranspiration, chemical precipitation is identified as the main factor responsible for the removal of significant quantities of dissolved solutes from solution.

Aggradation of the floodplain appears to be a combination of both clastic and chemical sedimentation. Estimated clastic sedimentation rates, derived from ^{210}Pb and ^{137}Cs dating, ranged from 0.24 to 0.39 cm/yr, with most of this accretion expected to be associated with seasonal flooding events. It is suggested that chemical sedimentation is an important contributor to long-term floodplain evolution, as it has the potential to modify the chemical and physical characteristics of wetland sediment. When viewed over long timescales, chemical sedimentation will affect the local landscape by altering hydrological flowpaths, vegetation distribution and topography. A conceptual model for chemical sedimentation on the Mkuze Floodplain is proposed and it is suggested that similar processes are probably occurring in other southern African wetland systems.

PREFACE

The experimental work described in this dissertation was carried out in the School of Chemistry, University of KwaZulu-Natal, Durban, from January 2005 to December 2008, under the supervision of Prof. A. Kindness, Prof. W.N. Ellery and Prof. J. Hughes.

This study represents the author's original work and has not been submitted before for any degree or to any other university. Where use has been made of the work of others, it has been duly acknowledged in the text.

_____

Marc Humphries

December 2008

AKNOWLEDGEMENTS

I thank Professor Andrew Kindness, Professor Fred Ellery and Professor Jeffery Hughes for supervision of this research and for their support and advice. I thank them for giving me the freedom to take the project in the direction I wished.

Thanks are also due to Dr Claudia Benitez-Nelson (University of South Carolina) and Professor Michael Witcomb (University of the Witwatersrand) who kindly assisted with radioisotope and TEM-EDS analysis, respectively.

Most importantly, I thank my friends Jonathan Bond, Jason Paraskevopoulos, Letitia Pillay, Kirsten van der Avoort and Michael van Niekerk who helped me on numerous data collection expeditions. Fieldwork would not have been as much fun without them. In particular, I thank Jonathan Bond for his constant assistance in the field and friendship throughout this study. Thank you!

The Ernst & Ethel Eriksen Trust and NUFU provided financial support for the study.

CONTENTS

Chapter 1
Introduction

Wetlands are complex systems that represent very important features in almost every environment. Wetlands are found at the interface of terrestrial and aquatic ecosystems, and cover about 6% of the earth's surface (Mitsch & Gosselink, 2007). Due to the wide range of hydrological, biogeochemical and ecological functions they perform, wetlands provide numerous environmental benefits, including water purification, river flow regulation, and habitat to a variety of plant and animal species. In South Africa, wetland systems are also vital to tourism, environmental education, wildlife protection, subsistence agriculture, and as a source of natural resources for rural communities.

Nevertheless, wetland systems worldwide have faced continuous degradation over the last century resulting from extensive drainage for agriculture, commercial forestry and urban development. The continuous loss of wetland areas around the world has resulted in wetlands becoming recognised as endangered ecosystems. Today, wetlands are among the most threatened habitats in South Africa, and it is estimated that up to 50% of South Africa's wetland areas have already been lost or degraded as result of human activities (Kotze *et al.,* 1995). As a result, wetlands have received increasing scientific and public attention over the last few years (Mitsch & Gosselink, 2007), with environmental policies and international programs (such as the Ramsar convention) being initiated to help conserve and manage wetlands sustainably.

Environmental conservation has witnessed a noticeable shift in emphasis in recent years, from the protection of individual species to ecosystems and landscapes (Saunders *et al*., 1991; Schwartz *et al.,* 2000; Prato, 2007). This is due to the fact that maintaining functioning ecosystems is of critical importance in providing habitats for species. In this context, the conservation, restoration and creation of wetlands is often justified in terms of the beneficial functions and values they provide. Being situated at the interface between two different ecosystem types, wetlands are typically biogeochemical hotspots of solute transformation that potentially accumulate large quantities of naturally occurring chemicals. Much research has therefore focused on nutrient transformations within wetlands and the potential of these systems to act as long-term sinks within the environment (Johnston, 1991; Day *et al*., 2004; Verhoeven *et al.,* 2006). However, research efforts have focused almost exclusively on plant macronutrients (nitrogen and phosphorus), with very little consideration being given to other natural chemicals (Grimm *et al.*, 2003, Fisher & Acreman, 2004). Moreover, most biogeochemical studies have been conducted on wetlands in the Northern Hemisphere, where conditions are characterised by cool, temperature environments. Very little scientific research, particularly in southern Africa, has been carried out on wetland systems where climatic conditions range from semi-arid to subtropical.

The Mkuze Wetland System in northern KwaZulu-Natal is one of South Africa's largest wetland areas (Stormanns, 1987). The diverse wetlands of this system not only play a valuable role in trapping sediment and attenuating discharge into Lake St Lucia, but they are also the largest supplier of freshwater to this estuary. The long-term survival of Lake St Lucia, the largest and one of the most important estuarine systems in Africa, thus depends on the conservation and wise management of the Mkuze wetlands. Due to their great ecological importance, both the Mkuze Wetland System and Lake St Lucia are protected in terms of the Ramsar Convention (Cowan, 1995) and have World Heritage status.

Preliminary investigations in the Mkuze Wetland System have indicated that this wetland is acting as a sink for certain solutes, particularly silicon, potassium, calcium, and to a lesser extent sodium and magnesium (Barnes *et al*., 2002). Extensive solute immobilisation and accumulation within the Mkuze Wetland System not only has significant implications for Lake St Lucia, but could also have significant impacts on the ecology and geomorphology of the wetland system itself. This process of chemical sedimentation has not been widely appreciated and has often been overlooked in wetland science (Ellery *et al.*, 2007). The potential importance of this process can be appreciated by

considering that the total quantity of chemical sediments accumulating annually in the Okavango Delta is approximately 450 000 tonnes (McCarthy & Ellery, 1998), which amounts to well over twice the clastic load. In the Okavango, chemical sedimentation is believed to occur primarily through transpiration by plants which cause solutes in the groundwater to concentrate to the point where they become saturated and precipitate out of solution. The accumulation of solutes in the soil has been shown to play a vital role in governing wetland structure and function (McCarthy *et al.*, 1993; McCarthy *et al.*, 1997). Recent studies emerging from Brazil show that similar concentration and precipitation processes may be operating within the Pantanal wetland (Barbiéro *et al*., 2002; Furquim *et al*., 2004).

Results from these studies indicate that wetland systems in the southern hemisphere may function very differently from their more well-studied counterparts in Europe and North America. Transpiration appears to be a key mechanism controlling the retention of large quantities of chemicals in these systems, and this raises the question as to whether similar chemical sedimentation processes are occurring in other wetland ecosystems. The aim of this study is to therefore investigate the presence and/or extent of chemical sedimentation on the lower Mkuze Floodplain, in order to develop a more generalised understanding of this process and improve our understanding of wetland functioning in South Africa.

The main objectives of this study are to:

- characterise sediment on the Mkuze River Floodplain by examining floodplain stratigraphy, sediment chemistry and mineralogy;
- examine variation in sediment porewater and groundwater chemistry;
- identify and characterise biogeochemical processes that contribute to variation in sediment, groundwater and porewater chemistry;
- investigate the use of radioisotopic measurements in estimating floodplain sediment deposition rates;
- assess the extent to which chemical sedimentation may influence the structure and functioning of the Mkuze Wetland System and
- integrate new insights gained from this study into existing chemical sedimentation models.

Chapter 2

Conceptual framework

Wetland research has benefited greatly from a variety of studies conducted within the fields of hydrology, ecology, chemistry and soil science. This has considerably improved our general understanding of wetland functioning. However, many of these studies have shown that an integrated and interdisciplinary approach is necessary to fully understand and assess the complex nature of wetland systems. This chapter provides an overview of the processes that characterise wetland systems, and in particular, those of southern Africa.

2.1 Introduction

Due to low mean annual rainfall (<500 mm) and high rates of evapotranspiration (>2000 mm per annum) over much of the subcontinent, southern Africa has relatively few wetlands, with the majority being small and often seasonal (Ellery *et al*., 2007). However, the region does contain a large variety of wetland systems which occur in diverse settings and under a variety of climatic conditions (McCarthy & Hancox, 2000). Heterogeneity arises from the range of climatic and geomorphic settings in which wetlands occur, ranging from the coastal plain of northern KwaZulu-Natal, to the highlands of the eastern escarpment, and the floodplains of the high plateau that dominates the southern African interior. Wetlands also range in size from small sites such as those found at the head of streams, to large complex ones such as the Okavango Delta. However, despite their great range in variety and size, wetlands share specific structural and functional characteristics.

2.2 Factors that shape wetland structure and function

Wetlands occur where there is a surplus of water at or close to the earth's surface for an appreciable period each year. Wetland structure and function are thus primarily a product of hydrologic forces (Figure 2.1). Water shapes the physical template of a wetland through the long-term cumulative action of flow, erosional and depositional processes. Hydrological flows are also responsible for transporting chemicals, nutrients and sediment into and out of wetlands. In South Africa where water is generally a scarce resource, many wetlands, especially large systems, are thus linked to streams (Ellery *et al*., 2007). In these systems, hydrology is the single most important driving variable as changes in river flow alter the extent, duration and frequency of inundation (Tockner & Stanford, 2002).

Hydrologic variables, such as water depth and frequency of flooding, create the unique physicochemical conditions that characterise wetland ecosystems. In this respect, hydrology plays a crucial role in the biogeochemistry of wetland soils through changes in pH, redox potential, and sediment properties (Mitsch & Gosselink, 2007). The rate at which chemicals and sediment are delivered to and flushed from a wetland are important variables which determine the extent to which biogeochemical reactions modify the chemistry of inflowing water. Wetlands generally have a high capacity for reducing the velocity of water, resulting in longer hydrologic residence times and greater contact time between water and sediment for biogeochemical reactions to take place.

The physicochemical conditions established by the hydrology of a wetland often determine a wetland's biotic response (Figure 2.1). Even small changes in hydrologic conditions may result in significant changes in species composition and ecosystem productivity. The hydrological regime of most wetlands is dynamic and may vary significantly from year to year or fluctuate seasonally. Many floodplain wetlands, in particular, are maintained, in part, by natural disturbances such as annual floods. The structure and functioning of these ecosystems is greatly influenced by the nature, strength and duration of inundation events. Alternating periods of inundation and drought together maintain the distinctive plant and animal communities of individual wetlands. Plant communities develop distinct patterns of vegetation zonation in response to the interaction of stresses imposed by both the degree and duration of inundation and exposure, with those tolerant of flooding being situated in areas of frequent flooding and inundation, and with those less tolerant being found in areas of prolonged dry periods (Breen *et al*., 1988).

Although hydrology controls many of the abiotic and biotic characteristics of wetlands, control is often not unidirectional. Wetlands can exert feedback controls that affect hydrology and their physicochemical environment (Figure 2.1). For example, wetland vegetation can alter hydrologic conditions through mechanisms such as sediment trapping, nutrient retention, peat accumulation and evapotranspiration (Mitsch & Gosselink, 2007). The activities of animals such as hippopotami (*Hippopotamus amphibious*) have also been shown to modify hydrologic conditions in wetlands by creating hydraulically efficient flow paths (McCarthy *et al*., 1998a; Ellery *et al*., 2003).

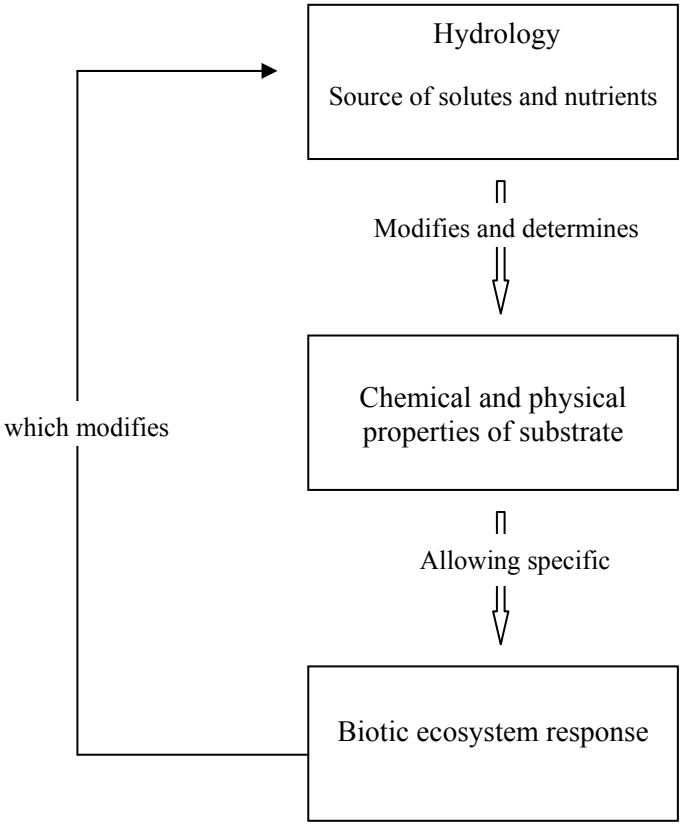

Figure 2.1 A conceptual model of the interrelation between wetland processes
Source: Gosselink & Turner (1978)

2.3 Wetland Soils

Although fluvial processes are the major mechanisms responsible for chemical transportation into wetlands, sediment is the ultimate chemical sink. Chemicals are introduced into wetlands primarily as solutes in the water or through adsorption on sediment particles. Once deposited, sediments are subjected to a series of biogeochemical transformations that occur during early diagenesis.

Wetlands are characterised by soils that are saturated for a substantial part of the year (Mitsch & Gosselink, 2007). Under conditions of prolonged saturation, most wetland soils become anoxic due to high microbial activity and the low rate of oxygen diffusion into the soil. A wide variety of redox transformations commonly occur at the boundary between oxic and anoxic conditions. Elements may be transformed from relatively immobile particulate forms to soluble components (Davison, 1993; Warren & Haack, 2001). Changes in redox status may also lead to variations in the composition of sediment porewaters and to the generation of new or altered mineral phases, such as hydroxide, carbonate, phosphate and sulphide compounds.

Under anoxic conditions, various chemical transformations take place in a predictable sequence and in predictable redox ranges (Table 2.1). Once oxygen and nitrogen are depleted, sediment microbes turn to Fe^{3+}, Mn^{4+} and SO_4^{2-} as terminal electron acceptors, resulting in the reduction of these species. It is such changes in the redox status of wetland soils that govern, in part, chemical transformations within wetland systems. Both the biological and chemical functions of wetlands are controlled to a large degree by oxidation-reduction reactions and the effects of these reactions on major nutrient cycles in wetlands have been well studied and documented (Mitsch & Gosselink, 2007; Vepraskas & Faulkner, 2001).

Table 2.1 Oxidised and reduced forms of elements and approximate redox potentials for transformations in wetland sediments

Element	Oxidised form	Reduced form	Approximate redox potential for transformation (mV)
Nitrogen	NO_3^-	N_2O, N_2, NH_4^+	250
Manganese	Mn^{4+}	Mn^{2+}	200 to 225
Iron	Fe^{3+}	Fe^{2+}	120
Sulphur	SO_4^{2-}	S^{2-}	-75 to -150
Carbon	CO_2	CH_4	-250 to -350

Source: Bohn (1971) and Mitsch & Gosselink (2007)

The behaviour of Fe and Mn in wetland soils has received a great deal of attention because of the central role that these metals play in the geochemical cycling of other elements (Gambrell, 1994). These metals undergo valence changes as a function of changing soil redox conditions, which greatly affect their solubility and plant availability. In aerated soil, iron exists as Fe^{3+} and manganese as Mn^{4+}, both of which are found as very sparingly soluble compounds. Manganese exists primarily as the black mineral MnO_2, while ferric iron typically occurs as an oxide (Fe_2O_3) or as the oxyhydroxide FeOOH. Under conditions of saturation, the oxidised forms of Fe and Mn are reduced to Fe^{2+} and Mn^{2+}, making them more soluble.

The formation of iron and manganese oxyhydroxides also plays an important role in scavenging other metals from solution. Thus, variation in redox conditions not only controls the solubility of Fe and Mn oxyhydroxides, but also indirectly the concentration and distribution of elements that may be adsorbed onto these redox sensitive mineral phases (Viers *et al*., 2005).

Periodic flooding of soils may cause frequent alternation between reduced and oxidised conditions, resulting in the periodic dissolution and precipitation of minerals. Field redox measurements can thus be useful in quantifying the tendency of soils to oxidise or reduce substances (Table 2.2). Redox assessments have been shown to be of particular importance in understanding long-term hydrology and the dynamic processes driving seasonal wetlands (Karathanasis *et al.,* 2003).

Table 2.2 Classification of sediment based on redox potential

Redox status of sediment	Approximate redox potential (mV)
Oxidised	>400
Moderately reduced	100 to 400
Reduced	-100 to 100
Highly reduced	-100 to -300

Source: Bohn (1971)

2.4 The sediment-water interface

The biogeochemical behaviour of metals in wetlands is complex, with the capacity of wetlands to transform chemicals being controlled primarily by the processes operating at the sediment-water interface (Donahoe & Liu, 1998). The rapid exchange of dissolved species, and chemical reactions occurring at the sediment-porewater interface affects the composition of the surface and groundwater (Martin *et al*., 1987). However, despite these important processes having been recognised, relatively little research has been published on how wetland sediments function in their control of chemicals at the sediment-water interface (Donahoe & Liu, 1998).

Porewater originates from the trapping of water during sedimentation, and is modified by the movement of water and the chemical reactions in the porewater-sediment environment. During the process of sediment deposition, chemical species that are found in the water column or adsorbed to sediment become isolated from surface water. Under these conditions chemicals in the water are subjected to a variety of diagenetic processes, which may result in the chemical composition of the porewater differing considerably from that of the inflowing water (Bufflap & Allen, 1995). Chemical reactions between porewater and solids may include the precipitation or dissolution of mineral phases, as well as the adsorption or remobilisation of chemicals from binding phases such as organic matter, metal oxides or clay particles. Investigation of such changes through porewater studies have been used to identify chemical processes occurring within sedimentary environments (Shaw *et al.*, 1990; Man *et al*., 2004).

2.5 Biogeochemistry and the role of plants in the movement of chemicals

Biogeochemical cycling refers to the movement of elements between various components in the natural environment as a consequence of their involvement in biological, geological and chemical processes. In this regard, they have biogeochemical cycles that are not shared by many other ecosystems (Mitsch & Gosselink, 2007). The transport and transformation of chemicals in wetlands involves a variety of interrelated physical, chemical and biological processes, which not only result in the spatial movement of resources but also in changes in the chemical forms of material. As a result, biogeochemical processes are recognised as being the ultimate control on overall wetland productivity (Mitsch & Gosselink, 2007).

Individual wetlands function, in part, through interaction with the adjacent landscape, and are typically viewed as sources, sinks or transformers of solutes within the environment (Mitsch & Gosselink, 2007). Considerable research has been directed at nutrient cycling in wetlands and determining the role of these ecosystems as sources, sinks or transformers of nutrients (Johnston, 1991; Morse *et al*., 2004; Verhoeven *et al.,* 2006). A wetland is a sink if it shows a net retention for a particular solute, while a net loss indicates it as being a source. Many wetlands act as sinks for particular inorganic nutrients while many are sources of organic material to nearby ecosystems. Wetlands act as transformers when they result in changes in oxidation state or from dissolved to particulate form. A given wetland may perform different functions for different substances.

The nature of chemical transformations and interactions in wetlands are complex and rely on cycling through the water system, sediments and biota. These interactions are affected by many factors including pH, redox potential, plant uptake and evapotranspiration. A general model of chemical cycling for a wetland is shown in Figure 2.2, which illustrates the main pathways and storages that are important in the movement of materials through wetland systems. Of particular importance are wetland plants, which play a major role in chemical transformations. Plants interact with the chemical and physical environment, and are able to modify resource flows within wetlands, affecting both the concentration and spatial distribution of available nutrients in a variety of ways.

Plants require essential macronutrients such as nitrogen and phosphorus, as well as a range of other micronutrients including iron and manganese. Plants selectively absorb these elements from the porewater, incorporating them into their tissues. Since wetlands contain abundant plant biomass and display high biological productivity, this can lead to high rates of element uptake (Kotze & Breen, 1994). Once in the plant tissue, these elements may then be incorporated into the soil as part of the organic matter pool.

Numerous studies have suggested that wetlands act as important sinks for certain chemicals, with attention having been focused primarily on the macronutrients of nitrogen and phosphorus (Grimm *et al.*, 2003; Fisher & Acreman, 2004). These elements are referred to as nutrient solutes as they are typically present in concentrations that are limiting to primary productivity in wetlands (Johnston *et al.*, 2001). Such nutrients usually lead to an increase in plant growth when their concentrations are increased. Wetland plants typically “scrub” inflowing water of nutrients, leading to a decrease in their concentration (Table 2.3). Less commonly considered solutes are those whose concentration

does not limit primary production rates, such as sodium, potassium and silicon. These solutes are used sparingly by plants and are typically present in greater concentrations than required by plants, resulting in their accumulation in groundwater.

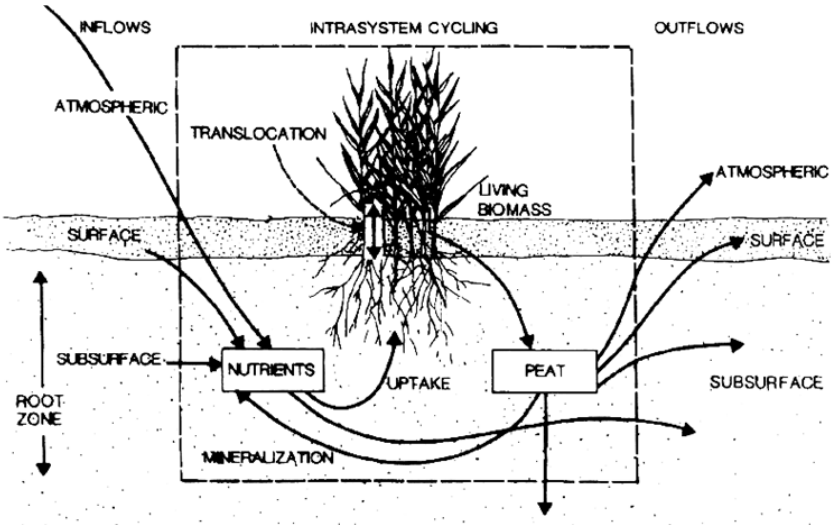

Figure 2.2 Generalised model of chemical cycling in wetlands
Source: Mitsch & Gosselink (2007)

Table 2.3 Typical solute concentrations of water entering and leaving the Okavango Delta (µg/ml)

Solute	Inflow	Outflow	Outflow / inflow
Total N	3.07	1.02	0.33
Total P	0.042	0.038	0.90
Ca	5.0	9.0	1.8
Mg	0.6	2.0	3.3
Na	2.0	6.5	3.3
SiO_2	15	35	2.2

Data sources: Cronberg *et al.* (1995); Ashton *et al*. (2002)

The role of plants in chemical transformation is emphasized by considering two of the world's largest wetland systems. In the Everglades, Florida in the USA, the relationship between ecosystem structure and nutrient dynamics on tree islands has received a great deal of attention recently (Troxler Gann *et al*., 2005; Wetzel *et al.*, 2005). In this environment, subsurface water flows

generated by evapotranspiration of trees create tree island hotspots of nutrient accumulation. This is due to higher evaporation rates on tree islands than in surrounding areas causing groundwater and dissolved nutrients to flow towards tree islands. The accumulation of limiting nutrients, particularly phosphorus, has been implicated in the maintenance and expansion of tree islands, in both elevation and size (Wetzel *et al*., 2005). Such islands not only represent an important internal sink for phosphorus in the region but it is suggested that the resulting change in elevation provides environmental conditions that support a wide variety of trees and other plants that would otherwise not exist within the unvarying landscape of the Everglades.

Similar processes have been identified within the Okavango Delta, northern Botswana. Situated in a semi-arid climatic region, approximately 96% of the annual discharge into this system is lost to the atmosphere (McCarthy & Metcalfe, 1990). Much of this is believed to occur through evapotranspiration, especially by deep-rooted trees, which *exclude* many solutes from the water they take up. This leads to the concentration and precipitation of dissolved compounds from the groundwater, resulting in mineral phases such as calcite and amorphous silica. It is believed that chemical precipitation is a major depositional process occurring in the Okavango basin and is responsible for the formation and growth of tree islands (McCarthy *et al*., 1993). Evapotranspirational water loss and associated chemical sedimentation create topographic relief and lead to the production of highly saline groundwater in the centre of islands, which plays a crucial role in influencing vegetation distribution (Ellery *et al*., 2000).

2.6 Wetland dynamics: Sedimentation and erosion as driving forces

Overall dynamics within wetland systems are the product of variation in hydrological inflows and outflows, and of erosional and depositional processes (Ellery *et al*., 2007). Most wetlands are regarded as sediment sinks within the landscape, as material lost within a river catchment generally accumulates in downstream wetlands. Deposition of sediment affects local and regional gradient in that slope is reduced upstream from the point of deposition and increased downstream of it. Erosion has the opposite effect and may potentially threaten the existence of a wetland when increases in the wetland gradient occurs due to a change in natural sediment transport. This may be caused by greatly increased sedimentation at the head of the wetland or by sediment starvation in the lower reaches of the system (DeLaune *et al*., 2003). Aggradation in wetlands is considered to be brought about by three types of sedimentation, namely clastic, organic, and chemical sedimentation.

2.6.1 Clastic sedimentation

Clastic sedimentation is the most common form of sedimentation that has been studied in streams and wetlands (Harter & Mitsch, 2003; Sanchez-Carrillo *et al.*, 2001; Furness, 1983). Clastic sedimentation takes place in areas where there is a reduction in the ability of a stream to carry its sediment load. Accumulation of clastic sediment in most systems takes place preferentially at the head of a wetland, predominantly in close proximity to the river channel. Deposits generally decrease in mean grain size as distance from the channel increases, with sand deposited near to the channel and fine sediment at greater distances. High rates of clastic sedimentation in localised regions of large wetlands can occasionally lead to the diversion of water from one area to another through channel avulsion. This process influences the dynamics of many floodplain wetlands (Stouthamer & Berendsen, 2007; Makaske *et al.,* 2002). Fine sediment also plays an important role in the transportation of chemicals through river systems, with overbank sediment deposits acting as valuable sinks for adsorbed chemicals.

2.6.2 Organic sedimentation

Where primary production exceeds consumption or decomposition, wetland systems are producers of organic matter. The fate of this excess production is strongly influenced by the hydrologic regime; either accumulating in the wetland or being exported out of it (Gosselink & Turner, 1978). In areas of slow moving or standing water, anaerobic conditions can slow down the decomposition of organic matter, resulting in the accumulation of peat. Such sedimentation has been shown to take place in low energy environments, such as the backswamp regions of wetland systems, where it leads to the infilling of basins deprived of clastic sediment (McCarthy & Ellery, 1998). Many of the coastal marshes along the east coast of the United States rely primarily on organic matter accumulation for accretion (DeLaune *et al*., 2003). Peatlands also represent a long-term sink of atmospheric CO_2 and a source of atmospheric methane, and thus play an important role in the global carbon cycle (Price & Waddington, 2000).

2.6.3 Chemical sedimentation

Chemical sedimentation generally occurs under evaporative conditions, which causes dissolved solutes in the groundwater to concentrate and precipitate in the soil. Reference has already been made to this process that has been documented in the Okavango Delta by many researchers. However, very little attention has been given to chemical sedimentation and it consequences in other wetland systems. In general, wetland research has focused almost entirely on clastic and

organic sedimentation, with chemical sedimentation being a potentially important process that is generally overlooked. It is suggested that this may be a particularly important type of sedimentation in southern African wetlands where potential evaporation generally exceeds rainfall. Under these conditions evapotranspiration is the dominant means of water loss from these systems, providing ideal conditions for chemical sedimentation.

2.6.4 Sedimentation and wetland longitudinal gradient

The three types of sedimentation described are speculated to play an important role in maintaining wetland longitudinal gradients (McCarthy *et al.,* 1997), with each being thought to take place in different regions of a wetland system. In sufficiently large wetlands, clastic sediment is typically deposited in the upper reaches, while organic sedimentation dominates middle reaches where there is an abundant water supply and limited clastic sediment input. Chemical sedimentation tends to predominate in the lower reaches of wetland systems, where solute concentrations are higher and hydrological residence times are longer. McCarthy *et al*. (1997) suggest that that the gradient on the Okavango fan represents a balance between clastic sedimentation in the upper fan and chemical sedimentation in the distal seasonal swamps. McCarthy *et al.* (1997) note the sensitivity of such systems to subtle changes in gradient.

2.7 Chemical precipitation under evaporative conditions

In a wetland, water can be lost to the atmosphere through direct evaporation from saturated soils and open water bodies, or by transpiration of soil porewater. Transpiration results from the root uptake of water by emergent plants and its subsequent loss through the leaf surface. Estimates of transpiration rates are related to vegetation density, soil moisture content, and depth of the rooting zone in relation to groundwater elevation. Although estimates in wetlands have been reported (Abtew, 1995; Martin *et al.*, 2003; Koch & Rawlick, 1993), transpiration rates remain a very difficult component to measure and quantify. For this reason, evaporation and transpiration are usually combined in wetland water balance studies into a single estimate of water loss (evapotranspiration).

The net effect of evapotranspiration is to remove water from solution, thereby increasing the concentration of dissolved chemicals. Although this process takes place in all climates, it is only under relatively arid conditions that the accumulation of dissolved chemicals through

evapotranspiration is a major control on water composition. Concentration of shallow groundwater driven by evapotranspiration has been documented in a variety of environments, from semi-arid systems in Western Australia (Salama *et al.,* 1993) to the tropical semi-humid climates of Brazil (Barbiéro *et al.,* 2002) and Argentina (Logan *et al*., 1999; Logan & Rudolph, 1997) as well as the temperate regions of the United Kingdom (Batty *et al*., 2006) and Denmark (Jørgensen, 2002). In southern Africa, wetlands are generally subjected to conditions where potential evaporation exceeds rainfall in most months of the year. As such, transpiration is likely to be the dominant means of water loss, and chemical sedimentation in wetland soils is likely to be an important process.

2.7.1 Evolution of closed-basin brines: The Hardie-Eugster model

The aqueous geochemistry of hydrologically restricted basins has been the subject of considerable study. The chemical evolution of such systems was first documented by Garrels & Mackenzie (1967), and subsequently expanded on by Hardie & Eugster (1970) and Eugster & Jones (1979). Much of this attention has been directed towards the closed-basin and playa-type lakes of central and east Africa. In such settings, solutes are found to precipitate as various mineral phases under evaporative concentration (Eugster & Jones, 1979).

The precipitation of a mineral from aqueous solution during evaporative water loss occurs when the concentration of that mineral exceeds its solubility. Such precipitation reactions control the composition of porewaters and produce minerals that are indicative of the waters from which they precipitated. In addition, the precipitation of a mineral phase significantly affects the composition of the residual solution, and may then prevent the crystallisation of other salts.

Hardie & Eugster (1970) developed a general model that covers a wide range of evaporative environments, and which treats the chemistry of water undergoing evaporation as a series of chemical divides (Figure 2.4). Whenever a binary salt is precipitated during evaporation, and the ratio of the two ions in the salt is different from the ratio of the concentrations of these ions in solution, further evaporation will cause the ion present in higher relative concentration to build up in solution, while the ion present in lower relative concentration will precipitate, reducing its concentration in solution. Thus, while some solutes are removed preferentially from solution, others increase in relative abundance. In almost all natural waters, the first mineral to precipitate, thus causing the first chemical divide, is $CaCO_3$ (calcite). Once calcite begins to precipitate, the

composition of the remaining solution changes as solutes are removed, and the path taken by the solution depends on the equivalent concentrations of calcium and alkalinity. The solution then evolves along a new chemical pathway until the next mineral reaches saturation. Subsequent precipitation of sulphates and silicates is controlled by the relative concentrations of Ca, Mg, Si, HCO_3, SO_4 and Cl. Final solutions are characterised by high pH and are usually dominated by two or three species, with sodium generally the dominant cation.

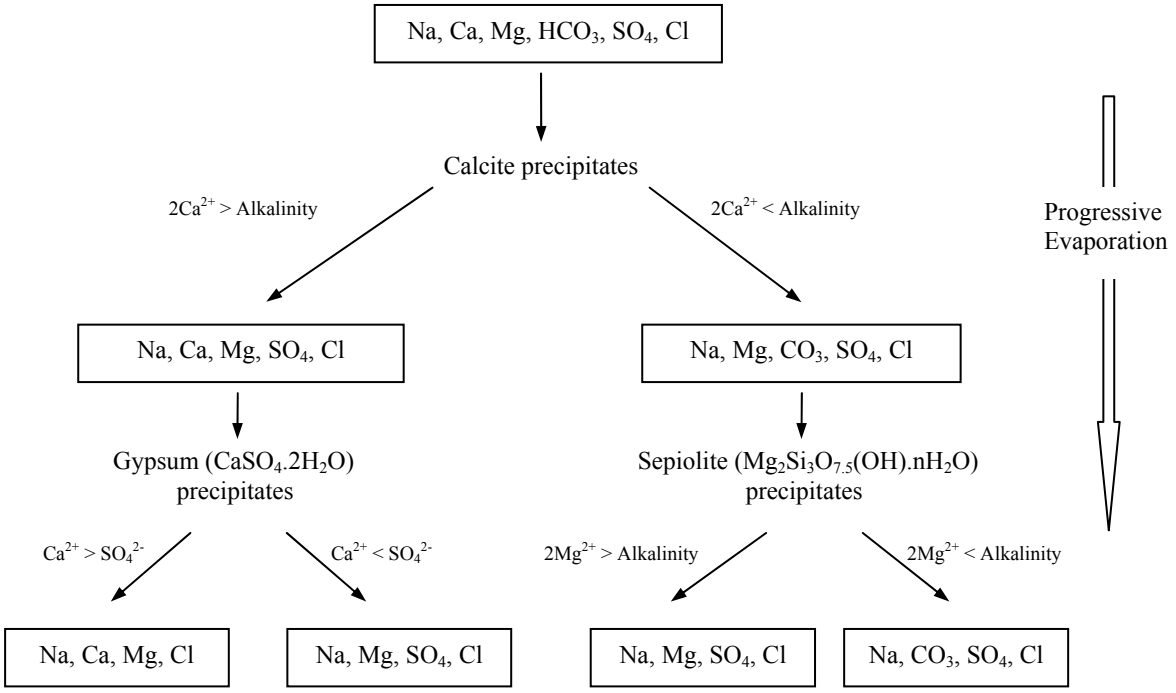

*Concentrations in equivalents

Figure 2.4 The chemical divides concept applied to the evaporation of natural waters
Source: Drever (1997)

Although the Hardie-Eugster model has been applied in a variety of environments, there are a number of important processes that were not included in the original model. Subsequent work by Gac *et al.* (1977), Yuretich & Cerling (1979) and Von Damm & Edmond (1984) has demonstrated the active presence of a silicate sink for magnesium. Most detailed investigations have been carried out on the lakes of central and east Africa (Lake Chad, Lake Turkana), where major soluble ions are being removed on a large scale. In these environments, the formation of aluminosilicate minerals is a major process and is the primary control on magnesium concentration.

In addition, ion exchange and sorption processes are also recognised as being important to the chemistry of waters, particularly for potassium (Eugster & Jones, 1979). Potassium does not form any salts, except at very high concentration, and thus calculations by Garrels & Mackenzie (1967) and Hardie & Eugster (1970) predict that potassium should, like sodium, simply build up in solution during evaporation. In reality however, potassium is almost always found depleted relative to sodium. Biological uptake from solution and adsorption appear to be important in regulating potassium concentrations in saline waters.

2.7.2 Carbonate precipitation

One of the primary sinks for solutes in the Hardie-Eugster model is the precipitation of carbonates. Primary carbonate precipitation may be represented by the following reaction:

$$Ca^{2+} + 2HCO_3^- \leftrightarrow CaCO_3 + CO_2 + H_2O$$

The above reaction illustrates the controls that govern $CaCO_3$ precipitation. Increases in soil CO_2 partial pressure or decrease in pH will drive the reaction to the left, causing calcite to dissolve and release Ca^{2+} and HCO_3^- to solution. The production of CO_2 by plant roots has been shown to be a particularly important factor limiting $CaCO_3$ precipitation (Deocampo & Ashley, 1999). Conversely, $CaCO_3$ precipitation is favoured by a decrease in CO_2 partial pressure, rise in pH, or increase in solute concentration.

Carbonate precipitation is governed by the equilibrium constant, K, which is defined as:

$$K = \frac{a_{Ca^{2+}} a_{CO_3^{2-}}}{a_{CaCO_3}}$$

where $a_{Ca^{2+}}$ and $a_{CO_3^{2-}}$ are the respective activities (concentrations) of Ca^{2+} and CO_3^{2-} in solution, and a_{CaCO_3} is the activity of $CaCO_3$. Given that the ion activity product (IAP) is defined as $a_{Ca^{2+}} + a_{CO_3^{2-}}$, the degree of saturation in water with respect to $CaCO_3$ can then be obtained by calculating the saturation index (SI):

$$\mathrm{SI} = \frac{\mathrm{IAP}}{\mathrm{K}}$$

Saturation index calculations can be useful in examining water composition for the stability of a mineral of interest. Positive SI values indicate solution supersaturation and mineral precipitation, while negative values are indicative of conditions favouring mineral dissolution.

2.7.3 Clay mineral neoformation

The geochemical importance of clay minerals stems from their ubiquity and their ability to strongly influence the properties of soils. Clays form an important group of phyllosilicate minerals, which are composed of sheets having the chemical composition $(Al,Si)_3O_4$. Clay minerals can be categorised depending on differences in chemical composition and the way that these sheets are packed into layers (Hillier, 2003). Clays are typically categorised into four main groups (Table 2.4), although they are rarely found separately. Natural clay samples usually contain a variety of clay minerals along with small amounts of feldspars, carbonates, and quartz.

Table 2.4 Classification of clay mineral groups

Mineral Group		**Generalised formula**
Kaolinite		$Al_2Si_2O_5(OH)_4$
Smectite	Montmorillonite Beidellite Nontronite Hectorite Saponite Sauconite	$(Ca, Na, H)(Al, Mg, Fe, Zn)_2(Si, Al)_4O_{10}(OH)_2 - xH_2O$
Illite		$(K, H)Al_2(Si, Al)_4O_{10}(OH)_2 - xH_2O$
Chlorite		Highly variable

Clay minerals present in the environment may be derived from two main sources: a) detrital inheritance or b) neoformation. Detrital clays are inherited as a result of weathering, and are typically introduced into sedimentary environments by fluvial transportation. Neoformed clays are produced *in situ*, by direct precipitation or crystallisation from solution (Hillier, 1995; Meunier, 2005). Although clay minerals that are detritally derived from catchments are by far the major component of clastic material transported by rivers (Chamley, 1989), neoformed clays are not uncommon in nature. While not abundant, neoformed clay minerals have been studied in a variety of settings because they provide much information about geochemical processes occurring in the

environment (e.g. Yuretich & Cerling, 1983; Hover *et al.,* 1999 Liutkus & Ashley, 2003; Meunier, 2005). In continental settings, neogenesis is dominated by smectite formation, and this group constitutes the most widely studied neoformed minerals. Their formation typically occurs under semi-arid or evaporative conditions where silica and basic cations become concentrated in the soil subsurface. Under these conditions, smectite precipitates directly from soil solutions. Neogenesis tends to occur at the boundary of alternating wet and dry environments, caused by strong evaporation and periodic groundwater rise (Chamley, 1989).

Neoformation has been documented in a number of central and eastern African lakes. Lake Chad is a particularly well-studied geochemical environment that displays widespread *in situ* formation of minerals. Subjected to an arid climate and characterised by high pH and silica concentrations, the evaporation of river water leads to the precipitation of Mg-smectite minerals, along with calcite and amorphous silica (Gac *et al.,* 1977). It is estimated that large quantities of solutes are lost from solution through chemical clay sedimentation (Chamley, 1989). Darragi & Tardy (1987) and Yuretich & Cerling (1983) have studied alkaline lakes in similar settings and have identified *in situ* formation of smectite and $CaCO_3$. The precipitation of minerals controls the evolution of pH, alkalinity and Ca, Mg and Si concentrations in these environments.

2.8 Conclusion

Tooth & McCarthy (2007) identify the process of chemical sedimentation as being one of the key differences between wetlands in southern Africa and wetlands from more humid or temperate regions. This is due to high potential evapotranspiration and frequent periods of desiccation that characterise many of the region's wetland systems. This belief is based on a limited number of case studies that have been conducted in the region. Very little research in southern Africa has explicitly examined chemical sedimentation in wetland systems, with previous studies focusing primarily on a single study area, the Okavango Delta. These studies have shown that chemical sedimentation is an important geomorphological and ecological process, which warrants further investigation. In order to gain a more detailed understanding of this process, other wetland environments in the region need to be studied. The following detailed study of the lower Mkuze Floodplain represents an initial attempt at developing a more generalised model of chemical sedimentation in wetlands.

Chapter 3

Study area

The Mkuze Wetland System is located east of the Lebombo Mountains on the Maputaland Coastal Plain in northern KwaZulu-Natal, South Africa (Figure 3.1). The system covers an area of approximately 450 km^2 and encompasses a variety of different wetland types, ranging from seasonally flooded and riparian floodplains to permanent wetlands and shallow lakes (Stormanns, 1987).

The formation and functioning of a wetland is largely dictated by the evolution of its surrounding landscape in combination with local climatic conditions (Richardson & Vepraskas, 2001). Important driving forces controlling wetland genesis on the KwaZulu-Natal coastal plain include climate, geology, hydrology, topography, vegetation, as well as the impact of humans (McCarthy & Hancox, 2000). It is the interplay of these forces that shape the physical and ecological processes operating on the Mkuze Floodplain.

3.1 Geology, geomorphology and drainage

The formation of the present lower Mkuze River Floodplain is the result of a series of marine regressions and transgressions (McCarthy & Hancox, 2000). During the last ice age (approximately 18 000 to 8000 BP), sea-level was lowered ~120 m relative to present sea-level, exposing much of the continental shelf and causing rivers on the coastal plain to incise deep valleys (Ramsay &

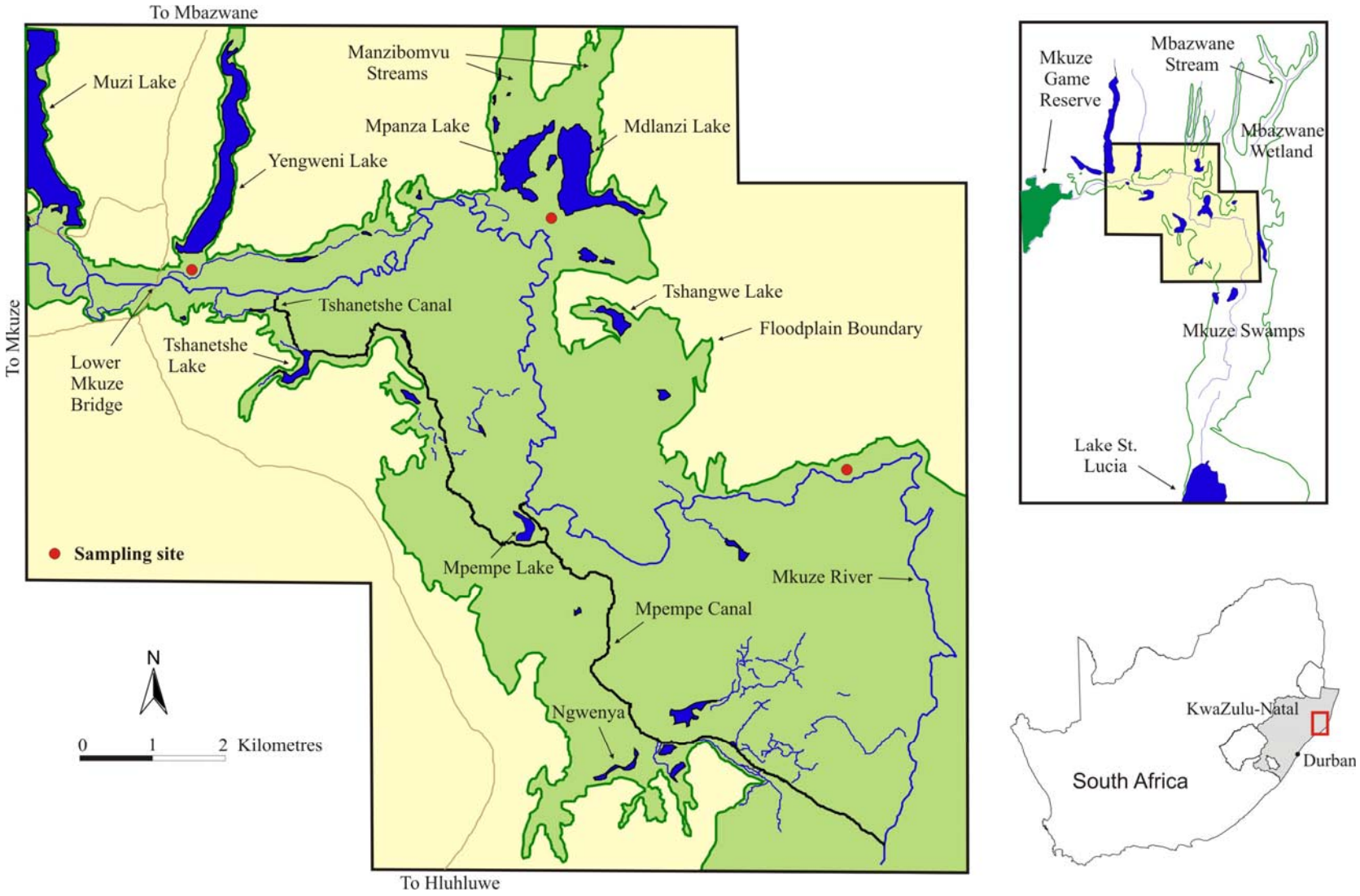

Figure 3.1 Location of study area (insets) and the main physiographic features of the Mkuze Floodplain (main figure)

Cooper, 2002). Subsequent sea-level rise, initiated ~6500 years ago, drowned these valleys. Unconsolidated shelf deposits were eroded and deposited to form some of the highest coastal dunes in the world. These dunes impeded the flow of major eastward-flowing rivers, flooding coastal valleys, resulting in the formation of an extensive and diverse wetland types, including Lake St Lucia and Kosi Bay, which are the largest estuarine wetland systems in Africa. Today, the coastal plain is predominantly covered by recent deposits of unconsolidated dune sand of Tertiary and Quaternary age (Figure 3.2). North-South trending dune cordons, representing former shorelines, dominate the coastal plain topography. These dune cordons control drainage patterns and play an important role in the development of wetlands.

The Mkuze River drains sedimentary strata of the Dwyka, Ecca and lower Beaufort Groups of the Karoo Sequence, as well as Pongola granites and rhyolites in the Lebombo mountains (McCarthy & Hancox, 2000; Figure 3.3). The river is 290 km in length and is characterised by moderate clastic sediment loads and comparatively high conductivities, ranging between 0.843 and 1.160 mS/cm (Stormanns, 1987). Overbank flooding of the Mkuze River constitutes the primary input of sediment onto the floodplain, with most of this comprising suspended silt and clay. The gradient of the river decreases significantly as it enters the coastal plain east of the mountains, resulting in the deposition of sediment (Alexander, 1986). Most deposition of sediment takes place in close proximity to the river channel and has resulted in the development of levees adjacent to the channel. Over time, elevation differences between the channel and floodplain create instability which occasionally results in the sudden shifting of the river to a new position on the floodplain in a process known as channel avulsion. Avulsion has been responsible for the formation of a number of the minor lakes associated with the floodplain (Watkeys *et al*., 1993). River levees, which are higher than the surrounding floodplain, also make it difficult for water to return to the stream once it enters the floodplain (Alexander, 1986), allowing areas of shallow water to collect on the floodplain for extended periods following floods. McCarthy & Hancox (2000) believe that sedimentary infilling of the Mkuze Wetland System has been occurring for the last 6500 years. Sedimentation and valley infilling continues, resulting in the aggradation and the west to east progradation of the Mkuze River floodplain (McCarthy & Hancox, 2000).

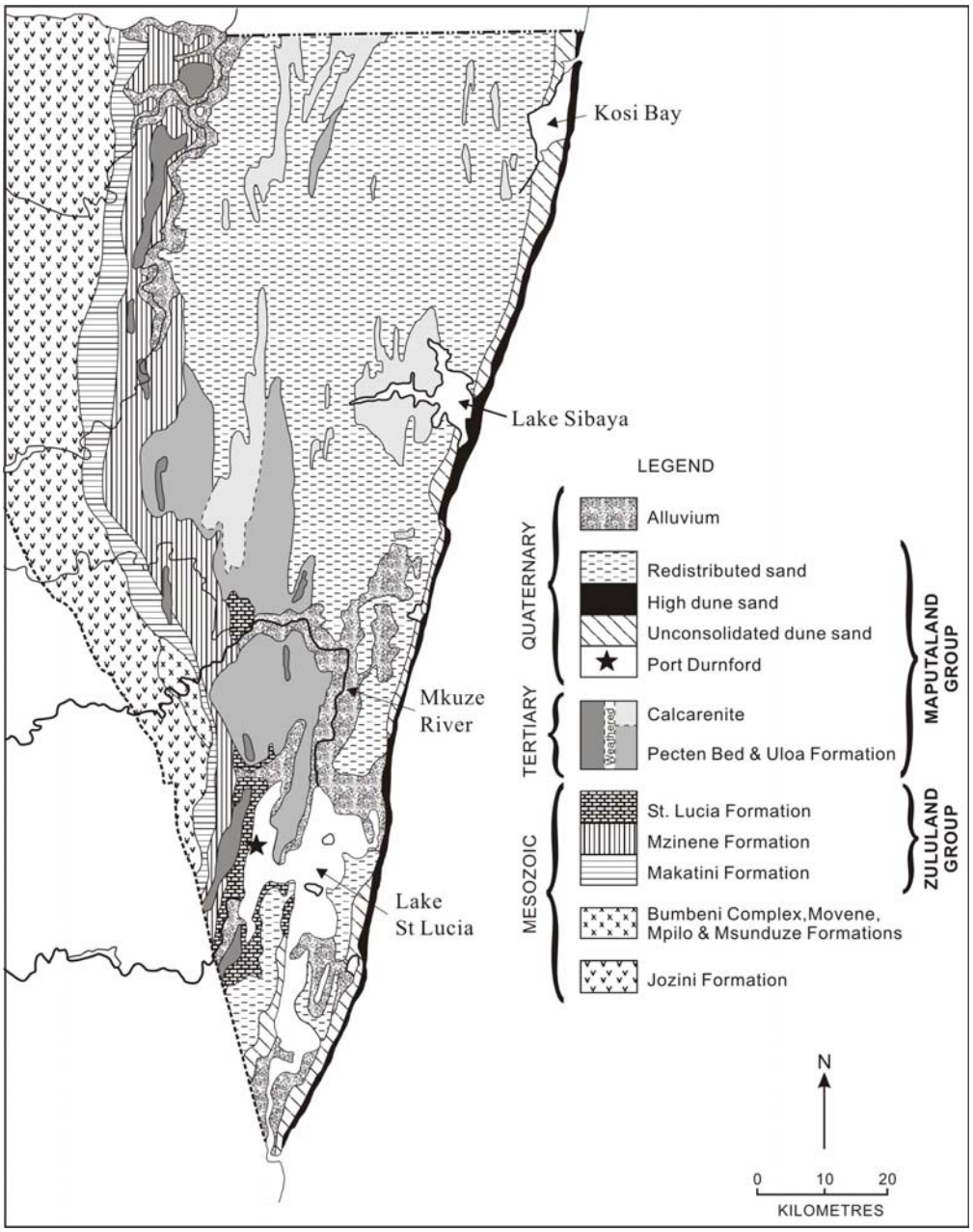

Figure 3.2 Geological sequences of the Maputaland Coastal Plain (Watkeys *et al.*, 1993)

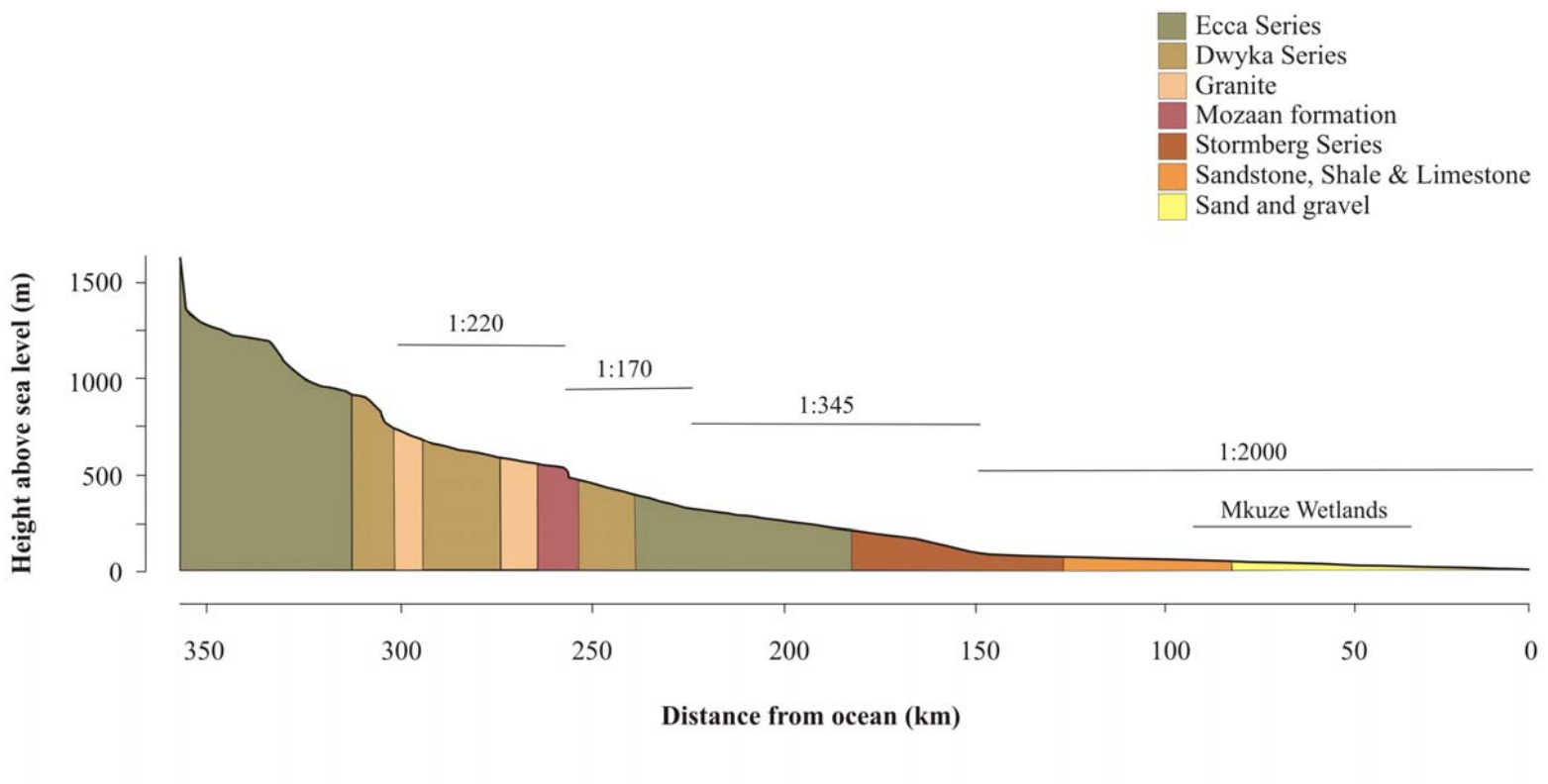

Figure 3.3 Mkuze River profile showing major geological groups and approximate location of the Mkuze Wetlands

Modified from Chew & Bowen (1971)

3.2 Climate

Northern KwaZulu-Natal experiences hot, wet summers and mild, dry winters. Mean monthly maximum temperatures vary between approximately 30 ^{o}C in summer to 25.5 ^{o}C in winter. Evaporation rates are high, and vary between ~190 mm per month in summer and ~80 mm per month in winter (Watkeys *et al*., 1993). Rainfall across the coastal plain is variable, decreasing from approximately 1000 mm/yr at the coast, to 600 mm/yr in the Mkuze Game Reserve west of the study area. The majority of rainfall occurs in summer (Figure 3.4) and is usually attributed to cold fronts moving northwards along the coast. Inter-annual variability of rainfall is high with rainfall varying between less than 300 mm per annum to over 1000 mm per annum. Flooding is seasonal and is usually associated with cutoff low pressure systems that typically occur several times a year, or occasional tropical cyclones (Watkeys *et al*., 1993). The most severe cyclone in recent history to have affected the Maputaland Coastal plain within South Africa was Cyclone Demoina that resulted in severe and widespread flooding in 1984.

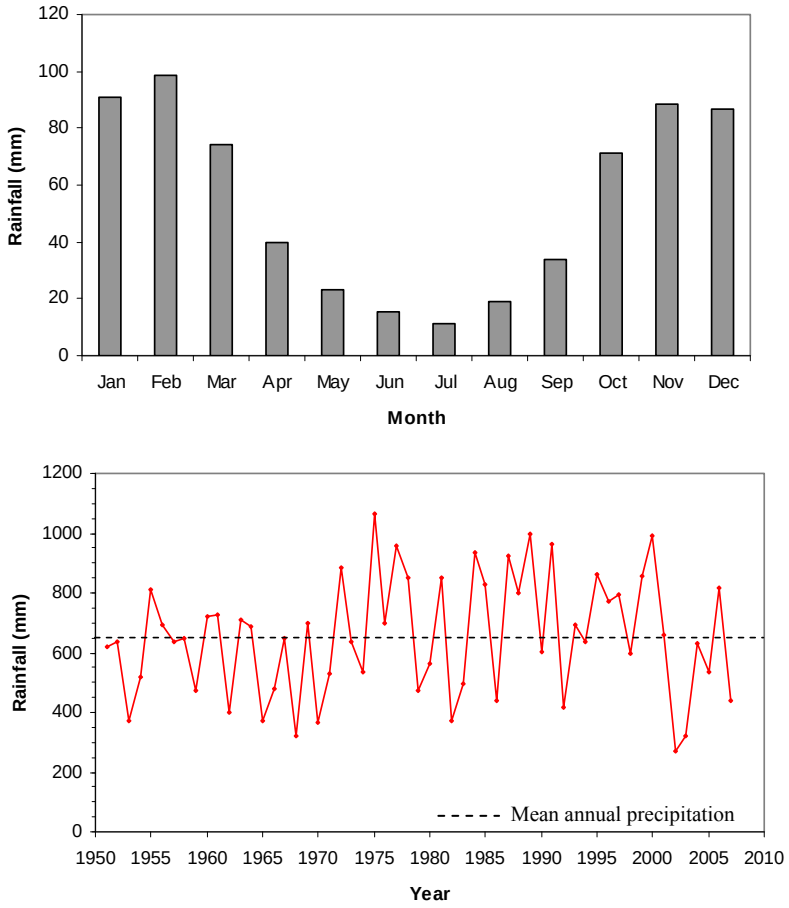

Figure 3.4 Monthly mean annual rainfall and variation in yearly rainfall recorded at Mkuze Game Reserve between 1950 and 2007.

3.3 Hydrology of the Mkuze Floodplain

The principal hydrological input into the wetland system is surface inflow via the Mkuze River, with rainfall and groundwater inflows playing minor roles (McCarthy & Hancox, 2000). Mean annual river flow is highly variable and ranges between 211 and 326 x 10^6 m^3 (Stormanns, 1987). This variation is due to the seasonal nature of rainfall within the Mkuze River catchment which produces two distinctly different hydrological seasons (Figure 3.5). During the summer rainfall season, the Mkuze River regularly overtops its banks and inundates the surrounding floodplain. The arrival of a flood takes place over a period of hours to days, with the flood wave typically persisting for a few days (Barnes, 2008). During the winter months of most years, there is little to no flow in the Mkuze River channel (McCarthy & Hancox, 2000).

Flow from the Mkuze River recharges floodplain lakes. These lakes also receive water from the predominately groundwater-fed Manzibomvu Streams located in interdune valleys north of the Mkuze River (Figure 3.1). Here the watertable is elevated relative to the floodplain, causing localised groundwater discharge into interdune depressions, recharging lakes and groundwater-fed swamps (McCarthy & Hancox, 2000). The southward-flowing Manzibomvu Streams drain onto the margin of the Mkuze Floodplain, which flows eastwards and then southwards into Lake St Lucia.

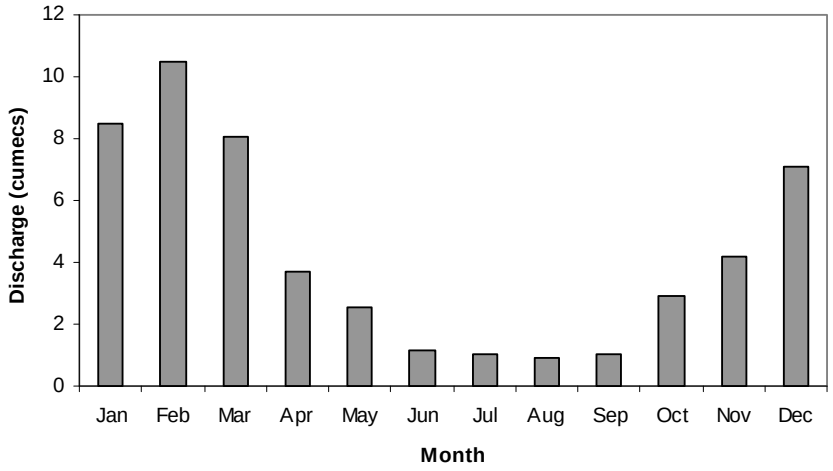

Figure 3.5 Monthly mean annual flows of the Mkuze River calculated between 1970 and 1987. Data supplied by the Department of Water Affairs and Forestry, South Africa.

Within the Mkuze Wetland, there are regions of groundwater recharge from surface water. These are particularly prevalent in the upper part of the system where aggradation of the floodplain has created relief that results in surface water recharging regional groundwater. During normal periods of low flow in the Mkuze River, there is gradual loss of water to subsurface water on the floodplain itself. This continual loss of water from the river to the surrounding floodplain is associated with a gradual decline in discharge downstream (McCarthy & Hancox, 2000). This results in a consistent decline in channel dimensions downstream on the floodplain (Ellery *et al.*, 2003).

The hydrological regime of the Mkuze Wetlands has been affected by the construction of two canal systems. In the late 1960s Lake St Lucia experienced hypersaline conditions as a result of severe drought. In an effort to increase the freshwater supply to the lake, authorities excavated the Mpempe Canal (Figure 3.1). Its purpose was to bypass the northern portion of the Mkuze River floodplain thereby shortening the route of water flow into Lake St Lucia. A second canal (the Tshanetshe Canal), was excavated by a local farmer for irrigation purposes. This canal has been subjected to rapid erosion such that approximately 80% of water is now diverted from the northern parts of the floodplain into the Tshanetshe Canal. Water only flows down the previous river course when discharges are greater than approximately 17.5 m^3/s (Ellery *et al.,* 2003). Efforts to restore flow down the original Mkuze River course have been unsuccessful.

3.4 Vegetation

The Maputaland Coastal Plain lies within a tropical-subtropical transition zone which results in a high vegetation biodiversity. Vegetation of the region is classified as Coastal Bushveld-Grassland (Low & Rebelo, 1996) and comprises a mixture of forest patches within a matrix of grassland and open savanna. The Mkuze River is fringed by fragmented patches of dense riverine forest characterised by trees such as *Ficus sycomorus, Rauvolfia caffr*a, *Voacanga thouarsii* and *Blighia unijugata* (Stormanns, 1987; Patrick & Ellery, 2006). The surrounding floodplain is characterised by open grasslands dominated by *Echinochloa pyramidalis*, while *Acacia xanthophloea* fringes the edges of floodplain lakes. The more permanently wet areas are dominated by various reeds and sedges such as *Phragmites australis* and *Cyperus papyrus* (Patrick & Ellery, 2006).

3.5 Land use and human activities

Land ownership and usage on the lower Mkuze Floodplain is controlled primarily by two main holders. Land to the north of the Mkuze River is controlled by Ezemvelo KwaZulu-Natal Wildlife, the provincial statutory conservation body, which is responsible for conserving and managing land that is not formally within protected areas. The floodplain to the west and south of the Mkuze River is communal tribal land. Subsistence agriculture is the main land use in this area, with crops such as sugar cane, maize, bananas and vegetables being cultivated on the floodplain. People from nearby communities derive the majority of their income through the selling of agricultural products and raw materials. Various wetland resources such as water, reeds, medicinal plants and firewood are also commonly harvested and utilized (Taylor, 1986). In recent years, farming has become more mechanised, which has led to the planting of cash crops and a dramatic increase in the area of the floodplain under cultivation (Figure 5.6).

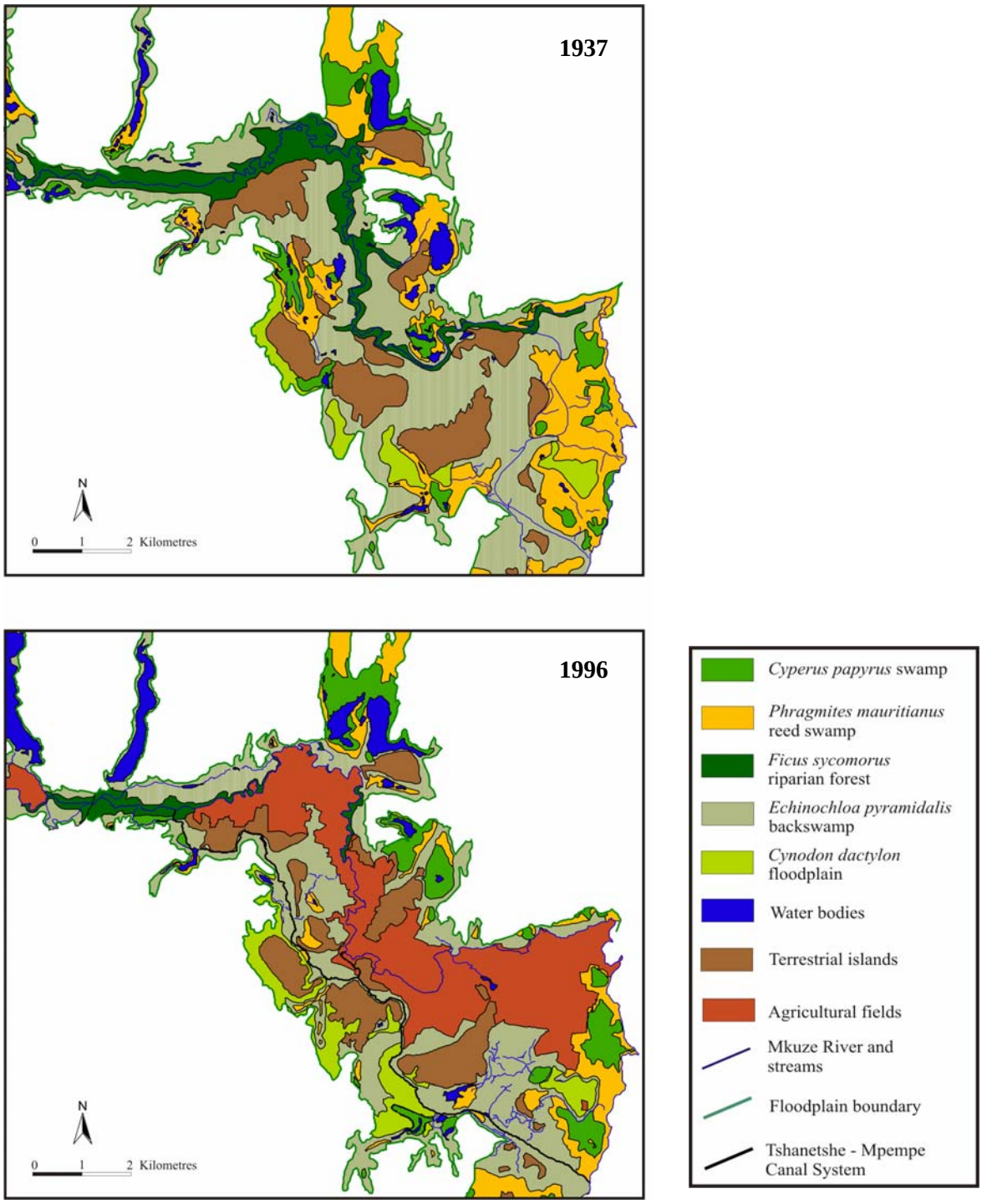

Figure 5.6 Change in vegetation cover of the Mkuze Wetland System from 1937 to 1996
Source: Neal (2001)

Chapter 4
Methodology

There are a number of analytical tools that can be used to determine the physical and chemical properties of aqueous and sediment samples. Detailed sediment characterisation and investigation of geochemical processes usually requires the application of several complementary analyses. This chapter provides a brief background to the major analytical techniques and procedures used in this study.

4.1 TECHNIQUES

4.1.1 Inductively Coupled Plasma-Optical Emission Spectroscopy (ICP-OES)

Inductively Coupled Plasma-Optical Emission Spectroscopy is now established as one of the most widely used techniques for elemental analysis. The technique is based on the fact that different atoms emit electromagnetic radiation at characteristic wavelengths. This allows individual elements to be determined without having to separate them chemically, resulting in the potential for rapid and simultaneous determination of a broad range of elements (Walsh, 1997). In addition to the major geochemical elements (Si, Al, Mg, Fe, Ca, Na, K, Mn), most trace elements are able to be determined using ICP-OES. This makes it a very cost effective technique and ideally suited to the analysis of a large number of samples.

In ICP-OES, an argon plasma source is employed to heat samples to temperatures in excess of 7000 ^{o}C causing them to decompose into atoms. These atoms undergo excitation, where electrons from the ground state are promoted to vacant higher-energy levels. In the excited state, the atom is unstable and almost immediately an electron will spontaneously drop back to fill the vacancy. In doing this, the atom emits radiation of characteristic wavelength for that element. For each transition, an emission spectral line is generated. However, electrons may move to more than one vacant energy level and may return to the ground state via several intermediate levels. As a result, a series of spectral lines for a particular element may be produced covering a range of different wavelengths. Every element will have its own set of emission lines, and a sample containing a variety of elements is likely to produce very complex emission spectra. Careful selection of an analysis line is thus important in eliminating or reducing spectral line interferences (Hill *et al*., 2004. The intensity of the radiation emitted is proportional to the concentration of the element producing the radiation and is used as a measure of the concentration of each element.

Inductively Coupled Plasma-Optical Emission Spectroscopy allows accurate and precise measurements with detection limits typically <1 ng/ml. The high operating temperature of the ICP eliminates most chemical interferences and the absence of self-absorption in the plasma gives calibration lines that are linear over a large concentration range (Skoog *et al*., 1996).

4.1.2 X-ray Diffraction (XRD)

X-ray diffraction is the main analytical technique used for the identification of mineral phases. It is particularly useful in the analysis of fine-grained material, which is difficult to study by other means (Schulze, 2002). The phenomenon of diffraction involves the scattering of X-rays by atoms of crystalline structures that are characterized by a regular and periodic arrangement of atoms. Each crystal contains planes of atoms that are separated by a constant distance and that are characteristic for that crystalline species. Since no two minerals have exactly the same interatomic distances, the angles at which diffraction occurs will be distinctive for a particular mineral. The interatomic distances within a mineral crystal then result in a unique array of diffraction maxima, which serves to identify a mineral. While the identification of minerals is the primary use of XRD, semi-quantitative estimates of mineral proportions can be made using peak height or area (Moore & Reynolds, 1997).

Well-crystallised minerals of sand and silt tend to give sharp diffraction lines, while clay-sized particles show broader lines caused by diffraction effects from the small particles. In some cases, the accurate determination of certain mineral phases cannot be made without the isolation and elimination of interferences caused by organic matter and other mineral phases (Amonette, 2002). In such cases samples need to be fractionated to decrease their complexity. This is particularly important in the case of very fine-grained and poorly crystalline clays, which are unlikely to give recognizable diffraction patterns in a bulk sample scan. In addition, a number of chemical treatments are usually required for the positive identification of specific clay minerals (Moore & Reynolds, 1997).

Clay minerals form a difficult group to study due to their small size and variable structural composition. In some cases, Transmission Electron Microscopy equipped with Energy Dispersive X-ray Spectrometry (TEM-EDS) can be useful in identifying minor accessory minerals whose peaks may be masked by the numerous diffraction peaks of the dominant minerals. TEM-EDS is also useful in identifying phases that give poor diffraction patterns which makes their identification by XRD problematic.

4.1.3 X-ray Fluorescence (XRF)

X-ray Fluorescence spectrometry is one of the most widely used and versatile of all instrumental analytical techniques for the determination of major and trace elements (Karathanasis & Hajek, 1996; Potts, 2004). The method is generally rapid, reliable, more accurate than conventional chemical analytical techniques, and allows the direct analysis of solid samples without the need for dissolution or other chemical pretreatment.

Elemental analysis by XRF is based on the principle that primary radiation can be used to excite secondary (fluorescent) X-ray emission from a sample. When a sample is irradiated with an intense beam of primary X-rays, it displaces electrons from the inner, most tightly bound electron energy level in an atom to a higher energy level. In this state the atom is unstable and returns to the ground state by the transfer of an electron from an outer energy orbital to the unfilled inner level. This transition releases energy (secondary X-ray radiation), equal to the difference in binding energy of electrons in the two levels. Since the energies of the electrons in each atom are fixed at various orbital levels, the wavelengths of the X-rays produced are unique for a given element. The intensity

of an emission line is proportional to the concentration of the element producing it. This allows the determination of the concentration of each particular element present in the sample to typically µg/g levels (Fitton, 1997).

4.1.4 Sequential extractions

While analytical techniques such as XRF are useful in providing information on total elemental concentrations in samples, they supply no insight into the chemical forms of particular elements. Total metal concentrations in sediments are thus of limited interpretative value as they do not necessarily reflect the biologically or chemically reactive fraction. The mobility and bioavailability of chemicals in soils and sediments is strongly dependent on their specific chemical and mineralogical forms and their binding characteristics (Baeyens *et al*., 2003; Gambrell, 1994). For example, those elements incorporated within primary crystalline silicates will be largely unaffected by either biological or diagenetic processes, and their behaviour will differ dramatically from easily exchangeable elements that are readily available for plant uptake. It is therefore generally recognised that the mobility and behaviour of chemicals in the environment can be better explained by determining their distribution among various geochemical phases rather than by their total concentration (Wang *et al.*, 2004; Fligueiras *et al.*, 2002). Knowledge of how elements are combined within sedimentary phases is of great interest in understanding their biogeochemical transformation and ultimate fate.

Metals in wetland sediments may be loosely bound to exchange sites, associated with carbonates, bound to iron or manganese hydroxides, fixed by organic matter and sulphides, or present in the structure of secondary and primary minerals (Gambrell, 1994). Environmental changes such as in pH, temperature or redox potential can greatly influence the behaviour of metals in these fractions. Therefore, to adequately assess the role of sediments as sinks or sources for chemicals, the measurement of the total content should be integrated with the determination of metal partitioning among the different sediment phases. It has generally been accepted that the most appropriate methods to evaluate solid speciation are selective sequential extraction procedures (Ianni *et al*., 2001).

Several sequential extraction methods have been developed and reported, many of which are variants of the procedure proposed by Tessier *et al*. (1979). However, because of a lack of

harmonisation between the different procedures, and the absence of standardised conditions for extraction and sample preparation, results obtained by different laboratories are very difficult to compare. Indeed, it has been shown that results obtained can vary widely under different extraction schemes and experimental conditions (Martin *et al*., 1987). Small changes in pH, temperature, leaching time, reagent concentration, particle size, and solid to extractant volume ratio can produce large variations in fractionation. As a result, the Community Bureau of Reference (BCR, now Measurements and Testing Programme) developed a standardised, three-step sequential extraction protocol for the fractionation of trace elements in sediment (Ianni *et al.*, 2001). This was aimed at harmonising sequential extraction schemes for the determination of extractable trace metals in soils and sediments. A series of interlaboratory studies also produced a reference material (BCR-701), certified for extractable Cd, Cr, Cu, Ni, Pb and Zn, allowing the quality and reliability of measurements to be controlled.

The BCR extraction scheme allows the partitioning of sediment into four specific fractions, i.e. acid soluble, reducible, oxidisable and residual (Figure 4.1). This is achieved by sequential treatments that involve the use of chemical reagents, which are applied in order of increasing reactivity so that the successive fractions obtained correspond to metal forms with lesser mobility. Under particular conditions some of these substrates will dissolve or release adsorbed metals.

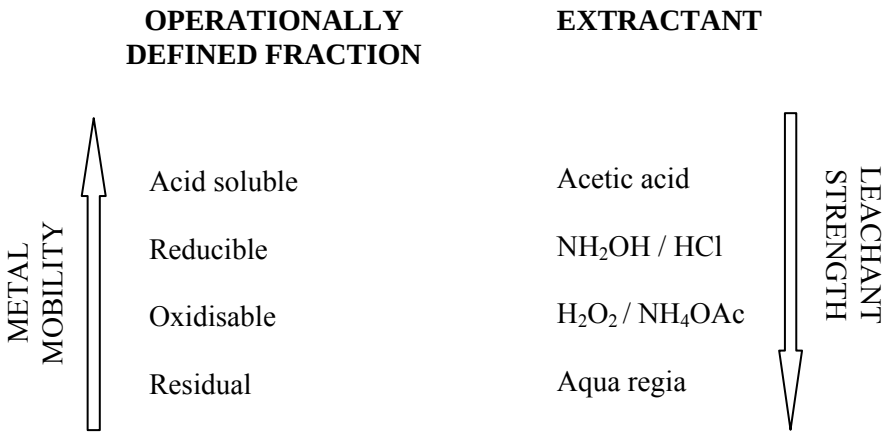

Figure 4.1 Relationship between metal mobility in different operationally-defined phases and leachant strength of chemical reagents used in the BCR sequential extraction.

Studies elsewhere have addressed the limitations of sequential extraction procedures (Filgueiras *et al.*, 2002; Martin *et al*., 1987). There is general agreement that results obtained by any sequential extraction scheme are operationally defined and therefore the significance of the analytical results is related to the extraction scheme used (Filgueiras *et al*., 2002). This is because extractants suffer from lack of selectivity and therefore leaching from a specific target mineralogical phase can be problematic. Despite this, sequential extractions are the most frequently applied analytical method for studying the solid phase speciation of environmentally relevant metals (Van Herreweghe *et al.*, 2003). Such experimental procedures have been used in a wide range of applications, including geochemistry, soil science, environmental science, and pollution studies. Although time consuming, sequential extraction procedures represent a useful means of assessing the origin of elements and their tendency to respond to certain physicochemical variations, making it attractive in the study of wetland sediments and the geochemical processes occurring within them.

4.1.5 Porewater extraction and analysis

In order to study the chemistry of interstitial waters, porewater must be separated from the sediment and preserved in conditions as close as possible to its natural state. Bufflap & Allen (1995) provide a detailed review of the various advantages and disadvantages of a variety of porewater recovery techniques. Although the sampling of soil porewater is considered most representative when conducted in the field, the remoteness of the present study site and the depth of sampling required precluded the use of *in situ* techniques. Centrifugation using solvent displacement was chosen as the most suitable technique for this study.

The application of a solvent displacement method for porewater separation, in which a dense, water-immiscible liquid is centrifuged with the soil, has been widely investigated and reported (Batley & Giles, 1979; Kinniburgh & Miles, 1983). During centrifugation, the more dense solvent displaces water from the sediment due to the resulting hydrostatic pressure caused by the density difference between the displacent and the porewater. The displaced water collects at the top of the tube and can then be removed for analysis. Suitable displacement solutions are characterised by inertness, having a high density, and low solubility in water. Solvents that have been previously used in studies include tetrachloroethylene, carbon tetrachloride and a variety of dense fluorocarbons.

4.1.6 Sedimentation rates: use of radioisotopes

Knowledge of the rate at which sediments have been accumulating can be of fundamental importance in understanding the sedimentary geochemical processes which may be taking place within a system. Such information may also assist in the interpretation of chemical profiles in sediments, and allow the effects of fluvial input to be separated from subsequent diagensis.

The use of radioisotopes is now established as the most common and reliable method to calculate sediment deposition and accumulation rates in estuarine, fluvial and lacustrine environments. (e.g. Kim, 2003; Benoit & Rozan, 2001; Robbins & Edgington, 1975; DeLaune *et al*., 1978). This is typically achieved using a combination of ^{210}Pb and ^{137}Cs dating procedures.

^{210}Pb technique

^{210}Pb, a naturally occurring radionuclide, is a product of the ^{238}U decay series with a half-life of 22.2 years. Its presence in the atmosphere is due to the diffusion of ^{222}Rn (daughter of ^{226}Ra) from the earth's crust into the atmosphere. The existence of ^{210}Pb in the atmosphere is short-lived, with a mean atmospheric residence time in the order of 5 to 10 days (Krishnaswami *et al.*, 1978). ^{210}Pb is deposited on the earth's surface as atmospheric fallout, where it quickly becomes adsorbed to fine-grained sediment. Approximately 90% of all ^{210}Pb fallout is derived through precipitation and therefore ^{210}Pb fluxes are strongly related to rainfall patterns (Binford, 1993). However, deposition rates are thought to be constant and spatially uniform within a limited geographic range (DeLaune *et al*., 1989).

Not all ^{222}Rn escapes the earth's crust before it decays, and a portion of the ^{210}Pb present in the soil is formed *in situ* by the decay of ^{226}Ra. A distinction is made between ^{210}Pb derived from the atmosphere (excess ^{210}Pb) and that derived from sediment (supported ^{210}Pb). It is the excess ^{210}Pb component of total ^{210}Pb activity that is used in sediment dating. Total ^{210}Pb activity should follow an exponential decay with depth, assuming a uniform sedimentation rate over a 100-150 year period. However, because of anthropogenic and environmental effects, this is seldom the case (Appleby & Oldfield, 1978). Several models for ^{210}Pb analysis have thus been developed, depending on environmental conditions and sediment processes.

The CRS (Constant Rate of Supply) model is the most widely accepted and employed model in determining ^{210}Pb derived sedimentation rates. The model is based on the assumption that no post-depositional mixing or sediment disturbance has occurred. Assuming a constant fallout of ^{210}Pb, the CRS model can be used to determine the age of a given depth (z) by:

$$^{210}Pb_{xs(z)} = {}^{210}Pb_{xs(0)}e^{-\lambda t}$$

where $^{210}Pb_{xs(0)}$ represents the excess activity of ^{210}Pb at the sediment surface, λ is the radioactive decay constant for ^{210}Pb (0.0311), and t is the deposition time. When $\ln^{210}Pb_{xs(z)}$ is plotted against depth, the resulting profile is linear and the accumulation rate can then be determined from the slope of this line.

Goldberg (1963), Krishnaswami *et al.* (1971) and Ritchie *et al*. (1973) pioneered the use of ^{210}Pb in sediment geochronology, which has now been widely applied by many researchers to a variety of environments such as wetlands (Fávaro *et al.,* 2006; Wang *et al*., 2004), estuaries (Pfitzner *et al*., 2004; Weis *et al*., 2001) and floodplains (Aalto & Dietrich, 2005; Saxena *et al*., 2002) to estimate sedimentation rates over the last 100-150 years. Typically, an accumulation rate of greater than 1 mm/year is considered sufficient for ^{210}Pb dating (Oldfield & Appleby, 1984). Post-depositional processes, such as compaction, bioturbation and erosion, that disturb the sediment column can interfere with the accuracy of ^{210}Pb sediment age dating. As a result, an independent tracer is typically used in conjunction with ^{210}Pb to validate calculations derived from ^{210}Pb activity (Smith, 2001). The accuracy and validity of ^{210}Pb derived geochronology is commonly confirmed using ^{137}Cs as an independent time-stratigraphic marker.

^{137}Cs technique

^{137}Cs (half-life 30 years) is an artificial radionuclide which was introduced into the environment by nuclear weapons testing during the late 1950s and 1960s (Ritchie & McHenry, 1990). ^{137}Cs released into the atmosphere by these weapons tests was dispersed globally and subsequently deposited as fallout on the earth's surface.

Significant fall-out levels first appeared in 1954, with peak quantities detected in 1963. Since then, global atmospheric ^{137}Cs deposition has decreased steadily as a result of an imposed testing ban,

with Cambray *et al.* (1985) reporting fallout deposition rates of ^{137}Cs to be below their limits of detection in 1983/1984. Fallout of ^{137}Cs resulting from the Chernobyl explosion of 1986 is reported to have been confined to Europe, having a limited impact on global fallout rates and patterns (Ritchie & McHenry, 1990).

Once deposited, ^{137}Cs is strongly adsorbed onto fine sediment particles, making it a useful marker in soils. Although ^{137}Cs deposition occurs primarily through rainfall, fine sediment containing ^{137}Cs can be transported downstream during flood events and deposited in floodplains, wetlands, lakes and oceans. The 1963 peak is frequently used as a marker layer in sediment studies, thus providing an average sedimentation rate since that time (Ritchie & McHenry, 1990). When used in conjunction with measurements of ^{210}Pb fallout, ^{137}Cs is recognised as a useful tool for the determination of sediment deposition history in a variety of environments.

Limitations in the southern hemisphere

Although both ^{210}Pb and ^{137}Cs have been successfully used, most of studies have been conducted in countries from the northern hemisphere. Very limited radioisotope research has been carried out in the southern hemisphere due to difficulties in obtaining ^{210}Pb concentration data that are above the detection limit of analysis (Bonotto & de Lima, 2006; Owens & Walling, 1996). Fallout of ^{210}Pb is much lower in the southern hemisphere due to the small ratio of land to sea. Oceans are not considered important sources of atmospheric ^{222}Rn (Wilkening & Clements, 1975) and as a result the annual supply of ^{210}Pb from the atmosphere can be eight times lower in the southern hemisphere in relation to European and North American countries. ^{210}Pb fallout also declines with increasing latitude due to decreasing precipitation rates (Outridge *et al*., 2002).

The southern hemisphere also received around 10 times less ^{137}Cs fallout than the northern hemisphere (McCallan *et al.*, 1980). Most nuclear testing took place in the northern hemisphere, making the nuclides from these tests very difficult to detect south of the equator (Figure 4.2). Due to the lack of a significant deposition peak and a much lower overall radionuclide concentration in sediment, ^{137}Cs has had a more restricted use as a tracer for sedimentation in southern hemisphere countries, with many studies being limited to sedimentation rate data derived solely from ^{210}Pb (Ashley *et al.,* 2004; Wilken *et al*., 1986).

Investigations in the southern hemisphere using ^{210}Pb or ^{137}Cs derived sedimentation rates have been confined primarily to Brazil (Sanders *et al.*, 2006) and Australia (Pfitzner *et al.*, 2004). Very few similar efforts have been carried out in southern Africa, with the exception of work done by Foster *et al.* (2007) and Owens & Walling (1996). This study represents the first known attempt to derive sediment accumulation rates using ^{137}Cs and ^{210}Pb in a southern African wetland.

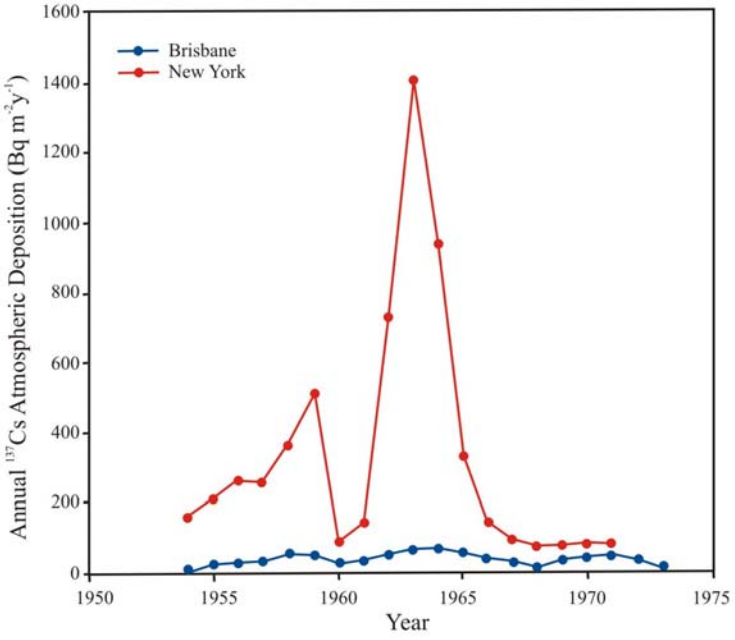

Figure 4.2 Annual deposition of ^{137}Cs for Brisbane (Australia) and New York (USA), highlighting differential in deposition rates between northern and southern hemisphere.
Source: Hancock (2002)

4.2 EXPERIMENTAL APPROACH

4.2.1 Fieldwork

Fieldwork was conducted over a period of 3 years (2005–2007). Site visits were usually conducted during the dry winter months (June to August) to ensure easy vehicle access to sampling sites. Sediment and groundwater samples were collected along three transects running roughly perpendicular to the Mkuze River at different locations on the lower floodplain (Figure 4.3). Transects were located to cover the three different reaches of the floodplain. Sediment samples at each site were collected by augering holes into the ground to a maximum depth of 5-7 m. Samples were collected every 0.5 m, or where there was a visible change in soil characteristics, and stored in sealed polyethylene bags to prevent water loss and limit air exposure. At sites where the groundwater table was reached, a water sample was taken and stored in air-tight polyethylene bottles. Soil morphology (colour and degree of mottling) was described on field moist samples. A total of 178 sediment samples and 15 water samples were obtained. Topographic elevation was measured along each transect using a dumpy level, and sample location sites were recorded using differential GPS with a remote base station. Figures 4.4 (a-d) illustrate some of the major physical features associated with sampling sites on the Mkuze Floodplain.

Two sediment pits (K and M), each approximately 85 cm deep, were excavated at two sites on the floodplain (Figure 4.3). This allowed large, undisturbed sediment samples (50 g dry weight) to be collected for radioisotopic analysis. Samples were sectioned at vertical intervals of ~2 cm, resulting in 50 samples at K and 55 samples at M.

4.2.2 Physicochemical parameters

The pH and redox potential of sediment and water samples collected were measured in the field using a Hanna™ portable pH/Eh combination electrode. For sediment samples, this was determined on a 1:2.5 soil-water suspension. Electrical conductivity (EC) measurements were similarly recorded in the field using a portable WTW™ conductivity meter. All electrodes were calibrated in the field using suitable buffer solutions. Particle size distribution was determined using a Malvern Mastersizer 2000 Laser Grainsize (measuring range: 0.02 – 2000 μm). Organic carbon was removed from samples prior to particle size analysis by loss on ignition at 450 ^{o}C (Ball, 1964).

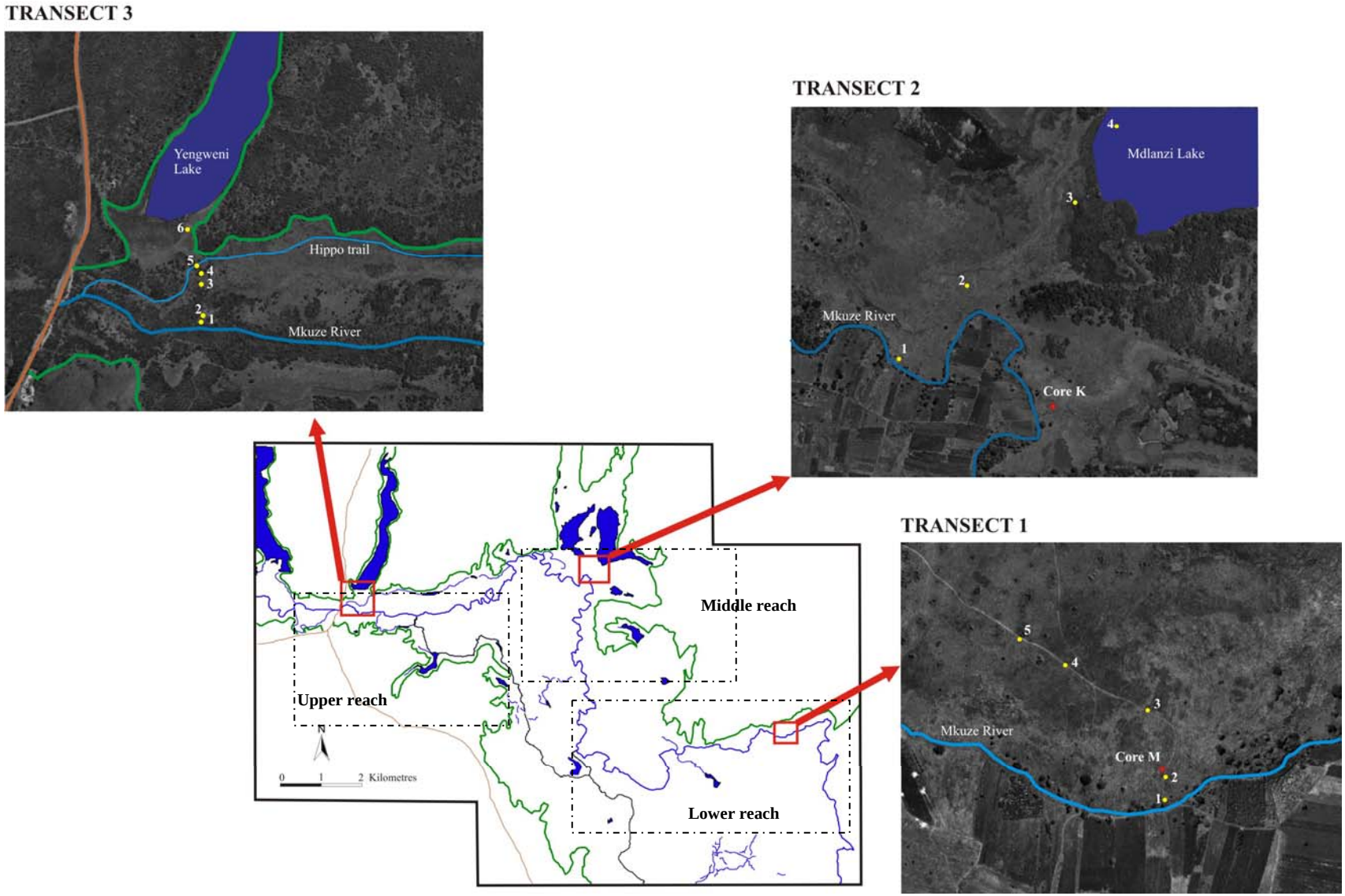

Figure 4.3 Location of sampling sites (main figure) and cores taken (aerial photographs).

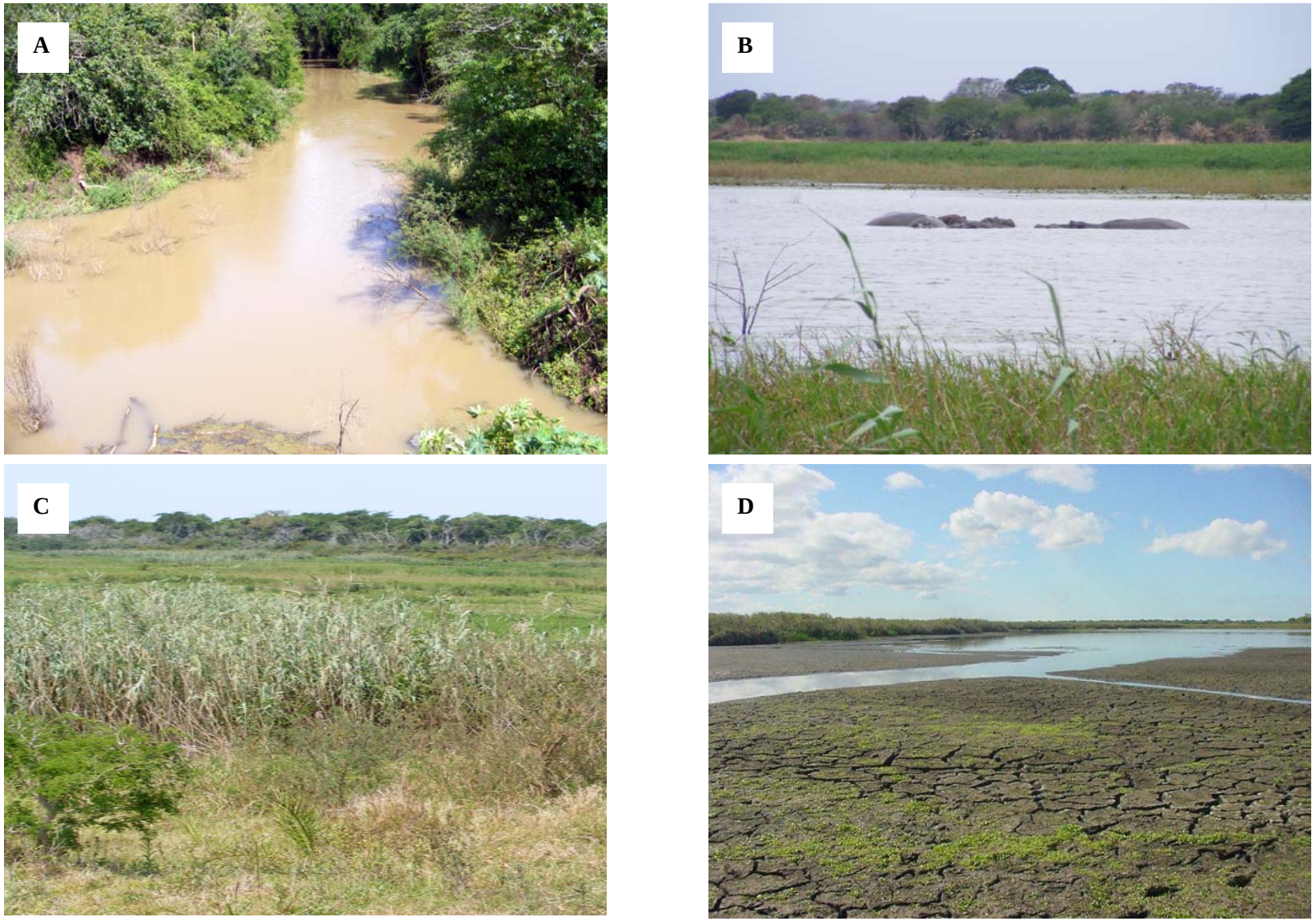

Figure 4.4 (A) The Mkuze River near the lower bridge after recent rains, November 2007, (B) floodplain lakes provide habitat to numerous wildlife including hippo, (C) the variety of vegetation types associated with the lower floodplain, (D) the effect of prolonged drought on Mdlanzi Lake, October 2004.

4.2.3 Water analysis

- *Groundwater*

Groundwater samples were filtered through 0.45 μm nylon syringe filters, acidified and analysed for the major cations (Ca, Mg, Si, Fe, Al, Mn, Na, K) using a Perkin Elmer Optima 5300 DV ICP-OES. Ion chromatography (Dionex ICS-90) was used to analyse for Cl, NO_3, SO_4 and PO_4. Total alkalinity of filtered samples was determined by acid titration with HCl (Gran, 1952).

- *Porewater*

Soil porewater was collected by centrifuging field moist samples of ~25 g at 12000 rpm for ~1 hour with CCl_4 in stainless steel tubes. This was performed 8 times for each sample, combining the collected water to provide a representative sample. Volumes of porewater collected varied depending on soil texture and moisture content. For some samples very little water (<1 ml) was separated, while other samples yielded no water at all. Increasing the time of centrifugation generally produced no significant increases in the volume of water separated. Every attempt was made to limit air exposure during the handling and centrifugation of sediment samples.

The displaced water was withdrawn using a micropipette and diluted using 2% HCl to produce workable solutions with measurable elemental concentrations. Any suspended material was removed by passing solutions through 0.45 μm syringe filters prior to analysis by ICP-OES for Ca, Mg, Si, S, Na, Fe and Al. For groundwater samples, results obtained for sulphate using ion chromatography and sulphur using ICP-OES were comparable. Sulphur measured in the porewater was thus assumed to be present in the form of sulphate. The small volumes collected precluded any further chemical porewater analysis.

4.2.4 X-ray Diffraction (XRD) and X-ray Fluorescence (XRF)

The clay fraction (defined by a particle size of <2 μm) of selected sediment samples was separated by centrifugation with distilled water. The mineralogy of this fraction was investigated by XRD using a Philips PW 1130 X-ray diffractometer (3 to 45^o 2θ) with monochromated Co Kα radiation at 1^o/min with a step size of 0.02^o on oriented samples following saturation of separate sub-samples with magnesium and potassium. Mg-saturated samples were examined air-dry, and after glycerol and ethylene glycol treatments. K-saturated samples were examined air-dry and after heating to

550 ^{o}C (Büchmann *et al*., 1985). Semiquantative estimates of mineral proportions were made based upon the peak height of characteristic XRD peaks before and after various treatments.

The major elements of bulk sediment samples and selected clay fractions were determined using XRF. Powdered samples were mixed with Spectroflux™ and heated to 1000 ^{o}C in a platinum-gold crucible. Discs were then analysed using a Philips PW 1404 spectrofluorometer.

4.2.5 BCR sequential extraction

- *Certified Reference Material*

Sequential extraction of samples was carried out as prescribed by the BCR sequential extraction procedure (Rauret *et al*., 2001). The reliability and reproducibility of this method was verified by analysing extractable trace elements in CRM BCR-701. The procedure followed is outlined briefly below and summarized in Table 4.1.

Step 1:

All glassware and centrifuge tubes were cleaned by rinsing with 4 M HNO_3 and then with double distilled water. A solution of 40 ml of 0.11 M acetic acid was added to an accurately weighed out (~1 g) sediment sample in a 50 ml polyethylene centrifuge tube. The tube was stoppered and extraction was performed by shaking on an orbital shaker overnight at room temperature (24 ^{o}C). The extract was separated from the residue by centrifugation and stored in a refrigerator prior to analysis.

Step 2:

The residue from Step 1 was shaken overnight at room temperature with 40 ml of 0.5 M hydroxylammonium chloride in HCl. The extract was separated from the residue by centrifugation and retained for analysis.

Step 3:

To the residue from Step 2, 10 ml of 30% hydrogen peroxide (acid-stabilised to pH 2-3) was added and allowed to digest at room temperature for ~1 hour with occasional manual shaking. Digestion was continued for ~1 hour at 85 ^{o}C over a water bath, followed by further heating of the uncovered test tube until the volume of liquid had been reduced to less than 3 ml. If needed, a further 10 ml

aliquot of H_2O_2 was added and heated at 85 ^oC until the volume of liquid had been reduced to approximately 1 ml. The solution was cooled and shaken overnight with 40 ml of 1.0 M ammonium acetate at room temperature. The extract was separated from the residue by centrifugation and retained for analysis as before. Between each extraction step described above, the residue was washed with ~20 ml of deionised water and separated by centrifugation at 3000 rpm for 10 min.

Step 4:

The residue from Step 3 was microwave digested using aqua regia (7.0 ml of 12 M HCl, 2.3 ml of 15.8 M HNO_3). Samples were in sealed Teflon^{TM} bombs and digested at 1400 W for 25 minutes using an Anton Paar microwave digestion system. This method was chosen over the recommended procedure of reflux digestion, as microwave-assisted digestions are easier and faster than conventional wet digestion techniques. In addition to the reduction in analysis time, microwave digestion tends to yield more reproducible results due to reduced loss of volatile species and lower contamination (Melaku *et al*., 2005; Tuzen *et al*., 2004; Sandroni & Smith, 2002). Once cooled, the extract was filtered and retained for analysis.

Table 4.1 BCR sequential extraction procedure employed in this study.

Step	Fraction	Operationally defined target phase(s)	Extractants
1	Exchangeable, water and acid soluble	Soluble species, carbonates, cation exchange sites	0.11 M acetic acid
2	Reducible	Iron and manganese oxyhydroxides	0.5 M hydroxylammonium chloride at pH 1.5
3	Oxidisable	Organic matter and sulphides	Hydrogen peroxide followed by 1.0 M ammonium acetate acidified to pH 2
4	Residual	Elements present in the lattice of primary and secondary minerals.	Aqua regia

All extracts were analysed by ICP-OES using multi-element, matrix matched standard solutions. Control samples were periodically run to account for any instrument drift. All determinants showed high linearity (R >99.98%) and good precision (generally <2%). Agreement between the certified and determined values was generally good (Table 4.2). All analytes fell within the certified ranges, except for Zn in Steps 1 (92% recovery) and 3 (83% recovery), where determined values were slightly lower.

Table 4.2 Determined, certified and indicative values (μg/g) for CRM BCR-701 extractable trace elements in sediments.

	Step 1		Step 2		Step 3		Step 4	
	Determined*	Certified	Determined	Certified	Determined	Certified	Determined	Indicative
Cd	7.10 ± 0.17	7.3 ± 0.4	3.70 ± 0.04	3.77 ± 0.28	0.28 ± 0.03	0.27 ± 0.06	0.10 ± 0.01	0.13 ± 0.08
Cr	2.30 ± 0.04	2.26 ± 0.16	45.8 ± 0.37	45.7 ± 2.0	139.3 ± 3.1	143 ± 7	63.3 ± 1.8	62.5 ± 7.4
Cu	48.7 ± 0.05	49.3 ± 1.7	125.2 ± 0.24	124 ± 3	57.67 ± 1.6	55.2 ± 4.0	47.4 ± 1.6	38.5 ± 11.2
Ni	14.9 ± 0.12	15.4 ± 0.9	26.4 ± 0.64	26.6 ± 1.3	14.9 ± 0.3	15.3 ± 0.9	38.6 ± 0.61	41.4 ± 4.0
Pb	3.20 ± 0.05	3.18 ± 0.21	125.3 ± 1.7	126 ± 3	7.8 ± 0.11	9.3 ± 2.0	10.08 ± 0.05	11.0 ± 5.2
Zn	188.4 ± 1.57	205 ± 6	113.6 ± 2.1	114 ± 5	37.9 ± 0.78	45.7 ± 4.0	85.1 ± 1.2	95 ± 13

*Results are expressed as the mean of three determinations ± standard deviation.
Certified and indicative values obtained from BCR certificate (Appendix 1).

- *Sediment Samples*

All sediment samples collected were analysed following the same procedure detailed above. Samples were air-dried, ground and sieved to 90 μm to achieve similarity with the CRM. Analysis of CRM extracts was also used to select appropriate spectral lines for ICP-OES analysis of samples. This was based on detection limit, reproducibility and lack of interference. Spectral lines used and their respective detection limits are provided in Appendix 1.

4.2.6 Carbonate analysis

Hand-picked carbonate nodules were analysed for Ca, Mg, and S. Accurately weighed out samples of approximately 1 g were digested in 20 ml 37% HCl for 20 minutes. The acid leachate was filtered and analysed by ICP-OES.

4.2.7 Electron microscopy

Analysis by TEM-EDS was used to identify minerals and precipitates in the clay fraction of selected sediment samples. Samples were dispersed in ethanol and mounted onto either Lacey Carbon or Formvar coated Cu grids. These were examined using a Philips CM 200 electron microscope at an accelerating voltage of 197 kV.

4.2.8 Sedimentation rates

All sediment samples for radioisotope analysis were air-dried, crushed and sieved to 125 μm. ^{137}Cs and ^{210}Pb measurements were made by gamma ray spectrometry performed at the University of South Carolina, using a low-energy Ge gamma spectrometer. A total of 24 samples were analysed. All activities were determined using a program called HYPERMET and all errors were determined from counting statistics and the error associated with the HYPERMET curve fitting routine (Phillips & Marlow, 1976). Total ^{210}Pb was measured by its emission at 46.5 KeV and supported ^{210}Pb by the weighted average decays of ^{226}Ra daughters at 295, 351, and 609 KeV. Excess ^{210}Pb was calculated as the difference between the measured total ^{210}Pb at 46.5 KeV and the estimate of the supported ^{210}Pb activity ($^{210}Pb_{ex}$ = ^{210}Pbtot – ^{226}Ra derived supported Pb). ^{137}Cs was determined using its gamma emission at 661 KeV. The distribution of excess ^{210}Pb with depth was used to calculate vertical accretion rates using the CRS model (Oldfield & Appleby, 1978). All results were corrected for salt content and porosity.

4.2.9 Geochemical modelling

The saturation status of minerals in groundwater and porewater samples was evaluated using the geochemical program PHREEQC (Parkhurst & Appelo, 1999). The program calculates mineral saturation indices (SI) from ion activity products and established equilibrium constants. The chemical parameters used in this study included pH and the concentrations of Na, Cl, Si, Fe, Al, Ca, Mg, SO_4, and HCO_3. For all porewater samples, a CO_2 partial pressure of 10^{-2} atm was used, as this is considered typical for wetland soils (Schrot & Wassen, 1993). The temperature was set to 20 ^oC for all calculations.

Chapter 5
Transect Geochemistry

This chapter is organised into three main sections, each concerned with the presentation and analysis of results from an individual sampling site. A brief discussion of results on each site is given in order to introduce and draw attention to concepts dealt with in more detail in Chapter 6.

5.1 TRANSECT ONE: THE LOWER REACH

5.1.1 Topography and general sediment characteristics

The location of Transect 1 and the surveyed profile is shown in Figure 5.1. Topographic relief of the floodplain is low, with topographic height varying by a maximum of ~2 m over a lateral distance of 400 m. The channel is small with an approximate depth of 1.25 m and width of 10 m. A distinctive small levee is present and there is an increase in slope from the channel towards the floodplain margin.

Particle size distribution and clay content of sediments across the floodplain is shown in Figure 5.2. All full data set is given in Appendix 2. Surface deposits in Cores 1-3 are composed predominantly of silt (70-80%), with minor amounts of clay and sand. This is underlain by a reddish, silty sand deposit, characterised by silt (~40%), fine sand (40-50%), and very little clay (<5%). Although 200 cm thick in Core 1, this deposit thins progressively away from the channel and is absent in Cores 4

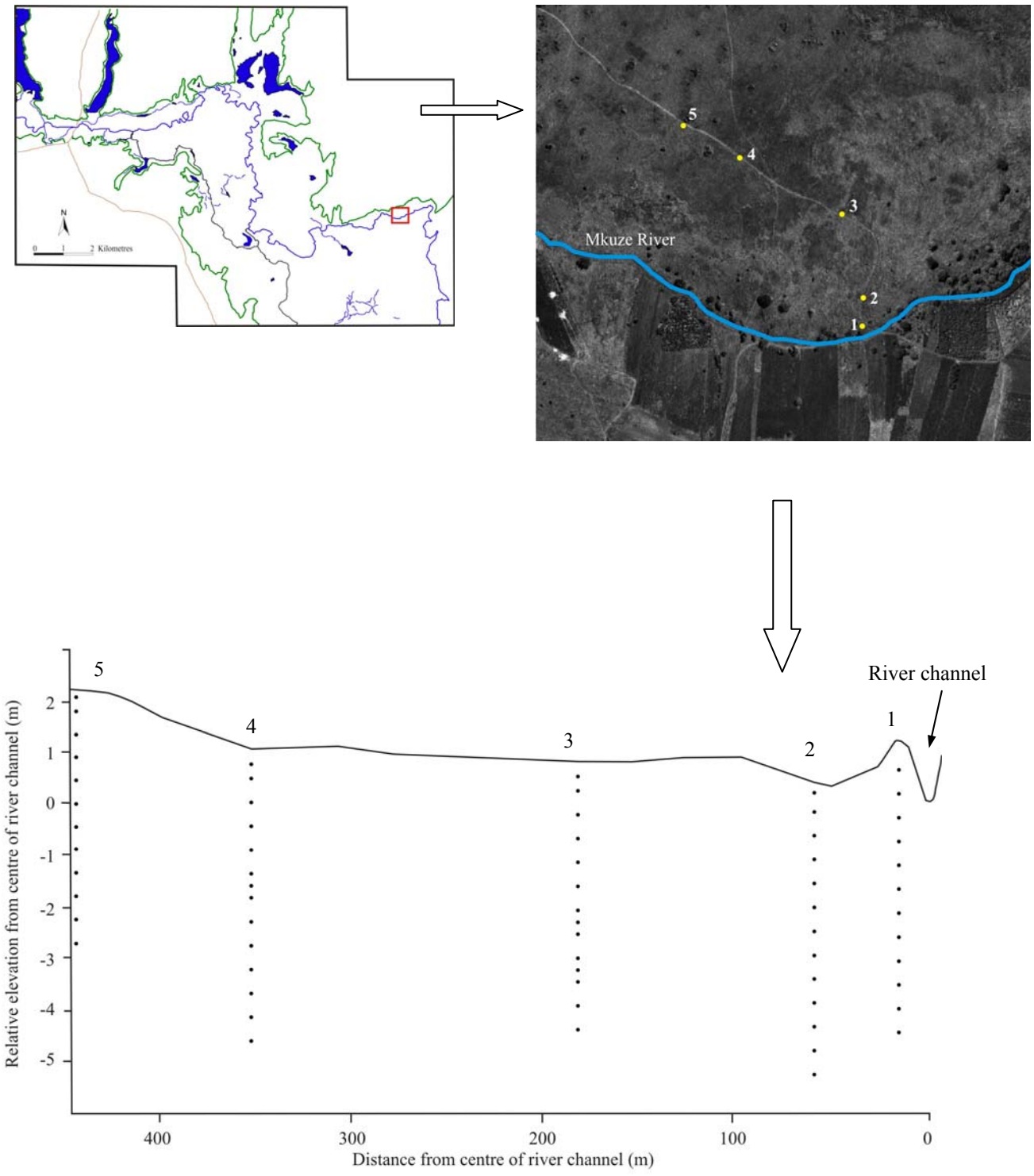

Figure 5.2 Location of sampling site on the lower Mkuze Floodplain and cores taken along the transect

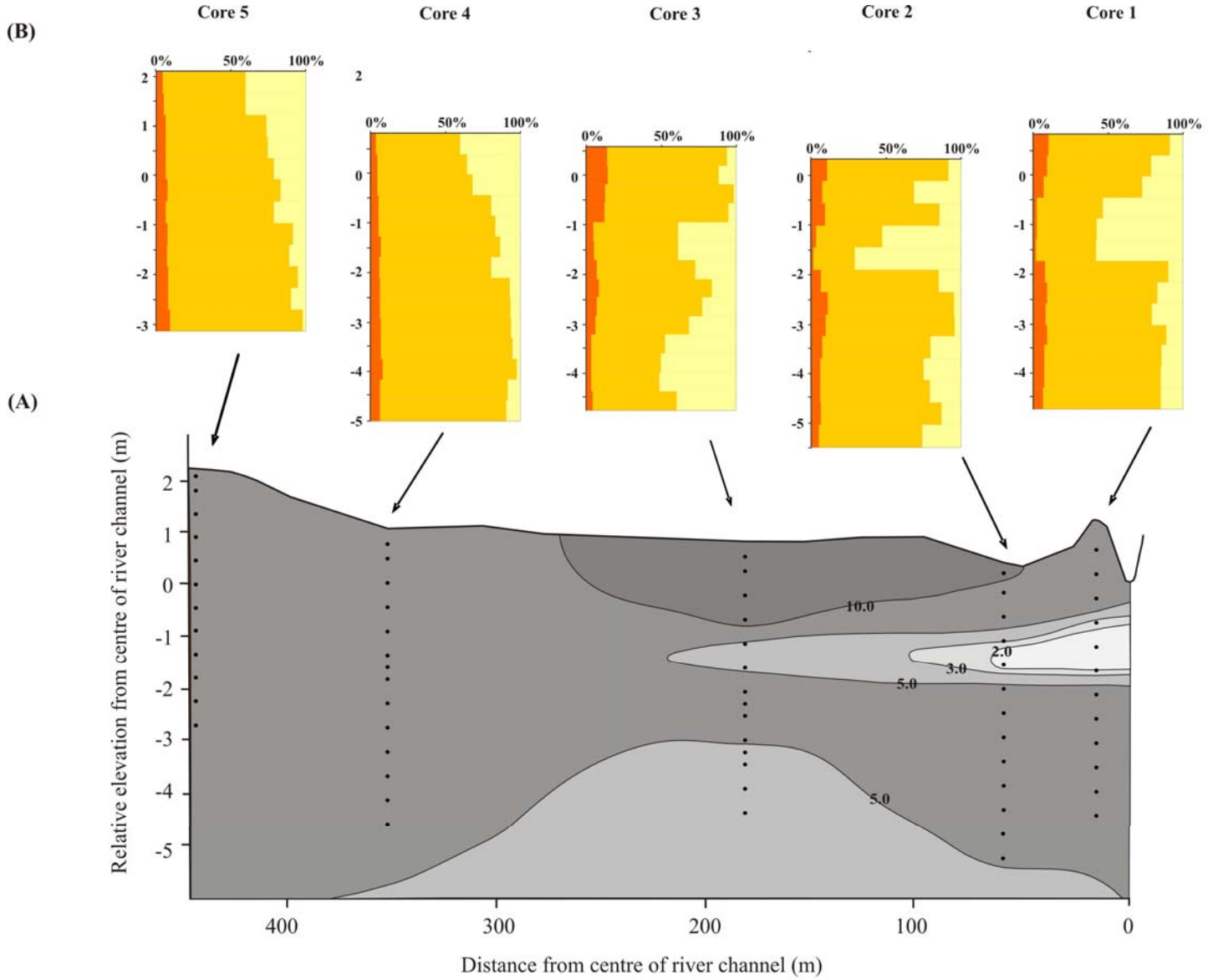

Figure 5.3 Generalised distribution of clay content (%) from sediments collected at Transect 1 (A), showing percentage clay (red), silt (orange) and sand (yellow) with depth in each core (B).

and 5. This layer likely represents the effect of a major flood event that deposited coarser sediment on the floodplain. In Cores 1 and 2, this deposit is underlain by sandy silt sediments displaying abundant iron mottling, although this diminishes below 400 cm, where deposits become characterised by very dark (black) sediment containing calcium carbonate nodules. The abundance of iron in Core 3 generally increases with depth, with Fe-Mn nodules present at 300 cm. Sediment at this depth is also characterised by numerous small calcium carbonate nodules, which become larger in size and more abundant at 400 cm (Figure 5.3). Sediment near the bottom of this profile gradually coarsens, containing higher fine and medium sand contents (>40%).

Particle size in Cores 4 and 5 coarsen upwards, with surface deposits characterised by relatively high total sand contents (30-40%). Substantial calcium carbonate accumulation is evident between 100 and 250 cm in Core 4, and between 150 and 450 cm in Core 5 (Figure 5.3). Iron mottling and Fe-Mn nodules are also present in these sediments.

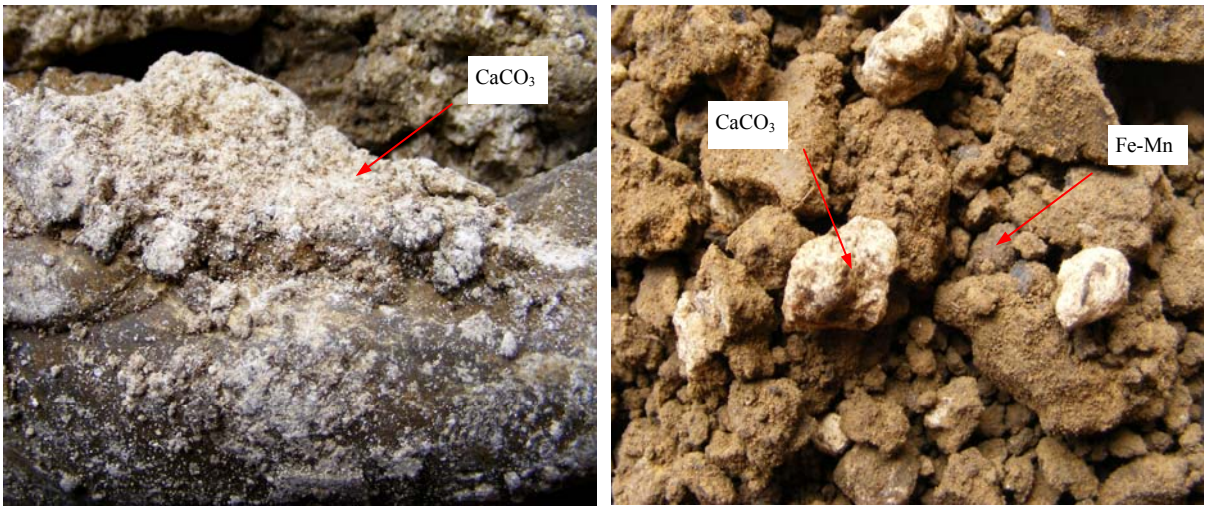

Figure 5.3 Calcium carbonate and Fe-Mn accumulations in sediments from Core 5 (left) and Core 3 (right). Nodules are typically 1-2 cm in diameter

5.1.2 Clay mineralogy and chemistry

Detailed sediment analysis and characterisation focused on Cores 1-4. X-ray diffraction patterns of clays from two typical samples are illustrated in Figure 5.4, with all other XRD traces provided in Appendix 3. The clay fraction of the majority of samples analysed is dominated by smectite, with lesser amounts of quartz, kaolin, vermiculite and mica. The presence of smectite is indicated by the shift in the d(001) peak from ~15 Å in the Mg air dried pattern to 16.5 Å in the ethylene glycol solvated sample. Weak 002 and 003 smectite reflections are seen at 8.46 Å and 5.53 Å in the ethylene glycol pattern. The identification of smectite is confirmed by K-saturation and heating to 550 ^{o}C, which results in the collapse of the basal smectite peak to ~10 Å. The presence of vermiculite is identified by its characteristic d(001) peak at 14-14.5 Å in the air-dried sample, which is retained after glycerol solvation. Weak reflections at ~10 Å and ~7.2 Å indicate the presence of minor amounts of mica and kaolin respectively. Non-clay minerals such as hematite (~2.67 Å), goethite (~4.16 Å) and K-feldspar (~3.24 Å) are also present in some samples in trace amounts (<5%).

Overall, sediments contain very little clay (5-10% on average), with surface sediments generally containing higher quantities. Differences in the mineralogical composition of the <2 μm fraction are also evident. In general, Cores 1-3 show increases in smectite content with depth. Surface samples typically contain 5-20% smectite, while deeper sediments may contain >60%. In Core 4, most samples contain 40-60% smectite. It appears that smectite as a proportion of total clay minerals increases with depth and with distance from the river channel. There is no apparent variation in kaolin or vermiculite through cores, although surface samples may contain higher quantities of mica and vermiculite.

The clay fractions of a few selected samples were analysed by XRF and these results are presented in Table 5.1. Overall, this fraction shows high Fe contents of up to 15% Fe_2O_3 by weight, with an average ratio of Fe to Al of approximately 0.65. Samples displaying slightly elevated ratios probably contain minor amounts of goethite or hematite, while samples with slightly lower ratios are likely to contain higher levels of non Fe-bearing minerals, such as quartz or kaolin. X-ray diffraction shows that, overall, very little hematite is present in the clay fraction, with <5% present in all samples. The majority of Fe is therefore attributed to the presence of clay minerals.

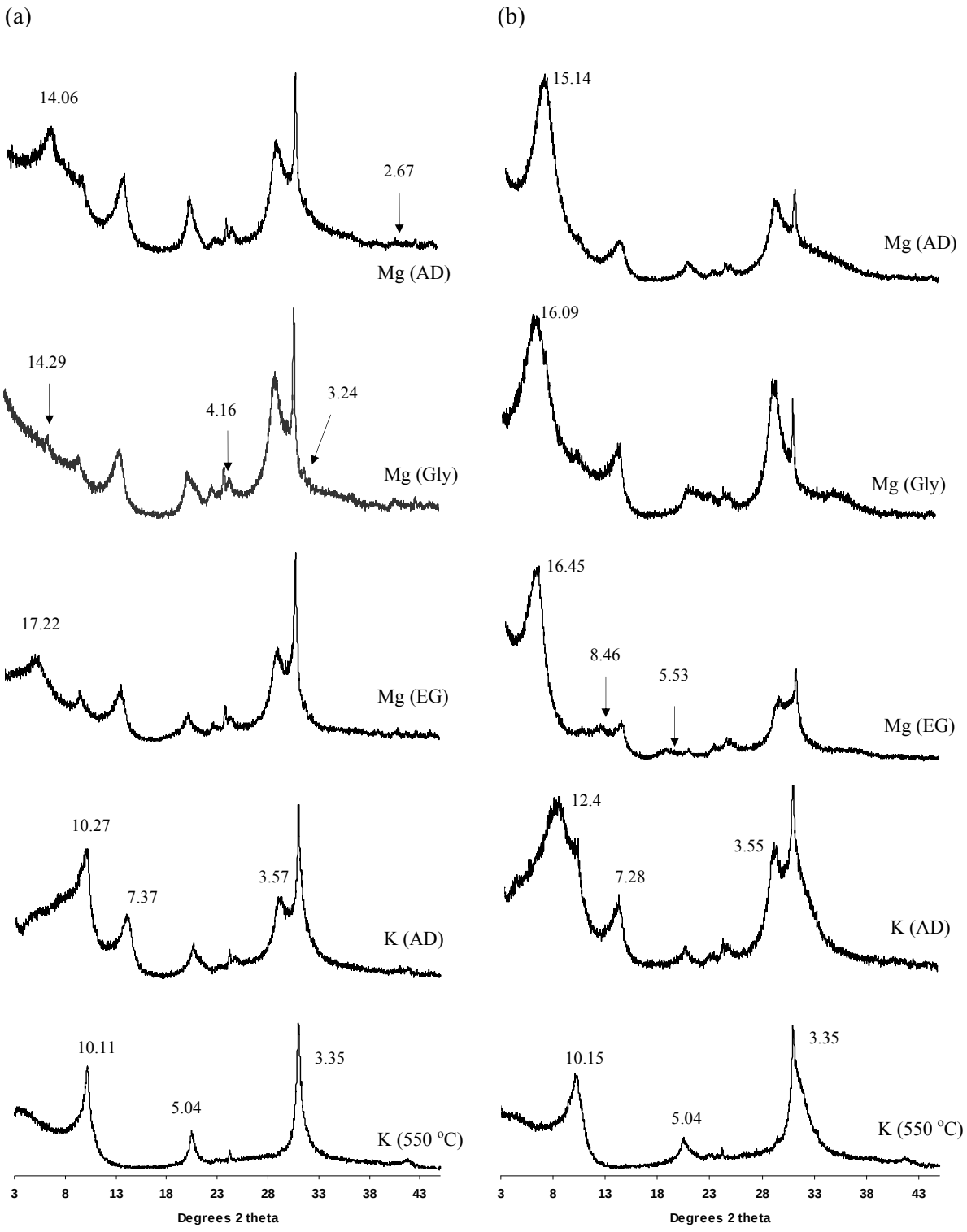

Figure 5.4 Clay XRD patterns from Core 3 (a) 50 cm and (b) 500 cm after various treatments
(Mg, magnesium saturated; K, potassium saturated; AD, air dry; EG, ethylene glycol; Gly, glycerol, d-spacings in Å)

Table 5.1 Major elements as weight percent in the clay fraction (<2 μm) for selected samples

Sample depth (cm)	SiO_2	Al_2O_3	Fe_2O_3	MnO	MgO	CaO	Na_2O	K_2O	TiO_2	L.O.I.*
Core1										
100	51.18	28.28	13.62	0.15	1.35	0.87	0.20	2.59	1.04	17.72
400	60.55	22.58	10.15	0.16	0.86	0.69	0.69	2.34	1.23	14.06
Core2										
100	55.10	25.17	12.92	0.20	1.20	0.89	0.45	2.42	1.17	16.59
300	53.76	26.37	13.23	0.11	1.53	0.93	0.32	2.38	1.09	17.22
450	54.93	25.58	12.82	0.10	0.95	1.08	0.35	1.54	1.78	18.68
600	53.16	26.14	14.93	0.06	1.36	0.67	0.27	1.43	1.15	18.75
Core3										
100	54.88	25.70	12.86	0.27	1.30	0.82	0.37	2.51	1.21	15.88
500	54.45	25.43	15.10	0.08	1.70	0.80	0.29	1.26	0.98	20.34
Core4										
100	54.94	25.90	12.40	0.19	1.52	1.20	0.33	1.03	1.55	19.03
200	53.99	25.90	13.48	0.08	2.17	0.51	1.05	1.06	1.15	19.63

*Loss on ignition

XRF and XRD values indicate that clay mineralogy is dominated by Fe-rich smectite. Examination of Fe-rich smectites studied elsewhere indicates that the chemical composition of this mineral is typically variable, with Fe_2O_3 contents ranging from 3 to 26% (Table 5.2). The chemical composition of smectite identified in this study falls within this range. Higher aluminum and potassium contents indicate the presence other clay minerals such as kaolin, mica and K-feldspar on the floodplain. Fe-rich smectities are differentiated from nontronite, the ferric endmember within the smectite group, based on their lower Fe_2O_3 and higher Al_2O_3 contents.

Analysis of selected clay fraction samples by TEM-EDS indicated the presence of both Mg-silicates (Figure 5.5) and opaline silica (Figure 5.6). Magnesian-silicates occur as irregular shaped particles, and are composed essentially of Mg (35%) and Si (55%). Opaline silica is found as extremely small (typically <0.1 μm), rounded spheres, similar to those reported by Pollard & Weaver (1973) and Drees *et al*. (1989). These occur as individual spheres or may coalesce to form chains.

Table 5.2 Chemical composition of nontronite (samples 1-5) and Fe-rich smectite (samples 6-13)

Sample*	SiO_2	Al_2O_3	Fe_2O_3	MnO	MgO	CaO	Na_2O	K_2O	TiO_2
1	51.36	8.15	35.94	-	0.19	3.57	0.03	0.01	0.02
2	46.3	2.77	33.2	-	0.29	0.04	2.36	0.16	0.02
3	49.90	0.27	29.50	-	1.75	0.77	0.12	0.01	-
4	44.8	7.80	29.1	-	0.40	0.03	3.17	0.10	0.17
5	42.1	4.7	29.0	0.15	0.85	1.15	0.45	0.58	0.26
6	60.15	5.64	25.98	0	2.82	1.17	0	3.58	0
7	51.46	2.20	24.70	0.03	3.27	1.45	1.06	0.24	0.05
8	52.08	6.92	18.40	0.06	3.39	1.31	0.31	0.07	0.06
9	42.72	15.03	12.06	0.06	6.90	3.21	0.13	0.60	0.03
10	49.3	17.8	10.7	-	1.68	0.38	2.08	0.40	1.05
11	44.64	22.04	8.02	0.08	3.44	0.94	0.19	0.29	0.06
12	55.3	18.7	6.70	-	2.54	0.19	2.46	0.17	0.02
13	56.59	20.06	3.19	0.03	3.10	0.68	2.17	0.45	0.06

*Sample localities and data sources: 1 South Australia, Keeling *et al.* (2000); 2 Germany, Köster *et al.* (1999); 3 Venezuela, Isphording (1975); 4 USA, Köster *et al.* (1999); 5 Lake Malawi, Müller & Förstner (1973); 6 Côte d'Ivoire–Ghana, Giresse & Wiewióra (1999); 7 Germany, Brigatti (1983); 8 USA, Brigatti (1983); 9 Italy, Brigatti (1983); 10 Austria, Köster *et al.* (1999); 11 Italy, Brigatti (1983); 12 France, Köster *et al.* (1999); 13 Italy, Brigatti (1983)

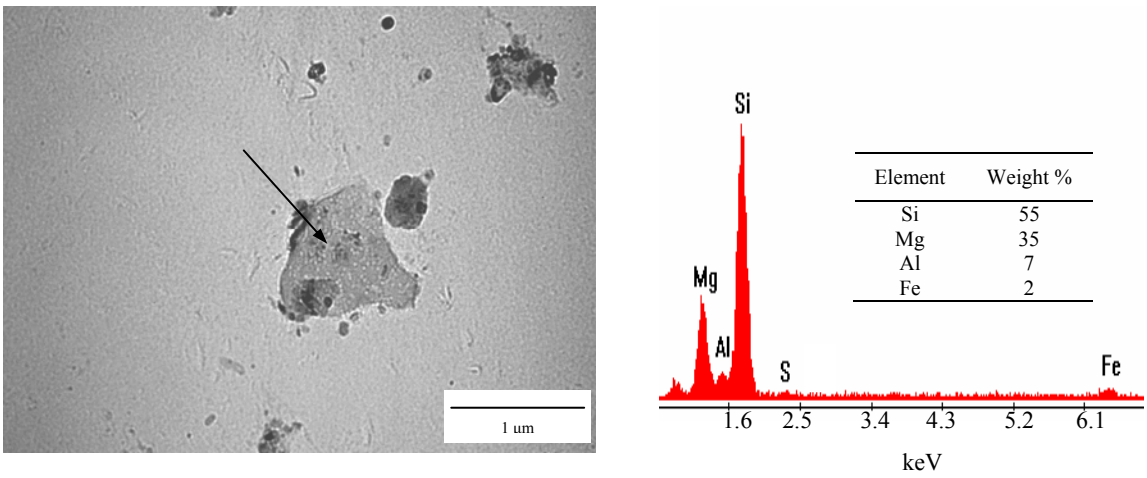

Figure 5.5 TEM image of Mg-silicate (Core 2 at a depth of 450 cm) and EDS spot analysis (arrow)

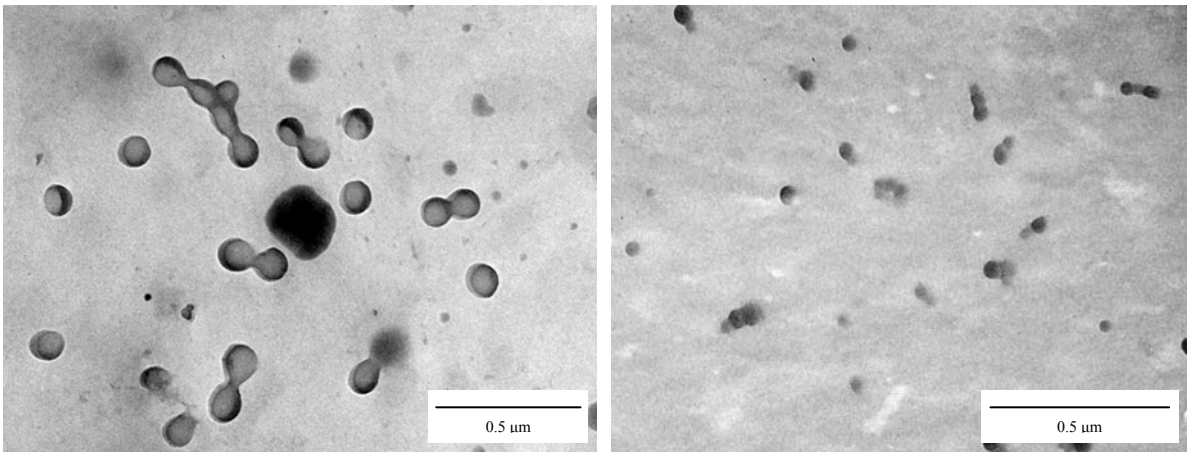

(a) (b)

Figure 5.6 TEM image of opaline silica spheres (a) from Core 5 at 400 cm and (b) Core 2 at 50 cm

5.1.3 Sediment redox and pH

Redox potential (Eh) and pH measurements described in methodology are presented in Figure 5.7. Sediment pH showed little variation in the top 300 cm of Core 1, although values seem to increase slightly with depth. Below this level, pH decreased sharply to 6.0 at 400 cm, thereafter showing a steady increase with depth. Redox potential was relatively constant to a depth of 450 cm, varying between 490 and 400 mV. Below this, Eh dropped dramatically to reach -124 mV at 550 cm. Sediment pH in the upper 350 cm of Core 2 remained fairly constant, varying between approximately 6.9 and 7.4. Below 400 cm, pH increased dramatically to a maximum of 8.34 at 500 cm. Eh dropped sharply from 531 mV near the surface to 254 mV at a depth of 100 cm. Readings at depths below this were remarkably stable except at a depth of 450 cm, where -43 mV was recorded. Sediment pH in Core 3 showed a general steady increase with depth, to a maximum of 9.01 at 325 cm. Overall, pH values encountered in this core were comparatively higher (average of 8.14) than those observed in Cores 1 and 2. The redox profile was highly variable, with values varying between 280 and 330 mV. Sediment in Core 4 was characterised by higher average pH values (8.89) when compared with the previous cores. pH initially increased from 8.20 near the surface to 9.39 at 150 cm, but thereafter showed gradual decline to 8.94 at 250 cm. Below a depth of 300 cm, pH remained relatively constant at approximately 8.7. The redox profile displayed moderately reducing conditions through the upper 400 cm of the core, with values varying between 250 and 300 mV. An increase in redox potential to 366 mV was encountered at 450 cm, with sediments below this level characterised by similar redox measurements.

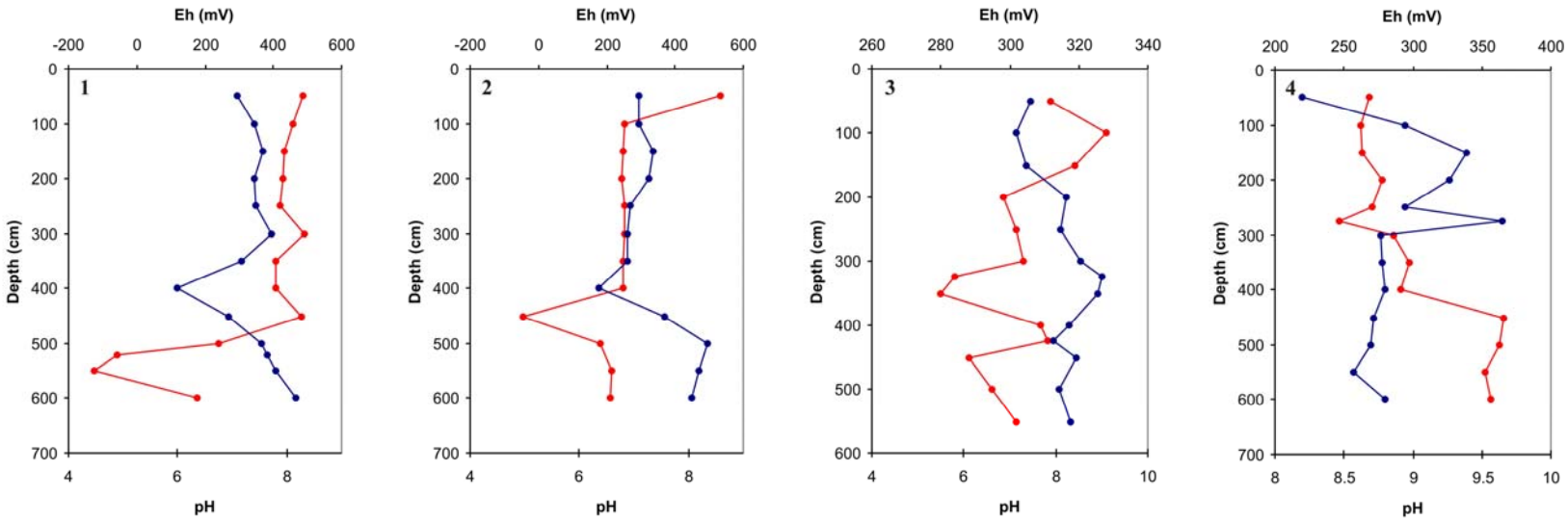

Figure 5.7 Variation of sediment pH (—) and redox potential (—) with depth in Cores 1-4 from Transect 1

Table 5.3 Groundwater chemistry data for Cores 2, 3 and 4 (concentrations expressed in µg/ml)

	Si	Mg	Ca	Fe	Al	Mn	K	Na	Cl	NO_3	SO_4	Alkalinity*	pH	EC (mS/cm)
Core 2	8.00	31.7	42.6	0.11	<0.1	0.61	0.54	1723	109	16.2	40.3	350	6.80	1.05
Core 3	9.10	19.5	19.6	<0.1	<0.1	<0.1	0.39	151	123	9.4	29.6	175	7.06	0.782
Core 4	21.3	17.2	10.6	<0.1	<0.1	<0.1	0.78	628	718	32.8	89.6	485	7.41	3.03

*Alkalinity expressed as $CaCO_3$ µg/ml
Watertable was not reached in Core 1

5.1.4 Groundwater chemistry

In general, groundwater chemistry was dominated by Na, Cl and HCO_3, with moderate amounts of Mg, Ca, Si and SO_4 (Table 5.3). Total concentrations of Fe, Al and Mn were typically low (<1 μg/ml).

There is lateral heterogeneity in groundwater composition, with conductivity increasing by a factor of three between Cores 3 and 4 (Figure 5.8). This is primarily due to considerable increases in dissolved Na and Cl. Soluble Si also shows a marked increase in concentration in Core 4, whereas Ca and Mg groundwater concentrations decline with distance from the channel. Groundwater pH appears to gradually increase with distance from the channel. There is a general decrease in the elevation of the watertable away from the channel, suggesting groundwater recharge from the channel towards the floodplain margin

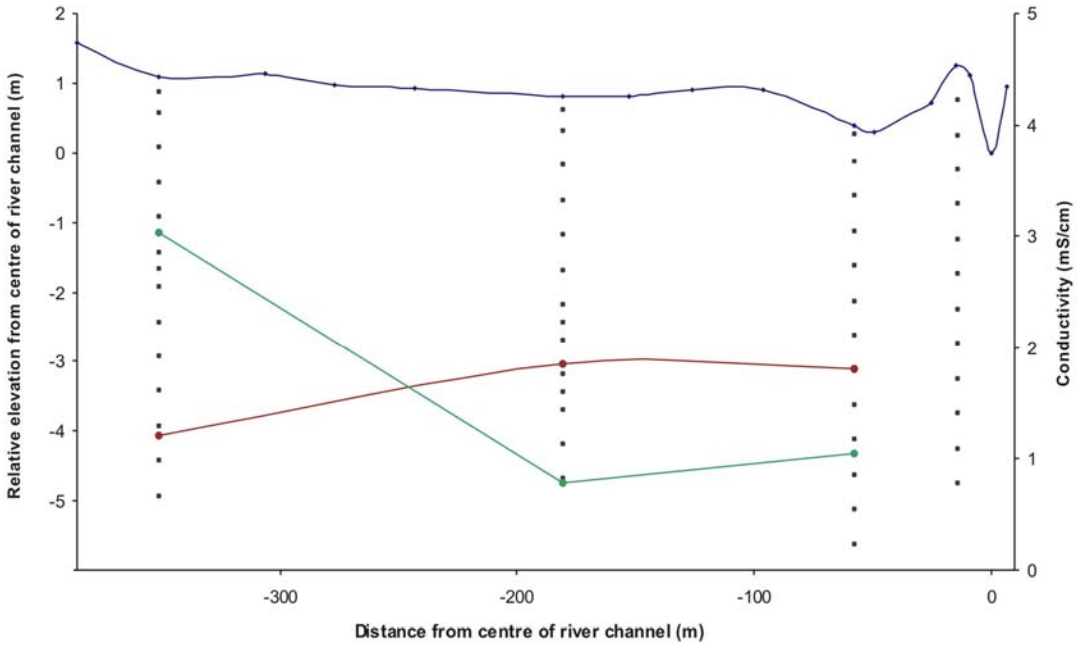

Figure 5.8 Transect profile showing groundwater conductivity (—) and elevation of the watertable (—)

5.1.5 Porewater chemistry

Porewater chemistry data for selected solutes are presented in Figures 5.9(a-c), with full data sets provided in Appendix 4. Only limited porewater information could be obtained for Cores 1-3, and these data are overlain with field conductivity measurements.

- Core 1

Core 1 shows pronounced subsurface maxima of Ca (178.2 μg/ml), Mg (89.2 μg/ml) and SO_4 (922.5 μg/ml) at 450 cm. This correlates well with an increase in conductivity at this depth. The concentration of these solutes declines with increasing depth below this. Porewater Na also shows a noticeable maximum concentration at 450 cm. The concentration of Na closely relates to measurements of electrical conductivity. Silicon, Al and Fe all show similar porewater profiles, with well-defined peaks in concentrations at 550 cm (Si = 62.6 μg/ml, Al = 28.0 μg/ml, and Fe = 26.9 μg/ml). These measurements are associated with a large decrease in sediment redox potential at this depth in the sediment profile.

- Core 2

Calcium and magnesium show similar porewater profiles, with very high concentrations at 300 cm (Ca = 138 μg/ml; Mg = 90.4 μg/ml). Below this depth, porewaters become gradually depleted in these two solutes. As observed in Core 1, Na also shows an elevated concentration at this depth. The correlation between these solutes and conductivity is not as clear as in Core 1, due to insufficient porewater volumes that could be extracted from sediments between 0 and 300 cm. Sulphate concentration remains relatively constant except for a distinct peak at 400 cm. Concentration profiles of Si, Al, and Fe are similar to each other, with enrichment at lower depths.

- Core 3

The porewater profile in Core 3 is characterised by a distinct and well-defined peak in all solute concentrations except Fe at 150 cm. Once again, a close relationship between Ca and Mg porewater concentrations is observed. Porewaters appear to be particularly enriched in Na and SO_4, with maximum concentrations in excess of 900 μg/ml and 200 μg/ml respectively. Iron, Al and Si appear to be enriched in the upper layers. There is, in general, good agreement between measured solute concentration and field conductivity measurements.

In general, sediment porewaters show higher solute concentrations than those found in the groundwater. Porewater Ca and Mg show good correlation in all samples analysed and there is reasonable agreement between porewater solute concentration and measured conductivity, particularly for Ca, Mg and Na. Although individual core profiles show similar overall trends, most solutes become increasingly concentrated with distance from the river channel. This is correlated with an overall increase in the average sediment conductivity away from the channel.

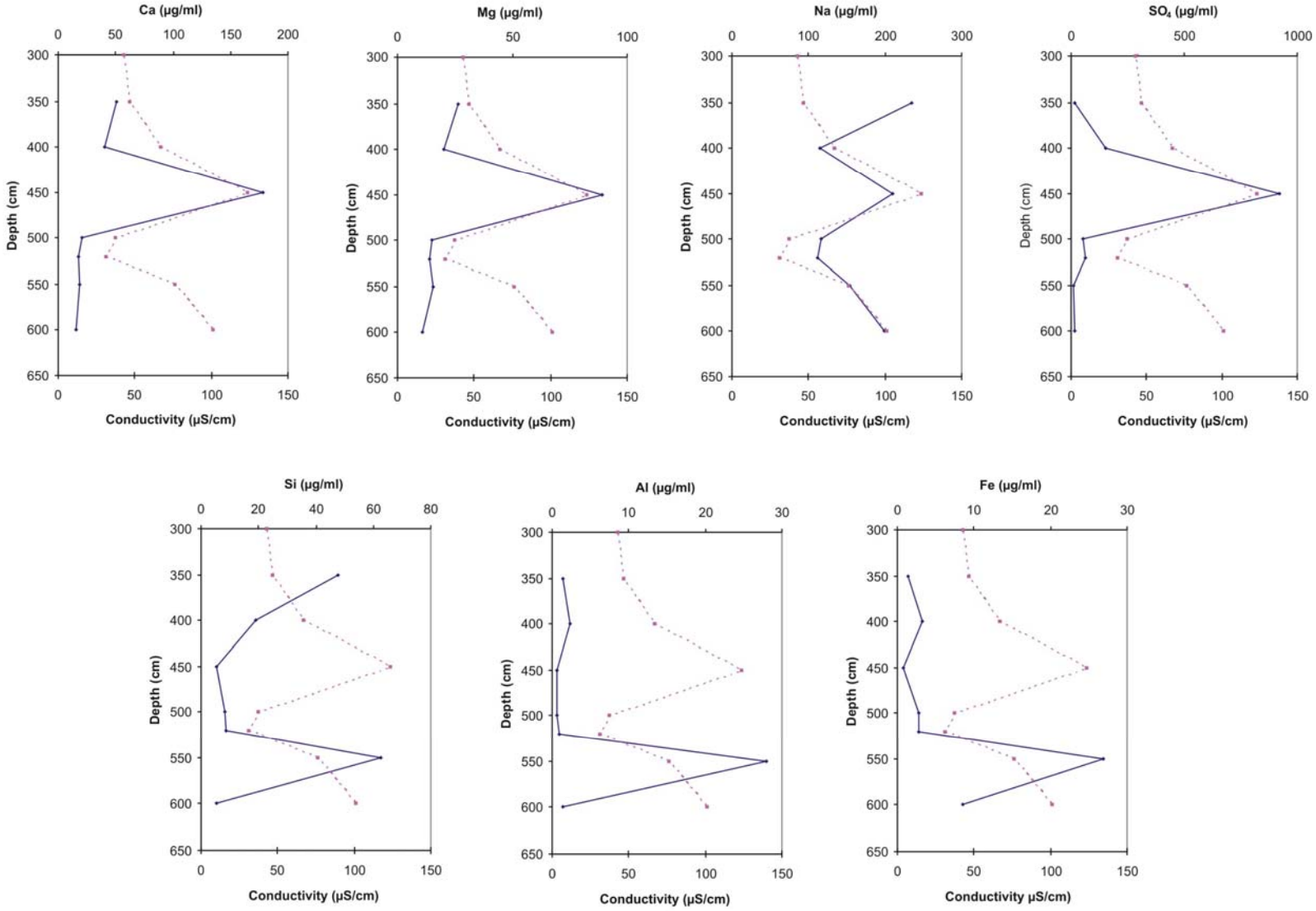

Figure 5.9(a) Variation in Core 1 porewater solute concentrations (solid line) and sediment conductivity (dashed line) with depth.

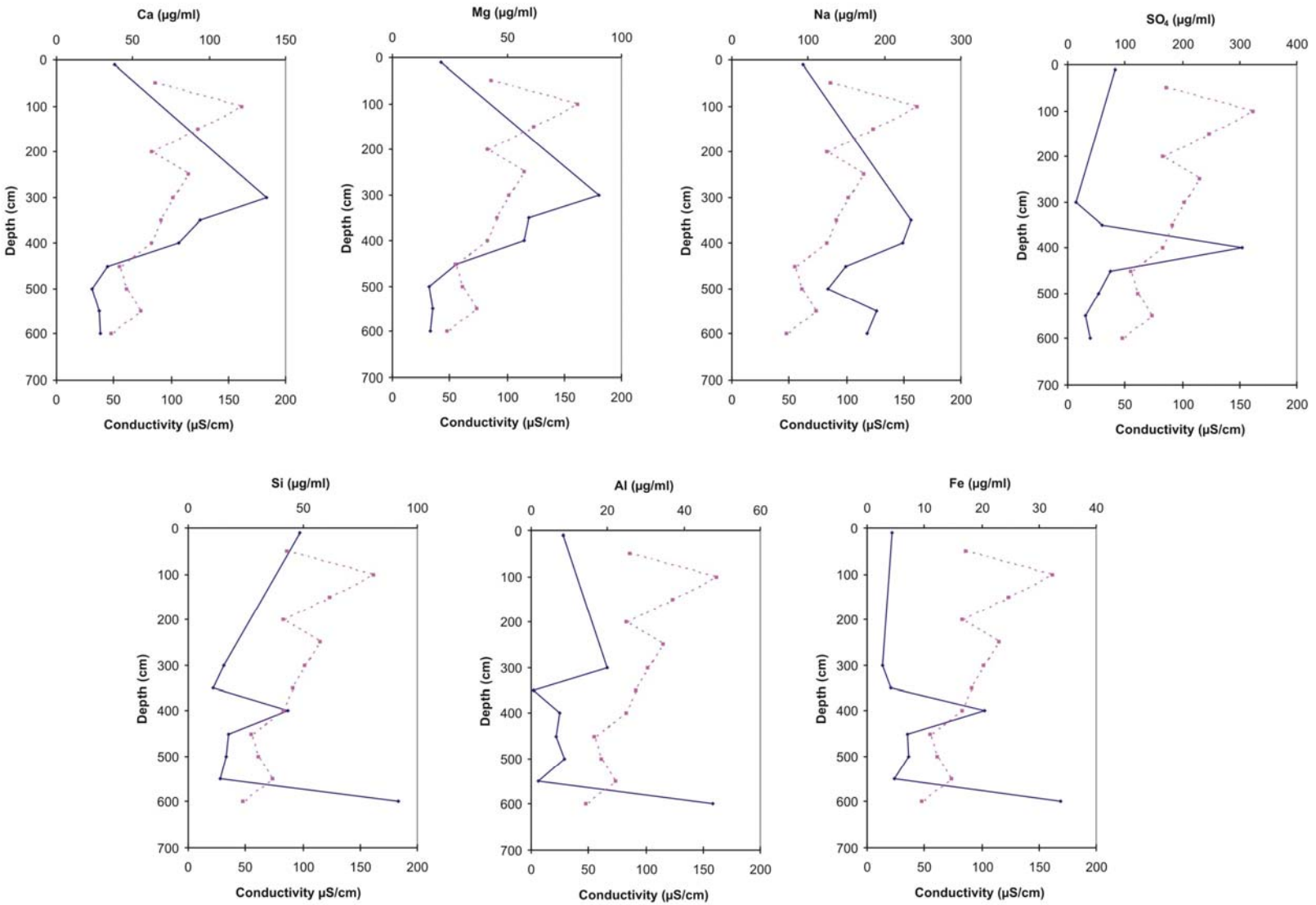

Figure 5.9(b) Variation in Core 2 porewater solute concentrations (solid line) and sediment conductivity (dashed line) with depth.

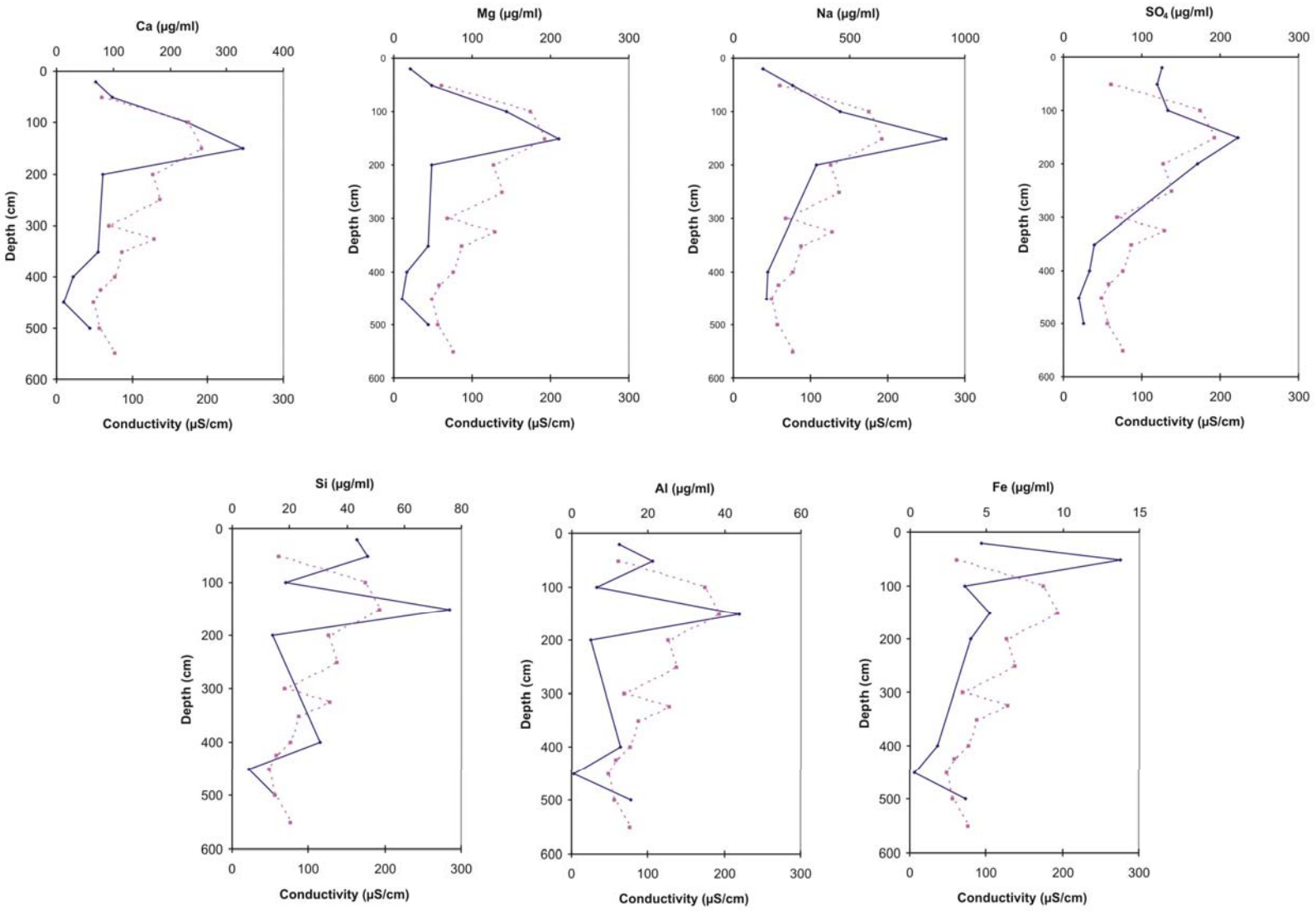

Figure 5.9(c) Variation in Core 3 porewater solute concentrations (solid line) and sediment conductivity (dashed line) with depth.

5.1.6 Geochemical modelling of groundwater and porewater

Groundwater saturation indices, as calculated using PHREEQC, are given in Table 5.4. Only minerals of interest are presented here, while a full data set is provided in Appendix 5.

Groundwater samples are undersaturated with respect to $CaCO_3$ (both calcite and aragonite). Saturation index profiles show that although porewaters from Cores 1 and 2 are also undersaturated with respect to $CaCO_3$ over the upper sections of each core, they become supersaturated with depth (Figure 5.10). There appears to be an increase in the degree of $CaCO_3$ saturation in the porewaters with increasing distance from the channel, with all porewater analysed from Core 3 being supersaturated with respect to $CaCO_3$.

Groundwater and porewaters are undersaturated with respect to amorphous silica, although porewater tends to be less undersaturated than groundwater, with some samples reaching equilibrium in respect with this phase (Figure 5.11). Gypsum remains undersaturated in both groundwater and porewater samples. Saturation indices for smectite suggest that conditions are favourable for the stability and/or formation of this clay mineral.

Table 5.4 Groundwater mineral saturation indices for selected minerals*

Mineral	Core 2	Core 3	Core 4
Calcite ($CaCO_3$)	-0.82	-1.16	-0.78
Aragonite ($CaCO_3$)	-0.96	-1.30	-0.92
Gypsum ($CaSO_4$)	-1.98	-2.37	-2.38
Smectite (nontronite)	18.91	17.54	19.63
SiO_2 (amorphous)	-0.99	-0.93	-0.36

*Negative values indicate undersaturation (dissolution), while positive values are indicative of supersaturation (precipitation)

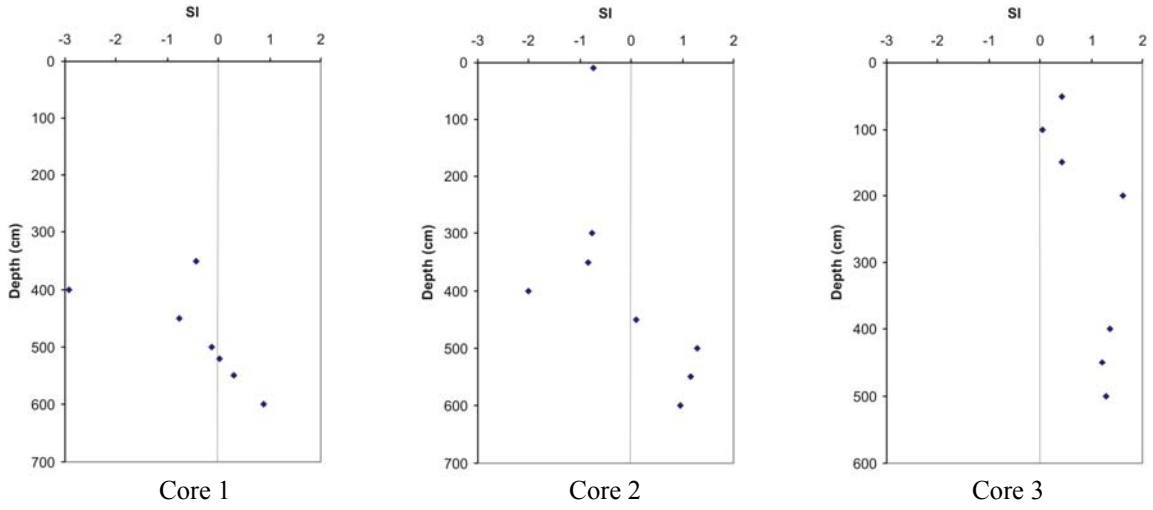

Figure 5.10 Calculated calcium carbonate saturation indices (SI) for Transect 1 porewater samples.

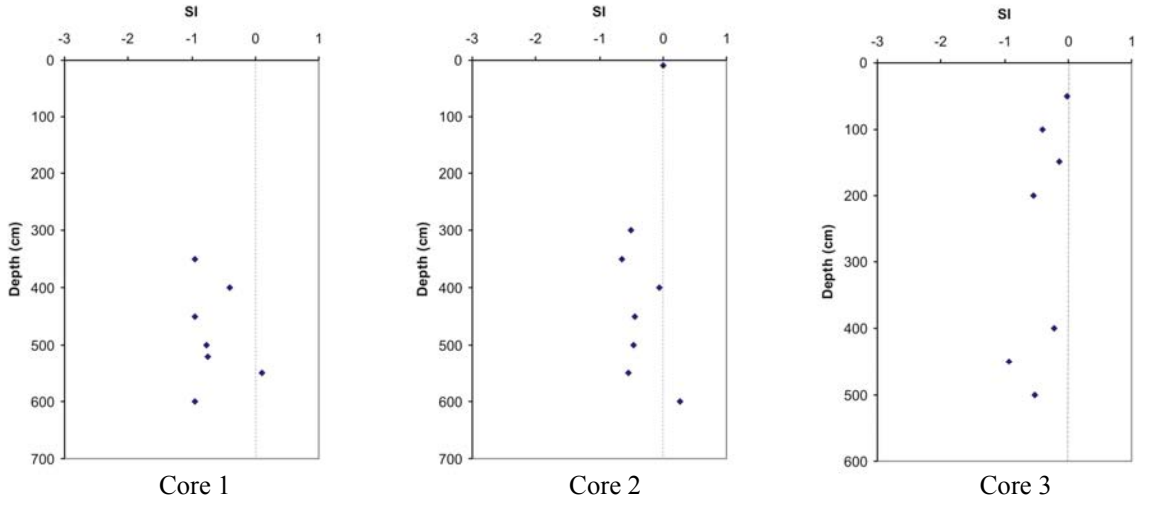

Figure 5.11 Calculated amorphous silica saturation indices (SI) for Transect 1 porewater samples.

5.1.7 Chemical fractionation

Metal percentages by fraction as a function of depth for each core are given in Appendix 6. Only elements in fractions of interest are presented and described here. The mapping programme Arc GIS™ 9.0 was used to assist in the interpolation of data and the construction of a series of isoplots showing areas of similar concentration.

- Reducible iron and manganese

Iron and manganese in the reducible fraction is considered to represent the presence of iron/manganese oxyhydroxides. Reducible iron concentrations generally decrease with distance from the channel, with higher levels present in surface sediments and at depths of 300-500 cm in Cores 1 and 2 (Figure 5.12). Enrichment at depth appears to be controlled by variation in redox potential, with peaks in concentration coinciding with dramatic changes in measured sediment redox status. Changes in redox status are due to the position of the watertable, which defines the boundary between reducing and oxidising conditions. Fluctuations in the watertable level thus control the geochemical behaviour of redox sensitive elements such as Fe and Mn, with repeated cycles of oxidation and reduction giving rise to mottles and concretions that are observable within the sediment profiles (Vepraskas & Faulkner, 2001).

Surface enrichment in iron oxyhydroxides are likely the result of biological activity. Infiltration of rainfall and occasional overbank flooding is likely to create periods which encourage the development of reducing conditions in surface sediments. Plants, however, require oxygen and wetland plants are adapted to surviving in stressful anoxic conditions by being able to release oxygen from their roots (Armstrong, 1975). This reoxidises reduced electron acceptors formed during the degradation of organic matter, resulting in the formation of Fe oxyhydroxide precipitates in the vicinity of plant roots.

Despite being present in relatively high concentrations, Fe oxyhydroxides account for a relatively small proportion of total iron. Most iron (80-95%) is accounted for by the residual fraction, and it is only in zones of alternating redox conditions that Fe oxyhydroxides show any appreciable contribution to overall iron concentration (about 30%). Although present in much lower concentrations, Mn oxyhydroxides account for the majority (up to 88%) of total manganese present

in all cores. Manganese is generally oxidised more slowly than Fe, resulting in the precipitation of these oxides at a higher position in the sediment profile.

Overall, Fe oxyhydroxides appear to be less important in cores further away from the channel, as indicated by lower Fe concentrations in the reducible fraction. This decline in iron oxyhydroxide concentration is likely to be due to the depletion of Fe in groundwater as it moves away laterally from the channel. Iron readily precipitates from solution in the presence of oxygen, and much of this seems to occur in close proximity of the channel. Water reaching areas further away from the channel is therefore depleted in soluble iron. This is supported by groundwater chemistry, which shows a reduction in concentration of both Fe and Mn with increasing distance from the channel. Sediments further away from the active channel are also likely to receive water less frequently and thus undergo changes in redox status less often.

- Oxidisable sulphur

Oxidisable iron and sulphur exhibit fairly similar patterns of distribution in Cores 1 and 2, suggesting that Fe partly precipitates as iron sulphide. This mineral is influenced by similar factors to those governing Fe oxyhydroxide precipitation, resulting in a similar distribution (Figure 5.13). Particularly high Fe sulphide concentrations occur in close proximity to the river channel at a depth of 400-500 cm, where water table fluctuations create anoxic conditions necessary for their formation. The formation of Fe sulphide adsorbed onto clay or silt particles is likely to be responsible for imparting the black colour to sediment, as observed in some of the samples. Elevated concentrations of Mn at these depths suggest that Mn sulphide may also be a possible mineral formed under these conditions.

Iron sulphide concentrations are also high in surface deposits, where the presence of organic matter is likely to promote bacterial sulphate reduction, providing conditions conducive to the precipitation and adsorption of sulphides. There is little correlation between oxidisable Fe and S in Cores 3 and 4, suggesting that sulphide minerals may be of limited importance further away from the channel.

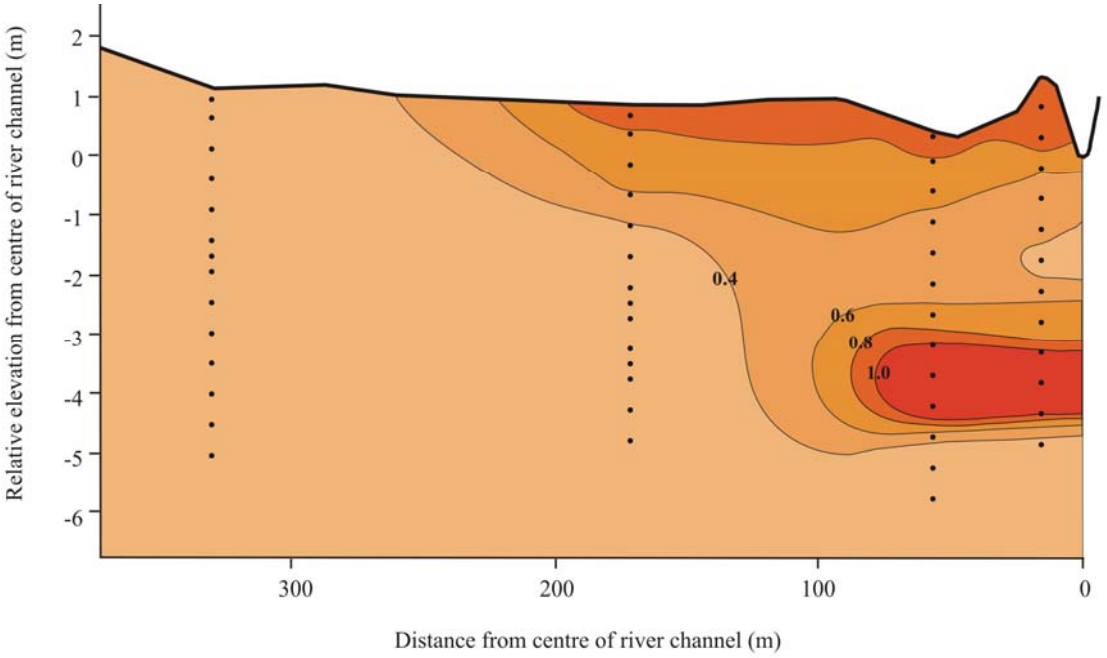

Figure 5.12 Isoplot showing the distribution of iron associated with the reducible fraction (expressed as % weight Fe) at Transect 1

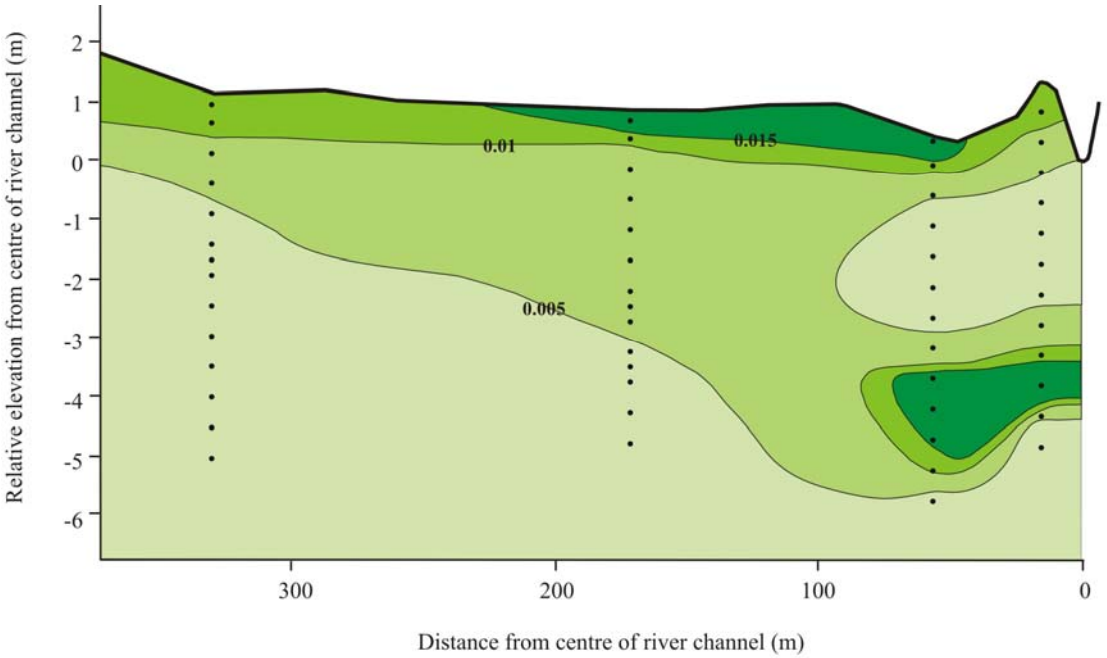

Figure 5.13 Isoplot showing the distribution of sulphur associated with the oxidisable fraction (expressed as % weight S) at Transect 1

- Acid soluble calcium and magnesium

Figure 5.14 shows the distribution of acid soluble Ca, with high concentrations being related to the presence of calcium carbonate. The majority of total calcium present in sediment samples seems to be found in this phase, with regions of high carbonate occurrence accounting for a high proportion of total calcium.

There is good correlation between the distribution of acid soluble calcium and magnesium, indicating the inclusion of magnesium in the carbonate phase. Although the concentration of Mg is substantially lower than that of Ca, carbonate accounts for a large proportion of total Mg. Appreciably higher concentrations of Ca and Mg are found in cores further away from the channel, indicating higher quantities of carbonate accumulation in these areas. In general, the percentage of Ca and Mg in the carbonate phase, as a proportion of total Ca and Mg present, also increases with distance from the channel, accounting for up to 90% of total Ca and 40-50% of total Mg in regions of high carbonate accumulation. While the carbonate fraction is important at certain depths, it often diminishes in favour of the reducible fraction. Adsorption with iron and manganese oxyhydroxides appears to be an important process controlling the distribution of calcium and magnesium.

Increases in Ca and Mg concentration are also accompanied by similar increases in acid soluble sulphur, suggesting some degree of sulphur sequestration in this phase, probably in the form of sulphate. In Cores 1 and 2, the carbonate fraction also shows clear peaks in Mn and Fe concentrations, which appear to coincide with large drops in redox potential. This is most likely explained by the development of anoxic conditions, which prevent Fe and Mn precipitating as oxyhydroxides. Instead, these species are probably sequestered in the carbonate phase by adsorption. Carbonate thus probably acts as an important adsorbent for Mn (up to 40% of total Mn) and Fe. Similar observations in other wetland environments have been reported by Wang *et al.* (2004).

5.1.8 Evapotranspiration and controls on chemical precipitation

Groundwater conductivity increases with distance from the river channel and a similar trend is seen in sediment conductivity (Figure 5.15). Sediment conductivity markedly increases, such that

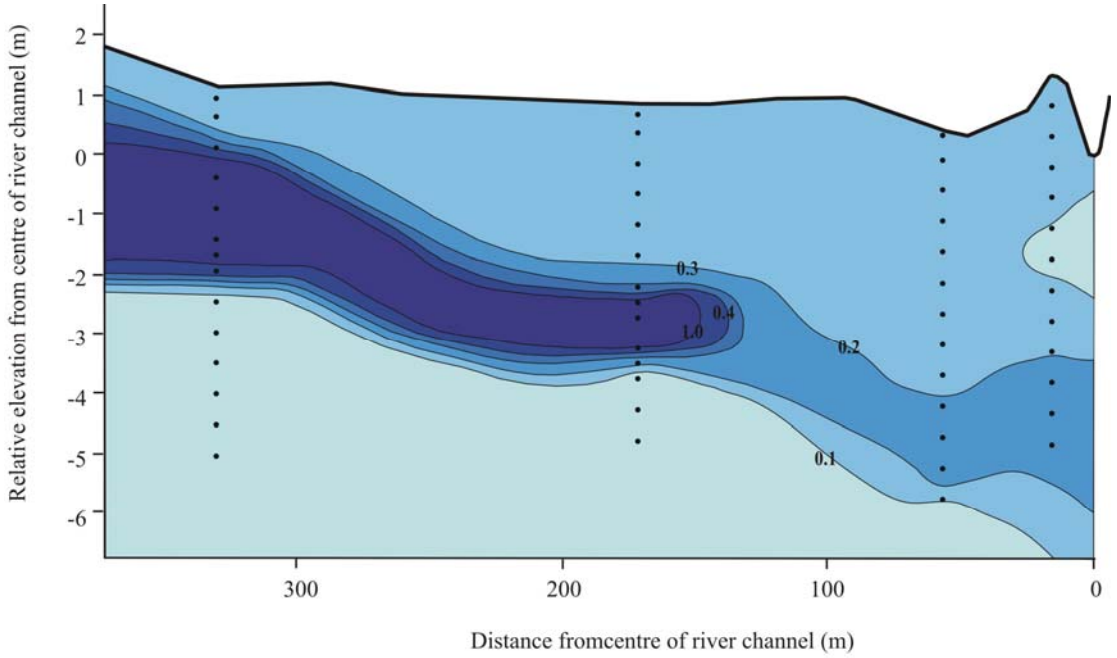

Figure 5.14 Isoplot showing the distribution of acid soluble calcium (expressed as % weight Ca) at Transect 1

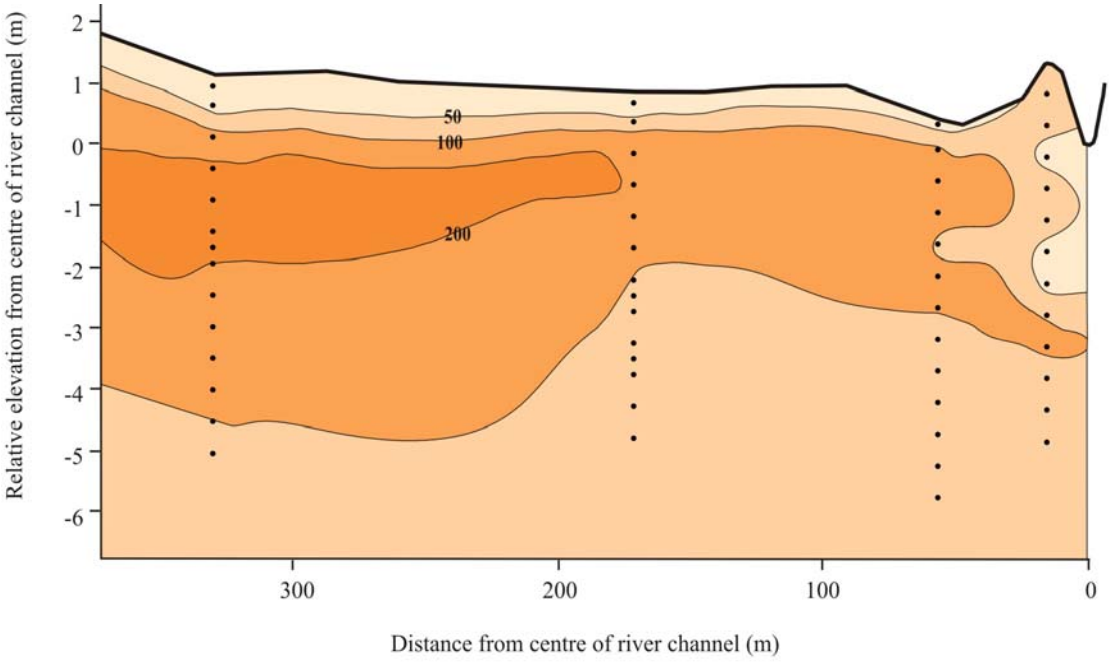

Figure 5.15 Isoplot showing the distribution of sediment conductivity (µS/cm) at Transect 1

conductivity in Core 4 is typically four times higher than conductivities encountered in Core 1. Areas of elevated conductivity appear to be confined to a subsurface band, which increases in prominence towards the floodplain margin. Sediments above and below this zone have very low conductivities. Overall distribution in sediment conductivity within the profile is considered to reflect water loss by evapotranspiration, with the band of high conductivity representing the rooting depth of plants. Due to groundwater recharge and continual evapotranspiration, sediment conductivity increases away from the river channel. Rainfall probably also plays a role in diluting and flushing soluble solutes downwards, such that the overall pattern observed in Figure 5.15 is a consequence of the interaction between groundwater flow, evapotranspiration and rainfall flushing.

The presence of $CaCO_3$ seems to be concentrated within a subsurface layer, which decreases in depth towards the floodplain margin. Similar trends in sediment conductivity and $CaCO_3$ support the idea that $CaCO_3$ in these sediments has precipitated under the influence of evapotranspiration. Higher sediment conductivities, representing higher evapotranspiration rates, results in greater $CaCO_3$ precipitation.

Surface sediments are generally depleted in $CaCO_3$ and this is most likely the result of local changes in CO_2 concentration. Dissolved CO_2 levels in soil solutions are typically an order of magnitude higher than atmospheric values due to plant root and microbial respiration. This lowers pH and results in greater calcite solubility (Stumm, 1996), thus explaining the build up of Ca and Mg observed in sediment porewaters. The behaviour of $CaCO_3$ in East African wetlands has been shown to be closely linked to CO_2 status, where the dissolution of carbonate minerals is driven by high CO_2 production in the root zone (Deocampo, 2005; Deocampo & Ashley, 1999). Precipitation of $CaCO_3$ thus takes place below the rooting zone, where the progressive increase in concentration of Ca in soil solution occurs as a result of water loss by evapotranspiration. Increases in soil pH with depth also promote $CaCO_3$ precipitation at depth, and in deeper anoxic sediments, carbonate precipitation may be assisted by sulphate reduction which results in increased alkalinity (Berner, 1971). Resulting precipitation of $CaCO_3$ depletes porewaters of Ca and Mg, causing decreases in Ca and Mg porewater concentrations (Figures 5.9 a-c).

There is high correlation between Ca and Mg in both groundwater and porewater samples (Figure 5.16). The Mg/Ca ratio in groundwater samples is 0.47, with this number increasing to 0.61 in porewater samples. This indicates the preferential removal of Ca relative to Mg and is attributed to

the preferential precipitation of $CaCO_3$ from solution, which increases the relative proportion of Mg to Ca during the evapotranspirational process.

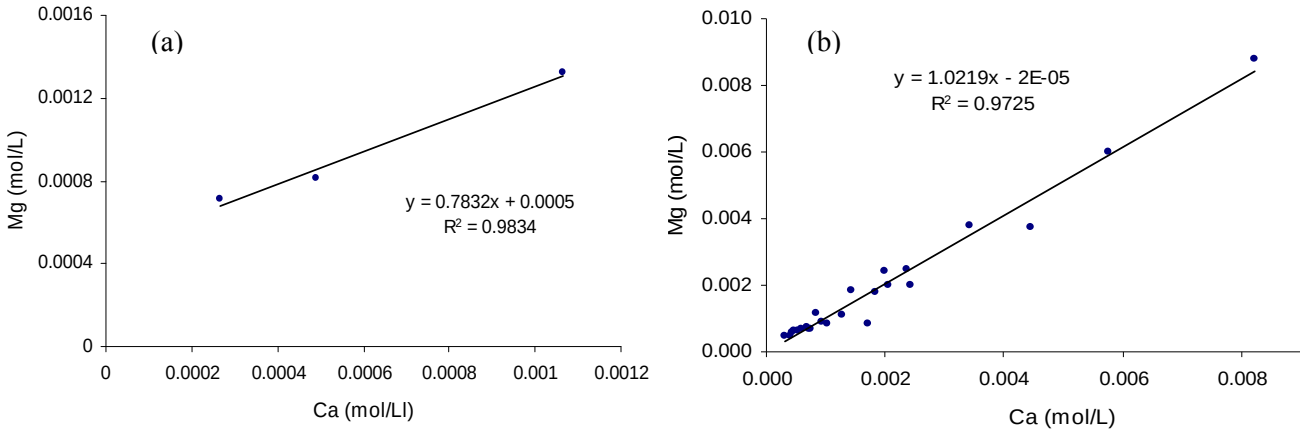

Figure 5.16 Correlation between calcium and magnesium in (a) groundwater and (b) porewater

More detailed analysis of calcium carbonate deposits reveals that precipitation of these compounds is more complex than originally suspected. X-ray diffraction carried out on handpicked samples shows that calcium carbonate is present as two polymorphs, calcite and aragonite. Calcium carbonate in Cores 1-3 is present as calcite, while Cores 4-5 contain aragonite (Figure 5.17). In both samples minor amounts of quartz and clay minerals exist as impurities.

Elemental analysis of carbonate samples shows that $CaCO_3$ present as calcite generally has a small amount of $MgCO_3$ coprecipitated with it (typically 3-4%). In nature, calcite has the tendency to accommodate Mg^{2+} into its structure to form magnesian calcite. This process has been extensively studied and is controlled in part by the Mg/Ca ratio of the water (Stumm, 1996). Preferential removal of Ca during carbonate precipitation causes the Mg/Ca ratio of the water to increase, which causes the Mg/Ca ratio of the calcite precipitate to increase (Eugster & Kelts, 1983). Thus, under conditions of continued evapotranspiration and higher porewater Mg/Ca ratios, carbonate near the river channel precipitates as low-magnesian calcite, with the Mg content of calcite increasing gradually away from the channel. Coprecipitation reactions can also be important for the removal of anions, particularly sulphate (Morse & Mackenzie, 1990), which explains the correlation between Ca, Mg and S in the carbonate fraction (see Appendix 6).

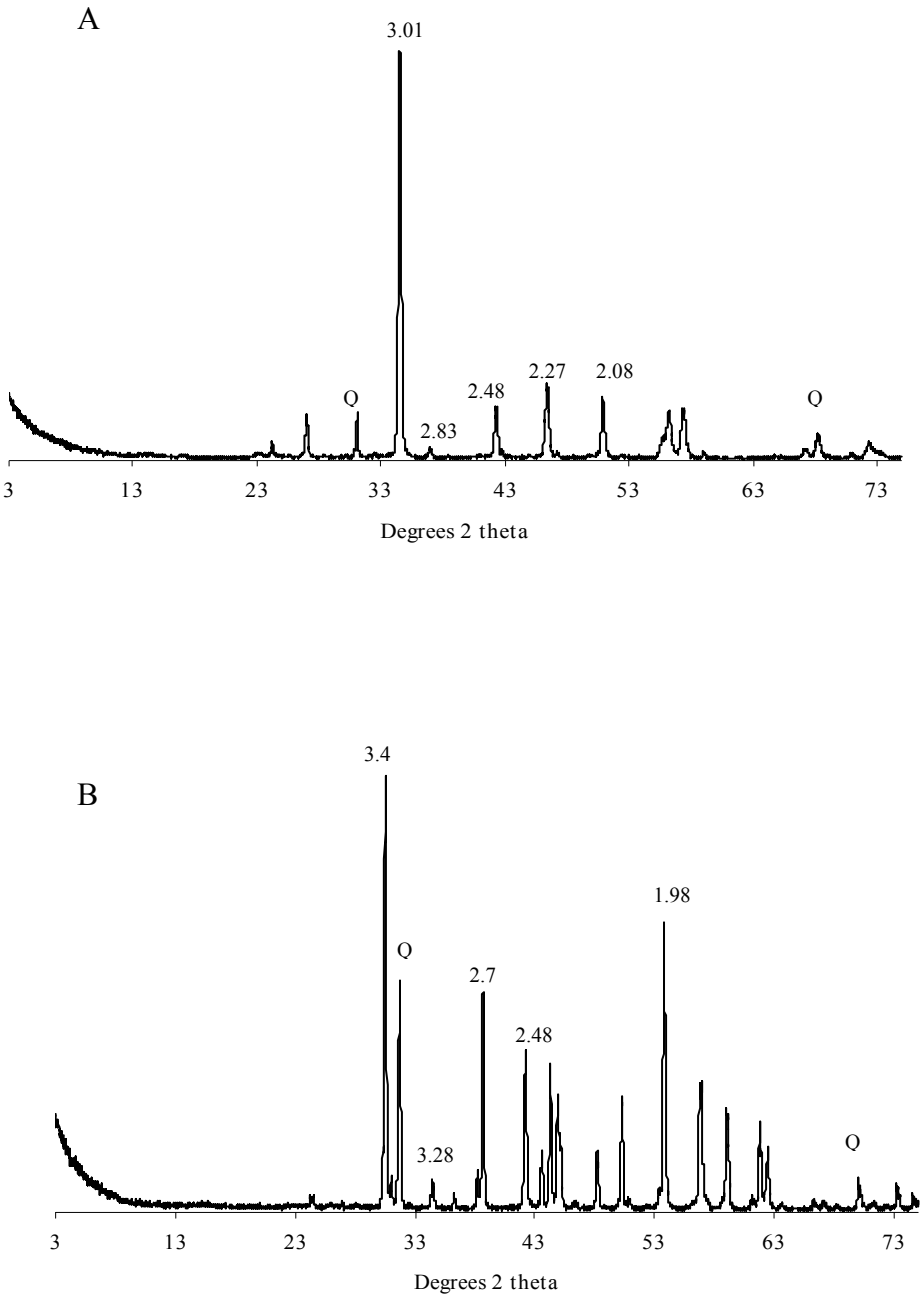

Figure 5.17 XRD patterns of (A) calcite (Core 3 at a depth of 325 cm) and (B) aragonite (Core 5 at depth of 400 cm), with the five most intense peaks for each mineral indicated. Q = quartz

In many environments the occurrence of co-existing aragonite and calcite is attributed to the diagenetic conversion of aragonite to calcite (Renaut & Jones, 1997). In such situations, carbonate accumulations would be expected to contain a mixture of both calcite and aragonite minerals. However, the presence of separate and essentially pure calcite and aragonite suggests that this is not a valid interpretation in this setting. Aragonite and calcite crystals are thus considered to represent primary precipitates, formed in response to spatial heterogeneity in the physicochemical environment.

Porewater modeling calculations show that the precipitation of both calcite and aragonite is thermodynamically favoured (Appendix 5). However, calcite is the less soluble polymorph of $CaCO_3$ and should always precipitate in preference to aragonite (Stumm, 1996). The presence of aragonite in nature is thus often considered to indicate the presence of conditions that inhibit calcite crystal growth (Morse & Mackenzie, 1990). In particular, it is well established that the presence of dissolved Mg^{2+} favours the precipitation of $CaCO_3$ as aragonite (Berner, 1985). High Mg/Ca ratios are commonly cited as the reason for aragonite rather than calcite precipitation in aquatic environments (Jørgensen, 2002; Renaut & Jones, 1997). High levels of dissolved Mg appear to have a strong retarding effect on calcite crystal growth. The Mg/Ca ratio needed to trigger aragonite in favour of calcite precipitation is unclear, although Folk (1994) argues that any solution with a Mg/Ca mole ratio of >1:1 should lead to aragonite precipitation. Based on this, the chemical composition of porewaters collected appears to reach levels conducive to aragonite precipitation, particularly in sediments further away from the river channel.

The change from calcite precipitation in Cores 1-3 to aragonite precipitation in Cores 4-5 can thus be explained by progressive changes in the composition of groundwater and porewater (see pg 72). It has already been shown that increases in the Mg/Ca ratio results in the precipitation of low-magnesian calcite close to the channel. Although no porewater information is available, it is likely that precipitation of calcite close to the channel raises the Mg/Ca ratio in the porewater to levels that inhibit calcite precipitation further away from the channel. This is consistent with the findings of Jorgensen (2002) who showed that although supersaturated with respect to both calcite and aragonite, only aragonite precipitates in the salt marshes of Denmark. This was attributed to the presence of dense plant communities that selectively removed water by transpiration, causing

progressive enrichment in Mg that inhibited calcite precipitation. High salinity and highly supersaturated solutions are also cited as factors favouring aragonite precipitation (Renaut & Jones, 1997). Thus, increases in both salinity and $CaCO_3$ supersaturation should favour aragonite precipitation in areas further away from the channel.

The precipitation of $CaCO_3$ under conditions of evaporation is often accompanied by the precipitation of other authigenic minerals (Garrels & Mackenzie, 1967; Gac *et al.*, 1977; Deocampo, 2005; Barbiero *et al.*, 2002). The identification of Mg-silicates and opaline silica suggests that evapotranspirative conditions probably also result in the precipitation of silica compounds. This is discussed in greater detail in Chapter 6.

5.2 TRANSECT TWO: THE MIDDLE REACH

5.2.1 Topography and general sediment characteristics

The transect surveyed at this site, from the river channel to the southern edge of Mdlanzi Lake, covers a distance of ~950 m (Figure 5.18). The river channel at this point is approximately 2.7 m deep and 15 m wide. Both the channel and Mdlanzi Lake were dry at the time of sampling.

The majority of sediments from this region of the floodplain are classified as silty sand and contain 50-90% total sand (Figure 5.19). Sediments show general coarsening with depth, with deeper sediments typically containing >90% sand. The majority of this coarse sediment is found within 400 m of the river channel (Cores 1 and 2). Sediments from Core 3 are characterised by intense Fe and Mn mottling, although this diminishes below 300 cm and is absent below 500 cm. Below 250 cm, sediments become very dark (black) and sticky. Mdlanzi Lake deposits (Core 4) are composed primarily of coarse sand (~40%) and silt (~25%), and contain large quantities of iron.

Clay content in all sediments ranged from 0 to 3.5%, with the majority of this clay being found within the top 200 cm of cores and in close proximity to Mdlanzi Lake. Organic carbon contents are very low, although surface sediments typically have slightly higher quantities (2-3%).

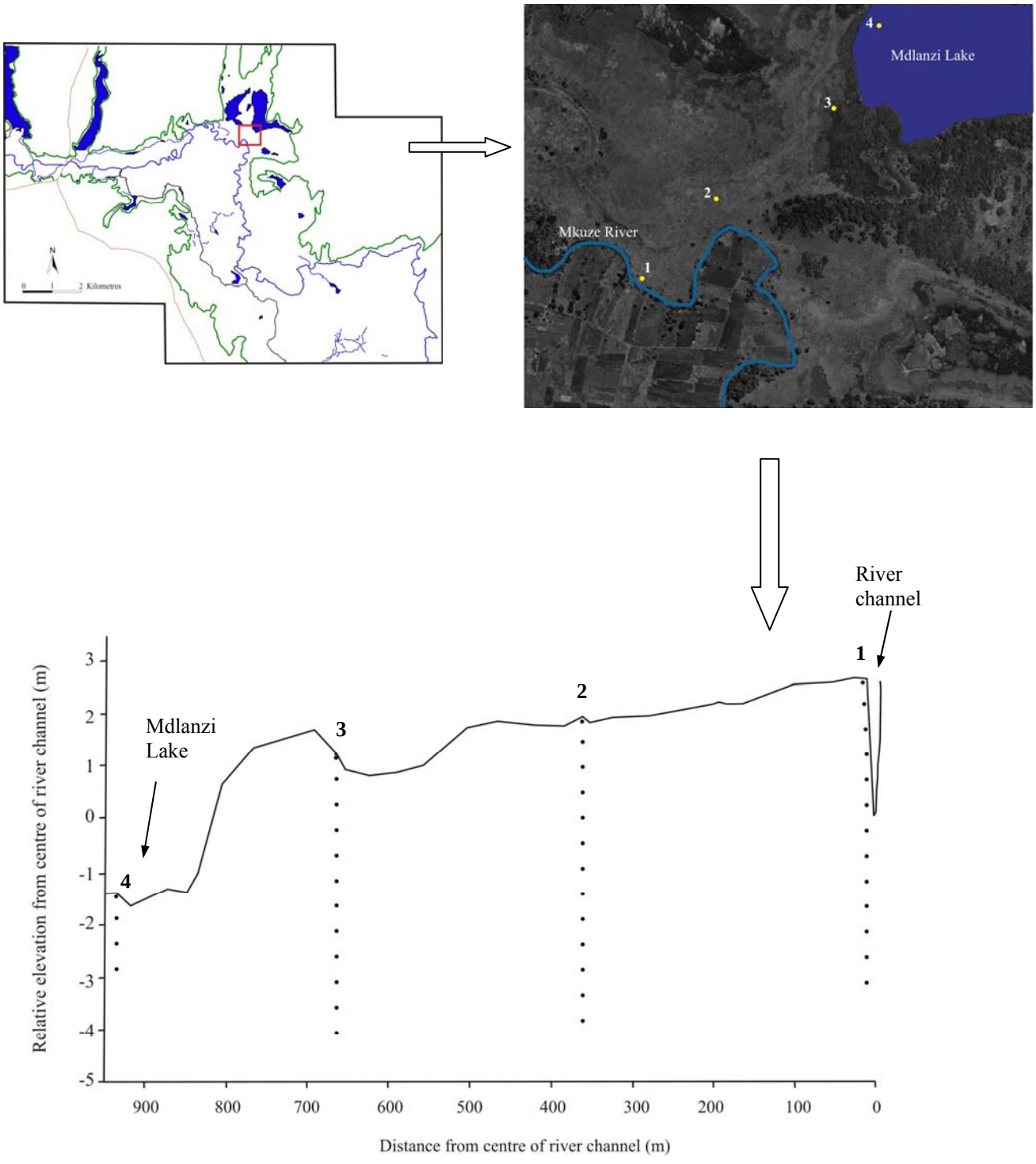

Figure 5.18 Location of sampling site on the lower Mkuze Floodplain and cores taken along the transect

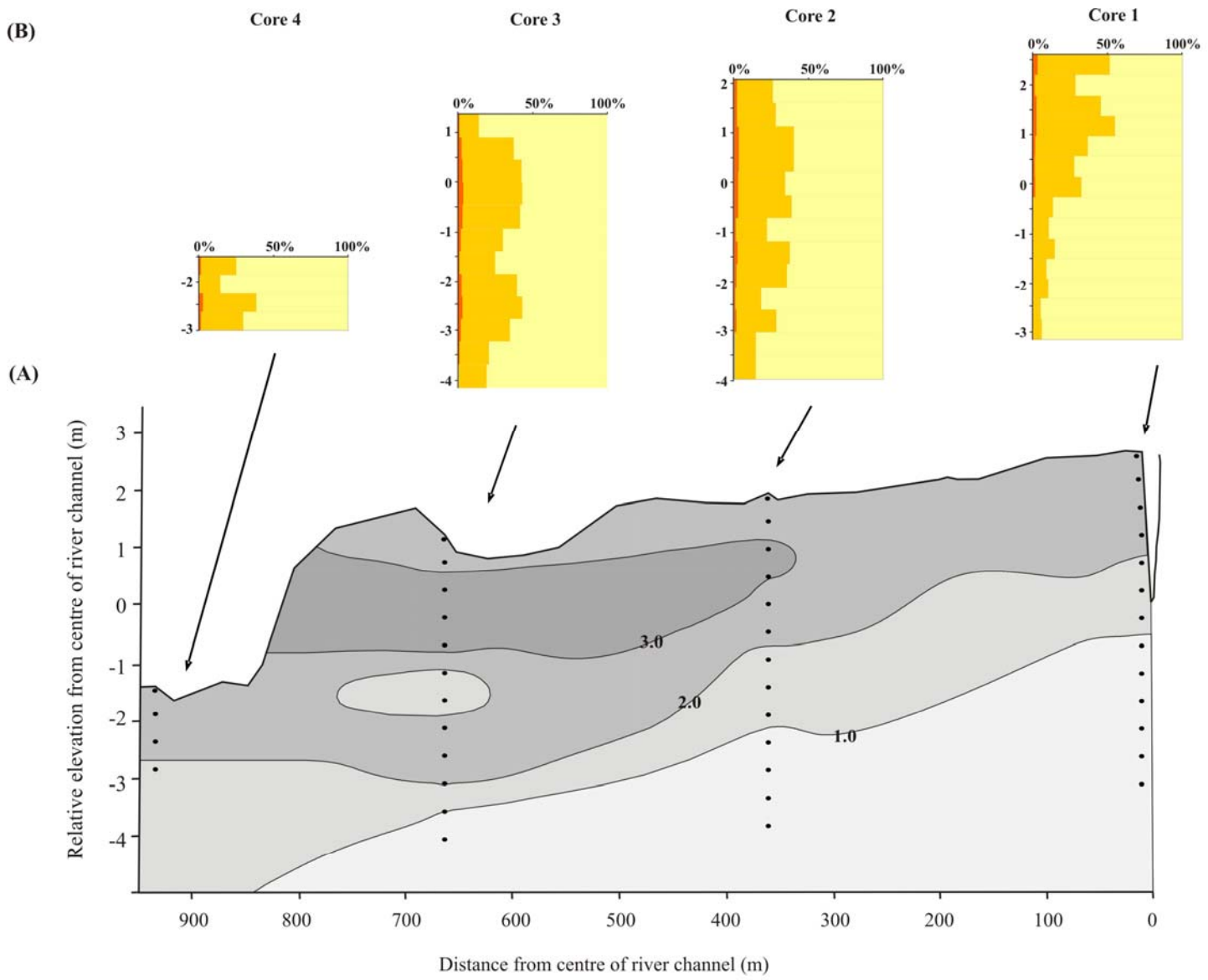

Figure 5.19 Generalised distribution of clay content (%) from sediments collected at Transect 2 (A), showing percentage clay (red), silt (orange) and sand (yellow) through each core (B).

5.2.2 Clay mineralogy and chemistry

Clay mineralogy is dominated by smectite, kaolin, vermiculite and mica, with minor amounts of hematite, goethite and K-feldspar present in certain samples. These clay minerals occur widely and show no obvious distribution pattern, although some samples from depth have slightly higher smectite contents. Most clay samples contain approximately 15% Fe_2O_3, with clay from Mdlanzi Lake sediment being particularly enriched in iron (Table 5.5). Significantly higher loss on ignition values indicate that sediments from the lake also have greater quantities of organic carbon.

Table 5.5 Major elements in the clay fraction (<2 μm) of sediment samples (as % weight)

Sample depth (cm)	SiO_2	Al_2O_3	Fe_2O_3	MnO	MgO	CaO	Na_2O	K_2O	TiO_2	LOI*
Core 1										
0	50.05	27.04	14.53	0.08	2.67	0.82	0.39	3.18	0.98	17.32
100	50.70	27.63	14.32	0.09	1.99	0.95	0.23	2.39	1.03	18.72
400	50.96	28.52	13.64	0.10	2.05	0.82	0.23	2.46	1.04	16.15
Core 2										
0	51.15	29.21	12.98	0.08	1.91	0.71	0.00	2.87	0.89	17.08
300	42.08	28.07	14.79	0.11	7.69	0.67	2.76	2.51	1.03	19.53
500	53.64	23.02	15.78	0.09	2.70	1.65	0.09	1.78	0.99	19.08
Core 3										
100	55.42	26.88	11.01	0.07	1.83	0.77	0.45	2.49	1.11	16.28
200	53.47	25.47	13.86	0.08	2.49	0.65	0.53	2.32	1.10	16.21
500	54.62	23.10	15.95	0.09	2.03	1.04	0.17	2.02	0.96	19.39
Core 4										
100	42.26	23.80	19.87	0.18	7.12	0.96	2.37	2.22	0.91	30.14

*Loss on ignition

5.2.3 Sediment redox and pH

Overall, sediment pH decreases towards Mdlanzi Lake (Figure 5.20). Sediment pH remains fairly constant at ~7.2 in the upper 350 cm of Core 1, but then declines steadily to 5.95 at 600 cm. Sediment from Cores 2 and 3 are characterised by similar trends in pH. Sharp increases in pH in the upper 50 cm are followed by a steady decline with increasing depth, reaching a minimum of 5.9 at 450 cm in Core 2 and 5.0 at 300 cm in Core 3. Sediment pH thereafter gradually increases with

depth. In Core 4, sediment pH remains fairly constant (~6.5) throughout the shallow depth analysed, while redox potential shows a sharp drop from moderately reducing conditions at the surface to strongly reducing conditions (-33 mV) at a depth of 150 cm. Large quantities of iron precipitated out of these sediments after sampling. No redox data for Cores 2-4 were obtained due to unforeseen circumstances in the field.

5.2.4 Groundwater chemistry

There appears to be little systematic variation in groundwater chemistry (Table 5.6), with no obvious trends in Ca, Mg or Si. Groundwater conductivity gradually increases from 0.527 mS/cm near the river channel to a maximum of 2.48 mS/cm at Core 3 (Figure 5.21). Maximum levels of Na (256.4 µg/ml) and Cl (814.6 µg/ml) are found in the groundwater of Core 3, which is also characterised by a relatively high concentration of Fe (27.17 µg/ml). Groundwater pH across this portion of the floodplain remains slightly acidic, varying between 5.94 and 6.43 in all samples.

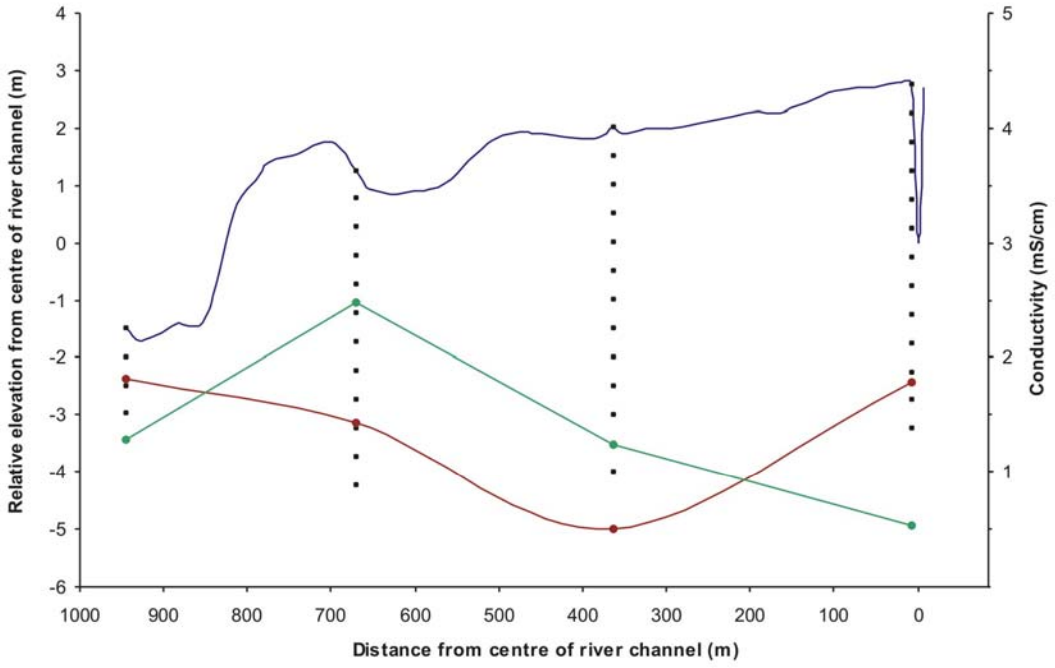

Figure 5.21 Transect profile showing groundwater conductivity (—) and elevation of the watertable (—)

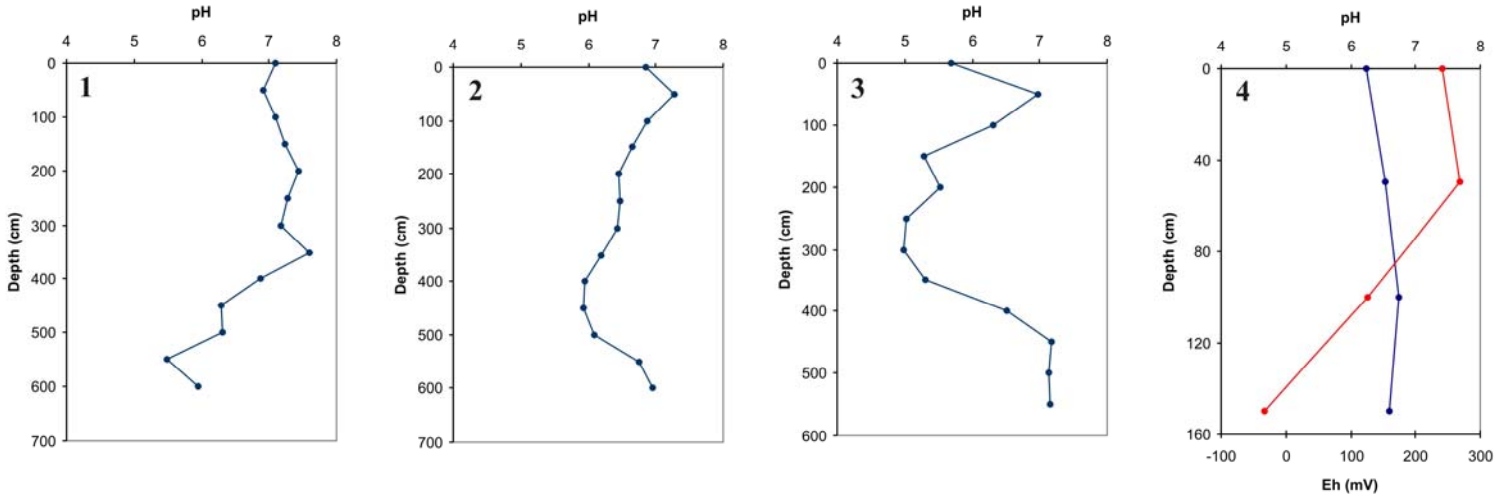

Figure 5.20 Variation of sediment pH (—) and redox potential (—) with depth in Cores 1-4 taken from Transect 2.

Table 5.6 Groundwater chemical composition for Transect 2 (concentrations expressed in µg/ml)

	Si	Mg	Ca	Fe	Al	Mn	K	Na	Cl	NO_3	SO_4	Alkalinity*	pH	EC (mS/cm)
Core 1	11.0	76.7	121	0.136	0.248	15.0	21.3	87.3	141	4.50	650	50.0	5.94	0.527
Core 2	17.2	52.6	99.6	0.422	<0.1	8.51	4.23	84.6	165	<5	26.7	432	6.12	1.234
Core 3	24.7	65.3	126	27.2	<0.1	3.41	9.52	256	814	4.54	95.0	46.0	5.92	2.48
Core 4	17.8	41.0	90.4	5.63	0.450	3.80	19.5	178	397	14.9	203	112	6.43	1.285

*Alkalinity expressed as $CaCO_3$ µg/ml

5.2.5 Porewater chemistry

Porewater from Cores 1, 3, and 4 was extracted and analysed. These data are shown in Figure 5.22(a-c) overlain with sediment conductivity measurements.

- Core 1

Porewater profiles for Ca, Mg and SO_4 are all similar and show gradual decreases in concentration with depth to 350 cm. Below this, concentrations increase with further increases in depth. There is little correlation between solute concentration and sediment conductivity, which may be due, in part, to the number of porewater samples that could be analysed. Both Fe and Mn profiles are characterised by relatively high concentrations near the surface (Fe = 8 μg/ml, Mn = 20 μg/ml), but this declines with depth, such that porewaters below 350 cm contain very little (<1 μg/ml) of either solute. There does not appear to be any systematic trend in Na or Si through the core.

- Core 3

There is good correlation between the porewater solutes Ca, Mg, S, Na, and sediment conductivity. These solutes all show decreases in concentration with increasing depth. Sodium, for example, decreases from over 500 μg/ml at 100 cm to ~60 μg/ml at 550 cm, which corresponds with a fourfold decrease in sediment conductivity over this range. The solutes of Si, Fe and Mn do not show this trend. Si concentration shows a broad peak in concentration between 200 and 500 cm, while a single sharp peak in Fe concentration (~13 μg/ml) occurs at 450 cm.

- Core 4

This core is too shallow to show any meaningful changes in porewater concentrations. Nevertheless, over the depth of sediment sampled, most porewater solutes show declines in concentration with depth. For Ca, Mg, S and Na, porewater concentrations at 150 cm are typically half of those at 50 cm. Marked decreases in Si, Al and Fe concentrations over the top 100 cm are also noticeable.

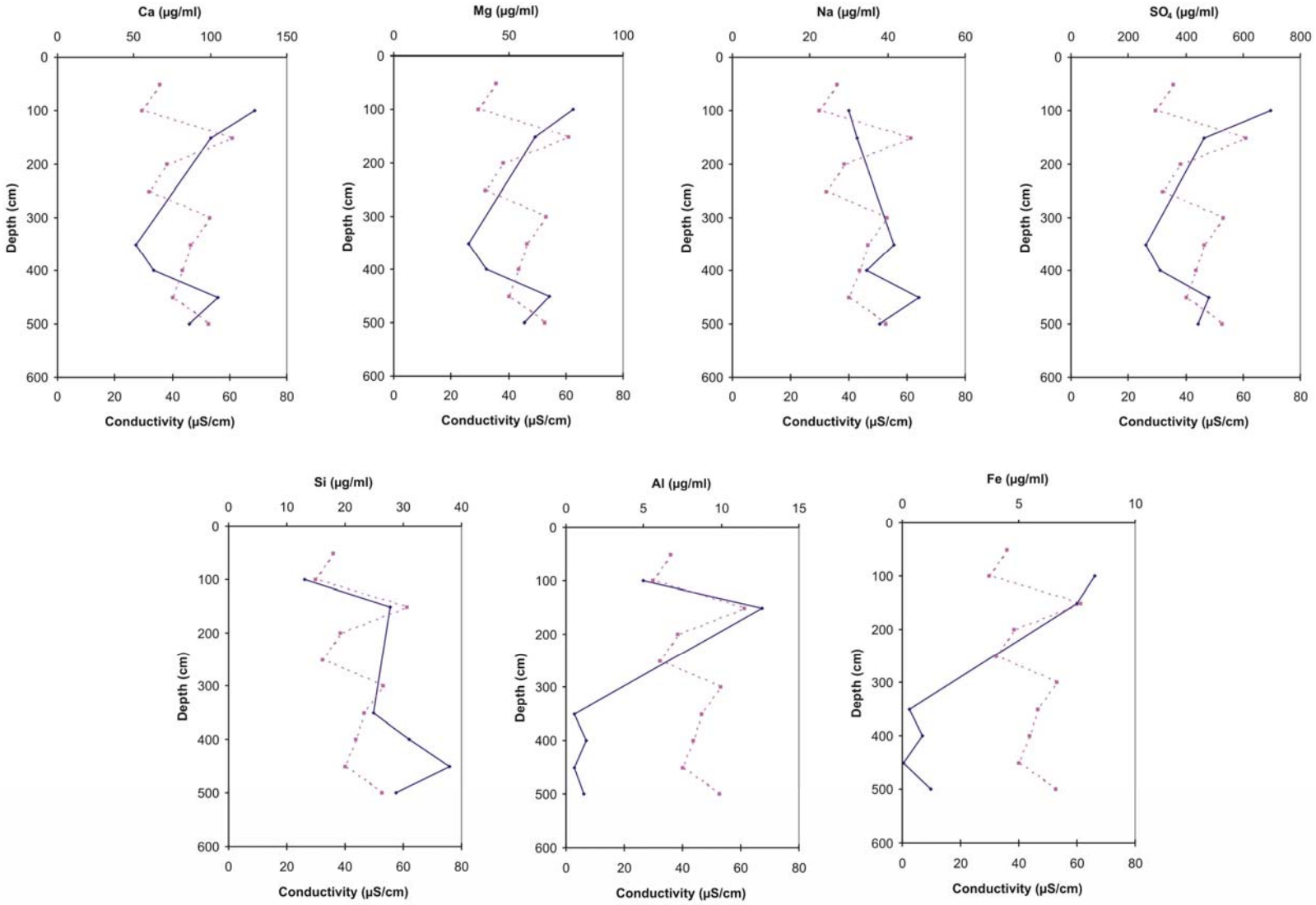

Figure 5.22(a) Variation in Core 1 porewater solute concentrations (solid line) and sediment conductivity (dashed line) with depth.

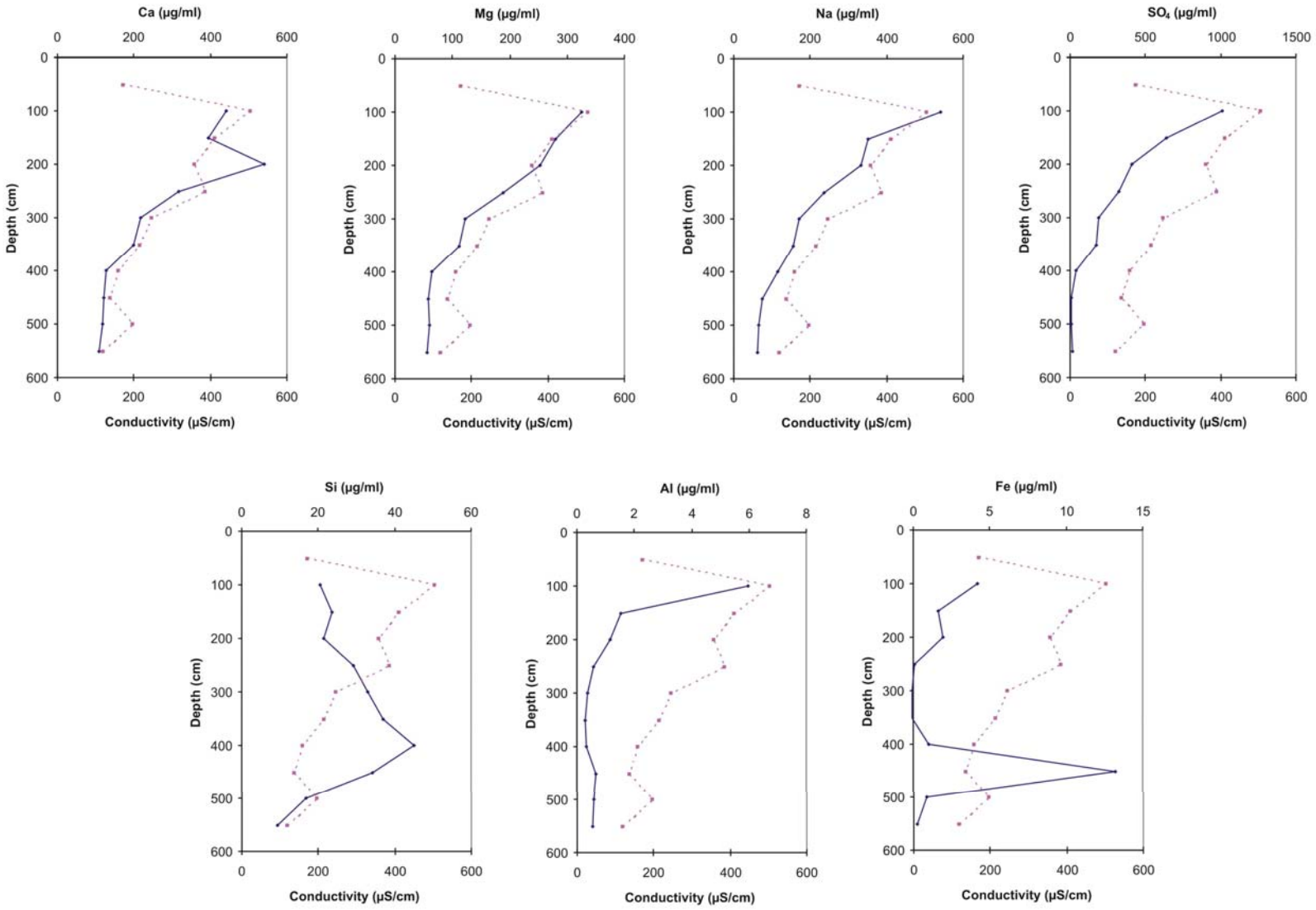

Figure 5.22(b) Variation in Core 3 porewater solute concentrations (solid line) and sediment conductivity (dashed line) with depth

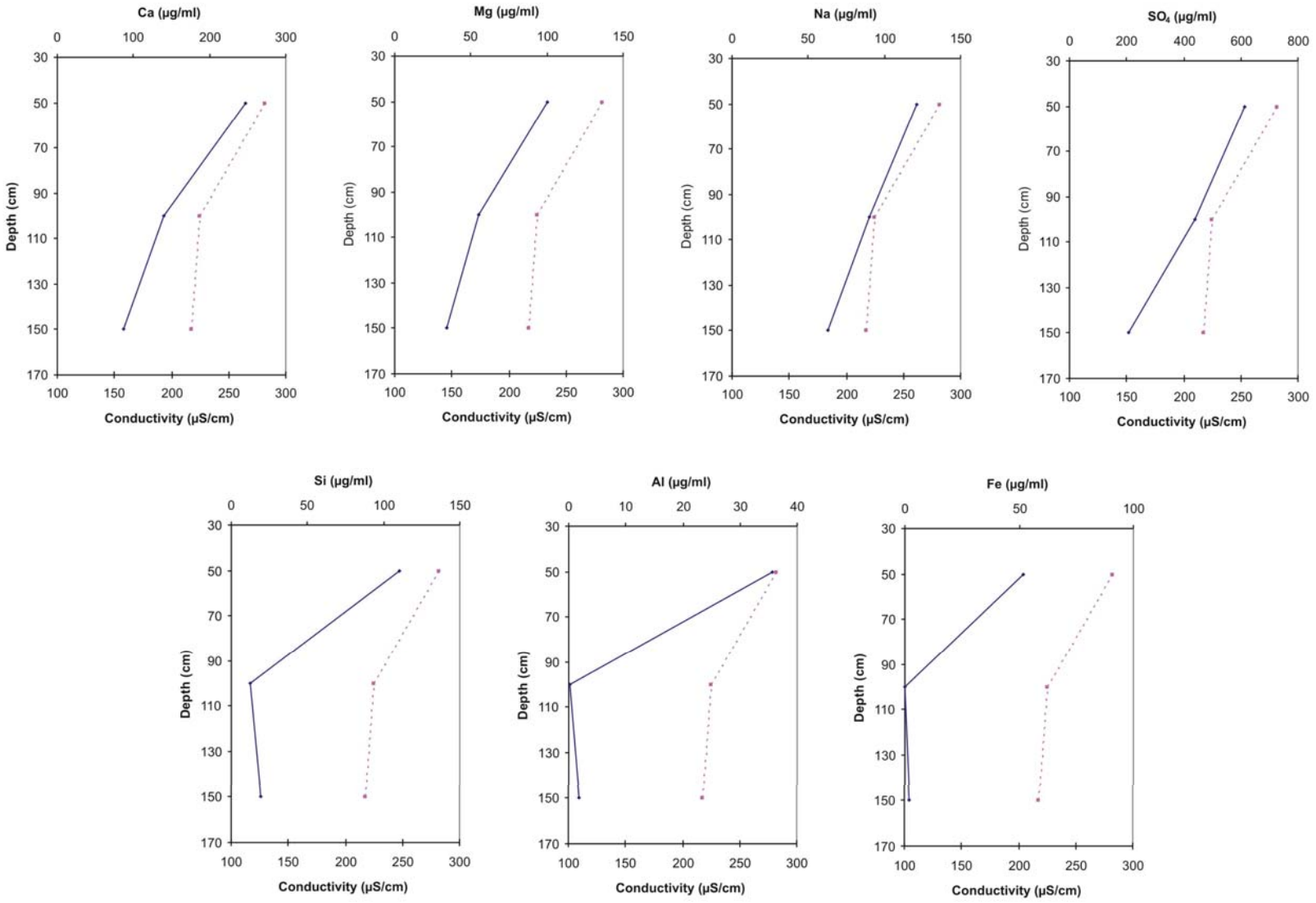

Figure 5.22(c) Variation in Core 4 porewater solute concentrations (solid line) and sediment conductivity (dashed line) with depth

5.2.6 Geochemical modelling of groundwater and porewater

Calcium carbonate, gypsum and amorphous silica do not attain saturation in any of the groundwater samples collected (Table 5.7). All porewaters also appear to be undersaturated with respect to these minerals (Figures 5.23 and 5.24).

Table 5.7 Calculated groundwater mineral saturation indices for selected minerals

Mineral	Core 1	Core 2	Core 3	Core 4
Calcite ($CaCO_3$)	-2.26	-1.06	-2.21	-1.46
Aragonite ($CaCO_3$)	-2.40	-1.20	-2.35	-1.60
Gypsum ($CaSO_4$)	-0.57	-1.87	-1.35	-1.09
Smectite (nontronite)	7.46	6.41	6.89	10.13
SiO_2 (amorphous)	-0.64	-0.45	-0.29	-0.44

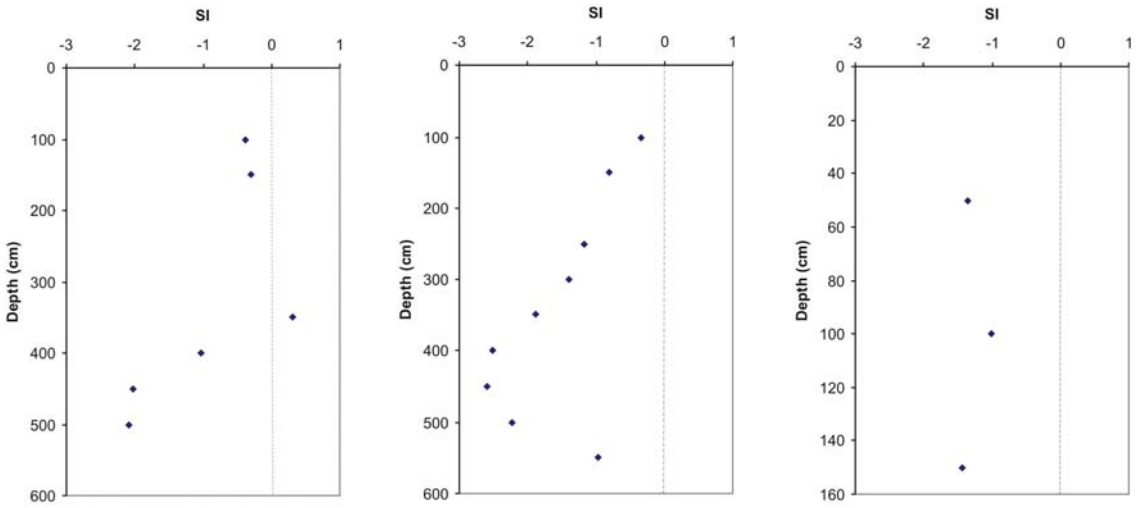

Figure 5.23 Calculated calcium carbonate saturation indices for Transect 2 porewater samples

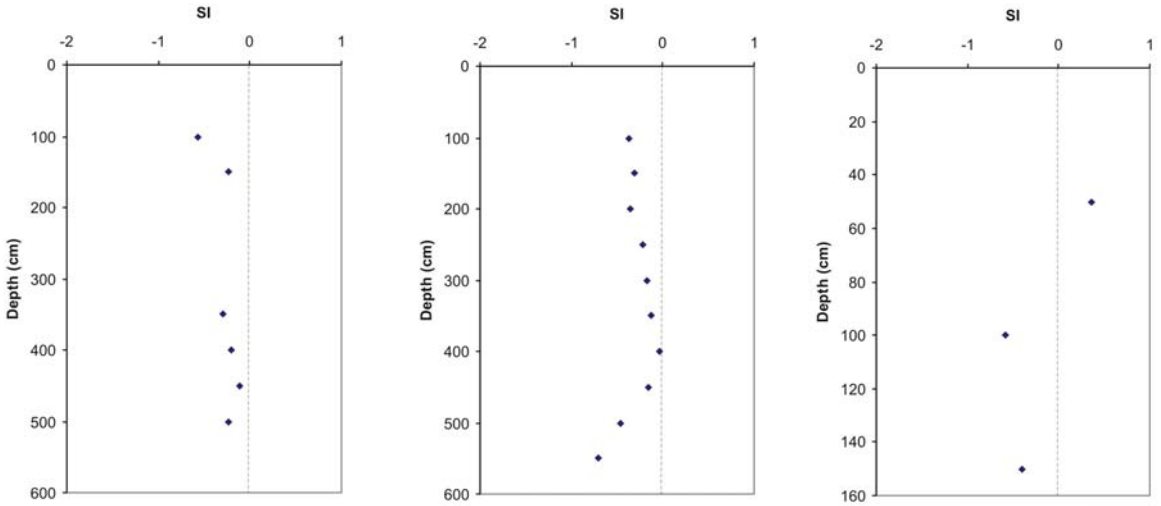

Core 1 Core 3 Core 4

Figure 5.24 Calculated amorphous silica saturation indices for Transect 2 porewater samples

5.2.7 Chemical fractionation

- Reducible iron and manganese

There is striking heterogeneity in the quantity of reducible iron contained in these sediments (Figure 5.25), with reducible iron becoming much more abundant with proximity to Mdlanzi Lake. There is over a five-fold increase in iron concentration from the river channel to the Lake, such that sediments from Mdlanzi Lake contain over 3% (w/w) reducible iron. In these sediments, approximately 45% of all Fe is present in this fraction. Most other sediments contain <0.8% reducible iron, although slightly higher concentrations are found close to the watertable near the river channel. Relative to iron, the quantity of reducible Mn present is low, and there does not appear to be much variation in concentration between cores.

Sediment and groundwater samples collected in the vicinity of Mdlanzi Lake contained relatively high concentrations of Fe and Mn. It appears as though water from Mdlanzi Lake, which represents the terminal floodplain margin lake of a tributary stream draining onto the floodplain, is an important source of soluble iron. The drainage line itself contains peat accumulations of more than 5 m thick (Fischer, 2000). The presence of this organic material results in the water and sediment from this region being acidic, and this is likely to encourage the solublisation of iron-containing minerals. Most of this soluble Fe appears to precipitate out in sediment close to the lake in response to seasonal water level changes and associated redox transformations.

- Oxidisable sulphur

Oxidisable sulphur shows a similar distribution trend to that of reducible iron, and is concentrated predominantly in close proximity to Mdlanzi Lake (Figure 5.26). Up to 80% of all sulphur in lake sediments may be present as iron sulphides. The very dark sediments collected from the region are probably the result of the large quantity of Fe sulphides that these deposits contain. In Cores 1-3, oxidisable sulphur is concentrated in sediments from the top 100 cm of each profile. Deeper sediments generally contain low levels of oxidisable sulphur, although sulphur increases dramatically below 550 cm in Core 1.

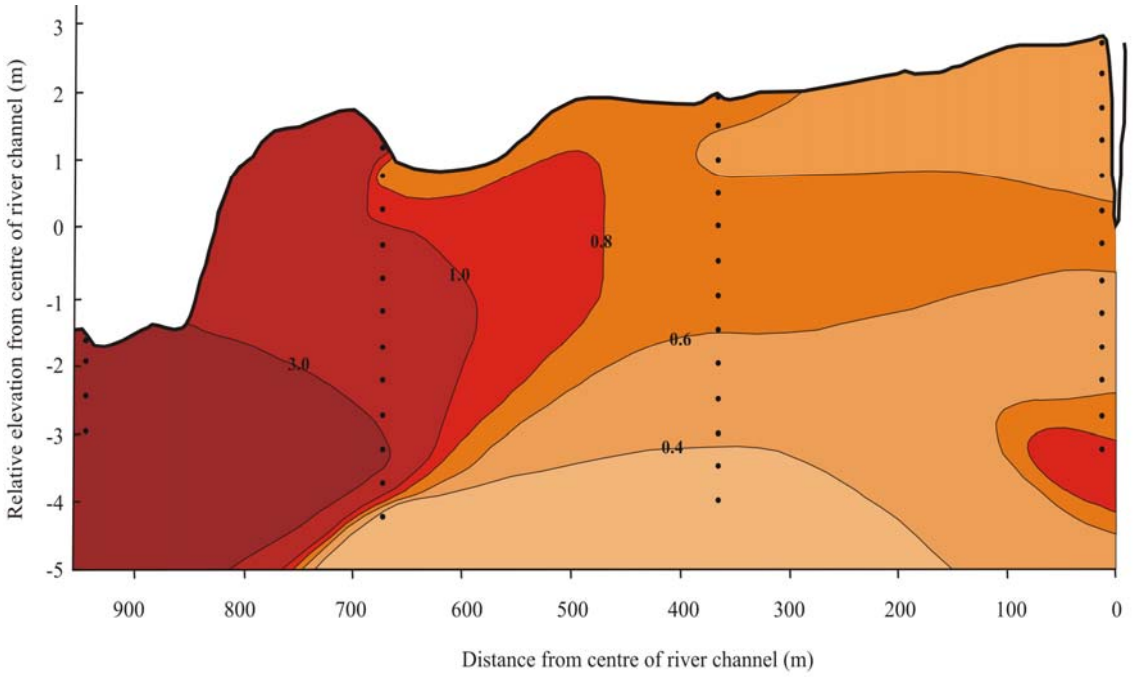

Figure 5.25 Isoplot showing the distribution of iron associated with the reducible fraction (expressed as % weight Fe) at Transect 2

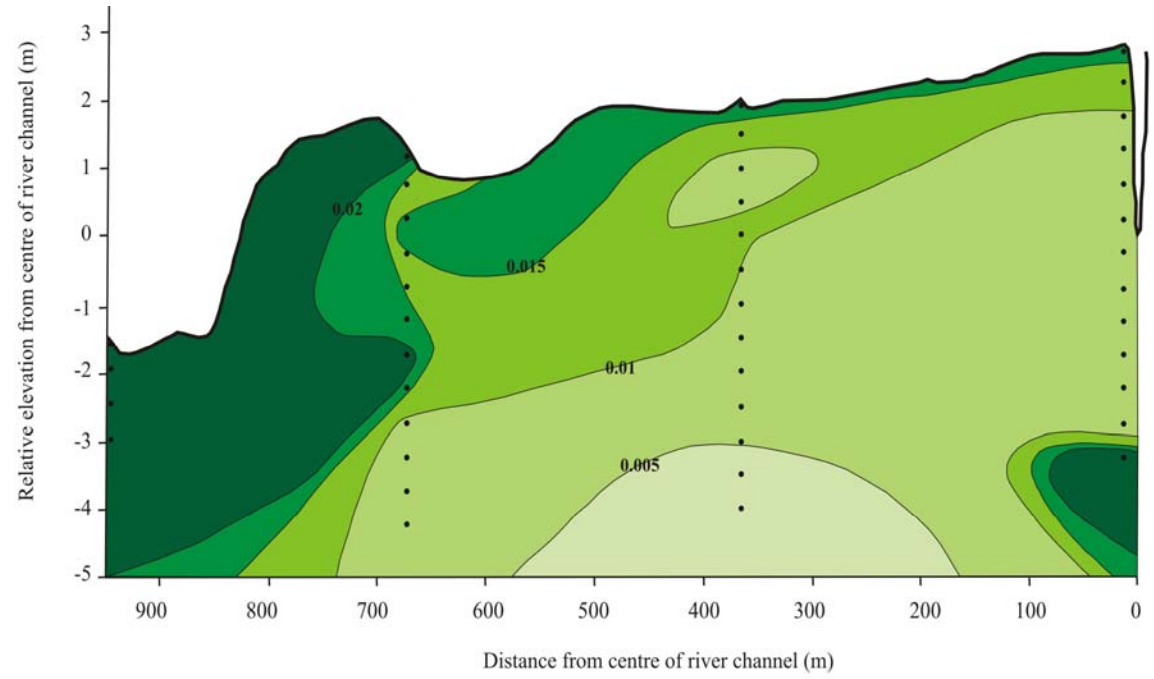

Figure 5.26 Isoplot showing the distribution of sulphur associated with the oxidisable fraction (expressed as % weight S) at Transect 2

- Acid soluble calcium and magnesium

Figure 5.27 shows that acid soluble calcium concentrations across much of the floodplain are generally <0.2% wt. The relatively low concentrations of acid soluble Ca and Mg found in these sediments indicates that this fraction probably represents water soluble and exchangeable cations. There is little significant variation in either Ca or Mg concentration, although slightly higher Ca concentrations are found in Core 4. There was no evidence of any $CaCO_3$ precipitation in these sediments, and it therefore does not appear as though calcium carbonate reaches saturation point. All groundwater and almost all porewater samples analysed were undersaturated with respect to $CaCO_3$, with precipitation probably being limited by the acidic pH environment. Typically, 30-40% of calcium in sediments is found in the reducible fraction indicating that adsorption to Fe oxyhydroxides is an important factor controlling its distribution.

Conductivity measurements show that sediments become increasingly concentrated towards Mdlanzi Lake, with highest levels recorded in Core 3 (Figure 5.28). A similar trend is seen in both groundwater conductivity and porewater solute concentrations, with most of this concentration being focused 100-300 cm below the surface.

5.2.8 Evapotranspiration and controls on chemical precipitation

There appears to be little evapotranspiration effect on chemical precipitation at Transect 2. This is indicated by relatively low groundwater conductivities and the lack of visible $CaCO_3$ precipitation. Factors limiting solute retention at this site are discussed in Section 6.7.

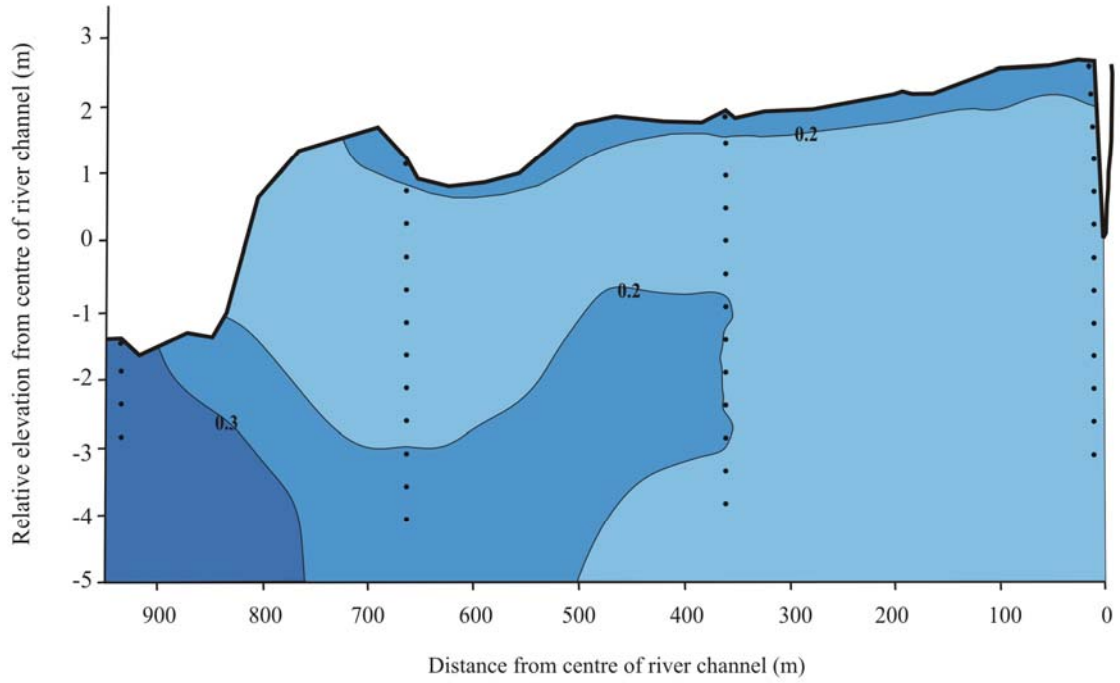

Figure 5.27 Isoplot showing the distribution of acid soluble calcium (expressed as % weight Ca) at Transect 2

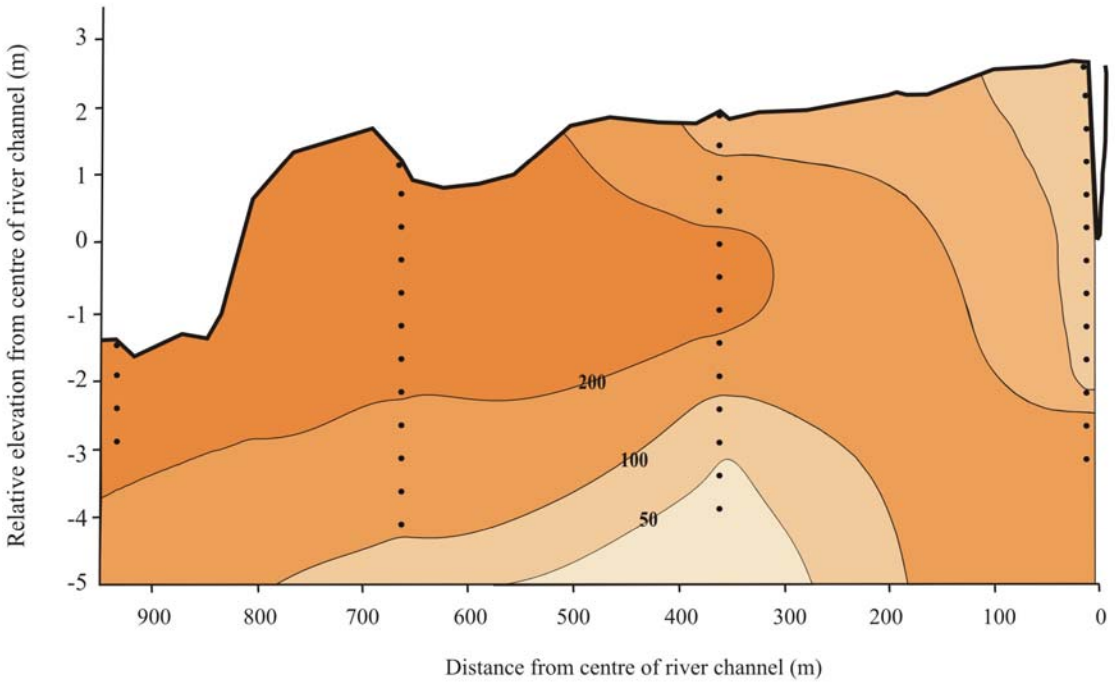

Figure 5.28 Isoplot showing the distribution of sediment conductivity (µS/cm) at Transect 2

5.3 TRANSECT THREE: THE UPPER REACH

5.3.1 Topography and general sediment characteristics

The transect surveyed at this site, running from the Mkuze River channel to the southern edge of Yengweni Lake, covers a distance of ~600 m (Figure 5.29). The river channel at this point is approximately 16 m wide and 4.3 m deep, and is flanked by a broad levee, roughly 100 m in width. At the time of sampling, water level in the river channel was approximately 1 m deep. Topographic relief over the rest of the floodplain is relatively low, although an eroded hippo trail (2.5 m deep) is present ~340 m from the main Mkuze River channel.

Particle size distribution of sediments is shown in Figure 5.30, with all samples collected from this site being classified as either sand or silty sand. Deposits in general contain very little clay, with most samples having less than 2%, as well as very little organic matter (typically <1%). Sediment from Cores 1 and 2 are similar in texture, and are dominated primarily by fine and medium sand, although samples between 150 and 300 cm are particularly coarse in Core 2. Slight Fe mottling is evident at 400 cm in Core 1 but is absent throughout Core 2. A higher quantity of finer material is found in Core 3 and particularly Core 4. Some samples between 400 and 600 cm in Core 4 contain up to 10% clay and 90% silt. Sediments from Cores 5 and 6 are generally coarse (70-80% sand), particularly at depth. Slightly finer sediments occur in the top 300 cm of Core 6, while deposits between 225 and 350 cm are very dark and characterised by numerous, small calcium carbonate nodules.

5.3.2 Clay mineralogy and chemistry

Clay mineralogy is dominated by smectite, kaolin, vermiculite and mica. Trace amounts of non-clay minerals such as hematite, goethite and K-feldspar are present in some samples. The proportion of smectite tends to be higher at depth, with surface samples typically containing 5-20% smectite, while samples from deeper layers generally contain 30-40% smectite. Smectite is iron rich (Table 5.8) and appears to be particularly abundant in sediments near Yengweni Lake. There appears to be little vertical or lateral variation in other clay minerals, with vermiculite, kaolin and mica each accounting for approximately 20-30% in most samples.

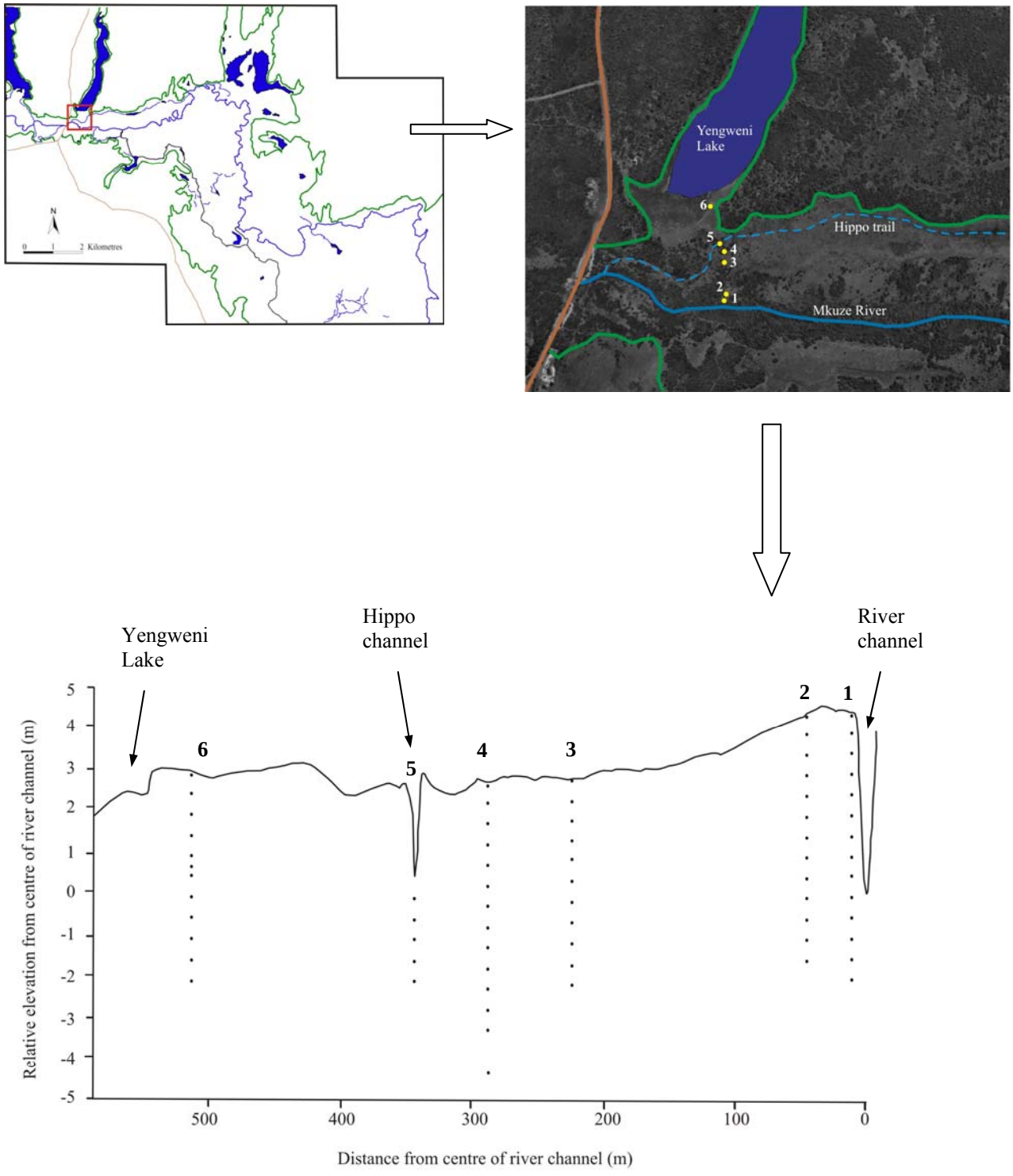

Figure 5.29 Location of sampling site on the lower Mkuze Floodplain and cores taken along the transect

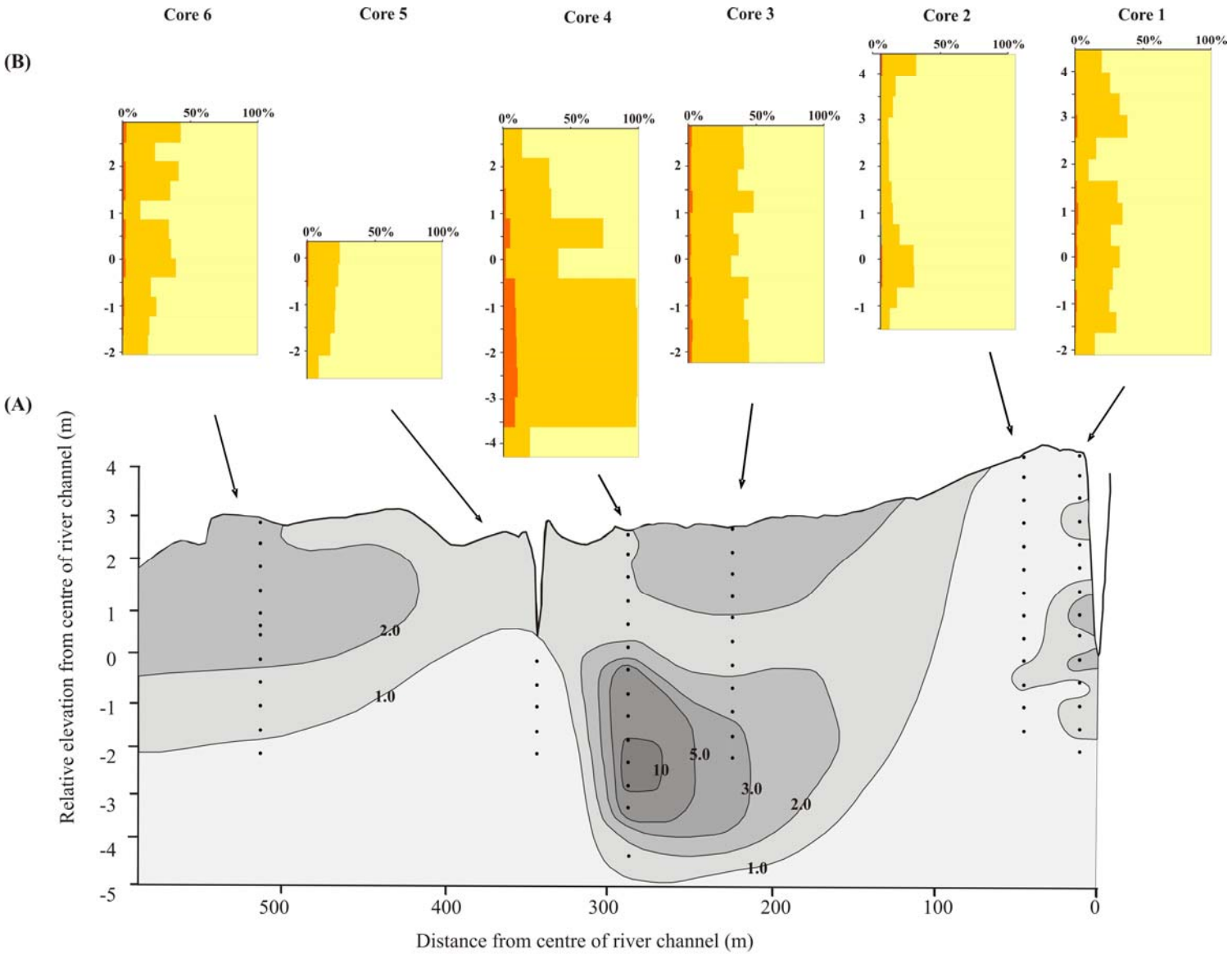

Figure 5.30 Generalised distribution of clay content (%) from sediments collected at Transect 3 (A), showing percentage clay (red), silt (orange) and sand (yellow) through each core (B).

Electron microscopy investigations reveal the presence of amorphous silica in the clay fraction of sediment samples from the bottom of Cores 3 and 4 (Figure 5.31). Elemental microanalysis (Table 5.9) shows that these irregular shaped particles are composed almost entirely of silica (>90%) and diffuse electron diffraction rings confirm their amorphous nature. Based on electron microscopy observations, amorphous silica appears to be locally abundant in this region.

Table 5.8 Major elements as weight percent in the clay fraction (<2 μm) for selected samples

Sample depth (cm)	SiO_2	Al_2O_3	Fe_2O_3	MnO	MgO	CaO	Na_2O	K_2O	TiO_2	LOI*
Core 1										
300	49.38	27.88	15.45	0.14	2.51	0.87	0.37	2.35	0.96	16.21
600	48.33	27.33	18.06	0.16	2.18	0.43	0.00	2.54	1.00	19.07
Core 2										
100	64.12	15.00	10.79	0.19	3.27	2.11	1.20	1.83	1.20	19.46
600	53.54	22.24	16.52	0.20	2.80	1.30	0.28	1.98	0.96	15.56
Core 3										
0	51.09	28.16	14.08	0.11	2.10	0.86	0.12	2.59	0.97	17.80
100	44.89	26.78	21.23	0.18	2.65	0.54	0.00	2.82	1.02	20.72
300	54.03	22.99	15.37	0.20	2.52	1.20	0.52	1.93	1.01	18.45
500	46.28	23.54	14.65	0.25	6.62	0.96	4.44	2.12	0.92	19.73
Core 4										
50	46.51	26.53	13.59	0.15	7.05	0.65	1.82	2.76	1.00	18.34
500	47.48	24.70	15.14	0.13	4.68	1.40	2.57	2.04	0.85	21.23
Core 5										
300	52.76	23.42	17.35	0.17	2.08	0.97	0.00	1.79	1.03	18.37
Core 6										
0	54.59	25.45	12.61	0.04	2.72	0.62	0.50	2.33	1.06	18.90
100	51.85	22.33	19.75	0.19	2.67	0.24	0.00	2.18	1.04	22.38
300	56.37	26.42	10.50	0.03	2.43	0.55	0.35	1.77	1.10	17.95

*Loss on ignition

Table 5.9 EDS elemental microanalysis (% mass) of amorphous silica identified in Figure 5.27

Sample	% Si	% O	% Fe	% Al	Total	Si : O
Core 3 (450 cm)	43	55	2	0	100	1 : 2.2
Core 4 (600 cm)	40	54	2	4	100	1 : 2.4

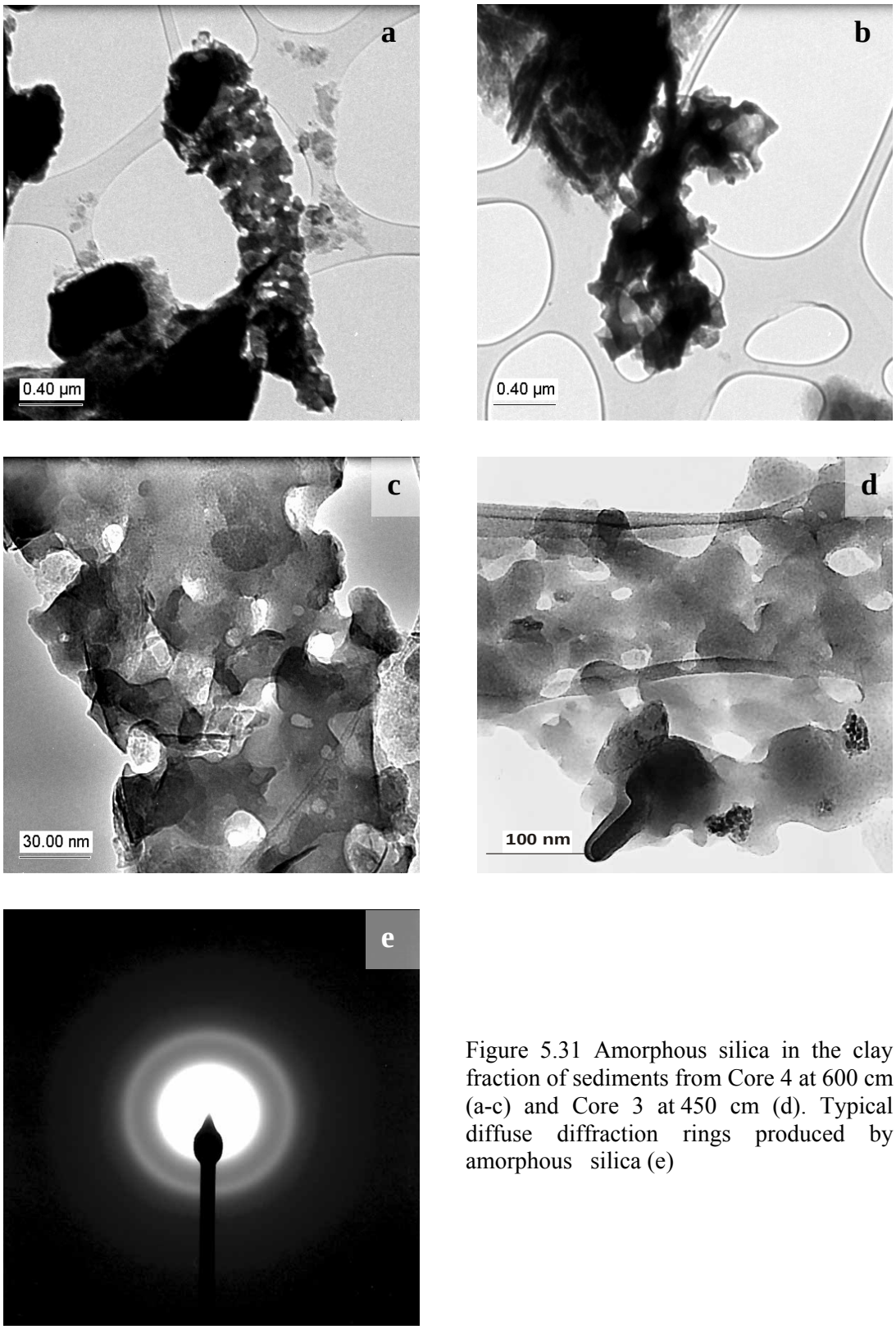

Figure 5.31 Amorphous silica in the clay fraction of sediments from Core 4 at 600 cm (a-c) and Core 3 at 450 cm (d). Typical diffuse diffraction rings produced by amorphous silica (e)

5.3.3 Sediment redox and pH

Redox potential and pH measurements recorded in the field are presented in Figure 5.32. Sediment pH through cores 1-6 remained fairly consistent, varying between 5.5 and 7.8. Sediment pH in Core 1 ranged from 5.5 to 6.9 and showed an overall decline with depth, although a sharp increase is noticeable between 600 and 650 cm. Redox potential remains relatively constant at ~300 mV through the profile until 650 cm, where a sudden drop in redox potential to -120 mV occurs. The upper portion of Core 2 is characterised by a general increase in sediment pH to a maximum of 7.7 at a depth of 350 cm. Thereafter, sediment pH steadily declines to 7.1 at 600 cm. Redox potential varies between 250 and 300 mV throughout the core, with slightly more reducing conditions found within the top 100 cm. In Core 3, pH increases sharply from 6.0 at the surface to 7.1 at 100 cm, where it remains constant to a depth of 200 cm, then gradually declines to 6.4 at 500 cm. Sediment throughout the core is moderately reduced, with redox values varying between approximately 320 and 250 mV. pH values in the upper part of Core 4 increase steadily from 6.5 at the surface to 7.8 at 200 cm. Recorded values then decline to 6.8 at 700 cm, although a distinct peak in pH to 7.8 is evident at 550 cm. There is little variation in sediment redox potential, with values varying between approximately 210 and 260 mV. Very little variation in both sediment pH and redox potential is seen in Core 5, although Eh gradually increases with depth. pH remains constant at ~6.7 over the depth analysed. Significantly higher sediment pH conditions are encountered in Core 6. Sediment near the top of the core is characterised by a steady increase in pH with depth, from 5.2 at the surface to 8.9 at 350 cm, where it then remains constant. No redox potential data was obtained for this core.

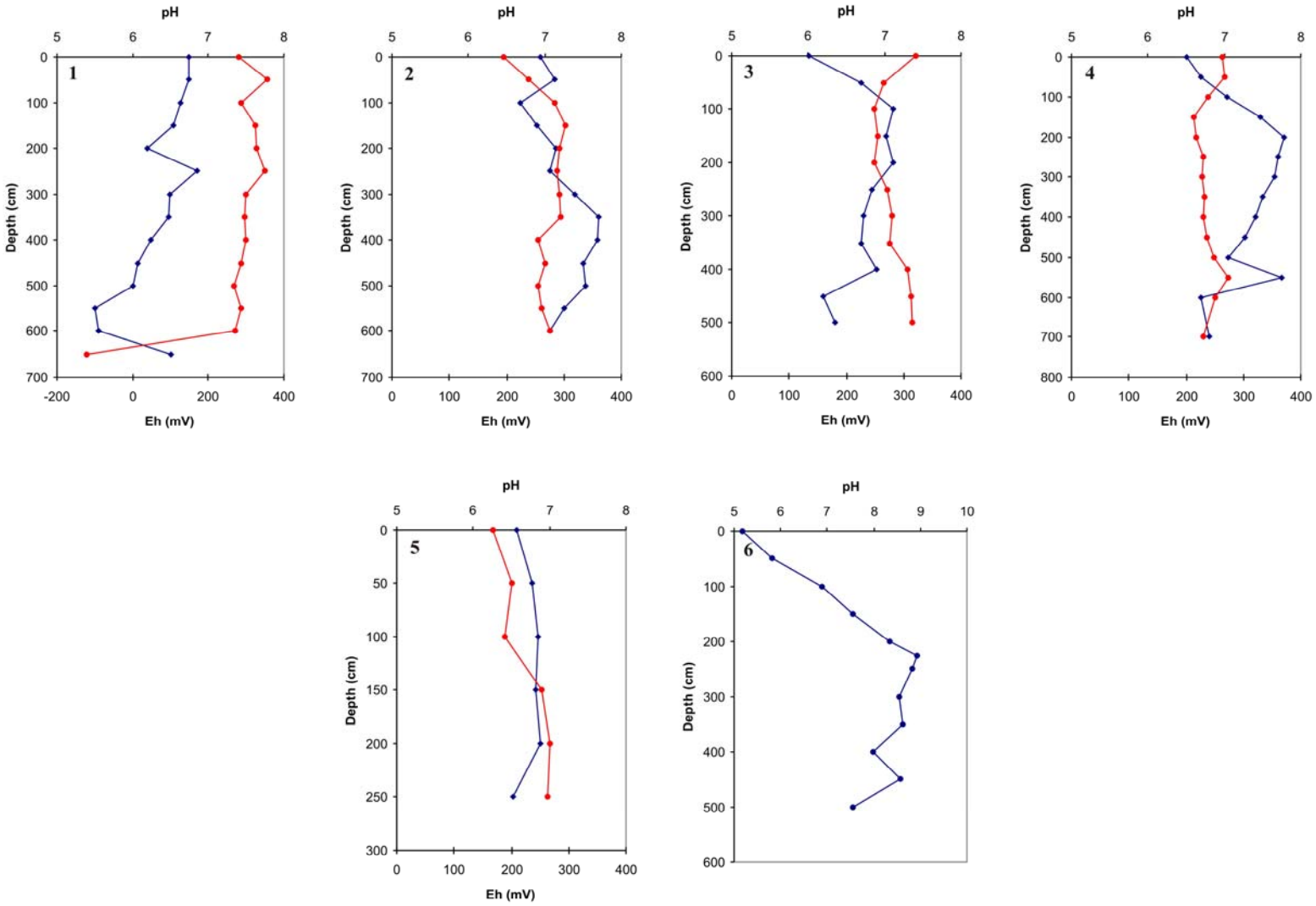

Figure 5.32 Variation of sediment pH (—) and redox potential (—) with depth in Cores 1-6 taken from Transect 3.

5.3.4 Groundwater chemistry

There is considerable chemical variation in groundwater chemistry across this portion of the floodplain (Table 5.10). Groundwater close to the river channel (Cores 1 and 2) is characterised by moderate solute concentrations, with overall concentrations being comparable to Mkuze River water. Groundwater in Cores 3 and 4 is significantly more concentrated, with considerable Cl, Na, Ca and Mg concentrations. Over a lateral distance of approximately 250 m, groundwater Cl concentration increases ~50 times, with similar increases in Ca, Mg and Na over this distance. This substantial increase in solute concentration is accompanied by significant increases in groundwater conductivity (Figure 5.33), from relatively low conductivities (<1 mS/cm) in Cores 1 and 2, to saline conditions in Core 3 (19.00 mS/cm) and Core 4 (22.6 mS/cm). Solute concentrations and groundwater conductivity decrease markedly towards Yengweni Lake, although Cores 5 and 6 are characterised by groundwater concentrations higher than those in Cores 1 and 2. Samples collected from Yengweni Lake show that solute concentrations in the lake are relatively low and similar to Mkuze River water. Concentrations of Al and Fe remain low in all samples, although significant amounts of Mn are present in Core 4. Groundwater pH remains moderately acidic across Cores 1-5, varying between 5.82 and 6.35. Alkaline conditions are encountered in groundwater from Core 6 (7.71) and surface water from Yengweni Lake (7.94).

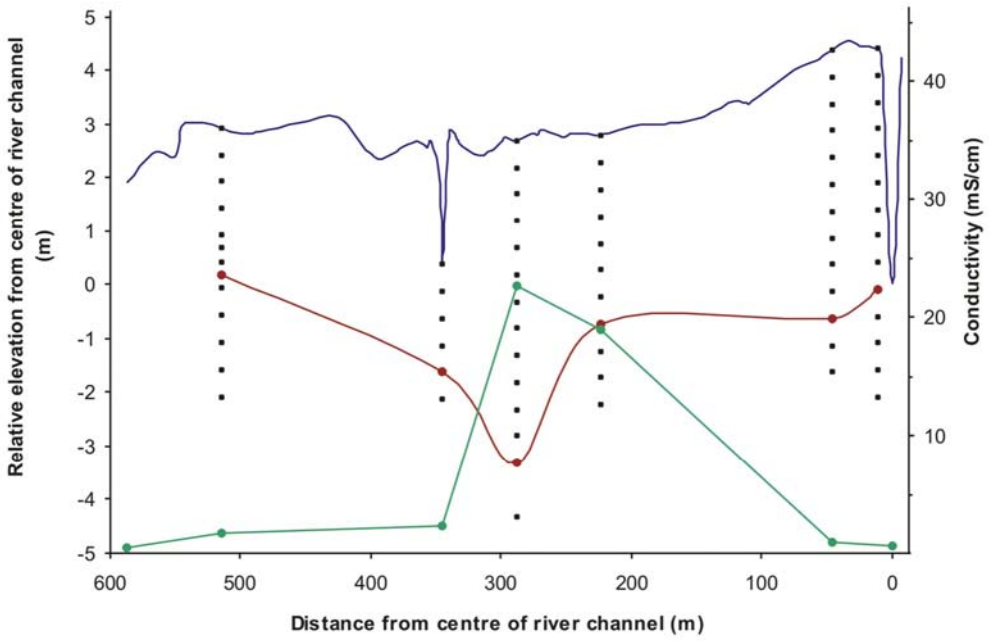

Figure 5.33 Transect profile showing groundwater conductivity (—) and elevation of the watertable (—)

Table 5.10 Groundwater chemistry data for Transect 3 (concentrations expressed in µg/ml)

	Si	**Mg**	**Ca**	**Fe**	**Al**	**Mn**	**K**	**Na**	**Cl**	**NO_3**	**SO_4**	**Alkalinity***	**pH**	**EC (mS/cm)**
Core 1	12.0	36.6	56.6	2.71	0.256	6.84	4.19	113	177	11.0	36.2	81.3	5.85	1.15
Core 2	23.1	61.0	117	<0.1	<0.1	8.22	5.49	175	150	96.9	250	671	6.35	1.75
Core 3	13.4	783	991	<0.1	0.367	10.4	4.95	2388	8138	19.4	463	230	6.33	19.0
Core 4	20.8	1212	1779	<0.1	<0.1	72.4	3.78	1181	8623	<5	71.9	350	5.82	22.6
Core 5	23.8	91.7	122	0.808	0.990	0.840	0.748	215	795	<5	86.2	75.1	5.94	2.34
Core 6	13.2	90.1	65.2	<0.1	<0.1	<0.1	0.640	249	154	5.18	291	601	7.71	1.68
Mkuze River	8.14	18.7	22.8	0.150	0.203	<0.1	5.15	73.6	81.0	<5	54.1	165	7.21	0.563
Yengweni Lake	2.40	20.4	27.5	<0.1	<0.1	<0.1	10.6	49.0	62.5	<5	11.4	185	7.94	0.483

* Alkalinity expressed in µg/ml $CaCO_3$

5.3.5 Porewater chemistry

Porewater chemistry data (Core 1 – 3) for selected solutes, overlain with field conductivity measurements, are presented in Figures 5.34(a-c).

- Core 1

Core 1 shows Ca and Mg porewater profiles that have similar trends. Calcium and Mg both initially decrease in concentration to reach minima at depths of 300 to 400 cm, but thereafter show steady increases in concentration with depth. This trend is fairly well related to changes observed in sediment conductivity. Porewater sulphate is also relatively well correlated with sediment conductivity, with peaks in concentration at 500 and 600 cm. Sodium and Si show similar profiles, with well-defined peaks in concentration (Na = 83.05 µg/ml, Si = 25.11 µg/ml) at 350 cm. Porewaters are generally depleted in Fe and Mn, although peaks in concentration are observed at 650 cm for both these solutes. This correlates with a dramatic decrease in sediment redox potential at this depth.

- Core 2

Calcium, Mg, SO_4 and Na all show similar porewater trends, with distinct peaks in concentration at 400 cm. Despite poor sample resolution in the top 400 cm of the profile, the observed trend correlates well with sediment conductivity measurements. Silicon shows a slight overall increase in concentration with depth. Manganese and Fe concentrations for all samples analysed where below 0.1 µg/ml.

- Core 3

Calcium and Mg show very similar porewater profiles, with significant increases in concentration with depth, from 84.20 µg/ml and 63.15 µg/ml at 50 cm, to 1271 µg/ml and 982 µg/ml, respectively, at 450 cm. This trend corresponds well with the marked increase in sediment conductivity. A similar trend is apparent for Na, which increases from 109.3 µg/ml to 1093 µg/ml at 450 cm. Silicon varies between 14.04 µg/ml and 25.56 µg/ml.

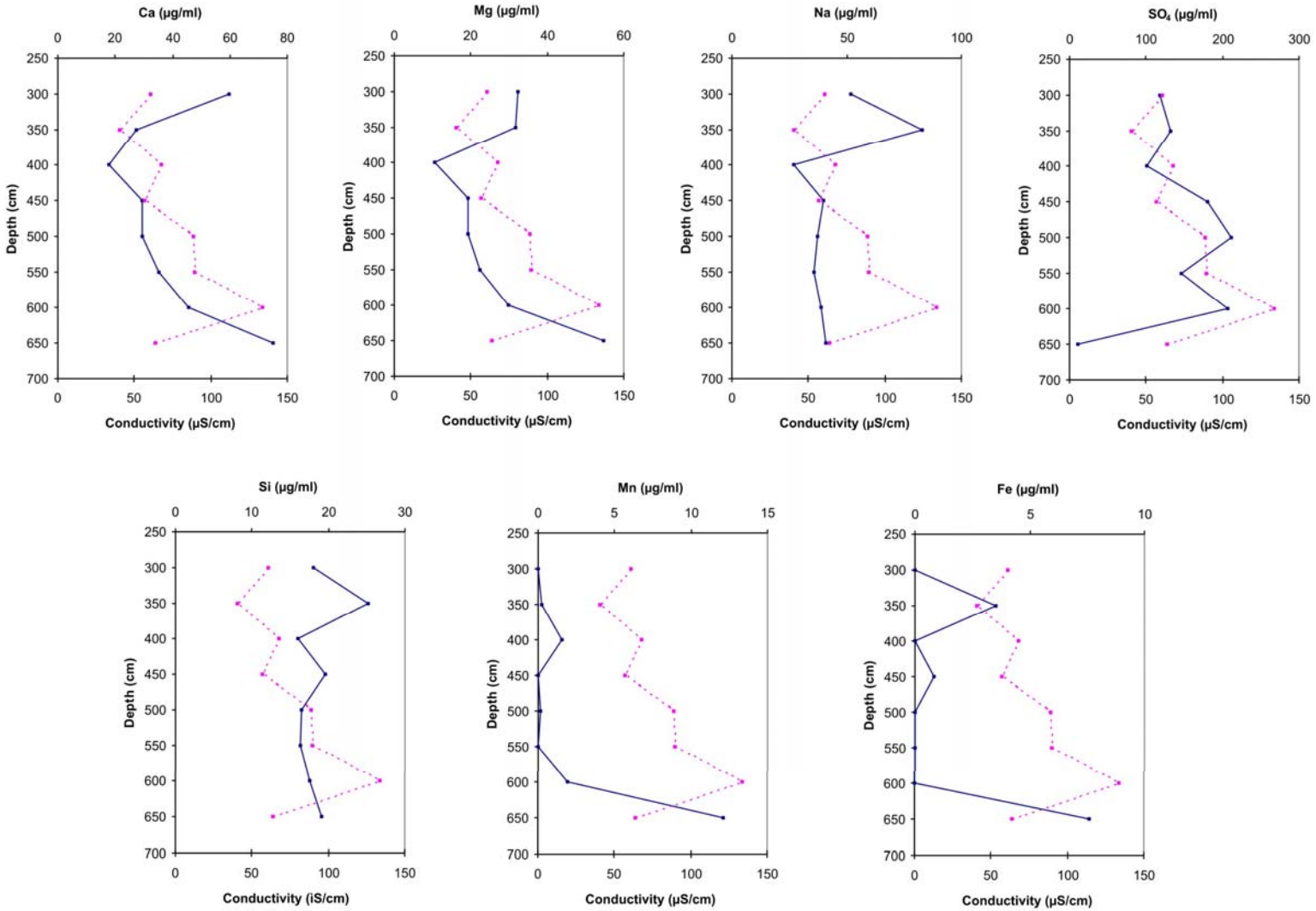

Figure 5.34(a) Variation in Core 1 porewater solute concentrations (solid line) and sediment conductivity (dashed line) with depth.

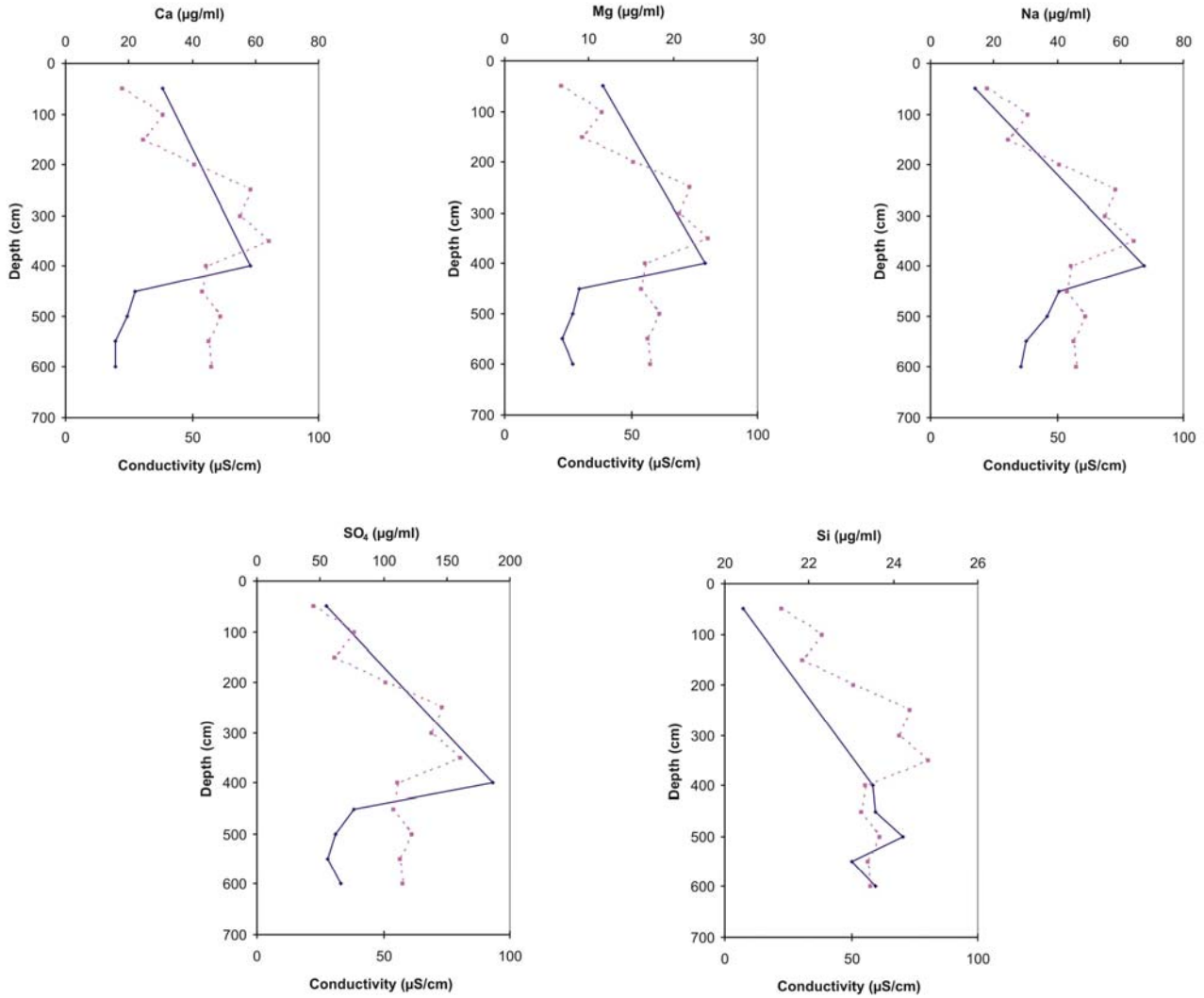

Figure 5.34(b) Variation in Core 2 porewater solute concentrations (solid line) and sediment conductivity (dashed line) with depth.

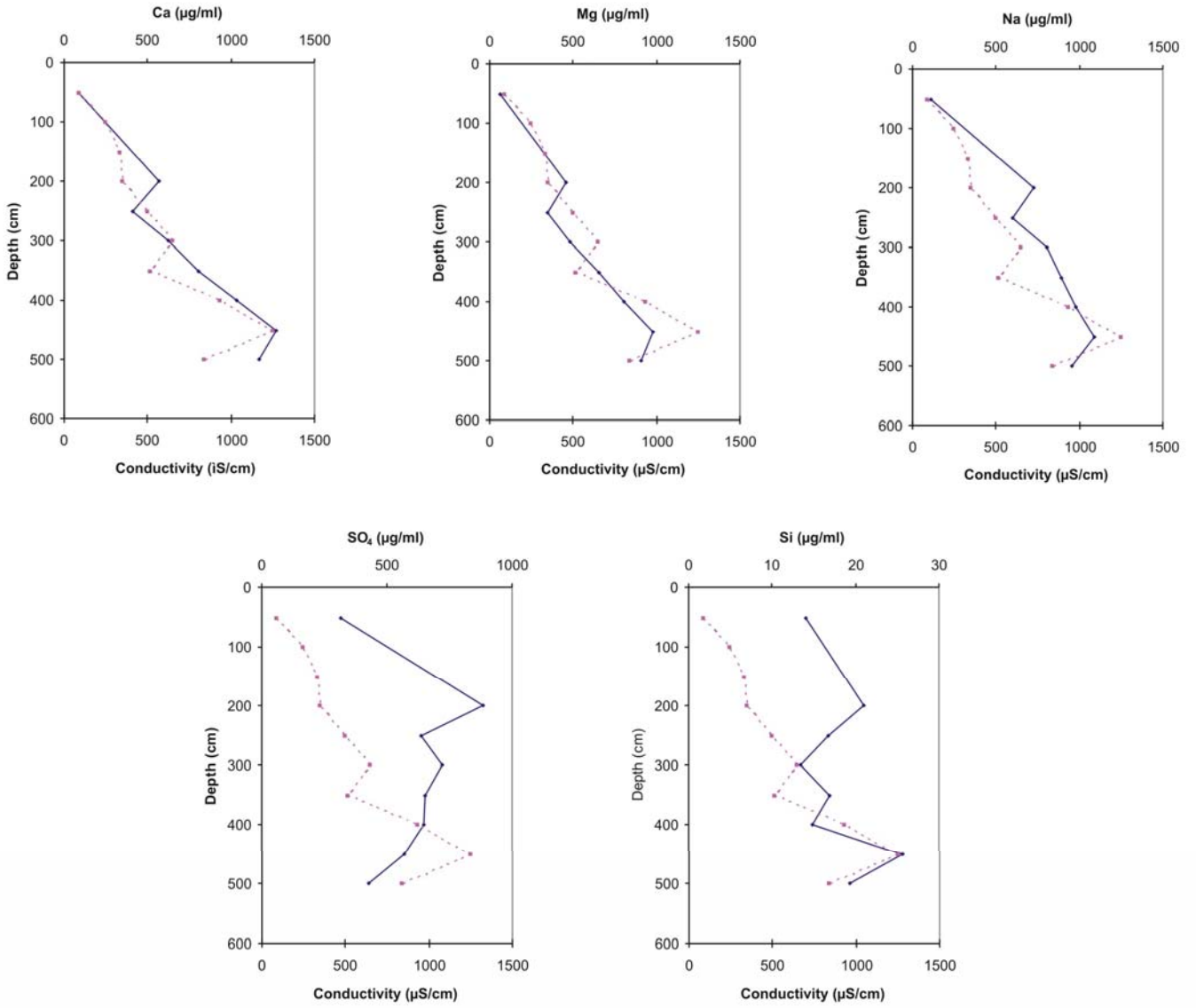

Figure 5.34(c) Variation in Core 3 porewater solute concentrations (solid line) and sediment conductivity (dashed line) with depth.

5.3.6 Geochemical modelling of groundwater and porewater

Saturation indices indicate that groundwater samples collected from Cores 1-5 are all undersaturated with respect to $CaCO_3$ (Table 5.11). Water samples collected from Yengweni Lake and the Mkuze River are also undersaturated with respect to $CaCO_3$. However, $CaCO_3$ saturation is reached in the groundwater of Core 6. Gypsum and amorphous silica remain undersaturated in all samples.

Table 5.11 Calculated groundwater mineral saturation indices for selected minerals

Mineral	Core 1	Core 2	Core 3	Core 4	Core 5	Core 6	Yengweni Lake	Mkuze River
Calcite ($CaCO_3$)	-2.28	-0.67	-0.56	-0.68	-2.04	0.38	-0.08	-0.97
Aragonite ($CaCO_3$)	-2.42	-0.81	-0.70	-0.82	-2.18	0.24	-0.22	-1.11
Gypsum ($CaSO_4$)	-1.90	-0.95	-0.48	-1.14	-1.41	-1.14	-2.59	-2.02
Smectite	7.65	7.04	6.12	6.01	10.03	7.81	4.76	8.99
SiO_2 (amorphous)	-0.61	-0.32	-0.65	-0.32	-0.31	-0.57	-1.31	-0.78

Most porewater samples analysed do not attain saturation with respect to $CaCO_3$, although some porewaters in Cores 2 and 3 do appear to be in equilibrium with this phase (Figure 5.35). While porewater from the sediments of Core 6 could not be extracted and analysed, they are likely to be supersaturated with respect to $CaCO_3$ given that groundwater from this core was supersaturated. All porewaters analysed are undersaturated with respect to amorphous silica (Figure 5.36) and gypsum.

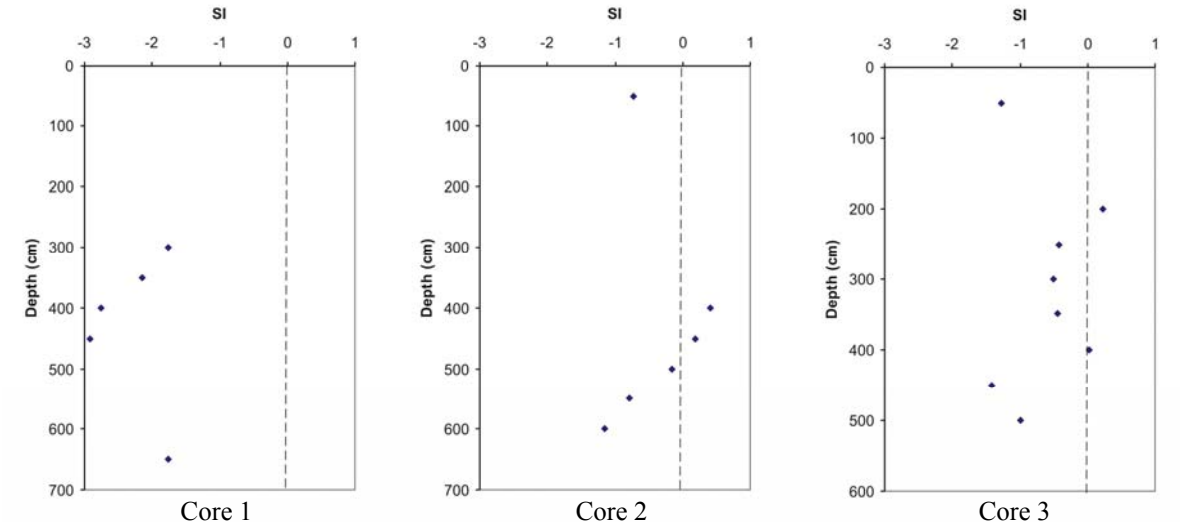

Figure 5.35 Calculated calcium carbonate saturation indices for Transect 3 porewater samples

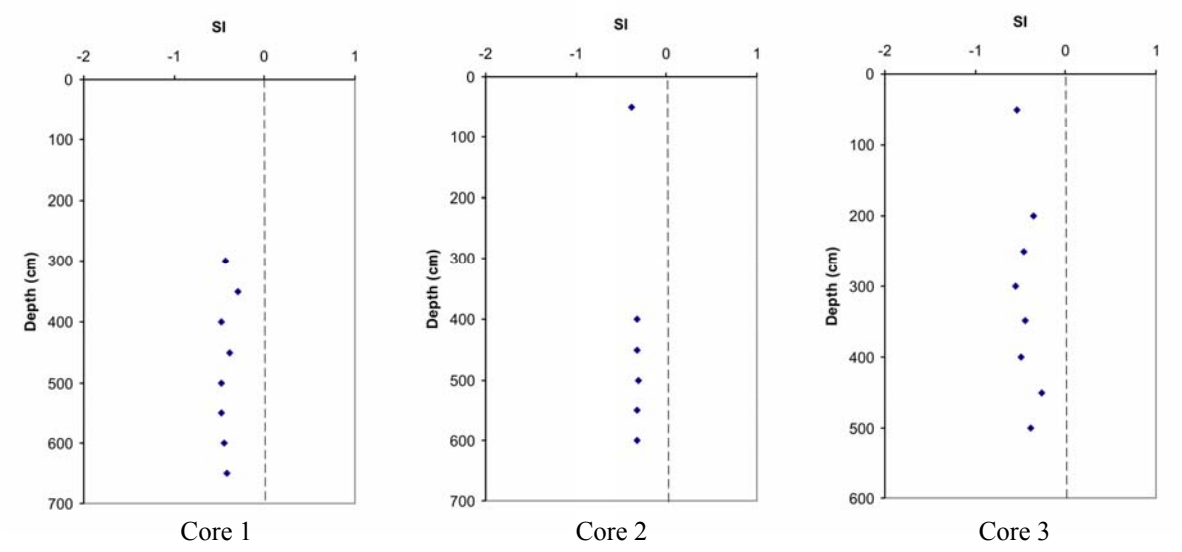

Figure 5.36 Calculated amorphous silica saturation indices for Transect 3 porewater samples

5.3.7 Chemical fractionation

- Reducible iron and manganese

Overall reducible Fe concentrations are fairly low, with higher concentrations being confined to sediments near the hippo channel and surface deposits close to Yengweni Lake (Figure 5.37). These regions of higher concentration are likely to become regularly saturated and thus promote the formation of Fe oxyhydroxides over time. While the reducible fraction of sediments is dominated in terms of concentration by Fe, only a very small proportion (typically 10%) of total Fe is present in this form. The majority (80-98%) of iron is found in the residual phase, representing primarily clay minerals. Although present in much lower concentrations, the reducible fraction accounts for a large quantity (approximately 50-80%) of total Mn present.

Surface Fe oxyhydroxide enrichment near Yengweni Lake probably result from the interaction between lake water and rainfall which saturate these sediments, and plant growth which precipitates soluble iron. Surface sediments here also have higher organic matter contents relative to the rest of the floodplain, which should promote the development of reducing conditions. It does not appear as though water from Yengweni Lake provides any significant iron input to the floodplain, with deposits from depth near the lake having negligible Fe oxyhydroxides contents. Samples from this lake show that this water contains very little soluble iron (<0.1 μg/ml). The extent of floodplain inundation during high river discharges is likely to be limited by the presence of the large hippo channel, such that very little water reaches the extreme northern areas of the floodplain during normal or moderate flows. Sediments here are thus starved of a regular supply of Fe from the river. Sediments near the hippo channel show elevated Fe concentration as it is likely to become frequently waterlogged due to rainfall that collects in the channel.

Sediment texture appears to play a role in determining Fe oxyhydroxide distribution. Particularly sandy deposits, like those characteristic of Cores 1 and 2, are unlikely to retain moisture for any significant period of time. Such conditions limit the potential for Fe oxyhydroxide formation in close proximity to the river channel. Finer sediments, located further from the channel, would be expected to retain soil moisture for longer periods of time, thereby favouring the development of anoxic conditions and the accumulation of Fe over time.

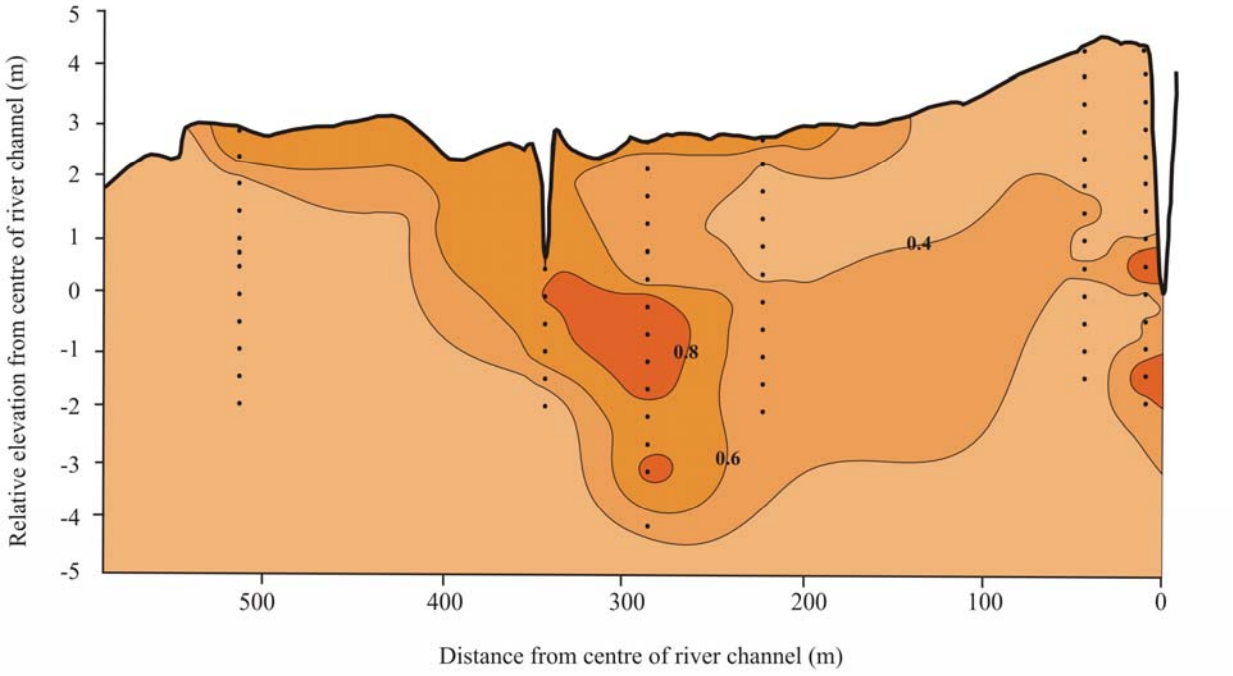

Figure 5.37 Isoplot showing the distribution of iron associated with the reducible fraction (expressed as % weight Fe) at Transect 3

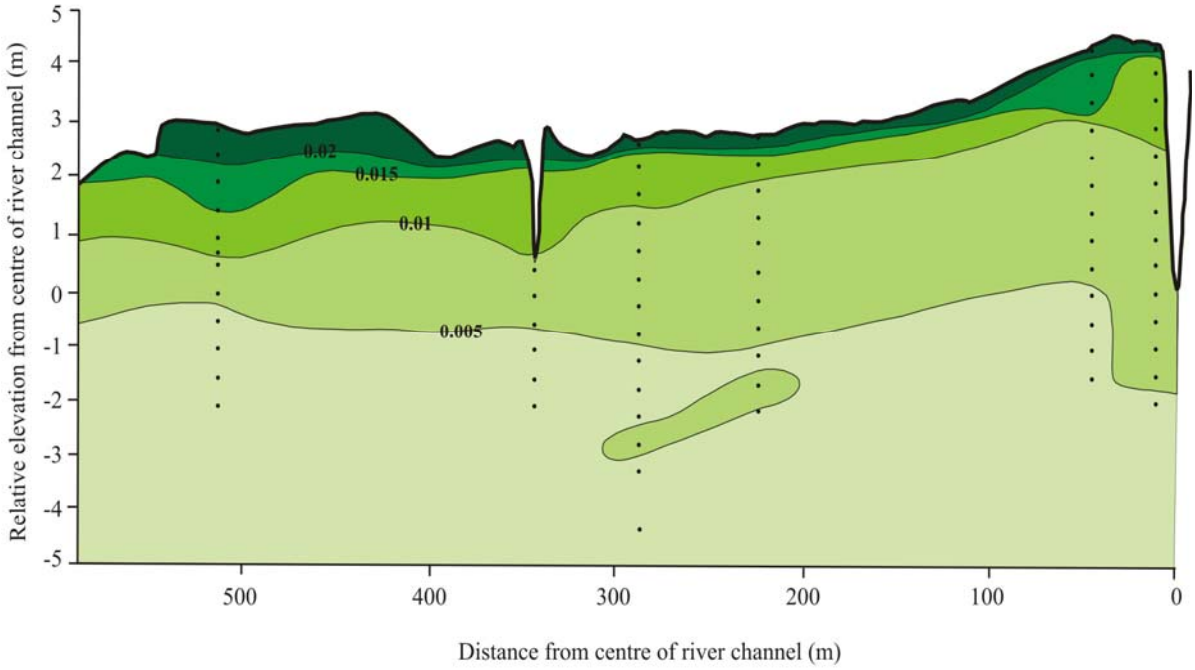

Figure 5.38 Isoplot showing the distribution of sulphur associated with the oxidisable fraction (expressed as % weight S) at Transect 3

- Oxidisable sulphur

The oxidisable fraction is dominated in terms of concentration by sulphur, with approximately 50% of all sulphur present in sediment samples occurring in this fraction. High amounts of oxidisable sulphur are confined to surface deposits, where the influence of plants and bacterial reducing processes are greatest (Figure 5.38). In these areas, over 90% of all sulphur appears to precipitate as iron sulphide. Deeper sediments are depleted in oxidisable sulphur

- Acid soluble calcium and magnesium

Concentrations of acid soluble calcium and magnesium over most of the floodplain are low, suggesting that this fraction represents primarily water soluble or easily exchangeable cations. In most cores, acid soluble calcium accounts for approximately 30% of total calcium. It is only in Core 6 where significantly elevated amounts of acid soluble calcium are encountered (>1% wt), particularly between 150 and 300 cm (Figure 5.39). This region of high concentration is attributed to the accumulation of $CaCO_3$. Approximately 70-80% of all calcium and 35-45% of all magnesium in these sediments is present in the acid soluble phase.

5.3.8 Evapotranspiration and controls on chemical precipitation

A distinct zone of substantial increase in sediment conductivity occurs between 200-600 cm in Cores 3 and 4 (Figure 5.40). Evapotranspiration appears to be strongly focused in this region, with sediment conductivities approximately 15-20 times higher than conductivities from surrounding floodplain sediments. Associated with these elevated conductivity readings are depressions in the position of the watertable. The relationship between conductivity and watertable elevation suggests a process by which groundwater is removed and solutes are concentrated.

Much of the floodplain at Transect 3 is covered by *Echinochloa pyramidalis*, with areas near the river channel being characterised by *Ficus sycomorus* (riparian forest). However, this zone of high conductivity is dominated by a band of *Acacia xanthophloea* (fever trees). These trees appear to be responsible for the removal of large quantities of water through transpiration, which results in the subsurface concentration of groundwater solutes. Hydraulically restrictive sediments and the continual removal of water by these deep-rooted trees are the likely causes of the significant decline in watertable elevation. The strong solute concentration mechanisms operative here also result in the precipitation of large amounts of amorphous silica. Although groundwater and porewater were

both slightly undersaturated with respect to amorphous silica at the time of sampling, evapotranspiration appears to provide conditions that are conducive to amorphous silica precipitation. Such conditions may also lend themselves to the chemical precipitation of Fe-smectite.

Sediments near Yengweni Lake contain abundant $CaCO_3$. Analysis shows that $CaCO_3$ is present as low magnesian calcite containing 4-7% $MgCO_3$. Elevated conductivity levels recorded in these sediments favour the interpretation that $CaCO_3$ has precipitated here in response to the evaporation and concentration of Yengweni Lake water. Yengweni Lake is fringed by *Acacia xanthophloea* and precipitation of $CaCO_3$ is likely to result from the transpiration by these trees. The alkaline waters of Yengweni Lake encourage $CaCO_3$ precipitation, resulting in sediment calcium concentrations of up to 2.3% wt. This process probably intensifies during periods of low rainfall which cause water levels in the lake to recede, thereby exposing water-saturated sediment.

Acid soluble calcium concentrations elsewhere are generally very low (Figure 5.39). It thus appears that conditions are not met for $CaCO_3$ precipitation across the rest of the floodplain, despite calcium groundwater and porewater concentrations reaching very high levels. Saturation indices indicate that $CaCO_3$ is typically undersaturated, with precipitation likely to be limited by the generally acidic sediments (pH 6.3 – 7.2). This causes porewater calcium and magnesium concentrations to build up in solution under the effect of evapotranspiration.

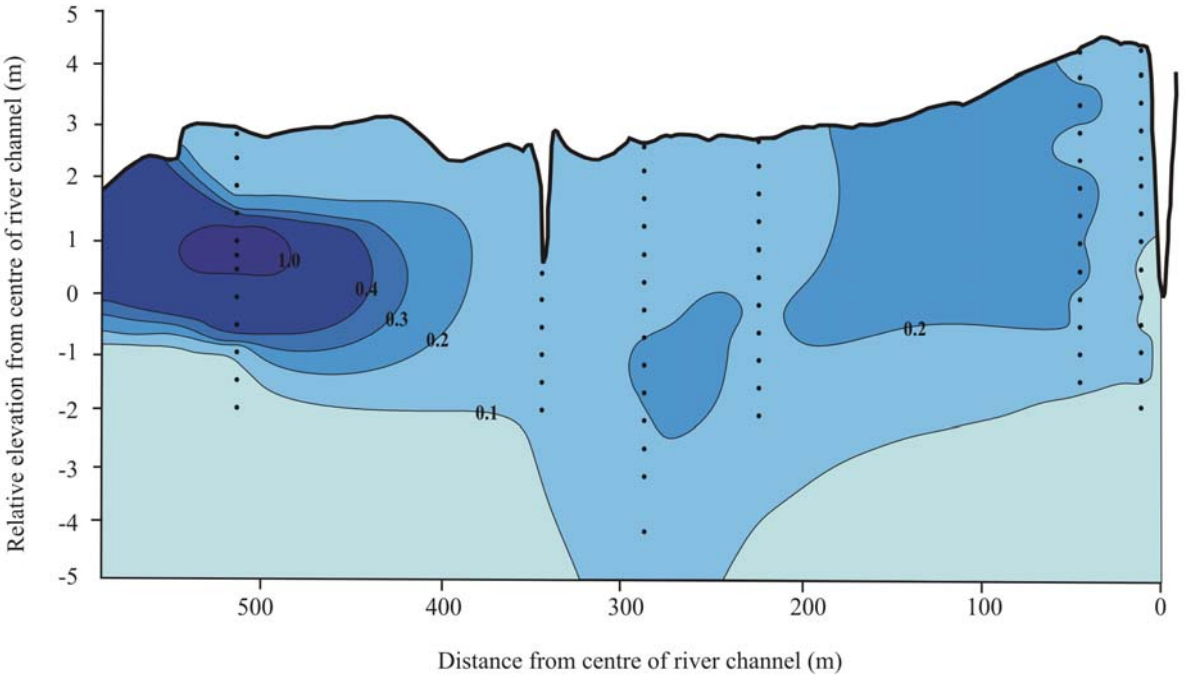

Figure 5.39 Isoplot showing the distribution of acid soluble calcium (expressed as % weight calcium) at Transect 3

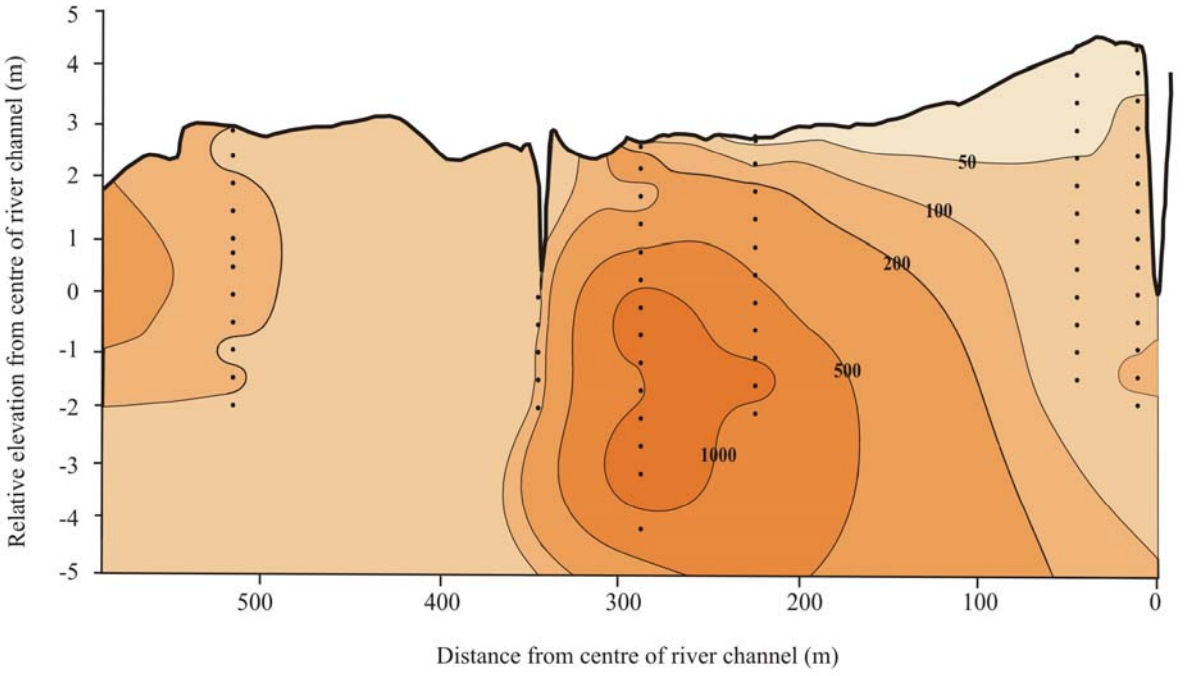

Figure 5.40 Isoplot showing the distribution of sediment conductivity (µS/cm) at Transect 3

5.4 SEDIMENTATION RATES

Sediment accumulation rates were calculated for both pits using ^{210}Pb and ^{137}Cs activities (Figure 5.41). Excess ^{210}Pb showed good exponential decay to 23 cm in Core M and 14 cm in Core K, with activities below these depths being highly variable. Average sedimentation rates were obtained by plotting the linear regressions of ln(^{210}Pbex) activities against depth for both cores (Figure 5.42 and Table 5.12). This yielded similar sedimentation rates of 0.24 cm/yr and 0.26 cm/yr for Cores K and M, respectively. Sediment mass fluxes were calculated from the average bulk density of samples from each core (Table 5.13).

Total ^{137}Cs in all samples analysed was very low, with most levels falling below analytical detection limit. Core M shows two significant ^{137}Cs events, with peaks in activity at depths of approximately 7-11 cm and 17-20 cm (Figure 5.41). These peaks in concentration are due to either rapid sedimentation or actual ^{137}Cs fallout. The second (deeper) of these two peaks is probably attributed to fallout from weapons testing in 1963. This gives a sedimentation rate of ~0.39 cm/yr. This then dates the first (shallower) peak to 21-26 years ago, the time when the area experienced widespread flooding due to tropical cyclone Domonia. In Core K, the excess ^{210}Pb and ^{137}Cs data suggest that the upper 8-22 cm is well mixed and may have all been deposited at the same time. Attributing the peak in ^{137}Cs concentration at 16 cm to weapons testing fallout, a sedimentation rate of 0.36 cm/yr is obtained. This dates the first ^{137}Cs peak at 8 cm to ~22 years ago, around the time of the flood event. The good correlation between ^{137}Cs peaks and environmental events indicates that little post-depositional mixing has occurred.

Calculated sedimentation rates using ^{137}Cs are slightly higher than those derived using ^{210}Pb, suggesting either compaction of surface deposits or more rapid accretion during recent years (Table 5.13). Average sedimentation rates on the floodplain are likely to be in the order of 0.25 to 0.35 cm/yr. This represents a mean value over the last 100-150 years, as it is likely that sedimentation is not constant over time but rather varies in cycles relative to overbank flood events. It is emphasized that sediment deposition on the Mkuze Floodplain is likely to be spatially variable and that the values reported reflect the sediment deposition at the individual sampling sites. Areas closer to the river channel are likely to experience rates of slightly higher deposition, while areas near the floodplain margin, where sediment supply is limited, are likely to display slightly lower accretion rates.

Core M

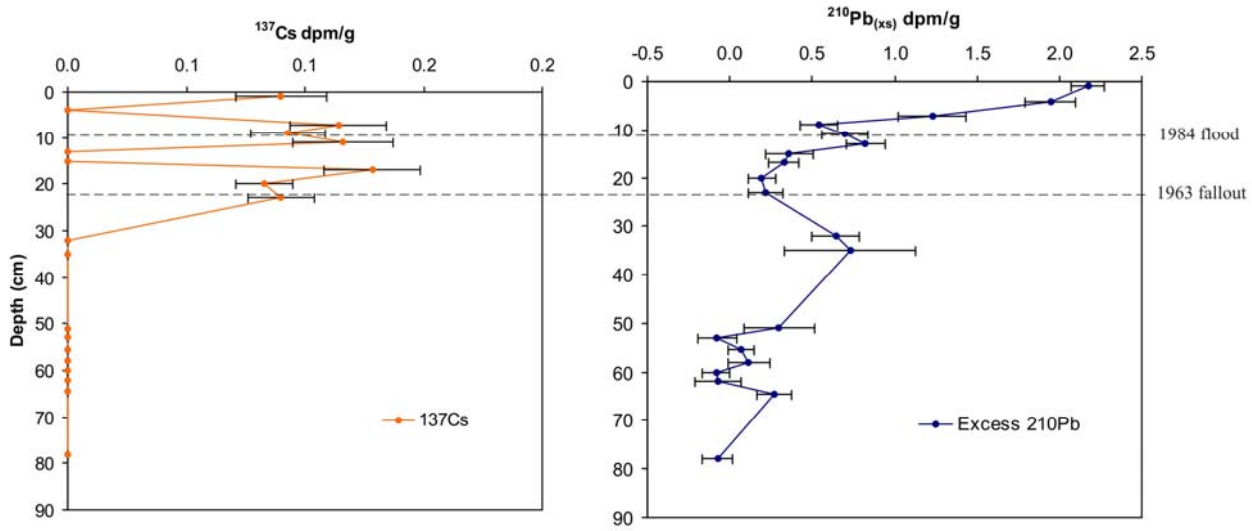

Core K

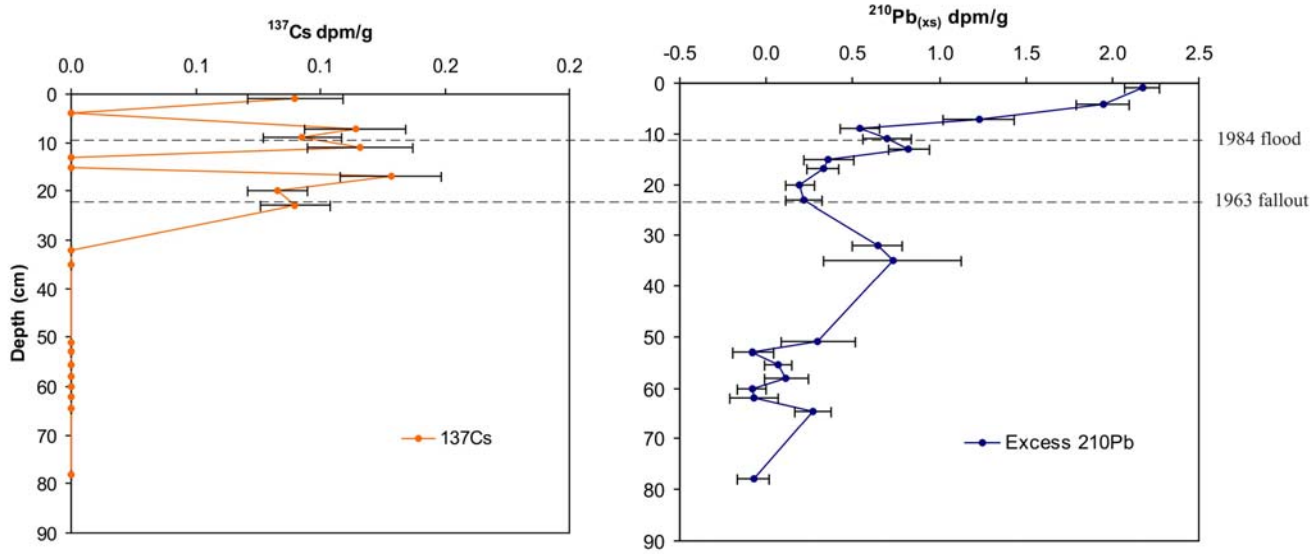

Figure 5.41 Depth distribution of excess ^{210}Pb and ^{137}Cs through Cores M and K indicating the likely time of peak ^{137}Cs fallout (1963) and the cyclone Domonia flood event (1984). Bars indicate error associated with analytical measurement.

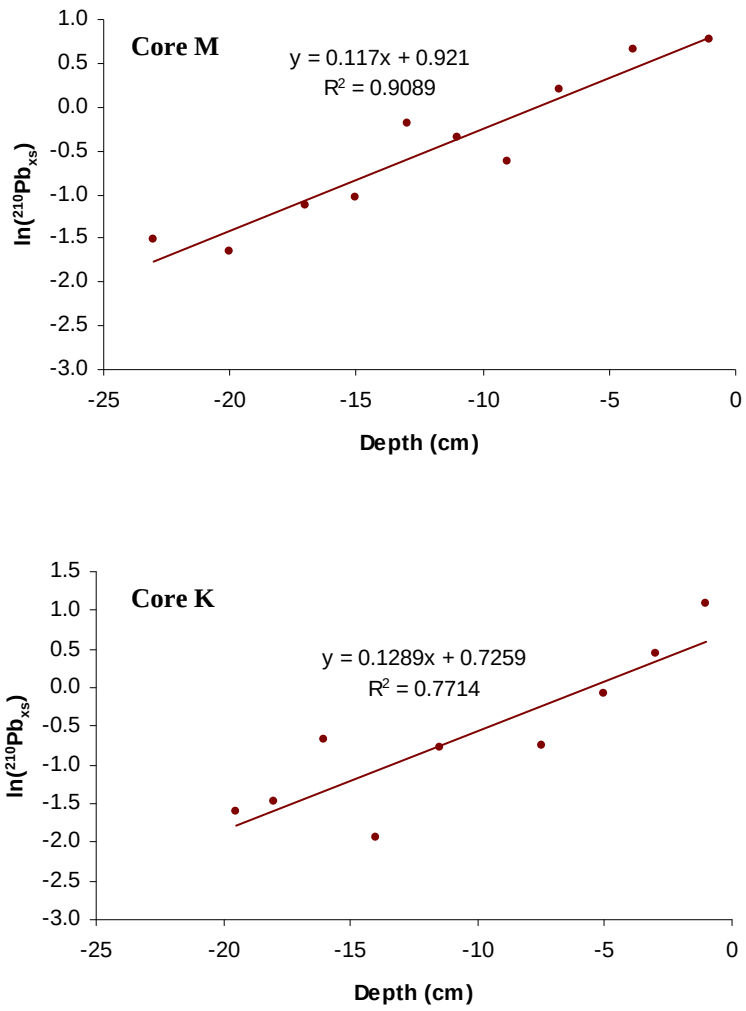

Figure 5.42 $^{210}Pb_{ex}$ versus depth for sediment Cores M and K

Table 5.12 Vertical distribution of ^{210}Pb and ^{137}Cs in cores

Depth (cm)	Total ^{210}Pb (dpm/g)	Supported ^{210}Pb (dpm/g)	Excess ^{210}Pb (dpm/g)	Error (+/-)	^{137}Cs (dpm/g)	Error (+/-)
Core M						
0-02	3.689	1.516	2.173	0.100	0.090	0.019
02-06	3.467	1.521	1.946	0.153	0.000	0.000
06-08	2.832	1.605	1.228	0.207	0.114	0.020
08-10	2.418	1.876	0.542	0.113	0.093	0.016
10-12	2.358	1.660	0.698	0.142	0.116	0.021
12-14	2.528	1.703	0.825	0.121	0.000	0.000
14-16	2.290	1.931	0.359	0.143	0.000	0.000
16-18	2.275	1.948	0.328	0.094	0.128	0.020
18-21	2.264	2.071	0.193	0.083	0.083	0.012
21-25	2.137	1.919	0.218	0.102	0.090	0.014
30-34	2.641	1.997	0.644	0.143	0.000	0.000
34-36	2.462	1.732	0.730	0.400	0.000	0.000
50-52	2.160	1.861	0.299	0.214	0.000	0.000
52-54	1.891	1.971	-0.080	0.118	0.000	0.000
54-57	1.911	1.845	0.066	0.078	0.000	0.000
57-59	1.910	1.795	0.115	0.126	0.000	0.000
59-61	1.959	2.042	-0.083	0.086	0.000	0.000
Core K						
0-02	4.319	1.323	2.996	0.205	0.000	0.000
02-04	3.244	1.676	1.568	0.128	0.115	0.022
04-06	2.807	1.888	0.918	0.160	0.203	0.028
06-09	2.507	2.035	0.472	0.115	0.235	0.031
09-13	2.538	2.083	0.455	0.074	0.203	0.012
13-15	2.307	2.165	0.142	0.141	0.213	0.060
15-17	2.646	2.134	0.512	0.129	0.244	0.030
17-19	2.257	2.028	0.228	0.169	0.182	0.035
19-20	2.280	2.079	0.201	0.108	0.206	0.031
20-22	2.413	1.985	0.427	0.176	0.272	0.031
56-58	2.624	1.957	0.667	0.060	0.027	0.007
78-80	2.294	1.834	0.460	0.123	0.000	0.000

Table 5.13 ^{210}Pb and ^{137}Cs derived sedimentation and accumulation rates

	^{210}Pb		^{137}Cs	
Sample site	Sedimentation rate (cm/yr)	Accumulation rate ($g/cm^2/yr$)	Sedimentation rate (cm/yr)	Accumulation rate ($g/cm^2/yr$)
Core K	0.24	0.21	0.36	0.32
Core M	0.26	0.22	0.39	0.33

Calculated sedimentation rates compare well with other estimates of aggradation. Data from a core taken during the construction of the lower Mkuze Bridge showed 42 m of sediment present at that location. Given that the valley started filling approximately 6500 years ago (McCarthy & Hancox, 2000), this translates to a sedimentation rate of around 0.65 cm/yr. This figure is approximately double the short-term estimate derived in this study, and suggests that average sedimentation rates on the Mkuze Floodplain have decreased in response to valley infilling and decline in valley cross-sectional area.

Chapter 6

Sedimentation and biogeochemical processes across the Mkuze Floodplain

This chapter aims to integrate findings outlined in Chapter 5 in an attempt to identify and explain a variety of chemical and physical processes occurring on the Mkuze Floodplain. Controls on sedimentation and biogeochemical processes are highlighted by drawing comparisons between results from different regions on the floodplain.

6.1 Regional topography and the influence of sediment characteristics

The Mkuze River flows within a shallow valley that is narrow in the west of the study area, but becomes progressively broader eastwards (Figure 6.1). North-south oriented drainage lines enter this valley on its northern margin, feeding floodplain lakes such as Muzi, Yengweni and Mdlanzi. The river channel near Yengweni Lake is ~15 m wide from the edge of one bank to the other, and 4-5 m deep. Both the width and depth decrease downstream such that in its lower reaches the channel is <10 m wide and 1 m deep. Changes in channel dimensions are as a consequence of constant water loss from the river to the surrounding floodplain McCarthy & Hancox, 2000).

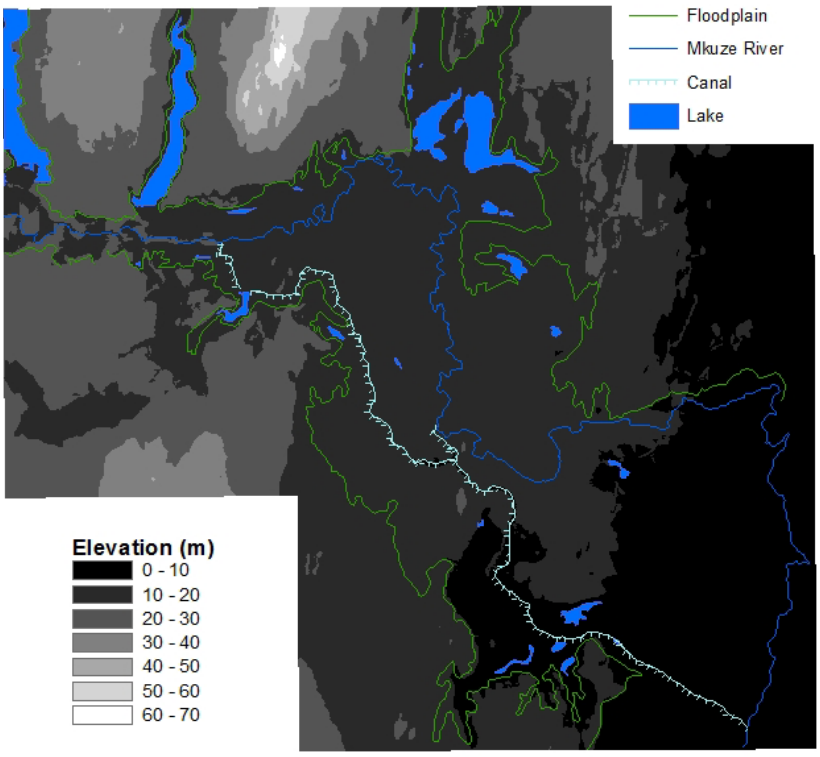

Figure 6.1 Digital elevation model showing elevation (above mean sea level) of the Mkuze Floodplain

Patterns of clastic sediment deposition on the floodplain are, to a large extent, a product of river channel morphology. Sediments show a gradual fining trend downstream, from predominantly sand or silty sand in the upper sections of the floodplain to sandy silt or silt in its lower reaches (Figure 6.2). In the upper reaches of the system, the Mkuze River channel is large and thus able to accommodate substantial volumes of water and suspended sediment. During times of high discharge, the Mkuze River regularly overtops its banks, depositing clastic sediment on the floodplain. Much of this fluvially introduced material accumulates in close proximity to the channel resulting in the development of well-developed river levees comprising predominantly of medium and coarse sand. Dense riverine vegetation, which typically flanks the Mkuze River channel, plays an important role in reducing the ability of floodwaters to transport suspended sediment, thus promoting deposition near the channel. Finer sediments (silt and clay) are transported laterally on the floodplain and further downstream, to be deposited in the lower reaches of the system. It is only during times of exceptional flood that significant volumes of coarse material are likely to reach the

lower regions of the floodplain. The large flood deposit identified in the sediment profile on the lower reach represents the effect of a massive flooding event experienced by the system. The enormity of this event is highlighted when it is considered that the effects of the Domonia flood in 1984 (the largest flood event on record) are barely discernible in the sediment profile. Such a severe event probably only occurs once every few thousand years.

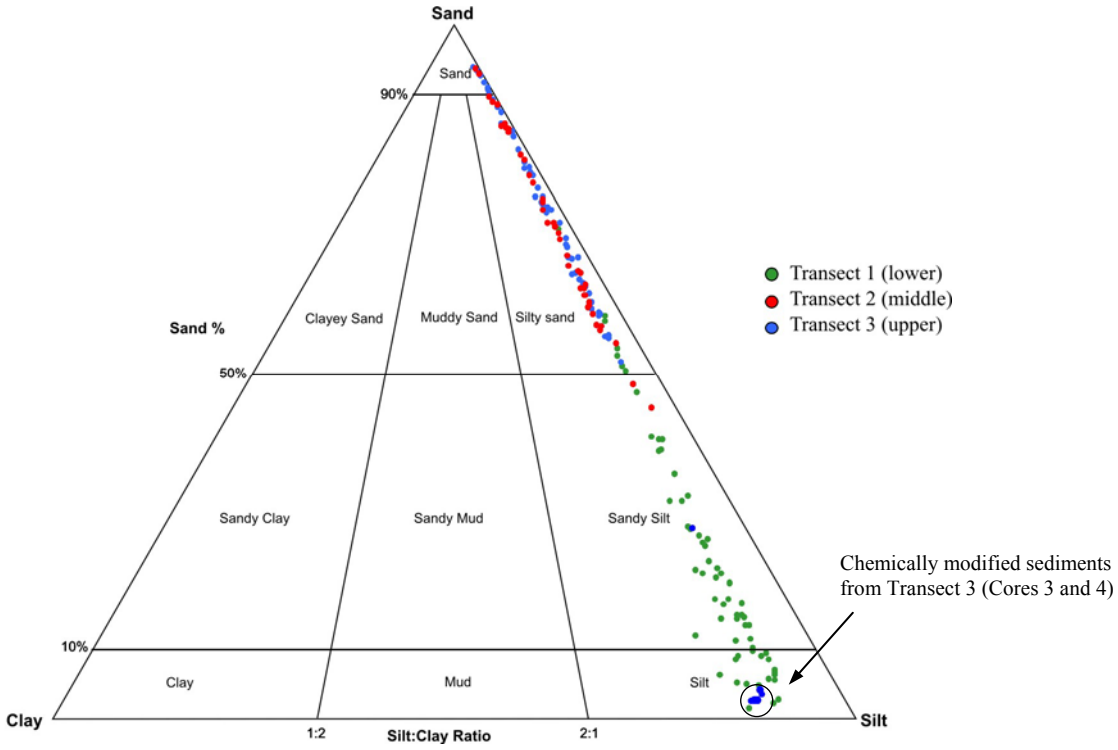

Figure 6.2 Sand-silt-clay ternary diagram showing the distribution of floodplain sediment samples
Plotted using Gradistat (Blott & Pye, 2001)

Sediment characteristics have a strong influence on biogeochemical processes, as variation in sediment deposition has the potential to create complex flow pathways of varying hydraulic conductivity. The hydraulic conductivity of the sediments is typically determined by particle-size (Arya *et al.,* 1999; Chakraborty *et al.,* 2006) with finer grained material (clay and silt) giving rise to sediments of lower hydraulic conductivity. Variations in hydraulic conductivity can markedly alter drainage, hydrological residence times, solute exchange, redox conditions, and biogeochemical

reactions. Since the chemical evolution of groundwater depends on its residence time in the sediment, sediment characteristics are expected to exert strong control on chemical accumulation within the wetland system.

6.2 Floodplain sediment chemistry

All sediment samples collected from the floodplain show good correlation between silica and alumina, with SiO_2 and Al_2O_3 varying between approximately 55-90% and 5-30% respectively (Figure 6.3). High silica contents are attributed to the presence of quartz, while greater alumina contents are indicative of higher clay contents.

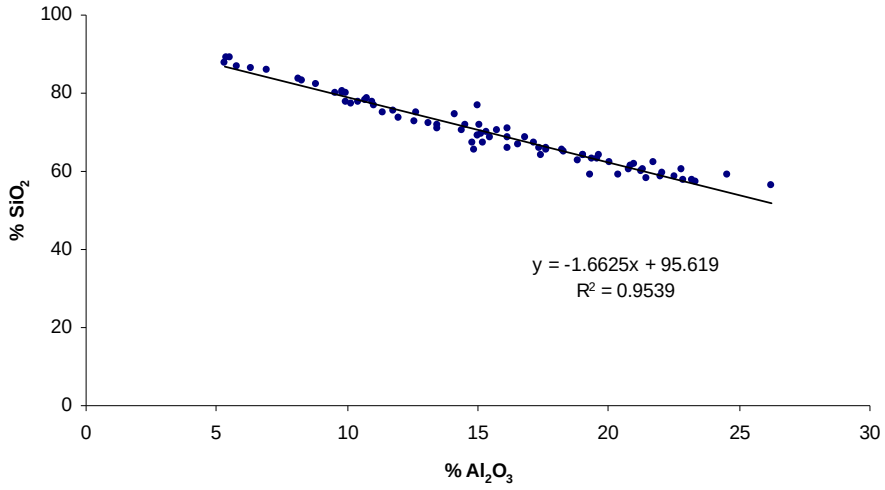

Figure 6.3 Correlation between SiO_2 and Al_2O_3 in bulk sediment samples from cores across the Mkuze Floodplain. (All XRF data given in Appendix 7)

Variation of aluminum in the environment is often considered to reflect mineral weathering (Kersten & Smedes, 2001) and it is thus often useful to plot elements of interest against Al_2O_3. Fluctuations with respect to aluminum may reflect diagenetic processes occurring within the sediment subsequent to deposition. Iron abundance co-varies with aluminum (Figure 6.4), although a number of samples are displaced towards higher iron compositions, suggesting the presence of iron-rich components in some samples.

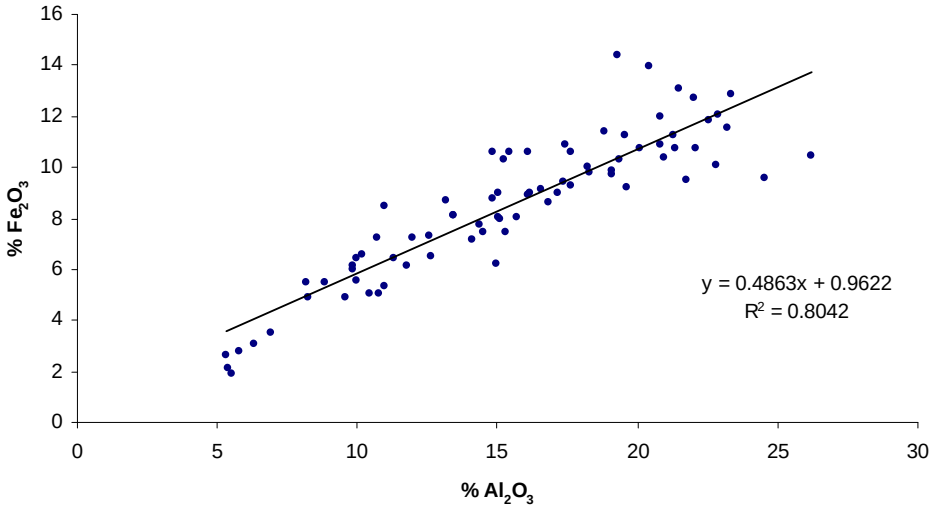

Figure 6.4 The relationship between total Fe_2O_3 and Al_2O_3 in bulk sediment samples

There is reasonable correlation (R^2 = 0.59) between magnesium and aluminum, suggesting that magnesium is derived partly from fluvial clastic input (Figure 6.5). Calcium and aluminum abundances show no apparent relationship, indicating that calcium in floodplain samples is largely unrelated to fluvially introduced clastic material (Figure 6.5).

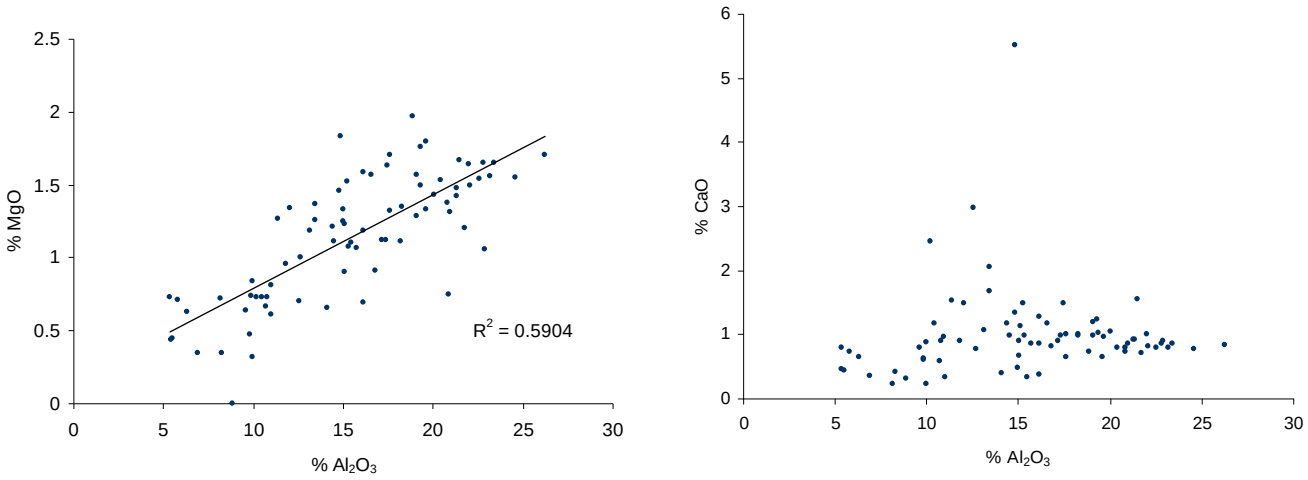

Figure 6.5 Plot of total MgO and total CaO against Al_2O_3 for bulk sediment samples

6.3 Influence of pH and redox conditions

Sediment redox conditions play an important role in determining many biogeochemical reactions. These reactions are responsible for the cycling of various chemicals, particularly iron and manganese. However, sediment pH and redox status are transient in nature and may change over short periods (Cresser *et al.,* 1993). Eh-pH diagrams are thus useful for depicting the most likely form of a particular element under certain environmental conditions.

Sediment Eh and pH data from samples collected in this study show that Fe and Mn are present predominantly as the oxyhydroxides Fe_2O_3 and Mn_2O_3, respectively (Figure 6.6). This is consistent with other field studies that have shown that Fe_2O_3 minerals may account for 30 to 60% of Fe minerals in hydric soils (Richardson & Hole, 1979). In general, Mkuze floodplain sediments are moderately reduced (100 to 400 mV) and above redox thresholds for both Fe and Mn reduction. However, progressively more reducing conditions are typically found at greater depths, with reduced (-100 to 100 mV) and highly reduced (-100 to -300 mV) conditions being encountered near the watertable in some cases. Here, anaerobic conditions facilitate the reductive dissolution of Fe(III) and Mn(IV) to produce soluble Fe(II) and Mn(II) present in sediment porewaters. Accumulation of Fe and Mn oxides typically occurs just above the anoxic zone, as Fe(II) and Mn(II) diffuse upwards from deeper, more reduced sediment zones and react with oxygen in the aerobic horizons above.

There is typically a strong relationship between the position of the watertable in a wetland and redox potential, as fluctuation in the height of the watertable changes the extent of unsaturated and saturated zones (Fiedler & Sommer, 2004; Dahm *et al*., 1998). Seasonal variations in sediment redox chemistry have been widely documented in a number of sedimentary environments (Korestsky *et al.,* 2006), with increased Fe mobilisation typically associated with increasing duration of saturation. Thus, the periodic flooding and drying cycles experienced by the Mkuze system are likely to exert strong controls on the redox status of floodplain sediments and therefore other biogeochemical reactions.

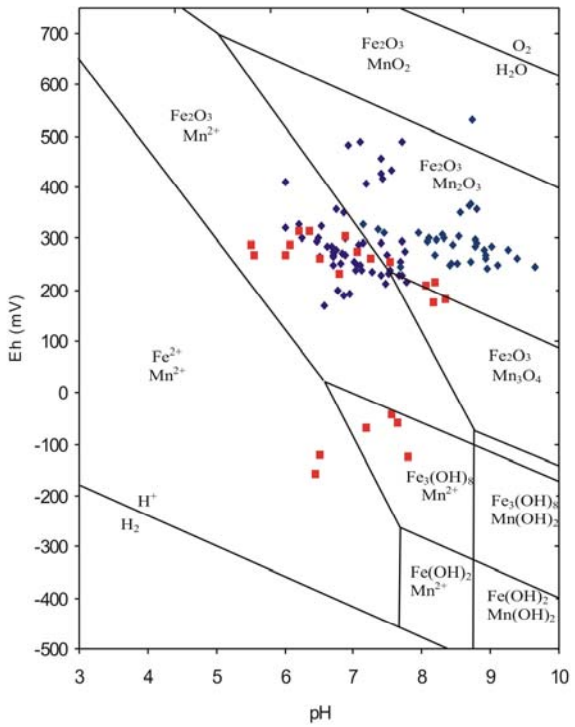

Figure 6.6 Eh-pH diagram showing predominant iron and manganese forms, with samples close to or below the watertable shown in red
Redrawn from Collins & Buol (1981)

The majority of sediment sampling for this study was done during winter months and thus redox results obtained are likely to represent conditions that prevail during dry periods. During this time, zones of reduction appear to be limited to sediments near and below the watertable. While it was not the aim of this study to document seasonal changes in sediment geochemistry and no such data were collected, it is anticipated that the extent of the reduced zone would increase in response to a rising watertable with the onset of the rainy season. During this period, iron is likely to be remobilized, making its readily available for biogeochemical reactions. In winter, as rainfall diminishes and floodplain sediments dry out, redox potential would once again rise above the threshold for iron reduction and cause Fe oxyhydroxides to precipitate out of solution. The low hydraulic conductivity of floodplain sediments may, however, reduce oxygen diffusion to the point where saturated conditions are maintained long after the flooding event.

While the distribution of Fe oxyhydroxides at depth is likely controlled by seasonal fluctuations in the level of the watertable, surface Fe and Mn accumulations are most probably due to the cycling

of these elements by wetland plants. Wetland plants are adapted to surviving in stressful anoxic conditions by being able to release oxygen through their roots. This has the potential to change redox stratification and typically results in Fe and Mn oxide ‘‘plaques’’ forming in sediments surrounding plant roots.

The primary hydrological input to the Mkuze Floodplain is flow via the Mkuze River. The majority of Fe precipitating in the sediment must therefore be supplied by flow from the channel. The concentration of Fe in Mkuze River water varies seasonally between 0.065 and 0.43 µg/ml (Barnes, 2008), and much of this Fe would be expected to precipitate out in close proximity to the river channel as water seeps into the floodplain. Higher iron concentrations near the river channel further downstream are likely to be a consequence of floodplain sediment texture. Very coarse and porous deposits, such as those that dominate regions near the river channel in the upper reach, are unlikely to retain water for a significant period of time. This lowers the likelihood of reducing conditions developing for any length of time. However, finer sediments further downstream are associated with lower hydraulic conductivities, which support longer periods of saturation and encourage the development of redoximorphic features in the sediment.

6.3.1 Redoximorphic features on the floodplain

Two kinds of redox features appear to form in Mkuze Floodplain sediments as a consequence of seasonal changes. The accumulation of soft, orange/red Fe, and black Mn deposits occurs across the floodplain. The most likely phases produced by oxidation are amorphous iron oxyhydroxides and amorphous Mn(IV) (Stumm & Morgan, 1981). These are found in great abundance predominantly in surface sediments and those near the watertable. Such formations probably represent an early process in the precipitation of Fe and Mn, which form when Fe and Mn oxidise within the sediment pores. The formation of these deposits is probably favoured by the silty texture of the floodplain sediments that provides sites for the reoxidation of reduced Fe and Mn.

The formation of hard, black Fe-Mn nodules, the occurrence of which is limited to on the lower reach, represents the second type of redoximorphic feature found on the floodplain. Nodules are usually recognised as being characteristic of poorly drained soils (Richardson & Hole, 1979; D’Amore, 2004). Thus, the lower hydraulic conductivity of sediments at on the lower reach (due to

a higher proportion of fine sediments) results in poorly drained sediments and conditions which favour Fe-Mn nodule formation.

Overall, high Fe oxyhydroxide concentrations (exceeding 3%) are thus likely to be a consequence of secondary accumulation, resulting from the precipitation of Fe introduced as a solute in Mkuze River water. Iron preferentially accumulates in surface sediments and in horizons closest to the mean groundwater level, producing distinct sediment mottling (Figures 5.12 and 5.25). Floodplain sediments thus appear to be an important sink for iron, whose distribution is linked to the interdependencies between hydrology, sediment texture, and vegetation.

6.4 Evolution of groundwater chemistry and the influence of evapotranspiration

Chloride is very soluble and is usually conserved in solution under evaporation. It is thus typically used as a concentration tracer and reliable indicator of chemical processing (Logan & Rudolph, 1997; Love *et al*., 1993). Figure 6.7 shows that groundwater chloride concentrations are well correlated with conductivity, making chloride a suitable concentration tracer in the Mkuze Wetland. A plot of solute concentration against chloride concentration can thus be used to investigate the effect that evapotranspiration has on the chemical composition of groundwater.

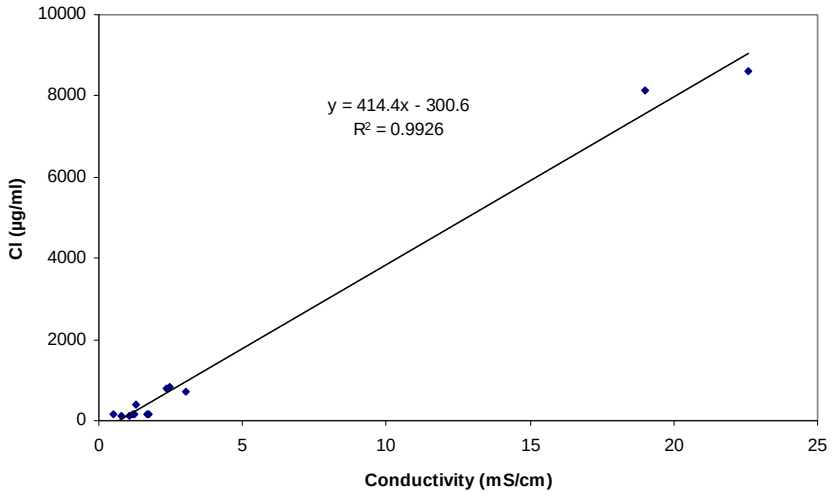

Figure 6.7 Relationship between groundwater conductivity and chloride concentration

The influence of evapotranspiration on groundwater calcium concentrations varies considerably across the floodplain (Figure 6.8). At Transect 3, calcium builds up in solution under evaporation, reaching substantial levels of up to 1780 µg/ml. Despite apparently high levels of evapotranspiration, $CaCO_3$ does not precipitate in these sediments. In contrast, higher chloride values are associated with decreasing calcium concentrations at Transect 1. This is due to the precipitation of abundant $CaCO_3$ which draws soluble calcium out of solution (Figure 5.14). There appears to be little evaporation effect on groundwater calcium concentrations at Transect 2, confirming that $CaCO_3$ precipitation probably does not take place within these sediments (Figure 5.27).

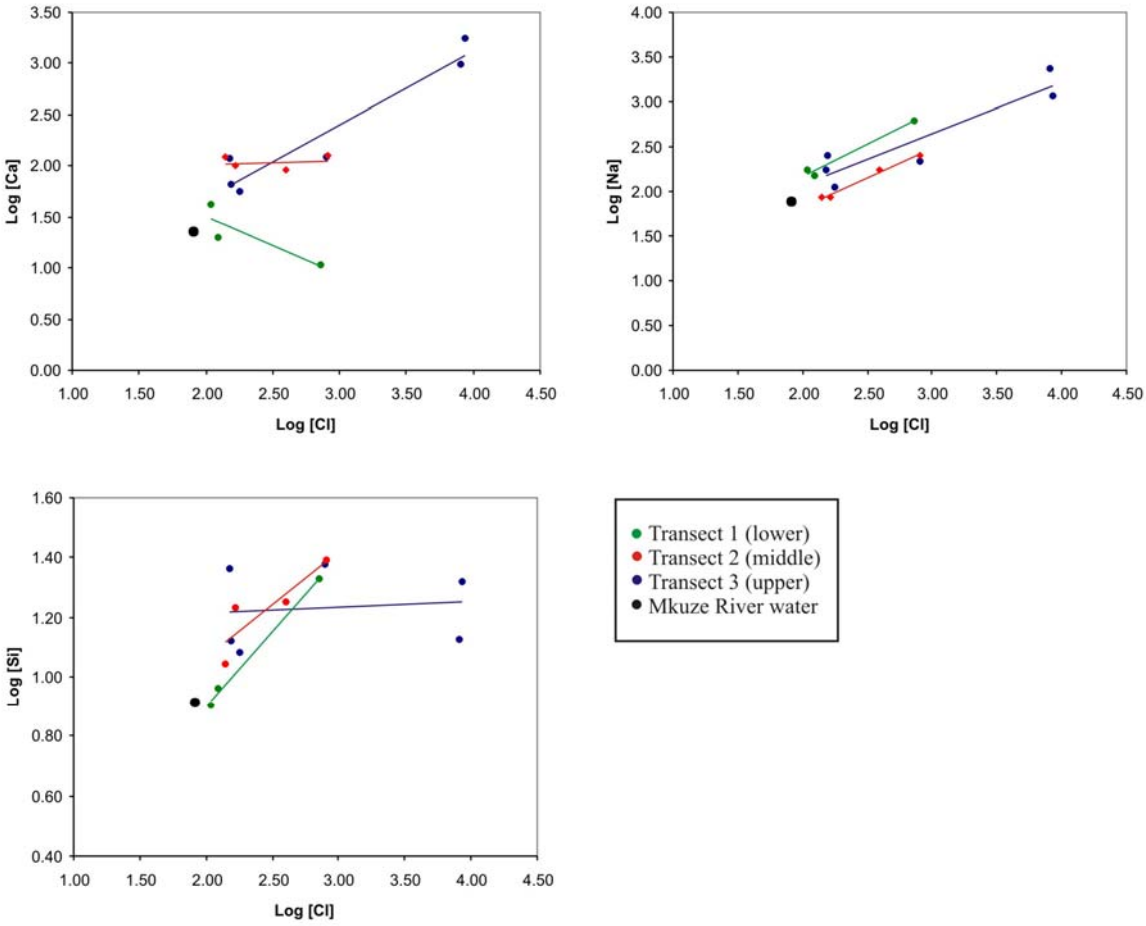

Figure 6.8 Effect of evapotranspiration on the concentration of groundwater calcium, sodium and silicon

Groundwater silicon concentrations at Transects 1 and 2 increase under the influence of evaporation. At Transect 3, higher salinities do not show corresponding groundwater silicon enrichment, indicating that silicon-containing compounds are probably precipitating in this region. At all sites, groundwater Na becomes increasingly concentrated under the effects of evapotranspiration, and thus appears to remain soluble over the range of groundwater solute loads measured across the floodplain.

Flow from the Mkuze River represents the major hydrological input into the wetland system and is characterised by moderate solute loads and conductivities ranging from 0.563 to 1.456 mS/cm (Barnes, 2008). Rainwater constitutes the most dilute input to the system) and is therefore not considered a significant solute input. High groundwater conductivities (up to 22 mS/cm) recorded on the floodplain thus indicate that a concentration process is modifying the relatively dilute chemical inputs to the Mkuze System.

The development of salinity and elevated solute concentrations in this system appears to result from evapotranspirative concentration of groundwater. Concentration of groundwater driven by vegetation transpiration has been widely documented in a variety of wetlands and lakes (Barbiero *et al*. 2002; Jørgensen, 2002; Logan *et al*., 1999; Jacks, 1973). In such situations, progressive evapotranspiration and groundwater concentration often initiates the precipitation of minerals.

Evapotranspiration appears to be the driving mechanism controlling chemical accumulation on the Mkuze Floodplain. The selective removal of water by floodplain plants and trees causes solutes to concentrate in solution, which under the right conditions, may precipitate as minerals/compounds. Mineral saturation on the Mkuze Floodplain is likely to be aided by limited groundwater flushing, restricted drainage, and sediments of lower hydraulic conductivity.

6.5 Evaporation modelling

When water is removed from solution, compounds start to saturate and precipitate out. The type of mineral formed and the sequence of precipitation is determined by the relative ratios of ions in solution and by the solubility of the relevant mineral. The precipitation of a number of minerals from Mkuze River water was modelled as a function of evaporative concentration (Table 6.1).

Modelling results are consistent with the findings from this study and show that $CaCO_3$ is the first mineral predicted to precipitate from solution. This occurs between 50% and 80% evaporation, and is followed by the precipitation of amorphous silica at 80-90% evaporation. Although dolomite saturation appears to be reached at 80% evaporation, it was not detected in any samples, possibly due to its unfavourable precipitation kinetics (Stumm & Morgan, 1981). Recorded chloride concentrations indicate that groundwaters may be concentrated by a factor of up to 50 times. Under such conditions (98% evaporation), gypsum is predicted to begin precipitating from solution, although no evidence of this was found. Halite remains undersaturated even at higher degrees of evaporation.

Table 6.1 Calculated saturation indices in response to the evaporation of Mkuze River water

Mineral	Mkuze River	50%* (2x)	80% (5x)	90% (10x)	95% (20x)	98% (50x)
Calcite ($CaCO_3$)	-0.97	-0.46	0.17	0.62	1.04	1.56
Aragonite ($CaCO_3$)	-1.11	-0.60	0.03	0.48	0.90	1.42
Dolomite ($CaMg(CO_3)_2$)	-1.80	-0.78	0.49	1.39	2.24	3.26
Gypsum ($CaSO_4$)	-2.02	-1.56	-1.00	-0.61	-0.25	0.21
Halite (NaCl)	-6.78	-6.21	-5.46	-4.91	-4.36	-3.64
Smectite (nontronite)	8.99	10.81	13.21	15.02	16.84	19.25
SiO_2 (amorphous)	-0.78	-0.48	-0.08	0.23	0.54	0.96

Note: The PHREEQC modelling assumes that evaporation and evapotranspiration have the same effect and that evapotranspiration has no effect on the ion ratios.
*Percentage evaporation (concentration factor)

6.6 Chemical precipitation on the Mkuze Floodplain

6.6.1 Calcium carbonate precipitation

Overall $CaCO_3$ content of floodplain sediments is generally low (0 – 0.2%), with regions of significant accumulation being confined to specific areas on the floodplain. Very little $CaCO_3$ precipitation appears to occur on the floodplain at either Transects 2 or 3, with calcite nodules only being found in sediments surrounding Yengweni Lake. Yengweni Lake sediments appear to be an important sink for calcium, with Barnes (2008) reporting widespread $CaCO_3$ precipitation along the margin of this lake, especially near the southern edge. Extensive $CaCO_3$ precipitation also occurs on the lower reach, particularly towards the floodplain margin, where calcium concentrations can reach

levels in excess of 6% (wt). Calcium carbonate precipitation in this region of the floodplain appears to be a particularly intense process that eventually results in the precipitation of aragonite, which is thermodynamically not favoured.

Alkaline conditions favour $CaCO_3$ accumulation (Bohn *et al*., 2001) and pH appears to be one of the most important factors influencing $CaCO_3$ precipitation on the Mkuze Floodplain (Figure 6.9). Variation in pH is responsible for most of the observed changes in saturation state. Precipitation of $CaCO_3$ only occurs where groundwater and sediment generally have a pH 7. Almost all sediment and groundwater samples at Transect 1 are alkaline, with some samples reaching values greater than 9 (Figure 5.7). This allows porewater to become supersaturated, resulting in areas of high $CaCO_3$ precipitation. In contrast, sediment and groundwater from Transects 2 and 3 are generally characterised by lower pH. Groundwater pH from these regions is typically less than 6, and this appears to keep sediment porewaters undersaturated with respect to $CaCO_3$ in spite of high porewater calcium concentrations in certain areas. It is only in sediments near Yengweni Lake, where alkaline lake waters and evapotranspiration from *Acacia xanthophloea* that border the lake, where substantial quantities of $CaCO_3$ precipitate.

There is an obvious link between porewater chemistry and $CaCO_3$ distribution, with all regions of porewater supersaturation showing evidence of $CaCO_3$ precipitation. In terms of solubility, gypsum should be the next mineral to precipitate. However, it appears that removal of calcium and increases in pH produced by carbonate precipitation prevents these waters from reaching saturation with respect to gypsum, causing sulphate, present in relatively low concentrations in groundwaters, to become enriched in porewater under conditions of evapotranspirational water loss.

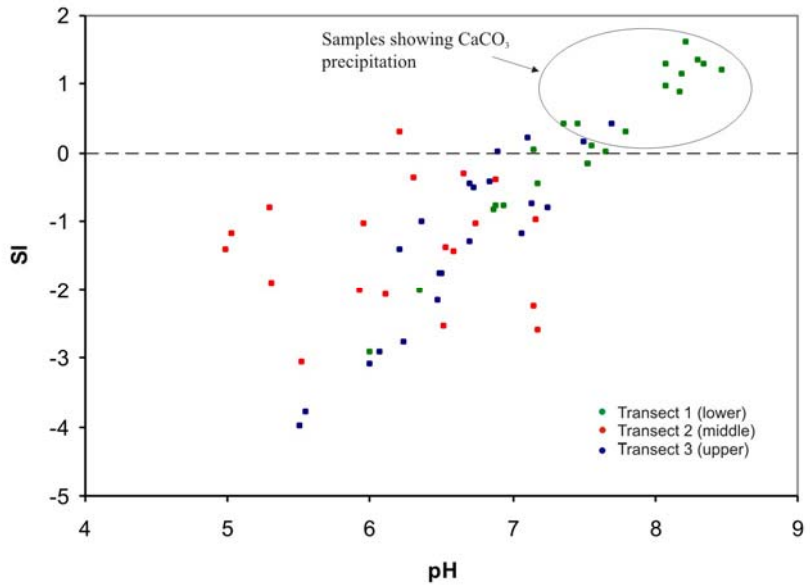

Figure 6.9 Plot of pH against saturation index (SI) of calcium carbonate in sediment porewaters

6.6.2 Silica precipitation

In many environments, the precipitation of $CaCO_3$ under conditions of evaporation is often accompanied by the *in situ* precipitation of other minerals. Investigations by Deocampo (2005), Barbiero *et al*. (2002) and Deocampo & Ashley (1999) have all shown that in wetlands subjected to evaporative conditions, $CaCO_3$ precipitation is accompanied by the precipitation of Mg-silicates and amorphous silica. The identification of Mg-silicates and amorphous silica in floodplain sediments suggests that similar processes are occurring in the Mkuze Wetland System. Although no direct evidence was presented, many studies carried out in the wetlands of the Okavango Delta suspected that the removal of vast quantities of silicon from solution was due to the precipitation of amorphous silica (McCarthy & Ellery, 1995; McCarthy *et al*., 1991). Electron microscopy results from this study prove that, under suitable conditions, amorphous silica precipitates within Mkuze Floodplain sediments (see Figure 5.31). Amorphous silica compounds are associated with highly saline sediments, suggesting that these compounds probably only form under intense evapotranspirational water loss.

Under the influence of strong evapotranspiration, a number of silica compounds are precipitating on the Mkuze Floodplain. Monosilicic acid, which is the main soluble form of silica in nature,

polymerises in response to solution concentration (Drees *et al*., 1989). As polymerization continues amorphous silica begins to precipitate, and with further loss of water and crystallization, opaline silica forms (Williams *et al.,* 1985). The extent to which silica precipitation is occurring is difficult to quantify in sediment containing abundant quartz and a variety of clay minerals. These compounds also cannot be detected by XRD due to their amorphous nature, unless present in very large amounts. Nevertheless, the precipitation of amorphous silica and Mg-silicates are recognised as important sinks and have been implicated in the consumption of large quantities of solutes from solution (Jones & Weir, 1983; Deocampo, 2005).

In addition to the precipitation of silica compounds, the production of phytoliths (silica bodies produced by plants) is common in wetland environments. The removal of silica from groundwater by plants has been documented in a variety of wetland environments (Wust & Bustin, 2003; Deocampo & Ashley, 1999; McCarthy & Ellery, 1995). Although no direct evidence of this was found, it is likely that silica is also precipitated as phytoliths by the grasses and sedges found on the floodplain. Wetland plants are generally highly productive, and are thus likely to be efficient at transforming dissolved silica into the solid phase.

6.6.3 Clay mineral neoformation

Iron containing smectites can form via three different processes: as a product of chemical weathering of basic rocks such as basalt and dolerite, by hydrothermal alteration which occurs in marine environments, or by chemical precipitation from solution (Stucki, 1988). In this respect, the origin of Fe-smectite on the Mkuze River Floodplain is problematic. Firstly, the Mkuze River appears to transport smectite as part of its sediment load. Analysis of Mkuze River sediment shows that smectite accounts for approximately 20% of total clay transported by the river. This is likely to be derived from the weathering of igneous rock (basalts) in the catchment, with subsequent transport and deposition on the floodplain. However, stratigraphical changes in clay mineral abundances in relation to variations in physico-chemical conditions, suggests that smectite on the floodplain may not be exclusively derived from fluvial sources. In certain cores, smectite increases in abundance with depth, resulting in some samples containing >60% smectite. Increased smectite contents also seem to be associated with areas of higher conductivity and $CaCO_3$ precipitation. This suggests that a portion of the smectite on the floodplain is chemically derived through neoformation reactions.

Wilson (1999) acknowledges that not enough emphasis has been placed upon neoformation processes. While smectites were once believed to be a product only of weathering or hydrothermal alteration, considerable evidence now exists that direct crystallisation or *in situ* precipitation are possible processes of formation. The neoformation of smectites has been reported in a wide range of environments, ranging from wetlands in Brazil (Furquim *et al*., 2004; Barbiéro *et al*., 2002), northern Spain (Armenteros *et al.,* 1995) and California (Lee *et al.,* 2004), to lakes and wetlands in central and east Africa (Hover *et al.*, 1999; Hover & Ashley, 2003; Liutkus & Ashley, 2003; Darragi & Tardy, 1987; Gac *et al*., 1977; Chamley, 1989). Although geomorphically diverse, these environments are similar in their ability to provide ions necessary for formation of smectite. In addition, climatic and hydrological conditions have been shown to be important variables that influence solute concentration and govern the precipitation of clay minerals. In particular, intense evaporation appears to favour smectite neogenesis.

In these settings, clay neoformation is commonly accompanied by $CaCO_3$ and silica precipitation (Furquim *et al*., 2004; Von Damm & Edmond, 1984; Gac *et al.,* 1977). This may explain the high smectite contents that typically accompany $CaCO_3$ and silica precipitations on the Mkuze Floodplain, particularly on the lower reaches and in sediments surrounding Yengweni Lake. Evapotranspiration that leads to the precipitation of $CaCO_3$ and silica, probably also results in the precipitation of smectite. This occurs at depth in the region of the watertable, resulting in increasing smectite abundance with depth.

At Transect 3, smectite neogenesis is also likely to occur in the region of Cores 3 and 4, where strong evapotranspiration causes the development of high solute concentrations. Results from this study have already shown that this process results in the precipitation of amorphous silica in this region. Under favourable conditions, a portion of soluble silica may also be incorporated into the formation of clay minerals. In a series of laboratory experiments, Harder (1972) found that the formation of clay minerals only takes place from solutions that are undersaturated with respect to amorphous silica. Highly saturated SiO_2 solutions were not able to precipitate clay minerals. Geochemical modelling shows that, at the time of sampling, Mkuze sediments at Transect 3 are all slightly undersaturated with respect to amorphous silica. It is thus suspected that intense evapotranspiration causes silicon to saturate, resulting initially in the precipitation of amorphous silica. As the precipitation of amorphous silica removes silica from solution, conditions begin to

favour the neoformation of smectite. Research elsewhere has shown that amorphous silica can facilitate the neoformation of silicates (Hover & Ashley, 2003; Wust & Bustin, 2003).

Iron-smectite precipitation process

Pedro *et al.* (1978) describe the formation of Fe-rich smectite (nontronite) in the sediments of Lake Chad by the *in situ* precipitation of Fe with silica. They speculated that this process involved the transformation of Fe oxides, which under reducing conditions, combine with silica in a hydroxy complex that crystallizes into ferric smectite. This conversion has been implicated in the consumption of large amounts of silica from river water flowing into Lake Chad (Pedro *et al*., 1978). Harder (1972) also showed that amorphous hydroxides of Al, Fe and Mg are capable of co-precipitating silica even from very dilute surface solutions, which under the right conditions crystallize into clay minerals.

A similar mechanism for the occurrence of Fe-rich smectite on the Mkuze floodplain is proposed. Reductive dissolution of iron oxides, caused by prolonged sediment saturation, results in Fe^{2+} being made available for the formation of a Si-Fe^{2+} hydroxy complex. In laboratory synthesis experiments, Harder (1976) demonstrated that the formation of Fe-bearing smectites could only be accomplished from a solution which was initially under reducing conditions and suggested that a slightly alkaline pH favoured synthesis. Under these conditions, the amorphous Si-Fe^{2+} hydroxy complex transforms into Fe(III) smectite. Some uncertainty exists regarding the necessary and sufficient conditions for synthesis. Stucki (1988) suggests that the effect of pH may simply be kinetic, with lower pH environments requiring longer reaction times.

It is widely acknowledged that it is difficult to distinguish neoformed smectite from that which has been detritally derived (Allen & Hajek, 1989), and this is certainly the case for the Mkuze Floodplain. Surface clay deposits are undoubtedly the result of overbank flooding and deposition. Similarities in the distribution of vermiculite, mica, and kaolin suggest that these clay minerals are detrital. However, physicochemical conditions on the Mkuze floodplain appear to be favourable for smectite neogenesis. Such conditions include the build up of solutes under evapotranspiration, restricted drainage, and seasonal watertable fluctuations. While most clays form in upper horizons where factors of soil formation are most intense, it is suspected that smectite neogenesis occurs predominantly at depth, where solutes are highly concentrated and regular changes in redox conditions take place.

In most circumstances, smectite neogenesis is dominated by the formation of Mg-smectite (Hover *et al.,* 1999; Gac *et al.,* 1977). The occurrence of ferric smectite in shallow deposits appears to be rather rare (Pedro *et al*., 1978; Giresse & Wiewióra, 1999). The supply of iron and periodic development of reducing conditions appears to favour the precipitation of Fe-rich smectite on the Mkuze Floodplain. Iron-rich smectites are known to be more stable than Mg-smectites in acidic conditions (Robert & Veneau, 1979 in Delvaux *et al*., 1990).

6.7 Spatial variation in chemical sedimentation

Mass balance modelling by Barnes *et al.* (2002) provides some measure of the extent to which solutes are being retained within the Mkuze Wetland System (Table 6.2). This study has provided insight into the mechanisms involved in retaining these solutes. Calcium and magnesium are retained predominantly in a carbonate phase, which precipitates under the influence of evapotranspiration. This occurs extensively on the lower reaches of the floodplain, but also in sediments surrounding Yengweni Lake. The majority of soluble silicon that enters the Mkuze System is retained (80%), which appears to occur through the precipitation of silica compounds, including amorphous silica, Mg-silicates and neoformation of Fe-smectite.

Table 6.2 Estimated retention of solutes within the Mkuze Wetland System

Solute	Approximate % of mass retained
Silicon	80
Potassium	70
Calcium	50
Magnesium	20
Sodium	20

Source: Barnes *et al*. (2002)

Potassium and sodium are common exchangeable cations (Evans, 1989), and this represents the most likely sink for such elements. Sequential extraction data show that typically 30-70% of sodium in sediments is present in a loosely bound form. Potassium and sodium may also be accumulated by plants that take them up as nutrients.

The length of time required for compounds to saturate under the influence of evapotranspiration is dependent on the concentration of groundwater inflow, the ratio of rainfall to evapotranspiration, as well as the type of vegetation. Chemical sedimentation across the Mkuze Floodplain is thus not spatially uniform. Regional differences in chemical accumulation on the Mkuze Floodplain appear to be a product of variation in fluvial geomorphological processes, hydrological flow patterns and vegetation distribution, which create site-specific conditions on the floodplain that favour chemical sedimentation.

The large volume of clastic sediment deposition that has taken place on the floodplain over time has blocked the interdune tributaries that previously flowed into the Mkuze River from the north. The interruption of free flow from these drainage lines has affected local groundwater flows and resulted in a change from groundwater discharge to groundwater recharge. Local groundwater recharge conditions appear to be an important factor contributing to the retention of solutes as a result of longer hydrological residence times, particularly near Yengweni Lake (Barnes, 2008) and probably more so at Muzi Lake.

Figure 6.10 shows the elevation of Muzi, Yengweni and Mdlanzi Lakes relative to the Mkuze River. Being at a lower elevation than the Mkuze River, water must flow into Yengweni and Muzi Lakes during flood events. Given these differences in elevation and the aggradation of the Mkuze Floodplain over time, groundwater recharge must take place in the vicinity of Muzi and Yengweni Lakes. Floodplain sediments themselves also experience less frequent flushing, giving groundwater solutes time to build up in solution under evapotranspiration. High solute concentrations recorded on the floodplain at this site indicate that very little flushing occurs, which promotes chemical sedimentation in these regions.

The degree of groundwater and porewater concentration on the floodplain near Mdlanzi Lake is far less than that encountered near Yengweni Lake. This is partly due to groundwater discharge down the southward-flowing drainage lines in which Mpanza and Mdlanzi Lakes are situated. Fresh water recharge from the coastal plain thus does not allow solutes to reach sufficient concentrations to enable chemical sedimentation. The more acidic sediment environment, created by this groundwater discharge also appears to be an important factor preventing mineral saturation.

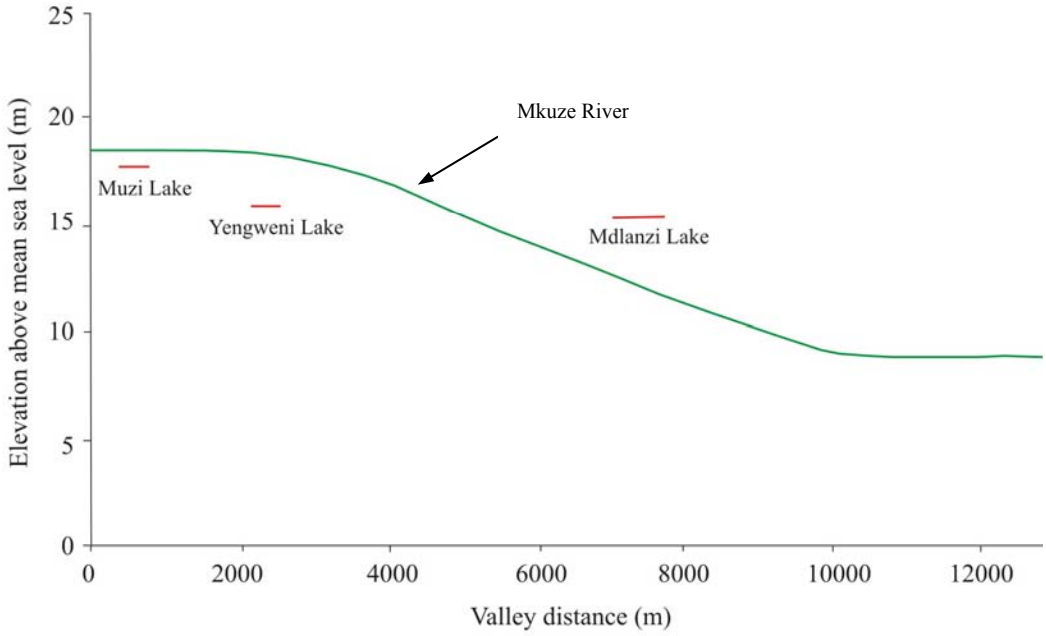

Figure 6.10 Elevation of Muzi, Yengweni and Mdlanzi Lakes relative to the Mkuze River

Water from the Mkuze River is continually lost to the surrounding floodplain, such that water flow in the lower reaches of the floodplain is less than in the upper reaches. Significantly finer sediments on the lower extremities of the floodplain also result in sustained floodplain inundation which promotes biogeochemical reactions. The presence of extensive $CaCO_3$ deposits suggests that hydrological residence times are sufficiently long for saturation of this mineral phase.

Salinity variations in wetlands have been correlated with vegetation distributions (Arndt & Richardson, 1993) and this relationship appears to play a key role in chemical sedimentation on the Mkuze Floodplain. As highlighted in Chapter 5, areas of extreme salinity on the floodplain near Yengweni Lake are dominated by the growth of *Acacia xanthophloea*. These trees occur in a band on the floodplain as well as lining the fringes of Yengweni Lake (Figure 6.11). It appears that these deep-rooted trees are particularly effective in selectively removing water through transpiration, resulting in the concentration and eventual precipitation of minerals at depth.

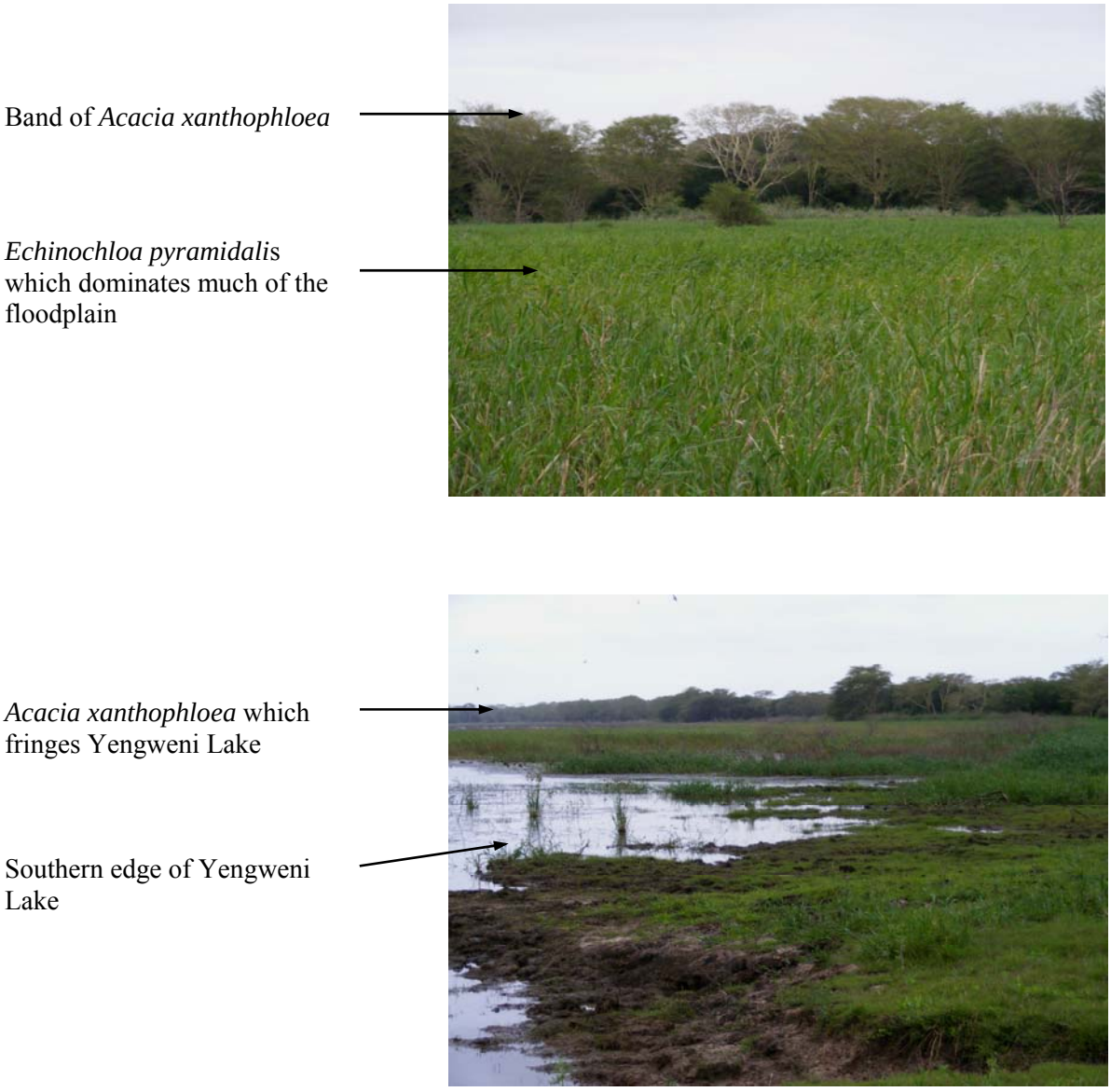

Figure 6.11 Vegetation distribution at Transect 3 showing growth of *Acacia xanthophloea* on the floodplain (top) and on the fringes of Yengweni Lake (bottom)

A. xanthophloea is widespread within the southern African region, typically occurring in swampy or riverine environments where water availability is high (Coates Palgrave, 2003). In Kenya and Tanzania, this species is frequently found associated with channels, swamps and alluvial fans (Deocampo, 2005; Ashley *et al*., 2004). In this region, high soil salinities, thought to be driven by climatic and human-induced factors, have been linked, by some researchers, to the mortality of *A. xanthophloea* (Western & van Praet, 1973; Mills, 2006). Based on this study it is clear that groundwater and soil chemistry is related to the distribution of *A. xanthophloea.* However, it appears as though transpiration from these trees produces areas of elevated sediment salinity. *A. xanthophloea* is drought tolerant, adapted to surviving in the arid and semi-arid savannas of southern Africa by being able to extract water from deep within the sediment profile through extensive root systems. It is also suggested that these trees have the ability to re-direct resources to important areas such as root growth to improve water uptake during times of stress (Otieno *et al*., 2005a; Otieno *et al.,* 2005b). High rates of water extraction from within the sediment profile must therefore contribute to the development of high salinity and thus probably to the documented precipitation of calcium carbonate and silicates in the sediments of east Africa.

A. xanthophloea on the Mkuze Floodplain does not appear to be under any stress, indicating that this species is particularly tolerant of salinities that would be toxic to most other plants. The high porewater and groundwater salinities produced (>20 mS/cm) must therefore play a role in controlling plant distribution. Loss of *A. xanthophloea* forests in Kenya and Tanzania is more likely to be a result of increased elephant (*Loxodonta Africana*) activity rather than salinity, as suggested by Western & Maitumo (2004).

6.8 Clastic sedimentation patterns

Floodplains are commonly recognised as important sinks for clastic sediment and associated chemicals introduced by river systems. Average sediment deposition rates on most floodplains are generally low, in the order of a few millimeters per year (Davidson *et al.,* 2004; He & Walling, 1996), although substantially higher sedimentation rates of up to a few centimeters per year have been recorded for certain rivers (Saxena *et al*., 2002). However, sediment deposition on floodplains is typically spatially variable. Sedimentation tends to occur at higher rates along and near river channels resulting in pronounced levees and channels that are elevated above the surrounding floodplain. This has the potential to create locally steepened gradients which can result in avulsion.

Channel avulsion, the abandonment of a part of the whole of a channel belt for a new course, is a common process in large floodplain wetlands around the world (Assine, 2005; McCarthy *et al*., 1992). Avulsion is driven by instability caused by high rates of sedimentation in localised regions of the landscape, which leads to natural channel diversions along hydraulically favourable pathways. This results in the diversion of water and sediment from one area of a floodplain to another.

Aggradation rate is considered to be the dominant mechanism driving such avulsion events (Bryant *et al.,* 1995; Ashworth *et al*., 2004). Studies of other river systems provide support for the link between aggradation rate and avulsion frequency (Figure 6.12). Frequent (decades to centuries) avulsion events appear to be characteristic of moderately to rapidly aggrading (0.7-1.5 mm/yr) systems, while very slowly aggrading systems (<0.1 mm/yr) typically experience infrequent avulsion. Given an approximate sedimentation rate of 3 mm/yr (Table 5.13), the lower Mkuze Floodplain represents a fairly rapidly aggrading system that should undergo frequent avulsion.

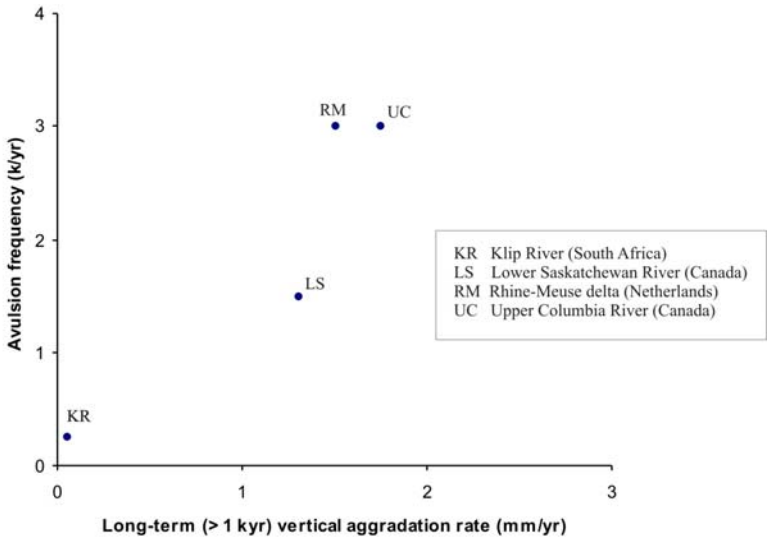

Figure 6.12 Graph showing the relationship between aggradation rate and avulsion frequency
Data for LS, RM and UC taken from Makaske *et al*. (2002), data for KR from Tooth *et al.* (2007)

Past avulsion events on the Mkuze Floodplain are abundantly evident, particularly in the middle reaches of the floodplain where abandoned channel-levee complexes elevated above the surrounding floodplain can be identified (Figure 6.13). Avulsion in this region has been responsible

for the formation of a number of the minor, irregularly shaped lakes associated with the floodplain, which are isolated by the levees of abandoned channels (Watkeys *et al*., 1993).

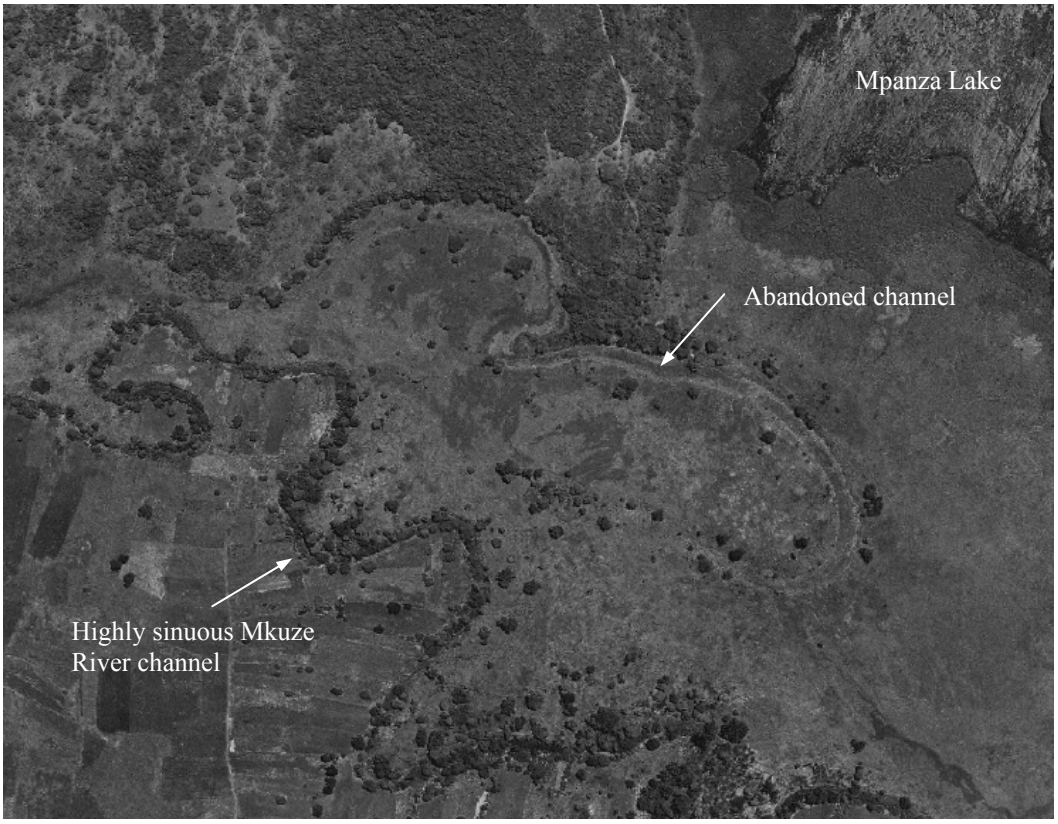

Figure 6.13 Aerial photograph showing evidence of past avulsion events associated with the middle reach of the floodplain

An avulsion event on a much larger scale occurred in 1986, when flow from the Mkuze River was altered by a private farmer who excavated a canal between the Mkuze River and Tshanetshe Lake. The canal was created by enlarging an existing hippo trail with the intention of increasing water supply for crop irrigation and livestock. The canal has subsequently been subjected to rapid erosion resulting in it capturing most of the flow that previously flowed down the Mkuze River course. While initiated by human activity, Ellery *et al.* (2003) believe that channel avulsion was probably inevitable at this point on the Mkuze Floodplain. This is due to the fact that the Mkuze River course is situated on a localised alluvial ridge, resulting in a substantial difference in elevation between the Mkuze River and the floodplain to the south. Hippo trails themselves have been recognised as an important factor determining the course of a new channel during avulsion (McCarthy *et al*., 1998).

Hippos move from the lakes to the surrounding floodplain to graze, resulting in the formation of extensive networks of trails. Repeated movement along these paths create favourable pathways for water flow that may erode into deeper channels. Hippo trails play a particularly prominent role in influencing the location of avulsion courses when they create depressions within the main channel levees, making it possible for water to leave the main channel without overtopping the crests of the levees themselves. Thus, the presence of a hippo trail leading from the river into the backswamp to the south of the Mkuze River may have naturally facilitated avulsion along a hydraulically more efficient pathway. Human intervention simply accelerated a natural process. Efforts to restore flow down the original river channel have been unsuccessful due to a more hydraulically favourable gradient along this alternative watercourse.

Avulsion of the Mkuze River has had important consequences for clastic and chemical sedimentation in the system. Today, water only flows down the original Mkuze course at discharges greater than approximately 17.5 m^3/s (Ellery *et al*., 2003). This represents only the highest 5% of historical flows, with flooding of the floodplain occurring at substantially higher discharges than this. This has had a great impact on floodplain inundation patterns, with lakes to the north of the river no longer being recharged to the same extent (Goodman, 1987). Deprived of a regular supply of solutes and sediment, clastic and chemical sedimentation in the northern sections of the floodplain is probably now limited. In many areas, vegetation has colonised the bed of the abandoned Mkuze channel.

In addition to the development of the canal system, chemical sedimentation processes have probably been affected by the loss of vast areas of riparian forest fringing the Mkuze River. Major sections of riparian forest and backswamp vegetation have been replaced by subsistence agriculture. The effect of vegetation changes on chemical sedimentation in the current study area can only be speculated upon, but replacement of natural vegetation (particularly deep-rooted trees) with cultivated land, which has a lower annual evapotranspiration rate, has in all likelihood reduced the ability of the wetland system to remove solutes from inflowing water.

Chapter 7

The chemical sedimentation model

Wetlands are chemically and biologically complex, and as such, there are many potential mechanisms by which chemicals may be immobilised within these systems. This study has focussed on non-nutrient solutes with data presented in Chapters 5 and 6 suggesting that chemical precipitation driven by evapotranspiration is the major mechanism driving the retention of these solutes in the Mkuze Wetland System. Annual rainfall in the region varies between 800-1000 mm, while evapotranspiration ranges between 1200-1600 mm per year. This translates to a precipitation deficit around 500 mm per year, and coupled with high watertables and restricted drainage, solutes in the groundwater are likely to concentrate under these conditions.

7.1 Mechanism of solute retention

Flow from the Mkuze River is the primary input of water, clastic sediment and solutes onto the floodplain system. Groundwater is fed primarily through channel seepage, although occasional overbank flooding may also supplement groundwater recharge. Due to low hydraulic conductivities and restricted groundwater flow, solutes become increasingly concentrated in solution under the effects of evapotranspiration. Progressive solute concentration eventually results in certain minerals reaching saturation point in the porewater. Under favourable pH conditions, calcium carbonate is probably the first mineral to precipitate (initially as calcite) due to its low solubility in water. This depletes porewaters of soluble calcium and causes an increase in the Mg/Ca ratio, which appears to

favour the precipitation of low-magnesian calcite and eventually aragonite (see Section 5.1.8). Overall, calcium carbonate distribution is controlled by variation in sediment pH, local CO_2 conditions and evapotranspiration. Increasingly saline conditions subsequently result in the precipitation of silica compounds, including amorphous/opaline silica and Mg-silicates.

Evapotranspiration also indirectly controls sediment redox conditions in its effect on the elevation of the watertable. Variations in redox status partially control the solubility and retention of Fe and Mn minerals. Under aerobic conditions, Fe and Mn precipitate in the soil as oxyhydroxides in zones where water levels fluctuate (see Section 6.3). Such redox sensitive minerals also appear to be effective scavengers of other major metals, which become adsorbed to their surface. In highly reduced sediments, sulphate reduction may also result in the formation of Fe sulphides.

Under reducing conditions and elevated silicon concentrations, the precipitation of Fe-rich smectite appears to be a potentially important process (see Section 6.6.3). The formation of clay minerals through neoformation depends upon the appropriate physicochemical conditions of the environment, and a combination of restricted drainage, alternating redox conditions and evapotranspiration appears to provide conditions conducive to the *in situ* formation of Fe-smectite on the Mkuze Floodplain. This process is likely to remove significant quantities of silicon and iron from solution.

Figure 7.1 summarises the complex array of biogeochemical processes that occur on the floodplain of the Mkuze Wetland. The chemical evolution of groundwater and composition of floodplain sediment appears to broadly support the Hardie-Eugster model. Calcium carbonate precipitates early in the evaporation sequence, followed by the precipitation of amorphous/opaline silica and Mg-silicates under higher degrees of evapotranspiration. This ultimately results in water dominated by Na, Cl, HCO_3 and SO_4.

It must be emphasised that while this study has focused on geochemistry, the role of the organic fraction may be important. In addition to the subsurface accumulation of inorganic solutes, there is likely to be substantial organic solute accumulation, which is likely to have an influence on groundwater and sediment geochemistry as described in other wetland environments (Bauer-Gottwein *et al*., 2007). In particular, it is suggested that dissolved organic matter has an important role in iron dissolution and mobilisation of Fe(II) under reducing conditions (Mladenov *et al.*,

2008). This may have some bearing on the availability of Fe(II) and formation of Fe-rich smectite in the Mkuze System.

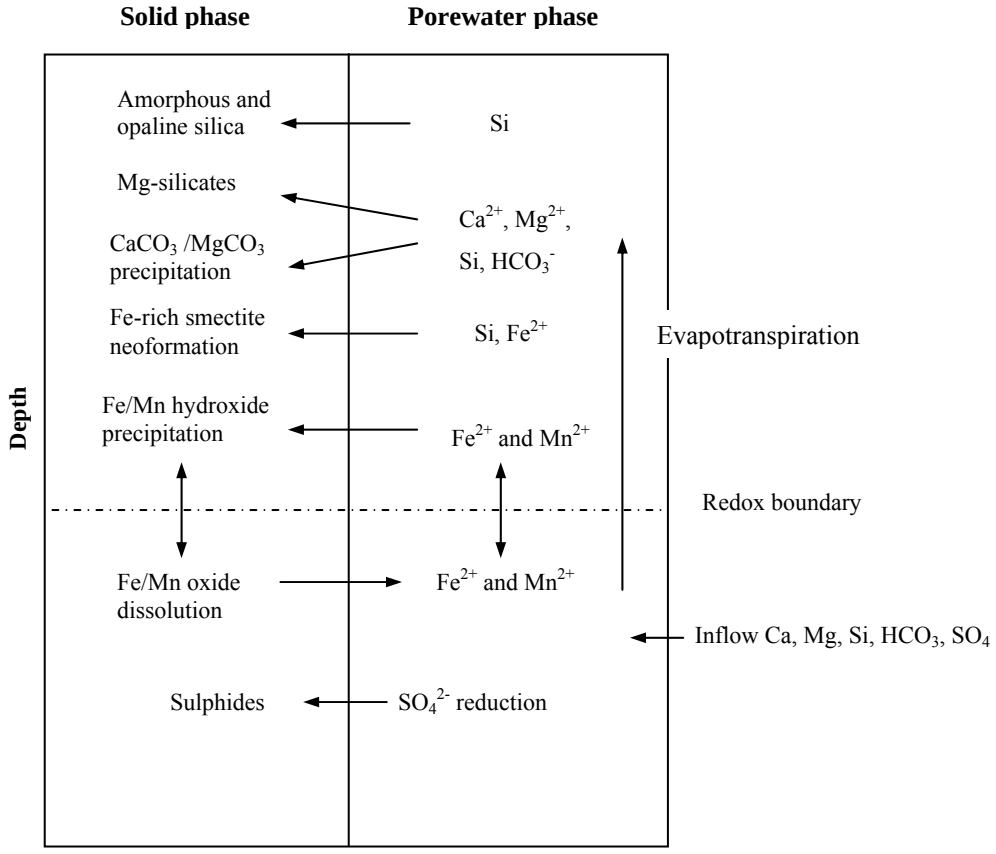

Figure 7.1 Conceptual diagram summarising the major geochemical processes, identified in this study, occurring on the floodplain of the Mkuze Wetland System.

7.2 Sedimentary processes on the Mkuze Floodplain

7.2.1 Clastic sedimentation

Floodplains are commonly recognised as important sinks for storing suspended sediment and associated chemicals in the landscape. Results from this study show that the lower Mkuze Floodplain is a relatively rapidly aggrading system. Calculated sedimentation rates (see Section 5.4) indicate that approximately 3300 tons/km^2 or 1485 000 tons of clastic sediment accumulates annually within the Mkuze Wetland System. The floodplain and its associated wetlands thus act as major sediment sinks, which results in little to no sediment from the Mkuze River entering Lake St

Lucia. This results in an actively evolving floodplain, which continues to prograde in a west-east direction as a result of sediment introduced onto the floodplain by the Mkuze River (McCarthy & Hancox, 2000). Sedimentation rates suggest that this system should undergo frequent avulsion. The activity of hippos is highlighted as playing an important role in this process.

7.2.2 Chemical sedimentation

Solutes introduced into the wetland system are being retained and stored in floodplain sediments, particularly in low-lying backswamp areas where surface-water residence times are long and groundwater recharge conditions prevail. River levees, which are higher than the surrounding floodplain, make it difficult for water to return to the stream once it enters the floodplain, allowing areas of shallow water to collect on the floodplain for extended periods following floods. Chemical sedimentation occurs principally through the evapotranspirational concentration of solutes in soil and groundwater, which causes solutes to precipitate out of solution. This process is likely to be influenced by seasonal variations in rainfall and discharge. Highest groundwater conductivities occur during July (winter), while lowest values are recorded in December, during periods of higher rainfall and water inflow from the Mkuze River (Barnes, 2008). Solute concentrations would thus be expected to intensify during winter months, which are characterised by little to no flow. Chemical sedimentation is thus probably variable over the annual cycle, occurring in an interrupted rather than in a continuous manner. Clastic sedimentation predominates during the high rainfall summer months, while chemical sedimentation is likely to take place preferentially during the drier winter season.

The overall spatial distribution of precipitated minerals is thus the result of the interaction of evapotranspiration and local hydrologic flow patterns developed over time. Major sedimentary and biogeochemical processes identified on the Mkuze Floodplain are summarized in Figure 7.2.

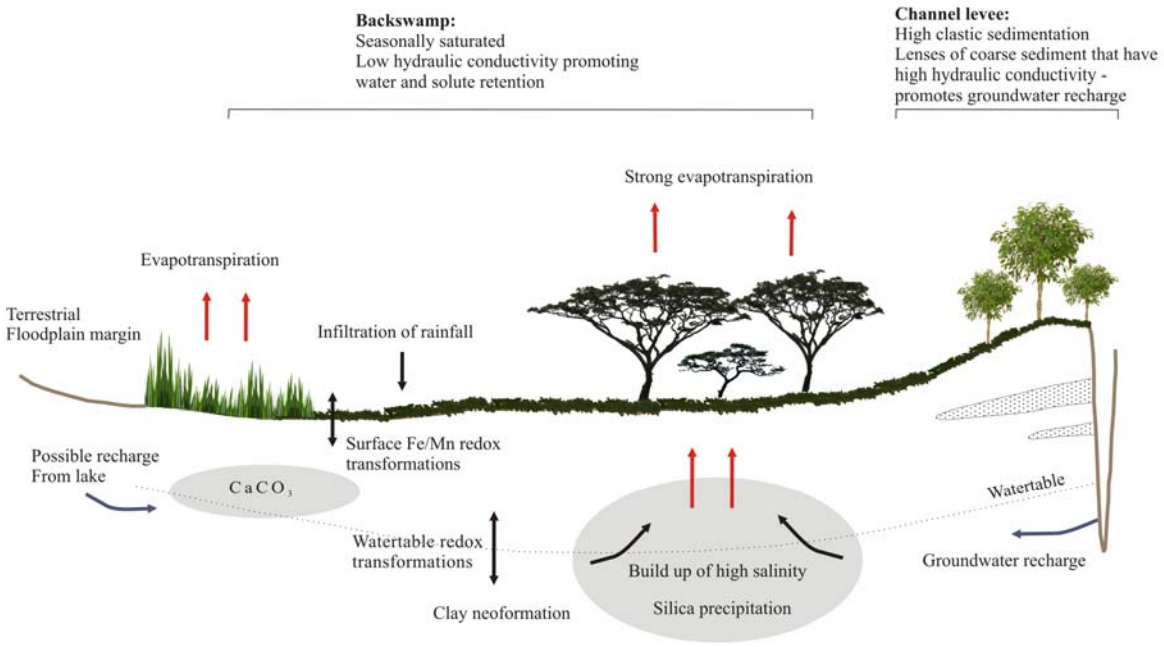

Figure 7.2 Overview of major sedimentary and biogeochemical processes occurring on the Mkuze Floodplain

7.3 Implications of chemical sedimentation for wetland structure and function

Sedimentary infilling in the Mkuze Wetland System has been occurring since the end of the Last Glacial Maximum about 6500 years ago. Resulting aggradation on the floodplain has created conditions favourable for chemical sedimentation. The ability of solutes to concentrate in the groundwater under evapotranspiration depends to a large extent on regional groundwater flows and the nature of the substratum. Deposition of fine sediments (silt and clay) on the coastal plain by the Mkuze River has modified the properties of the wetland substrate, from a relatively high hydraulic environment to one that supports water and solute retention. This has been aided by the formation of pronounced levees, which make it difficult for water to return to the river channel once it enters the floodplain. This allows areas of shallow water to collect on the floodplain for extended periods following flood events. Chemicals thus preferentially accumulate in low-lying backswamp areas where increased hydrological residence times allow solutes introduced into the system to become concentrated under the influence of evapotranspiration. Local groundwater recharge conditions, resulting from the blocking of interdune tributaries from the north, also limit flushing and increase hydrological residence times.

The rate at which chemicals have been accumulating in the system is difficult to determine or even speculate upon. It is likely, however, that this rate has been highly variable in the past, influenced by changing substrate properties and flow dynamics resulting from clastic sediment deposition. Clastic sedimentation must certainly have dominated during the initial formation of the system, caused by the rapid infilling of river valleys associated with sea level rise. Chemical sedimentation, on the other hand, may require hundreds of years to initiate and become noticeable in a wetland, the rate of which is dependent on the concentration of hydrological inputs and water flux within the system. The island complexes of the Okavango Delta, where large amounts of chemical accumulation has been documented, are estimated to be around 100 to 400 thousand years old (Ramberg & Wolski, 2008). Given this, the Mkuze Wetland System is still very young, and thus while clastic input continues to dominate sedimentary processes on the floodplain, it is proposed that as aggradation and progradation of the floodplain continues, it will drive and initiate further chemical sedimentation in the system. As aggradation of the floodplain continues, peat-filled basins, such as Mdlanzi Lake, will receive increasing sediment input, transforming it eventually into a system similar to Yengweni Lake. High flows and associated floodplain inundation thus play a major role in modifying the Mkuze Wetland landscape, through the introduction of clastic sediment and dissolved chemicals.

The accumulation of chemicals on the floodplain is suspected to have important consequences for the wetland system. Wetland soils and hydrology are intricately linked in the development and functioning of wetland ecosystems. Chemical sedimentation has the potential to modify the chemical and physical characteristics of wetland sediment, through changes in hydraulic conductivity, salinity and pH. Smectites, in particular, are well-known for their high cation exchange and water retention properties. Neoformed smectite may thus exert important control on the saturation and drying of the wetland surface, as documented in other wetland systems (D'Amore *et al.,* 2000).

The precipitation of minerals from solution is likely to result in the extraction of large quantities of chemicals from solution. Calcium, Mg, Si and Fe are therefore all expected to be consumed in large amounts as a consequence of mineral precipitation on the Mkuze Floodplain. On the floodplain itself, evapotranspirational water loss can result in the development of highly saline groundwater. Variations in groundwater salinity have been shown to play a crucial role in influencing vegetation distribution in other wetland systems (Ellery *et al*., 2000; Bernaldez & Rey Benayas, 1992). This

study shows that wetland plants, in particular *Acacia xanthophloea*, have the ability to modify their chemical environment through transpiration. This creates local chemical gradients, which are likely to influence vegetation distribution based on tolerance to variation in sediment salinity and pH. The development of salinity and precipitation of solutes may thus play a key role in creating and maintaining the biological and habitat diversity of the wetland

When viewed over longer time scales, cumulative chemical sedimentation may even play a role in modifying regional topography. In both the Okavango Delta (McCarthy *et al*., 1993) and the Everglades (Troxler Gann, 2005), chemical accumulation as a result of evapotranspiration has been implicated in altering local topography. The precipitation of chemicals in the soil results in vertical expansion, creating elevated "islands" that support a wide variety of plants. Given sufficient time, chemical precipitation is likely to represent a significant mechanism of accretion on the Mkuze Floodplain, especially given the fact that precipitation does not occur uniformly over the floodplain, but is restricted to localised areas. Small changes in elevation may translate to large changes in duration of inundation, thereby influencing habitat diversity on the floodplain.

7.4 Conclusion

Wetlands are well-known for their ability to act as sinks for sediment and chemicals in the landscape. Sedimentation within these systems, however, is commonly investigated by considering only clastic deposition. The considerable similarities between biogeochemical processes occurring in the Okavango Delta and those identified in the Mkuze Wetland System, indicate that chemical sedimentation can play an important role in overall wetland structure and function. In these systems it is the interplay between clastic and chemical sedimentation that appears to shape wetland geomorphology and ecology.

Although chemical sedimentation in wetlands has traditionally not been given much attention, studies from southern Africa have shown that it is potentially an important process, and that it is likely to have implications for wetland structure and function. It is suggested that wetlands from southern Africa, as well as wetlands from other regions of the world that experience similar climatic conditions, may therefore function very differently from their more well-studied counterparts in cool, temperate settings. Due to high rates of evapotranspiration (>2000 mm per annum) over much of the subcontinent, southern African wetlands are generally subjected to conditions where potential

evaporation exceeds rainfall. As such, evapotranspiration is expected to be the dominant means of water loss from these systems. This is in contrast to many wetlands in northern temperate settings where precipitation far exceeds potential evaporation. The following factors are identified as being necessary for chemical sedimentation in wetland systems:

- A sub-tropical or semi-arid climate with a water balance dominated by evapotranspirational water loss
- A substrate that encourages water retention
- Weathering in the catchment causing inflowing water to have high solute concentrations

In general, knowledge of sediment dynamics in wetland systems is poor. This study represents the first known successful attempt to measure sediment accumulation rates in a South African wetland using ^{137}Cs and ^{210}Pb isotopes. Due to difficulties in obtaining concentration data that are above detection limits, few investigations have been conducted in the region using ^{210}Pb and ^{137}Cs derived chronology. This study reveals the potential for using ^{137}Cs and ^{210}Pb in estimating deposition rates in South Africa. Both ^{137}Cs and ^{210}Pb are present in sufficient quantity to make them useful in determining sedimentation rates in South African systems. The ability to gain insight into the depositional history of such systems using radioisotopic methods may be an important development in fully understanding wetland formation, evolution and functioning in the region.

7.5 Future work

Given that chemical sedimentation is likely to be occurring in other wetland systems from subtropical and semi-arid regions, it as a mechanism of solute retention should me more widely investigated. With further research, the model of chemical sedimentation could be further developed, providing greater insight into wetland evolution. Within the Mkuze Wetland System, further research that could enhance our understanding of chemical sedimentation includes:

- Determining the quantity of chemicals accumulating within the system. This would require developing techniques that would allow the differentiation between clastic and chemical sediments.
- More detailed studies to determine the influence of seasonal flooding on sediment redox chemistry.

- Further investigation into the role vegetation distribution plays in initiating chemical sedimentation and the sequestration of solutes in plant tissues. Of particular interest is the mechanism employed by *Acacia xanthophloea* that enables it to survive in extremely saline conditions.

REFERENCES

Aalto R. & Dietrich W. (2005) *Sediment accumulation determined with ^{210}Pb geochronology for Strickland River flood plains, Papua New Guinea*. Seventh IAHS Scientific Assembly. Brazil.

Abtew W. (1996) Evapotranspiration measurements and modeling for three wetland systems in south Florida. *Water Resources Bulletin* 32: 465-473.

Alexander W.J.R. (1986) *Threats to the Mkuze river floodplain east of the Lebombo mountains and the Mkuze Swamp System*. Stormanns C.H. and Breen C.M. Proceedings of the Greater Mkuze Swamp System Symposium and Workshop. Institute of Natual Resources.

Allen B.L. & Hajek B.F. (1989) Mineral occurrence in soil environments. In Dixon J.B. and Weed S.B. (ed) *Minerals in Soil Environments*. Soil Science Society of America. Madison.

Amonette J.E. (2002) Methods for determination of mineralogy and environmental availability. In Dixon J.B. and Schulze D.G. (ed) *Soil mineralogy with environmental applications*. Soil Science Society of America. Madison

Appleby P.G. & Oldfield F. (1978) The calculation of lead-210 dates assuming a constant rate of supply of unsupported ^{210}Pb to the sediment. *Catena*. 5: 1-8.

Armenteros I., Bustillo M.A.A. & Blanco J. (1995) Pedogenic and groundwater processes in a closed Miocene basin (northern Spain). *Sedimentary Geology*. 99: 17-36.

Armstrong W. (1975) Waterlogged soils. In Etherington J.R. (ed) *Environment and Plant Ecology*. John Wiley & Sons. New York.

Arndt J.L. & Richardson J.L. (1993) Temporal variations in the salinity of shallow groundwater from the periiphery of some North Dakota wetlands (USA). *Journal of Hydrology*. 141: 75-105.

Arya L.M., Leij F.J., Shouse P.J. & van Genuchten M. (1999) Relationship between the hydraulic conductivity function and the particle-size distribution. *Soil Science Society of America Journal*. 63: 1063-1070.

Ashley G.M., Maitima Mworia J., Muasya A.M., Owens R.B., Driese S.G., Hover V.C., Renaut R.W., Goman M.F., Mathai S. & Blatt S.H. (2004) Sedimentation and recent history of a freshwater wetland in a semi-arid environment: Loboi Swamp, Kenya, East Africa. *Sedimentology*. 51: 1301-1321.

Ashton P.J., Masundire H., Hart R., Prince-Nengu J., Botshelo O., Lekhuru M., Mehlomakulu M. & Tylol I. (2002) *Water quality of the Okavango Delta, Botswana*. Aquatic Ecosystems of the Okavango Delta, Botswana. Centre for Applied Biodiversity Science. 38-53.

Ashworth P.J., Best J.L. & Jones M. (2004) Relationship between sediment supply and avulsion frequency in braided rivers. *Geology*. 32(1): 21-24.

Assine M.L. (2005) River avulsions on the Taquari megafan, Pantanal wetland, Brazil. *Geomorphology*. 70: 357-371.

Baeyens W., Monteny F., Leermakers M. & Bouillon S. (2003) Evalution of sequential extractions on dry and wet sediments. *Analytical and Bioanalytical Chemistry*. 376: 890-901.

Ball D.F. (1964) Loss-on-ignition as an estimate of organic matter and organic carbon in non calcareous soils. *Journal of Soil Science*. 15: 84-91.

Barbiero L., de Queiroz Neto J.P., Ciornei G., Sakamoto A.Y., Capellari B., Fernandes E. & Valles V. (2002) Geochemistry of water and ground water in the Nhecolândia, Pantanal of Mato Grosso, Brazil: variability and associated processes. *Wetlands*. 22: 528-540.

Barnes K. (2008) *The fate of solutes and processes of solute retention in the Mkuze Wetland System, KwaZulu-Natal.* PhD thesis. University of KwaZulu-Natal, Durban.

Barnes K., Ellery W.N. & Kindness A. (2002) A preliminary analysis of water chemistry of the Mkuze Wetland System, KwaZulu-Natal: A mass balance approach. *Water SA*. 28: 1-12.

Batley G.E. & Giles M.S. (1979) Solvent displacement of sediment interstitial waters before trace metal analysis. *Water Research*. 13: 879-886.

Batty L.C., Baker A.J.M. & Wheeler B.D. (2006) The effect of vegetation on pore water composition in a natural wetland receiving acid mine drainage. *Wetlands*. 26(1): 40-48.

Bauer-Gottwein P., Langer T., Prommer H., Wolski P. & Kinzelbach W. (2007) Okavango Delta islands: interactions between density-driven flow and geochemical reactions under evapo-concentration. *Journal of Hydrology*. 355: 389-405.

Benoit G. & Rozan T.F. (2001) ^{210}Pb and ^{137}Cs dating methods in lakes: a retrospective study. *Journal of Paleolimnology*. 25: 455-465.

Bernaldez F.G. & Rey Benayas J.M. (1992) Geochemical relationships between groundwater and wetland soils and their effects on vegetation in central Spain. *Geoderma*. 55: 273-288.

Berner R. (1975) The role of magnesium in the crystal growth of calcite and aragonite from sea water. *Geochimica et Cosmochimica Acta*. 39: 489-504.

Berner R.A. (1971) *Principles of Chemical Sedimentology*. McGraw-Hill. New York.

Binford M.W. (1993) Interpretation of ^{210}Pb profiles and verification of the CRS dating model in PIRLA project lake sediment cores. *Journal of Paleolimnology*. 9: 275-296.

Blott S.J. & Pye K. (2001) Gradistat: A grain size distribution and statistics package for the analysis of unconsolidated sediments. *Earth Surface Processes and Landforms*. 26: 1237-1248.

Bohn H. (1971) Redox potential. *Soil Science*. 112: 39-45.

Bohn H., McNeal B.L. & O'Connor G.A. (2001) *Soil Chemistry*. 3rd ed. John Wiley and Son. New York.

Bonotto D.M. & de Lima J.L.N. (2006) ^{210}Pb-derived chronology in sediment cores evidencing the anthropogenic occupation history at Corumbatai River basin, Brazil. *Environmental Geology*. 50: 595-611.

Borchardt G. (1989) Smectites. In Dixon J.B. and Weed S.B. (ed) *Minerals in soil environments*. 2nd ed. Soil Science Society of America. Madison.

Botha J., Witkowski E.T.F. & Shackleton C.M. (2002) A comparison of anthropogenic and elephant disturbance on Acacia xanthophloea (fever tree) populations in the Lowveld, South Africa. *Koedoe 45(1): 9–18.* 45(1): 9-18.

Breen C.M., Roger K.H. & Ashton P.J. (1988) Vegetation processes in swamps and flooded plains. In Symoens J.J. (ed) *Vegetation of Inland Waters*. Kluwer Academic Publishers. Dordrecht.

Brigatti M.F. (1983) Relationship between composition and structure in Fe-rich smectites. *Clay Minerals*. 18: 177-186.

Bryant M., Falk P. & Paola C. (1995) Experimental study of avulsion frequency and rate of deposition. *Geology*. 23(4): 365-368.

Bühmann C., Fey M.V. & de Villiers J.M. (1985) Aspects of the X-ray identification of swelling clay minerals in soils and sediments. *South African Journal of Science*. 81: 505-509.

Bufflap S.E. & Allen H.F. (1995) Sediment pore water collection methods for trace metal analysis: a review. *Water Research*. 29: 165-177.

Cambrey R.S., Playford K. & Lewis N.J. (1985) *Radioactive fallout in air and rain: results to the end of 1984*. UK Atomic Energy Authority.

Chakraborty D., Chakraborty A., Santra P., Tomar R.K., Garg R.N., Sahoo R.N., Choudhury S.G., Bhavanarayana M. & Kalra N. (2006) Prediction of hydraulic conductivity of soils from particle-size distribution. *Current Science*. 90(11): 1526-1531.

Chamley H. (1989) *Clay Sedimentology*. Springer. Berlin.

Chew J.A. & Bowen (1971) *Water Resources of Coastal Areas of northern Natal and Zululand*. Natal Town and Regional Planning report, v17.

Coates Palgrave K. (2003) *Trees of Southern Africa*. Struik. Cape Town.

Collins J.F. & Buol S.W. (1981) Effects of fluctuations in the Eh-pH environment on iron and/or manganese equilibria. *Soil Science*. 110: 111-118.

Cowan G.I. (1995) *Wetlands of South Africa*. South African Wetlands Conservation Programme Series. Department of Environmental Affairs and Tourism, Pretoria.

Craft C.B. & Casey W.P. (2000) Sediment and nutrient accumulation in floodplain and depressional freshwater wetlands of Georgia, USA. *Wetlands*. 20(2): 323-332.

Cresser M.S., Killham K. & Edwards T. (1993) *Soil chemistry and its applications*. Cambridge environmental chemistry series. Cambriddge University Press. New York.

Cronberg G., Gieske A., Martin E., Nengu J. & Stenstrom I.M. (1995) Hydrobiological studies in the Okavango Delta and the Kwando/Linyanti /Chobe River, Botswana. I Surface water quality analysis. *Botswana Notes and Records*. 27:151–226.

Dahm C.N., Grimm N.B., Marmonier P., Vallet H.M. & Vervier P. (1998) Nutrient dynamics at the interface between surface waters and groundwaters. *Freshwater Biology*. 40: 427-451.

D'Amore D.V., Stewart S.R. & Huddleston J.H. (2004) Saturation, reduction, and the formation of iron-manganese concretions in the Jackson-Frazier Wetland, Oregon. *Soil Science Society of America Journal*. 68: 1012-1022.

D'Amore D.V., Stewart S.R., Huddleston J.H. & Glasmann J.R. (2000) Stratigraphy and hydrology of the Jackson-Frazier Wetland, Oregan. *Soil Science Society of America Journal*. 64: 1535-1543.

Darragi F. & Tardy Y. (1987) Authigenic trioctahedral smectites controlling pH, alkalinity, silica and magnesium concentrations in alkaline lakes. *Chemical Geology*. 63: 59-72.

Davidson G.R., Carnley M., Lange T., Galicki S.J. & Douglas A. (2004) Changes in sediment accumulation rate in an oxbow lake following late 19th century clearing of land for agricultural use: a ^{210}Pb, ^{137}Cs, and ^{14}C study in Mississippi, USA. *Radiocarbon*. 46(2): 755-764.

Davison W. (1993) Iron and manganese in lakes. *Earth-Science Reviews*. 34: 119-163.

Day J.W., Ko J., Rybczyk J., Sabins D., Bean R., Berthelot G., Brantley C., Cadoch L., Conner W., Day J.N., Englande A., Feagley S., Hyfield E., Lane R., Lindsey J., Mistich J., Reyes E. & Twilley R. (2004) The use of wetlands in the Mississippi Delta for wastewater assimilation: a review. *Ocean and Coastal Management*. 47: 671-691.

DeLaune R.D., Jugsujinda A., Peterson G.W. & Patrick Jr W.H. (2003) Impact of Mississippi River freshwater reintroduction on enhancing marsh accretionary processes in a Louisiana estuary. *Estuarine, Coastal and Shelf Science*. 58: 653-662.

DeLaune R.D., Patrick Jr W.H. & Buresh R.J. (1978) Sedimentation rates determined by ^{137}Cs dating in a rapidly accreting salt marsh. *Nature*. 275: 532-533.

DeLaune R.D., Whitcomb J.H., Patrick Jr W.H., Pardue J.H. & Pezeshki S.R. (1989) Accretion and canal impacts in a rapidly subsiding wetland. 1: ^{137}Cs and ^{210}Pb techniques. *Estuaries*. 12(4): 247-259.

Delvaux B., Herbillion A.J., Vielvoye L. & Mestdagh M.M. (1990) Surface properties and clay mineralogy of hydrated halloysitic soil clays. II: Evidence for the presence of halloysite/smectite (H/Sm) mixed-layer clays. *Clay Minerals*. 25: 141-160.

Deocampo D. & Ashley G. (1999) Siliceous islands in a carbonate sea: Modern and Pleistocene spring-fed wetlands in Ngorongoro Crater and Oldupai Gorge, Tanzania. *Journal of Sedimentary Research*. 69(5): 974-979.

Deocampo D.M. (2005) Evaporative evolution of surface waters and the role of aqueous CO_2 in magnesium silicate production: Lake Eyasi and Ngorongoro Crater, northern Tanzania. *South African Journal of Geology*. 108: 493-504.

Donahoe R.J. & Liu C. (1998) Pore water geochemistry neat the sediment-water interface of a zoned, freshwater wetland in the southeastern United States. *Environmental Geology*. 33: 143-153.

Drees L.R., Wilding L.P., Smeck N.E. & Senkayi A.L. (1989) Silica in soils: Quartz and disordered silica polymorphs. In Dixon J.B. and Weed S.B. (ed) *Minerals in Soil Environments*. 2nd ed. Soil Science Society of America. Madison.

Drever J.I. (1997) *The geochemistry of natural waters: Surface and groundwater environments*. 3rd ed. Prentice-Hall. New Jersey.

Ellery W., Kotze D., McCarthy T., Tooth S., Grenfell M., Beckedahl H., Grundling P.-L., le Maitre D. & Ramsay L. (2007) *The origin and evolution of wetlands*. Water research commission wetlands research programme: Wetland rehabilitation. Water Research Commission, Durban.

Ellery W.N., Dahlberg A.C., Strydom R., Neal M.J. & Jackson J. (2003) Diversion of water flow from a floodplain wetland stream: an analysis of geomorphological setting and hydrological and ecological consequences. *Journal of Environmental Management*. 68(1): 51-71.

Ellery W.N., McCarthy T.S. & Dangerfield J.M. (2000) Floristic diversity in the Okavango Delta, Botswana as an endogenous product of biological activity. In Gopal B., Junk W. and Davis J. (ed) *Biodiversity in wetlands: assessment, function and conservation: volume 1*. Backhuys Publishers. Leiden.

Eugster H. & Kelts K. (1983) Lacustrine chemical sediments. In Goudie A. and Pye K. (ed) *Chemical sediments and Geomorphology*. Academic Press. London.

Eugster H.P. & Jones B.F. (1979) Behaviour of major solutes during closed-basin brine evolution. *American Journal of Science*. 279: 609-631.

Evans L.J. (1989) Chemistry of metal retention by soils. *Environmental Science and Technology*. 23(9): 1046-1056.

Favaro D.I.T., Damatto S.R., Silva P.S.C., Riga A.A., Sakamoto A.Y. & Mazzilli B.P. (2006) Chemical charactrization and ^{210}Pb dating in wetland sediment from the Nhecolandia Pantanal Pond, Brazil. *Journal of Radioanalytical and Nuclear Chemistry*. 269(3): 719-726.

Fiedler S. & Sommer M. (2004) Water and redox conditions in wetland soils - their influence on pedogenic oxides and morphology. *Soil Science Society of America Journal*. 68: 326-335.

Filgueiras A.V., Lavilla I. & Bendicho C. (2002) Chemical sequential extraction for metal partitioning in environmental solid samples. *Journal of Environmental Monitoring*. 4: 823-857.

Fischer D. (2000) *The retention of metals in a wetland peat deposit, Mkuze Wetland System, Northern KwaZulu-Natal*. Honours thesis. University of Natal, Durban.

Fisher J. & Acreman M.C. (2004) Wetland nutrient removal: a review of the evidence. *Hydrology and Earth System Sciences*. 8(4): 673-685.

Fitton G. (1997) X-ray fluorescence spectrometry. In Gill R. (ed) *Modern Analytical Geochemistry: An introduction to quantitative chemical analysis techniques for earth, environmental and materials scientists*. Longman. London.

Folk R.L. (1994) Interaction between bacteria, nannobacteria, and mineral precipitation in hot springs in central Italy. *Geographie physique et Quaternaire*. 48: 233-246.

Foster I.D.L., Boardman J. & Keay-Bright J. (2007) Sediment tracing and environmental history for two small catchments, Karoo Uplands, South Africa. *Geomorphology*. 90: 126-143.

Funess H.D. (1983) Wetlands as accreting systems: inogranic sediments. *Journal of Limnological Society of South Africa*. 9(2): 90-95.

Furquim S.C., Queiroz Neto J.P., Furian S., Barbiero L. & Graham R.C. (2004) Mg-mica formation in alkaline environment of the Nhecolandia, south Mato Grosso, Brazil. *Applied Minerology*.

Gac J.Y., Droubi A., Fritz B. & Tardy Y. (1977) Geochemical behaviour of silica and magnesium during the evaporation of waters in Chad. *Chemical Geology*. 19: 215-228.

Gambrell R.P. (1994) Trace and toxic metals in wetlands - A review. *Journal of Environmental Quality*. 23: 883-891.

Garrels R.M. & Mackenzie F.T. (1967) Origin of chemical compositions of some springs and lakes. *Advances in Chemistry Series*. 67: 222.

Giresse P. & Wiewióra A. (1999) Origin and diagenesis of blue-green clays and volcanic glass in the Pleistocene of the Cote d'Ivoire–Ghana Marginal Ridge. *Sedimentary Geology*. 127: 247-269.

Goldberg E.D. (1963) *Geochronology with lead-210 radioactive dating*. International Atomic Energy Agency.

Goodman P. (1987) Mkuze floodplain and swamps - wetland management case study. *African Wildlife*. 41(5): 269-270.

Gosselink J.G. & Turner R.E. (1978) The role of hydrology in the freshwater wetland ecosystems. In Good R.E., Whigham D.F. and Simpson R.L. (ed) *Freshwater Wetlands: Ecological processes and management potential*. Academic Press. New York.

Gran G. (1952) Determination of the equivalence point in potentiometric titrations (Part II). *Analyst*. 77: 661-667.

Grimm N.B., Gergel S.E., McDowell W.H., Boyer E.W., Dent C.L., Groffman P., Hart S.C., Harvey J., Johnston C., Mayorga E., McClain M.E. & Pinay G. (2003) Merging aquatic and terrestrial perspectives of nutrient biochemistry. *Oecologia*. 442: 485-501.

Hancock G., Edgington D.N., Robbins J.A., Smith J.N., Brunskill G. & Pfitzner J. (2002) *Workshop on radiological techniques in sedimentation studies: methods and applications*. Fernandez J.M. and Fichez R. Environmental changes and radioactive tracers. Proceedings of the South Pacific Environmental Radioactivity Association, Paris.

Harder H. (1972) The role of magnesium in the formation of smectite minerals. *Chemical Geology*. 10: 31-39.

Harder H. (1976) Nontronite synthesis at low temperatures. *Chemical Geology*. 18: 169-186.

Harder H. (1978) Synthesis of iron layer silicate minerals under natural conditions. *Clays and Clay Minerals*. 26(1): 65-72.

Hardie L.A. & Eugster H.P. (1970) The evolution of close-basin brines. *Mineralogical Society of America Special Publications*. 3: 273-290.

Harter S.K. & Mitsch W.J. (2003) Patterns of short-term sedimentation in a freshwater created marsh. *Journal of Environmental Quality*. 32(1): 325-334.

He Q. & Walling D.E. (1996) Rates of overbank sedimentation on the floodplains of British lowland rivers documented using fallout ^{137}Cs. *Geografiska Annaler*. 78(4): 223-243.

Hill S.J., Fisher A. & Cave M. (2004) Inductively Coupled Plasma Spectrometry. In Smith K.A. and Cresser M.S. (ed) *Soil and Environmental Analysis: modern instrumental techniques*. 3rd ed. Marcel Dekker. New York.

Hillier S. (1995) Erosion, sedimentation and sedimentary origin of clays. In Velde B. (ed) *Origin and mineralogy of clays*. Spinger. Berlin.

Hillier S. (2003) Clay Mineralogy. In Middleton G.V., Church M.J., Coniglio M., Hardie L.A. and Longstaffe F.J. (ed) *Encyclopedia of sediments and sedimentary rocks*. Kluwer Academic Publishers. Dordrecht.

Hover V., Walter L., Peacor D. & Martini A. (1999) Mg-smectite authigenesis in a marine evaporative environment, Salina Ometepec, Baja California. *Clays and Clay Minerals*. 47: 252-268.

Hover V.C. & Ashley G.M. (2003) Geochemical signatures of paleodepositional and diagenetic environments: A STEM/AEM study of authigenic clay minerals from an arid rift basin, Olduvai Gorge, Tanzania. *Clays and Clay Minerals*. 51: 231-251.

Ianni C., Ruggieri N., Rivaro P. & Frache R. (2001) Evaluation and comparision of two selective extraction procedures for heavy metal speciation in sediments. *Analytical Sciences*. 17: 1273-1278.

Isphording W.C. (1975) Primary Nontronite From the Venezuelan Guayana. *American Mineralogist*. 60: 840-848.

Jacks G. (1973) Chemistry of ground water in a district in southern India. *Journal of Hydrology*. 18: 185-200.

Johnston C., Bridgham S. & Schubauer-Berigan J. (2001) Nutrient dynamics in relation to geomorphology of riverine wetlands. *Soil Science Society of America Journal*. 65: 557-577.

Johnston C.A. (1991) Sediment and nutrient retention by fresh-water wetlands: effects on surface-water quality. *Critical Reviews in Environmental Control*. 21: 491-565.

Jones B.F. & Wier A.H. (1983) Clay minerals of Lake Abert, an alkaline, saline lake. *Clays and Clay Minerals*. 31: 161-172.

Jørgensen N.O. (2002) Origin of shallow saline groundwater on the Island of Læsø, Denmark *Chemical Geology*. 184: 359-370.

Karathanasis A.D. & Hajek B.F. (1984) Evaluation of aluminum-smectite stability equilibria in naturally acid soils. *Soil Science Society of America Journal*. 48(2): 413-417.

Karathanasis A.D. & Hajek B.F. (1996) Elemental analysis by X-ray fluorescence spectroscopy. In Sparks D.L. (ed) *Methods of soil analysis: Chemical methods. Part 3*. Soil Science Society of America. Madison.

Karathanasis A.D., Thompson Y.L. & Barton C.D. (2003) Long-term evaluations of seasonally sautrated "wetlands" in western Kentucky. *Soil Science Society of America Journal*. 67: 662-673.

Keeling J.L., Raven M.D. & Gates W.P. (2000) Geology and characterization of two hydrothermal nontronites from weathered metamorphic rocks at the Uley graphite mine, South Australia. *Clays and Clay Minerals*. 48(5): 537-548.

Kersten M. & Smedes F. (2002) Normalization procedures for sediment contaminants in spatial and temporal trend monitoring. *Journal of Environmental Monitoring*. (4): 109-115.

Kim J.G. (2003) Response of sediment chemistry and accumulation rates to recent environmental changes in the Clear Lake watershed, California, USA. *Wetlands*. 23(1): 95-103.

Kinniburgh D.H. & Miles D.L. (1983) Extraction and chemical analysis of interstitial water from soils and rocks. *Environmental Science and Technology*. 17: 362-368.

Koch M.S. & Rawlik P.S. (1993) Transpiration and stomatal conductance of two wetland macrophytes (*Cladium jamaicense* and *Typha domingensis*) in the subtropical Everglades. *American Journal of Botany*. 80(10): 1146-1154.

Koretsky C.M., Haas J.R., Miller D. & Ndenga N.T. (2006) Seasonal variations in pore water and sediment geochemistry of littoral lake sediments (Asylum Lake, MI, USA). *Geochemical Transactions*. 7(11).

Köster H.M., Ehrlicher U., Gilg H.A., Jordan R., Murad E. & Onnich K. (1999) Mineralogical and chemical characteristics of five nontronites and Fe-rich smectites. *Clay Minerals*. 34: 579-599.

Kotze D.C. & Breen C.M. (1994) *Agricultural land-use impacts of wetland functional values*. Water Research Commission.

Kotze D.C., Breen C.M. & Quinn N. (1995) Wetland losses in South Africa. In Cowan G.L. (ed) *Wetlands of South Africa*. Department of Environmental Affairs and Tourism. Pretoria.

Krishnaswami S. & Lai D. (1978) Radionuclide limnochronology. In Lerman A. (ed) *Lakes: chemistry, geology, physics*. Springer. New York.

Krishnaswami S., Lal D., Martin J.M. & Maybeck M. (1971) Geochronology of lake sediments. *Earth and Planetary Science Letters*. 11: 407-411.

Lee B.D., Graham R.C., Laurent T.E. & Amrhein C. (2004) Pedogenesis in a wetland meadow and surrounding serpentinitic landslide terrain, northern California, USA. *Geoderma*. 118: 303-320.

Liutkus C.M. & Ashley G.M. (2003) Facies model of a semiarid freshwater wetland, Oluvai Gorge, Tanzania. *Journal of Sedimentary Research*. 73: 691-705.

Logan W.S., Auge M.P. & Panarello H.O. (1999) Bicarbonate, sulfate, and chloride water in a shallow, clastic-dominated coastal flow system, Argentina. *Ground Water*. 37(2): 287-295.

Logan W.S. & Rudolph D.L. (1997) Microdepression-focused recharge in a coastal wetland, La Plata, Argentina. *Journal of Hydrology*. 194: 221-238.

Love A.J., Herczeg A.L., Armstrong D., Stadter F. & Mazor E. (1993) Groundwater flow regime within the Gambier Embayment of the Otway Basin, Australia: evidence from hydraulics and hydrochemistry. *Journal of Hydrology*. 143: 297-338.

Low A.B. & Rebelo A.G. (1996) *Vegetation of South Africa, Lesotho and Swaziland*. Department of Environmental Affairs and Tourism. Pretoria.

Makaske B., Smith D.G. & Berendsen H.J.A. (2002) Avulsions, channel evolution and floodplain sedimentation rates of the anastomosing upper Columbia River, British Columbia, Canada. *Sedimentology*. 49: 1049-1071.

Man K., Zheng J., Leung A.P.K., Lam P.K.S., Lam M.H. & Yen Y. (2004) Distribution and behaviour of trace metals in the sediment and porewater of a tropical coastal wetland. *Science of the Total Environment*. 327: 295-314.

Martin J.F., Hofherr E. & Quigley M.F. (2003) Effects of Typha latifolia transpiration and harvesting on nitrate concentrations in surface water of wetland microcosms. *Wetlands*. 23(4): 835-844.

Martin J.M., Nirel P. & Thomas A.J. (1987) Sequential extraction techniques: promises and problems. *Marine Chemistry*. 22: 313-341.

McCallan M.E., O'Leary B.M. & Rose C.W. (1980) Redistribution of cesium-137 by erosion and deposition on an Australian soil. *Australian Journal of Soil Research*. 18: 119-128.

McCarthy T.S., Barry M., Bloem A., Ellery W.N., Heister H., Merry C.L., Ruther H. & Sternberg H. (1997) The gradient of the Okavango fan, Botswana, and its sedimentological and tectonic implications. *Journal of African Earth Sciences*. 24: 65-78.

McCarthy T.S. & Ellery W.N. (1995) Sedimentation on the distal reaches of the Okavango fan, Botswana, and its bearing on calcrete and silcrete (Ganister) formation. *Journal of Sedimentary Research*. A65: 77-90.

McCarthy T.S. & Ellery W.N. (1998) The Okavango Delta. *Transactions of the Royal Society of South Africa*. 53: 157-182.

McCarthy T.S., Ellery W.N. & Bloem A. (1998a) Some observations on the geomorphological impact of hippopotamus (Hippopotamus amphibius L) in the Okavango Delta, Botswana. *African Journal of Ecology*. 36(1): 44-56.

McCarthy T.S., Ellery W.N. & Dangerfield J.M. (1998b) The role of biota in the initiation and growth of islands on the floodplain of the Okavango alluvial fan, Botswana. *Earth Surface Processes and Landforms*. 23: 291-316.

McCarthy T.S., Ellery W.N. & Ellery K. (1993) Vegetation-induced, subsurface precipitation of carbonate as an aggradational process in the permanent swamps of the Katanga (delta) fan, Botswana. *Chemical Geology*. 107: 111-131.

McCarthy T.S. & Hancox P.J. (2000) Wetlands. In Patridge T. and Maud R. (ed) *The Cenozoic of southern Africa*. Oxford University Press. Oxford.

McCarthy T.S., McIver J.R. & Verhagen B. (1991) Groundwater evolution, chemical sedimentation and carbonate brine formation on an island in the Okavango Delta swamp, Botswana. *Applied Geochemistry*. 6: 577-595.

McCarthy T.S. & Metcalfe J. (1990) Chemical sedimentation in the semi-arid environment of the Okavango Delta, Botswana. *Chemical Geology*. 89: 157-178.

Melaku S., Dams R. & Moens L. (2005) Determination of trace elements in agricultural soil samples by inductively coupled plasma-mass spectrometry: microwave acid digestion versus aqua regia extraction. *Analytica Chimica Acta*. 543: 117-123.

Meunier A. (2005) *Clays*. Springer. Berlin.

Mills A.J. (2006) The role of salinity and sodicity in the dieback of Acacia xanthophloea in Ngorongoro Caldera, Tanzania. *African Journal of Ecology*. 44: 61-71.

Mitsch W.J. & Gosselink J.G. (2007) *Wetlands*. 4th ed. John Wiley. New York.

Mladenov N., Huntsman-Mapila P., Wolski P., Masamba W.R.L. & McKnight D.M. (2008) Dissolved organic matter accumulation, reactivity, and redox state in groundwater of a recharge wetland. *Wetlands*. 28(3): 747-759.

Moore D.M. & Reynolds R.C. (1997) *X-ray diffraction and the identification and analysis of clay minerals*. 2nd ed. Oxford University Press. New York.

Morse J., Megonigal J. & Walbridge M. (2004) Sediment nutrient accumulation and nutrient availability in two tidal freshwater marshes along the Mattaponi River, Virginia, USA. *Biogeochemistry*. 69: 175-206.

Morse J.W. & Mackenzie F.T. (1990) *Geochemistry of Sedimentary Carbonates*. Elsevier Science. Amsterdam.

Müller G. & Förstner U. (1976) Primary nontronite from the Venezuela Quayqa: additional primary occurrences (Red Sea, Lake Malawi). *American Mineralogist*. 61: 500-501.

Neal M.J. (2001) *The vegetation ecology of the lower Mkuze River Floodplain, northern KwaZulu-Natal: A landscape ecology perspective*. MSc thesis. University of KwaZulu-Natal, Durban.

Oldfield F. & Appleby P.G. (1984) A combined radiometric and mineral magnetic approach to recent geochronology in lakes affected by catchment disturbance and sediment redistribution. *Chemical Geology*. 44: 67-83.

Otieno D.O., Schmidt M.W.T., Adiku S. & Tenhunen J. (2005a) Physiological and morphological responses to water stress in two Acacia species from contrasting habitats. *Tree Physiology*. 25: 361-371.

Otieno D.O., Schmidt M.W.T., Kinyamario J.I. & Tenhunen J. (2005b) Responses of Acacia tortilis and Acacia xanthophloea to seasonal changes in soil water availability in the savanna region of Kenya. *Journal of Arid Environments*. 62: 377-400.

Outridge P.M., Hermanson M.H. & Lockhart W.L. (2002) Regional variations in atmospheric deposition and sources of anthropogenic lead in lake sediments across the Canadian Arctic. *Geochemica et Cosmoshimica Acta*. 66(20): 3521-3531.

Owens P.N. & Walling D.E. (1996) Spatial variability of Caesium-137 inventories at reference sites: an example from two contrasting sites in England and Zimbabwe. *Applied Ratiation and Isotopes*. 47(7): 699-707.

Parkhurst D.L. & Appello C.A.J. (1999) *User's guide to PHREEQC (Version 2) - A computer program for speciation, batch reaction, one dimensional transport, and inverse geochemical calculations*. US Geological Survey, Water-Resources Investigations Report 99-4259, Colorado.

Patrick M.J. & Ellery W.N. (2006) Plant community and landscape patterns of a floodplain wetland in Maputaland, Northern KwaZulu-Natal, South Africa. *African Journal of Ecology*. 45: 175-183.

Pedro G., Carmouze J.P. & Velde B. (1978) Peloidal nontronite formation in recent sediments of Lake Chad. *Chemical Geology*. 23: 139-149.

Pfitzner J., Brunskill G. & Zagorskis I. (2004) ^{137}Cs and excess ^{210}Pb deposition patterns in estuarine and marine sediment in the central region of the Great Barrier Reef Lagoon, north-eastern Australia. *Journal of Environmental Radioactivity*. 76: 81-102.

Phillips G.W. & Marlow K.W. (1976) *Nuclear Instruments and Methods*. 137(3): 525-536.

Pollard C.O. & Weaver C.E. (1973) Opaline spheres - loosely-packed aggregates from silica nodule in diatomaceous miocene fullers earth. *Journal of Sedimentary Petrology*. 43(4): 1072-1076.

Potts P.J. (2004) X-Ray Fluoresence Analysis. In Smith K.A. and Cresser M.S. (ed) *Soil and Environmental Analysis: modern instrumental techniques*. 3rd ed. Marcel Dekker. New York.

Prato T. (2007) Selection and evaluation of projects to conserve ecosystem services. *Ecological Modelling*. 203(3-4): 290-296.

Price J.S. & Waddington J.M. (2000) Advances in Canadian wetland hydrology and biogeochemistry. *Hydrological Processes*. 14: 1579-1589.

Ramberg L. & Wolski P. (2008) Growing islands and sinking solutes: processes maintaining the endorheic Okavango Delta as a freshwater system. *Plant Ecology*. 196.

Ramsay P.J. & Cooper J.A.G. (2002) Late Quaternary sea-level change in South Africa. *Quaternary Research*. 57: 82-90.

Rauret G., Lopez-Sanchez J.F., Luck D., Yli-Halla M., Muntau H. & Quevauviller P. (2001) *The certification of the extractable contents (mass fractions) of Cd, Cr, Cu, Ni, Pb and Zn in freshwater sediment following a sequential extraction procedure: BCR-701*. European Commission Report.

Renaut R.W. & Jones B. (1997) Controls on aragonite and calcite precipitation in hot spring travertines at Chemurkeu, Lake Bogoria, Kenya. *Canadian Journal of Earth Sciences*. 34: 801-818.

Richardson C.J. & Hole F.D. (1979) Mottling and iron distribution in a Glossoboralf Haplaquoll hydrosequence on a glacial moraine in northwestern Wisconsin. *Soil Science Society of America Journal*. 43: 552-558.

Richardson J. & Vepraskas M.J. (2001) *Wetland Soils: Genesis, Hydrology, Landscapes and Classification*. CRC Press. Florida.

Ritchie J.C. & McHenry J.R. (1990) Application of radioactive fallout cesium-137 for measuring soil erosion and sediment accumulation rates and patterns: a review. *Journal of Environmental Quality*. 19: 215-233.

Ritchie J.C., McHenry J.R. & Gill A.C. (1973) Dating recent reservoir sediments. *Limnology Oceanography*. 18: 254-263.

Robbins J.A. & Edgington D.N. (1975) Determination of recent sedimentation rates in Lake Michigan using ^{210}Pb and ^{137}Cs. *Geochimica et Cosmochimica Acta*. 39: 295-304.

Robert M. & Veneau G. (1979) Stabilité des minéraux phylliteux 2:1 en conditions acides. Rôle de la composition octaédrique. *Proceedings from the 6th International Clay Conference*. Oxford: 385-394.

Salama R.B., Farrington P., Bartle G.A. & Watson G.D. (1993) The chemical evolution of groundwater in a first-order catchment and the process of salt accumulation in the soil profile. *Journal of Hydrology*. 143: 233-258.

Sanchez-Carrillo S., Alvarez-Cobelas M. & Angeler D.G. (2001) Sedimentation in the semi-arid freshwater wetland Las Tablas de Daimiel (Spain) *Wetlands*. 21(1): 112-124.

Sanders C.J., Santos I.R., Silva-Filho E.V. & Patchineelam S.R. (2006) Mercury flux to estuarine sediments, derived from Pb-210 and Cs-137 geochronologies (Guaratuba Bay, Brazil). *Marine Pollution Bulletin*. 52: 1085-1089.

Sandroni V. & Smith C.M.M. (2002) Microwave digestion of sludge, soil and sediment samples for metal analysis by inductively coupled plasma-atomic emission spectrometry. *Analytica Chimica Acta*. 468: 335-344.

Saunders D.A., Hobbs R.J. & Margules C.R. (1991) Biological consequences of ecosystem fragmentation - a review. *Conservation Biology*. 5(1): 18-32.

Saxena D.P., Joos P., Van Grieken R. & Subramanian V. (2002) Sedimentation rate of the floodplain sediments of the Yamuna river basin (tributary of the river Ganges, India) by using ^{210}Pb and ^{137}Cs techniques. *Journal of Radioanalytical and Nuclear Chemistry*. 251(3): 399-408.

Schot P.P. & Wassen M.J. (1993) Calcium concentrations in wetland groundwater in relation to water sources and soil conditions in the recharge area. *Journal of Hydrology*. 141: 197-217.

Schulze D.G. (2002) An introduction to soil mineralogy. In Dixon J.B. and Schulze D.G. (ed) *Soil mineralogy with environmental applications.* Soil Science Society of America. Madison.

Schwartz M.W., Brigham C.A. & Hoeksema J.D. (2000) Linking biodiversity to ecosystem function: implications for conservation ecology. *Oecologia*. 122(3): 297-305.

Shaw T.J., Gieskes J.M. & Jahnke R.A. (1990) Early diagenesis in differing depositional environments: the response of transition metals in pore water. *Geochimica et Cosmochimica Acta*. 54: 1233-1246.

Skoog D.A., West D.M. & Holler F.J. (1996) *Fundamentals of Analytical Chemistry*. 7th ed. Saunders College Publishing. Orlando.

Smith J.N. (2001) Why should we believe ^{210}Pb sediment geochronologies? *Journal of Environmental Radioactivity*. 55: 121-123.

Stormanns C.H. (1987) *An inventory and assessment of the conservation value of the Greater Mkuze Wetland System*. Investigational Report No 36. National Conservation Resources. CSIR.

Stouthamer E. & Berendsen H.J.A. (2007) Avulsion: The relative roles of autogenic and allogenic processes. *Sedimentary Geology*. 198: 309-325.

Stucki J.W. (1988) Structural iron in smectites. In Stucki J.W., Goodman B.A. and Schwertmann U. (ed) *Iron in Soils and Clay Minerals*. Reidel Publishing Company. Dordrecht.

Stumm W. (1996) *Aquatic chemistry : chemical equilibria and rates in natural waters*. John Wiley & Sons. New York.

Stumm W. & Morgan J.J. (1981) *Aquatic Chemistry: an introduction emphasizing chemical equilibria in natural waters*. 2nd ed. Wiley-Interscience. New York.

Taylor R. (1986) *The past and present human involvement in the Mkuze Swamp System*. Stormanns C.H. and Breen C.M. Proceedings of the Greater Mkuze Swamp System Symposium and Workshop. Institute of Natual Resources, Investigational Report No.22.

Tessier A., Campbell P.G.C. & Bisson M. (1979) Sequential extraction procedure for the speciation of particulate trace metals. *Analytical Chemistry*. 51: 844-851.

Tockner K. & Stanford J.A. (2003) Riverine flood plains: present state and future trends. *Environmental Conservation*. 29(3): 308-330.

Tooth S. & McCarthy T.S. (2007) Wetlands in drylands: geomorphological and sedimentological characteristics, with emphasis on examples from southern Africa. *Progress in Physical Geography*. 31(1): 3-41.

Tooth S., Rodnight H., Duller G.A.T., McCarthy T.S., Marren P.M. & Brandt D. (2007) Chronology and controls of avulsion along a mixed bedrock-alluvial river. *Geological Society of America Bulletin*. 119: 452-461.

Troxler Gann T.G., Childers D.L. & Rondeau D.N. (2005) Ecosystem structure, nutrient dynamics, and hydrologic relationships in tree islands of the southern Everglades, Florida, USA. *Forest Ecology and Management*. 214: 11-27.

Tuzen M., Sari H. & Soylak M. (2004) Microwave and wet digestion procedures for atomic absorption spectrometric determination of trace metals contents of sediment samples. *Analytical Letters*. 37(9): 1925-1936.

Van Herreweghe S., Swennen R., Vandecasteele C. & Cappuyns V. (2003) Solid phase speciation of arsenic by sequential extraction in standard reference materials and industrially contaminated soil samples. *Environmental Pollution*. 122: 323-342.

Vepraskas M.J. & Faulkner S.P. (2001) Redox Chemistry of Hydric Soils. In Richardson J.L. and Vepraskas M.J. (ed) *Wetland Soils: Genesis, Hydrology, Landscapes, and Classification*. CRC Press. New York.

Verhoeven J.T.A., Arheimer B., Yin C. & Hefting M.M. (2006) Regional and global concerns over wetlands and water quality. *Trends in Ecological Evolution*. 121: 96-103.

Viers J., Barroux G., Pinelli M., Seyler P., Oliva P., Dupre B. & Boaventura G. (2005) The influence of the Amazonian floodplain ecosystems on the trace element dynamics of the Amazon River mainstem (Brazil). *Science of the Total Environment*. 339: 219-232.

Von Damm K.L. & Edmond J.M. (1984) Reverse weathering in the closed-basin lakes of the Ethiopian rift. *American Journal of Science*. 284: 835-862.

Walsh J.N. (1997) Inductively coupled plasma-atomic emission spectrometry (ICP-AES). In Gill R. (ed) *Modern Analytical Geochemistry: introduction to quantitative chemical analysis techniques for earth, environmental and materials scientists*. Longman. London.

Wang G., Liu J. & Tang J. (2004) Historical variation of heavy metals with respect to different chemical forms in recent sediments from Xianghai wetlands, northeast China. *Wetlands*. 24: 608-619.

Warren L.A. & Haack E.A. (2001) Biogeochemical controls on metal behaviour in freshwater environments. *Earth-Science Reviews*. 54: 261-320.

Watkeys M., Mason T. & Goodman P. (1993) The role of geology in the development of Maputaland, South Africa. *Journal of African Earth Sciences*. 16: 1-16.

Watkeys M.K. (1997) The Mkuze River from the Lebombo Mountains to the Lower Mkuze bridge. In Botha G.A. (ed) *Maputaland: Focus on the quaternary evolution of the south-east African coastal plain. Field guide and abstracts*. Council for Geoscience.

Weis D.A., Callaway J.C. & Gersberg R.M. (2001) Vertical accretion rates and heavy metal chronologies in wetland sediments of the Tijuana Estuary. *Estuaries*. 24: 840-850.

Western D. & Maitumo D. (2004) Woodland loss and restoration in a savannah park: a 20-year experiment. *African Journal of Ecology*. 42: 111-121.

Western D. & van Praet C. (1973) Cyclical changes in the habitat and climate of an East African ecosystem. *Nature*. 241: 104-106.

Wetzel P.R., van der Valk A.G., Newman S., Gawlik D.E., Troxler Gann T., Coronado-Molina C.A., Childers D.L. & Sklar F.H. (2005) Maintaining tree islands in the Florida Everglades: nutrient redistribution is the key. *Frontiers in Ecology and the Environment*. 3(7): 370-376.

Wilken R.D., Moreira I. & Rebello A. (1986) Pb-210 and Cs-137 fluxes in a sediment core from Guanabara Bay, Brazil. *Science of the Total Environment*. 58: 195-198.

Wilkening M.H. & Clements W.E. (1975) The ocean as a source of atmospheric radon-222. *Journal of Geophysical Research*. 80: 3828-3830.

Williams L.A., Parks G.A. & Crerar D.A. (1985) Silica Diagenesis I: Solubility controls. *Journal of Sedimentary Petrology*. 55: 301-311.

Wilson M.J. (1999) The origin and formation of clay minerals in soils: past, present and future perspectives. *Clay Minerals*. 34: 7-25.

Wust R.A.J. & Bustin R.M. (2003) Opaline and Al-Si phytoliths from a tropical mire system of West Malaysia: abundance, habit, elemental composition, preservation and significance. *Chemical Geology*. 200: 267-292.

Yuretich R.F. & Cerling T.E. (1983) Hydrochemistry of Lake Turkana, Kenya: Mass balance and mineral reactions in an alkaline lake. *Geochimica et Cosmochimica Acta*. 47: 1099-1109.